Chiral Phase Transition in QCD and Vector Manifestation

Chihiro Sasaki

Department of Physics, Nagoya University,
Nagoya, 464-8602, Japan

February 2, 2008

Abstract

Spontaneous chiral symmetry breaking is one of the most important features in low-energy QCD. The chiral symmetry is expected to be restored at very high temperature and/or density. Accompanied by the chiral phase transition, properties of hadrons will be changed especially near the critical point. The study of the phenomena associated with the chiral phase transition will give us some clues on the connection between the chiral symmetry and the low-energy hadron dynamics.

We develop the theory based on the hidden local symmetry (HLS) at finite temperature, which is an effective field theory of QCD and includes pions and vector mesons as the dynamical degrees of freedom, and study the chiral phase transition in hot matter. We show that the chiral symmetry is restored as the vector manifestation (VM), in which the massless degenerate pion (and its flavor partners) and the longitudinal ρ meson (and its flavor partners) as the chiral partner. We also present several predictions based on the VM. We estimate the critical temperature T_c and show the following phenomena near T_c: the vector charge susceptibility becomes equal to the axial-vector charge susceptibility; the vector dominance of the electromagnetic form factor of the pion is largely violated; the pion velocity is close to the speed of light. Furthermore, we show that the remnant of the VM can be clearly seen in the system of heavy mesons. We expect that the VM and its predictions are testable by current and future experiments and the lattice analysis.

Contents

Chapter 1

Introduction

Quantum Chromo Dynamics (QCD) is the theory which governs the dynamics of quarks and gluons, and eventually the hadron dynamics. The QCD Lagrangian has an approximate global chiral symmetry in the light quark sector. The QCD vacuum, however, holds no longer the chiral symmetry which is spontaneously broken down caused by its strongly interacting dynamics. Spontaneous chiral symmetry breaking is one of the most important features in low-energy QCD. The phenomena of the light pseudoscalar mesons (the pion and its flavor partner), which are regarded as the approximate Nambu-Goldstone bosons associated with the symmetry breaking, are well described by the symmetry property in the low-energy region.

For the purpose to clarify the connection between the low-energy phenomena and the chiral symmetry, one of the most important techniques to study them is using effective field theories (EFTs) in which a systematic low-energy expansion is done, as in the chiral perturbation theory (ChPT). The EFTs are constructed based on the chiral symmetry, in which the non-perturbative effects are "dressed" around the (bare) quarks and gluons and the fundamental degrees of freedom are replaced with the relevant ones in the low-energy region, i.e., hadrons. In general, the EFTs have many parameters like hadron masses and coupling constants. Some of them can be determined in low-energy limit by the chiral symmetry, however others are not completely restricted by only the symmetry. When one performs the matching of the EFT to QCD to determine the parameters of the EFT, one can clarify how the hadron physics succeeds the dynamics of underlying QCD. Furthermore, including quantum effects into the parameters, we can understand the hadron physics based on QCD from many different angles and clarify the non-perturbative aspects of QCD.

However, the mechanism how hadrons acquire their masses as a result of the dynamics

is still an open problem of QCD. In order to find out some clues on this issue, it is efficient to consider a world where the QCD vacuum holds the chiral symmetry. Although the chiral symmetry is spontaneously broken in the real world, it is expected to be restored under some extreme conditions, e.g., very high temperature and/or density. Properties of hadrons will be changed at finite temperature/density, especially near the critical point of the chiral symmetry restoration [1, 2, 3, 4, 5, 6, 7].

Both theoretically and experimentally, it is important to investigate the physics near the phase transition point. In fact, the CERN Super Proton Synchrotron (SPS) observed an enhancement of dielectron (e^+e^-) mass spectra below the ρ/ω resonance [8]. This can be explained by the dropping mass of the ρ meson (see, e.g., Refs. [9, 3, 6]) associated with the chiral symmetry restoration following the Brown-Rho scaling proposed in Ref. [10]. The Relativistic Heavy Ion Collider (RHIC) has started to measure several physical processes in hot matter which include the dilepton energy spectra. In near future, the CERN Large Hadron Collider (LHC) and GSI are planning to measure them. These experiments will further clarify the properties of vector mesons in hot matter.

As indicated by the SPS data, the vector meson is the one of important degrees of freedom in studying the phenomena near the QCD phase transition. The theory based on the hidden local symmetry [11, 12] is an EFT including both pions and vector mesons, where the low-energy expansion is systematically done (for details, see Ref. [13]). The HLS theory has a wider energy range of the validity than the ordinary ChPT. In this thesis, we review the construction of the HLS theory in hot matter and its application to the chiral phase transition following Refs. [14, 15, 16, 17, 18].

There is no strong restriction concerning vector meson masses in the standard scenario of chiral symmetry restoration, where the pion joins with the scalar meson in the same chiral representation [see for example, Refs. [1, 19, 20]]. However there is a scenario which certainly requires the dropping mass of the vector meson and supports the Brown-Rho scaling: In Ref. [21], it was proposed that there can be another possibility for the pattern of chiral symmetry restoration, the vector manifestation (VM). The VM was proposed as a novel manifestation of the chiral symmetry in the Wigner realization, in which the chiral symmetry is restored by the massless degenerate pion (and its flavor partners) and the longitudinal ρ meson (and its flavor partners) as the chiral partner. In terms of the chiral representations of the low-lying mesons, there is a representation mixing in the vacuum [21, 13]. Approaching the critical point, we find that there are two possibilities for the pattern of the chiral symmetry

restoration (see chapter 5): One possible pattern is the standard scenario and another is the VM. Both of them are on an equal footing with each other in terms of the chiral representations. It is worthwhile to study the physics associated with the VM as well as that with the standard scenario of the chiral symmetry restoration.

It has been shown that the VM is formulated at a large number of flavor [21], critical temperature [14] and critical density [22] by using the HLS theory, where a second order or weakly first order phase transition was assumed. In the VM at finite temperature and/or density, the *intrinsic temperature and/or density dependences* of the *bare* parameters of the HLS Lagrangian played important roles to realize the chiral symmetry restoration consistently (see chapters 4 and 5): Since the HLS theory is an EFT of underlying QCD, the parameters of the HLS Lagrangian do depend on the temperature and/or density. In the framework of the HLS the equality between the axial-vector and vector current correlators at the critical point can be satisfied only if the intrinsic thermal and/or density effects are included. The intrinsic temperature and/or density dependences are nothing but the information integrated out which is converted from the underlying QCD through the Wilsonian matching [13, 14]. In other words, the intrinsic effects are the signature that the hadron has an internal structure constructed from the quarks and gluons.

The VM explains an anomalous enhancement of dielectron mass spectra observed at SPS. This is a theoretical support of the dropping mass of ρ meson following the Brown-Rho scaling, which can explain the SPS data.

In this thesis, we assume that only the pions and vector mesons are the relevant (light) degrees of freedom until near the critical temperature, say $T_c - \epsilon$, and that the chiral symmetry is partially restored already at $T_c - \epsilon$. Then we study whether the dropping ρ can be formulated in some EFT. We should note that, although we assume the dropping ρ meson mass $m_\rho \sim \mathcal{O}(\epsilon')$ as an input, it is non-trivial that the dropping ρ can actually be formulated in the framework of quantum field theory.

Now, what happens to other mesons? In Fig. 1.1, we sketch our view of the temperature dependences of the light mesons masses. We assume that the A_1 meson is still heavy at $T_c - \epsilon$. The scalar mesons and their fate near T_c may be more controversial. Several pictures on the construction of the scalar meson are proposed [see e.g., Refs. [23, 24, 25, 26]]. In our present picture, we do not introduce the scalar mesons as the dynamical degrees of freedom into the EFT because of the following naive speculations based on two kinds of picture on the quark content of scalar mesons.

Two-quark state : The light scalar meson is a bound state of a quark and an anti-quark. The

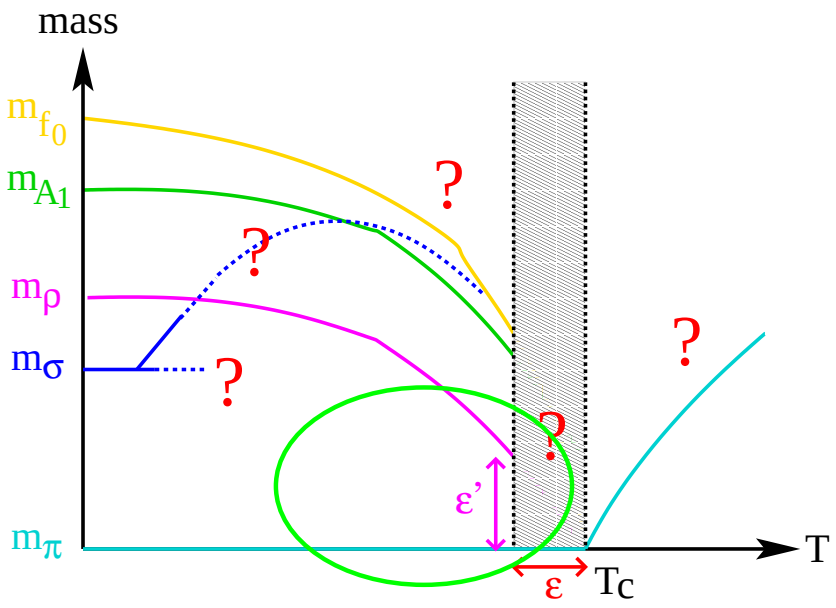

Figure 1.1: Our picture. The solid lines denote the temperature dependences of light mesons, π, σ, ρ, A_1 and $f_0(1370)$. Throughout this thesis, we concentrate on the region near $T_c - \epsilon$ (denoted by the green ellipsis) where we assume that only the pions and vector mesons are relevant degrees of freedom.

sigma meson mass $m_\sigma \sim 600\,\mathrm{MeV}$ in the real world can be explained by the existence of the disconnected quark diagram joined by the gluon exchange [27]. At finite temperature, we expect that the effective QCD coupling constant becomes weaker than that in the vacuum and that m_σ may go up. In that case, the m_σ may go to zero in the limit $T \to T_c$ although it might be still heavy until around $T_c - \epsilon$. There may be a possibility that the $f_0(1370)$ (or the mixture of σ and $f_0(1370)$) goes down at $T \to T_c$.

Four-quark state : The light scalar meson is a bound state of a diquark and an anti-diquark. The sigma meson may be melted at finite temperature less than T_c since the binding energy of qq is smaller than that of $\bar{q}q$. When there exists the light scalar meson near T_c (above $T_c - \epsilon$), such scalar meson might be related to the $f_0(1370)$ at $T = 0$.

In order to understand which universality class the VM belongs to, we may need to include the scalar and A_1 mesons other than pions and vector mesons for the analysis of critical exponents. In the chiral symmetric phase, on the other hand, an existence of some mesonic (soft) modes is proposed [see e.g, Refs. [28, 29, 30, 31, 32]].

Throughout this thesis, we concentrate on the region out of the window near $T_c - \epsilon$ where we assume that only the pions and vector mesons are relevant degrees of freedom. In that

region, we will see that the dropping ρ can be formulated within the EFT including both pions and vector mesons, related to the chiral symmetry restoration. Furthermore, the present framework gives several physical predictions which are closely related to the dropping ρ. These predictions can be tested in future experiments and numerical simulations on the lattice.

Now let us assume that the chiral symmetry of QCD is restored as the VM. Then can we see some remnant of the VM in the real world? In order to answer this question, in chapter 6, we study the heavy meson system which consists of one heavy quark and one light anti-quark following Ref. [33]. We construct an effective Lagrangian based on the VM and heavy quark symmetry at the restoration point, and then we introduce the effects of the spontaneous chiral symmetry breaking to go back to the real world. We will show that the EFT can describe the recent experimental data.

This paper is organized as follows:

In chapter 2, we give a general concept of EFTs and the matching between an EFT and the underlying theory in the Wilsonian sense. Then we apply the Wilsonian matching to the QCD in hot and/or dense matter. We give an account of the general idea of the intrinsic temperature and/or density dependences of the parameters, which are inevitably introduced as a result of the Wilsonian matching.

In chapter 3, we briefly review the HLS and the ChPT with HLS in hot matter following Refs. [14, 16]: In section 3.1, we review the theory based on the HLS and in section 3.2, we show details of the calculation of the hadronic thermal corrections as well as the quantum corrections in the background field gauge. In section 3.3, we construct the axial-vector and vector current correlators. Then in section 3.4, we study the temperature dependences of the vector meson mass, the pion decay constant and the pion velocity. We also study the validity of the vector dominance (VD) in hot matter. In section 3.5, we show the bare HLS Lagrangian without Lorentz invariance.

In chapter 4, we briefly review the Wilsonian matching at finite temperature following Refs. [14, 15, 16, 17, 18]: We extend the Wilsonian matching at zero temperature to the version at non-zero temperature. We also study in detail the effect of Lorentz non-invariance of the bare pion decay constants.

In chapter 5, we show how the VM is realized at the critical point in the framework of the HLS theory. We also study the predictions of the VM in hot matter: In section 5.1, we present the conditions for the bare parameters through the Wilsonian matching at the critical temperature. Further, we take into account the Lorentz non-invariance in the bare HLS theory

and present the extended conditions. Then we show that the conditions are still protected as the fixed point of the RGEs. In section 5.2, we review the formulation of the VM in hot matter following Ref. [16]. Then in section 5.3, we show how the pion decay constants vanish at the critical temperature following Ref. [15]. Next, in section 5.4, we summarize the predictions of the VM in hot matter studied in Refs. [14, 15, 16, 17, 18]: In subsection 5.4.1, we estimate the value of the critical temperature. In subsection 5.4.2, we focus on the vector and axial-vector susceptibilities very near the critical temperature T_c. Then we address the issue of what the relevant degrees of freedom can be at the critical point. In subsection 5.4.3, we shed some light on the validity of the vector dominance (VD) of electromagnetic form factor of the pion near the critical temperature. We find that *the VM predicts a large violation of the VD at the critical temperature*. This indicates that the assumption of the VD may need to be weakened, at least in some amounts, for consistently including the effect of the dropping mass of the vector meson. In subsection 5.4.4, we study the pion velocity at the critical temperature based on the VM. There we show the non-renormalization property on the pion velocity at the critical temperature, which is protected by the VM. Then using this property and through matching to the OPE, we estimate the value of the pion velocity. In section 5.5, we discuss the critical behavior of $m_\rho(T)$ near the critical temperature.

In chapter 6, we study the system of heavy mesons like D meson, following Ref. [33]. We construct an EFT based on the VM and the heavy quark symmetry motivated by the recent discovery of new D mesons ($J^P = 0^+$ and 1^+) in Babar, CLEO and Belle [34, 35, 36]. We show that the mass splitting between new D mesons and the existing D mesons ($J^P = 0^-$ and 1^-) is directly proportional to the light quark condensate. Further we study the characteristic decay modes and give the predictions on the decay widths and the branching ratios.

We give a brief summary and discussions in chapter 7.

Chapter 2

Effective Field Theory and Renormalization Group

Use of effective field theories (EFTs) is one of important implements to study strongly interacting system like low-energy QCD. An EFT works only in low energy below a characteristic scale, which is dependent on dynamics of the EFT, and is expanded in powers of momentum. At a given order, the theory has a finite number of counter terms and thus we can perform *an order-by-order renormalization* in the sense of momentum expansion although the EFT is conventionally non-renormalized.

In this chapter, we give a general idea of EFTs and the matching between an EFT and the underlying theory in the Wilsonian sense.

2.1 General Concept of Effective Field Theory

We consider the QCD Lagrangian with N_f massless quarks:

$$\mathcal{L}^{(0)}_{\rm QCD} = \bar{q} i\gamma^\mu (\partial_\mu - i g_s G_\mu) q - \frac{1}{2}{\rm tr}[G_{\mu\nu} G^{\mu\nu}]\,, \tag{2.1}$$

with G_μ and g_s being the gluon field and the QCD gauge coupling constant. The field strength $G_{\mu\nu}$ is defined by

$$G_{\mu\nu} = \partial_\mu G_\nu - \partial_\nu G_\mu - i g_s [G_\mu, G_\nu]\,. \tag{2.2}$$

We define the left- and right-handed quarks by

$$q_L = \frac{1}{2}(1-\gamma_5) q, \quad q_R = \frac{1}{2}(1+\gamma_5) q. \tag{2.3}$$

The interacting term between q_L and q_R never appear in the Lagrangian. It implies that the QCD Lagrangian has an $SU(N_f)_L \times SU(N_f)_R \times U(1)_V \times U(1)_A$ symmetry. In the real

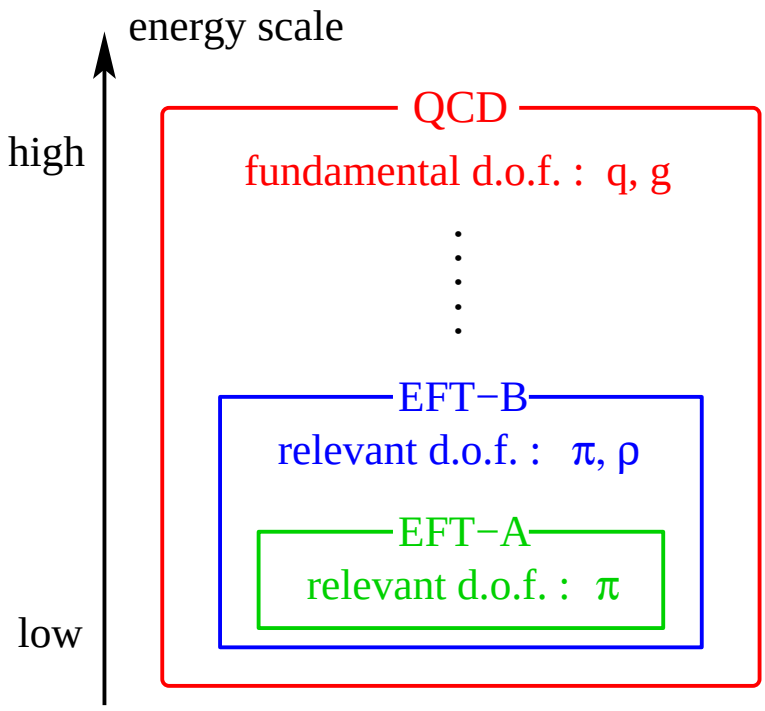

Figure 2.1: Schematic view of effective field theories (EFTs). Here q and g denote quarks and gluons respectively.

world, however, the chiral symmetry is spontaneously broken down by the strongly interacting dynamics, which makes pions to be much lighter than other hadrons. The pion are identified as massless Nabmu-Goldstone (NG) bosons associated with the spontaneous chiral symmetry breaking.

In the construction of an EFT valid in some energy region, it is important to specify the relevant degrees of freedom in the energy scale as well as to respect symmetries of the fundamental theory. The relevant degrees of freedom may be changed according to the energy scale that one is interested in. We show a schematic view of the relation between EFTs and their underlying QCD in Fig. 2.1: In low energies, the relevant degrees of freedom are hadrons. Especially pion is the lightest hadron, which is the most relevant degree of freedom in low-energy limit, and its dynamics is well described by EFTs based on the chiral symmetry of QCD like the chiral perturbation theory (ChPT) [37, 38, 39]. Here we consider an EFT, say EFT-A, which includes only pions as the relevant degrees of freedom. In the energy region where the EFT-A works well, other hadrons, e.g., vector mesons, nucleons and excited states, are sitting as the background. However at some energy scale, the EFT-A breaks down, and then one has to go to a more suitable theory which might be an EFT: As the energy scale

increases, other mesons like ρ mesons are elevated from the background and become relevant degrees of freedom as well as pions. The background matter now consists of other hadrons except for pions and ρ mesons. Thus one can switch over the EFT-A to new EFT, EFT-B, which includes both pions and ρ mesons as the relevant degrees of freedom.

Let us consider the QCD Lagrangian with external source fields:

$$\mathcal{L}_{\rm QCD} = \mathcal{L}^{(0)}_{\rm QCD} + \bar{q}(\gamma_\mu \mathcal{V}^\mu + \gamma_5\gamma_\mu \mathcal{A}^\mu)q - \bar{q}(\mathcal{S} - i\mathcal{P})q\,, \tag{2.4}$$

where the external vector ($\mathcal{V}_\mu$), axial-vector ($\mathcal{A}_\mu$), scalar ($\mathcal{S}$) and pseudoscalar ($\mathcal{P}$) fields are the hermitian $N_f \times N_f$ matrices in flavor space. If there is an explicit chiral symmetry breaking, it is introduced as the vacuum expectation value (VEV) of $\mathcal{S}$. In the case of $N_f = 3$,

$$\langle \mathcal{S} \rangle = \mathcal{M} = {\rm diag}(m_u, m_d, m_s). \tag{2.5}$$

The following functional of a set of source fields denoted by J,

$$Z[J] = \int \mathcal{D}q\mathcal{D}\bar{q}\mathcal{D}G \exp\left[i \int d^4x \mathcal{L}_{\rm QCD}[q, \bar{q}, G; J] \right], \tag{2.6}$$

generates Green's functions which have important information of the system. The basic concept of the EFT is based on the following assumption: The effective Lagrangian, which has the most general form constructed from the chiral symmetry, can give the same generating functional as in Eq. (2.6):

$$Z[J] = \int \mathcal{D}U \exp\left[i \int d^4x \mathcal{L}_{\rm eff}[U; J] \right], \tag{2.7}$$

where U denotes the relevant hadronic fields such as the pion fields and $\mathcal{L}_{\rm eff}$ is an Lagrangian expressed in terms of these hadrons. In the ChPT, $N_f \times N_f$ special-unitary matrix U is parametrized by the pseudoscalar fields $\pi = \pi^a T_a$ as

$$U = e^{2i\pi/F_\pi}, \tag{2.8}$$

where F_π denotes the pion decay constant. The leading Lagrangian in the chiral limit is given by [38, 40]

$$\mathcal{L}^{\rm ChPT}_{(2)} = \frac{F_\pi^2}{4} {\rm tr}[D_\mu U^\dagger D^\mu U], \tag{2.9}$$

where D_μ is the covariant derivative acting on U.

Corresponding to each Green's function derived from Eq. (2.6), we have the same Green's function obtained from the EFT through Eq. (2.7). We should note that according to the energy scale, the relevant degrees of freedom are different although both fundamental (q and g) and hadronic (U) degrees of freedom are integrated over all configuration space.

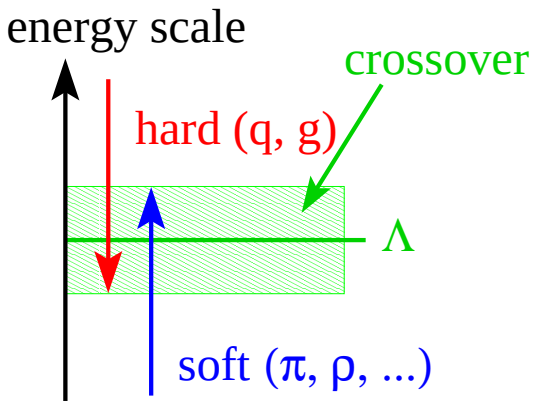

Figure 2.2: Separation over two regions (hard and soft). A crossover region where both theories are available is assumed. In this region, we can perform the matching between two theories.

The idea mentioned above is the most general construction of EFTs, where only the chiral symmetry gives constraints for the forms of the effective Lagrangian. Thus various EFTs consistent with the chiral symmetry form an "EFT space" and the real QCD holds a some region in the EFT space.

2.2 Matching in the Wilsonian Sense

In general, an EFT has many parameters like masses and coupling constants among hadrons. We can determine them by performing the matching between two Green's functions, Eqs. (2.6) and (2.7) at a scale.

In some matching schemes, the renormalized parameters of the EFT are determined from QCD. On the other hand, the matching in the Wilsonian sense is performed based on the following general idea:

Step 1 We imagine a some high-energy scale Λ which separates the perturbative (hard) region from the non-perturbative (soft) region [see Fig. 2.2]. Although the quarks and gluons are relevant degrees of freedom in the hard region, they are not relevant anymore in the soft region. Then we assume that one can replace the quarks and gluons with hadrons since "bare" quarks and gluons in the QCD Lagrangian become "dressed" ones by integrating out the high-energy quarks and gluons (i.e., the quarks and gluons above Λ), which eventually form hadrons.

Step 2 Under the above replacement of the degrees of freedom at Λ, we define the EFT at Λ as the *bare* EFT. Thus the generating functional derived from the bare EFT leads to

the same Green's function as that derived from Eq. (2.6) at Λ. The *bare* parameters of the EFT are determined after integrating out the quarks and gluons above Λ, and then carry information of the underlying QCD.

Once the bare theory is determined through the matching following the above steps, we can obtain the physical quantities in low-energy region within the EFT including quantum corrections, for instance, by using renormalization group equations (RGEs).

It is worthwhile mentioning the difference from the way to determine the renormalized parameters of the EFT through the matching to QCD. In this scheme, the theory at the matching scale Λ is *full quantum* (i.e., renormalized) theory which is achieved by starting over in low energies. While in the Wilsonian matching, one starts from the *bare* theory defined at Λ, and in order-by-order renormalizes quantum effects into the parameters to go down to low-energy scales. Both of them are almost equivalent in the case that Λ is much larger than a characteristic scale M of the EFT, e.g, energy, temperature and density. In this case, corrections $\mathcal{O}(M/\Lambda)$ are neglected and we can replace the bare parameter with the renormalized one at Λ and vice versa.

2.3 Application to Hot and/or Dense Matter

In this section, we apply the Wilsonian matching to the QCD in hot and/or dense matter. We first give an account of the general idea of the intrinsic temperature and/or density dependences of the bare parameters, which are inevitably introduced as a result performed the Wilsonian matching. We also discuss the effect of Lorentz symmetry violation at bare level.

In the following, we consider that one performs the Wilsonian matching of the EFT-B shown in Fig. 2.1 to perturbative QCD at finite temperature and/or density: In order to obtain the bare EFT-B, we integrate out high frequency modes in hot and/or dense matter. The hard modes integrated out are converted into the bare parameters and thus the temperature and/or density carried by them become temperature and/or density dependences of the bare parameters. We call the thermal and/or dense effects as *intrinsic* temperature and/or density dependences. They carry the information without (or behind) the EFT-B, i.e., the information of the underlying theory QCD. Ordinary hadronic thermal and/or dense effects are carried by the relevant degrees of freedom below Λ, π and ρ, which are generated by dynamics of the soft region. Thus in the Wilsonian matching, we can for convenience distinguish two kinds of temperature and/or density dependences:

Intrinsic temperature and/or density dependences : Carried by the relevant degrees of

freedom above Λ (hard region). Such degrees of freedom are integrated out in the EFT-B and contribute to bare parameters.

Hadronic temperature and/or density dependences : Carried by the relevant degrees of freedom below Λ (soft region). Such degrees of freedom interact to heat/particle bath and generate thermal and/or dense effects which appear in the Bose/Fermi distribution functions.

In the present case, the hard modes integrated out are all hadronic degrees of freedom except for π and ρ relevant below Λ. It should be noted that the intrinsic effects never appear in the bare parameters if one does not take into account these "residual" degrees of freedom. However, temperature and/or density of the system are provided by the hadronic matter formed by *all* hadronic degrees of freedom. The matter including only π andρ is not identical with the QCD matter. Thus we need to take into account "all the others" never incorporated in system within the EFT, which enable us to include the intrinsic effects.

Further, according to Step 1 mentioned in the previous section, we replace the hard modes with the quarks and gluons above Λ. The replacement indicates the following: The intrinsic temperature and/or density dependences are nothing but the signature that the hadron has an internal structure constructed from the quarks and gluons. This is similar to the situation where the coupling constants among hadrons are replaced with the momentum-dependent form factor in higher energy region since the hadronic picture becomes irrelevant. Thus the intrinsic thermal and/or dense effects play more important roles in the higher temperature region, especially near the phase transition point.

Intrinsic thermal/dense effects also cause Lorentz non-invariance in the bare theory: At finite temperature and/or density, theory has no longer the Lorentz invariance since we specify the rest frame of medium. The Lorentz non-invariance of hot and/or dense QCD is generated through the dynamics of quarks and gluons. Then the QCD Lagrangian takes the Lorentz invariant form. On the other hand, parameters of EFT have implicitly the information of the fundamental theory as the intrinsic effects. Thus the intrinsic temperature and/or density dependences carry the Lorentz non-invariance of hot/dense QCD, and eventually they cause the Lorentz symmetry breaking in the bare EFT.

Chapter 3

Hidden Local Symmetry Theory at Finite Temperature

The hidden local symmetry (HLS) theory [11, 12] is a natural extension of the non-linear chiral Lagrangian and it can describe a system including both pseudoscalars (pions) and vector mesons. In the present framework, the vector meson is introduced as the gauge boson of the HLS. We can introduce the vector mesons in other frameworks, e.g., matter field [41], massive Yang-Mills [42, 43, 44, 45, 46] and anti-symmetric tensor field [38, 47]. It was shown that these models are equivalent with the HLS theory at tree level [41, 48, 49, 50, 51, 52, 53]. However it is the most important advantage using the HLS theory that the systematic low-energy expansion can be performed.

In this chapter, we first briefly review the HLS and the chiral perturbation theory (ChPT) with HLS. (For details, see Ref. [13].) Next we apply the HLS theory to QCD at finite temperature following Refs. [14, 15, 16, 17, 18]. We present the predictions in the low temperature region: We show the temperature dependences of the vector meson mass and the pion parameters, and the validity of the vector dominance of the electromagnetic form factor of the pion.

3.1 Hidden Local Symmetry

The HLS theory [#1] is based on the $G_{\rm global} \times H_{\rm local}$ symmetry, where $G = SU(N_f)_L \times SU(N_f)_R$ is the chiral symmetry and $H = SU(N_f)_V$ is the HLS. The basic quantities are the HLS gauge

[#1] In the modern interpretation [54], implementing HLS in the chiral Lagrangian can be associated with the "ultraviolet completion" to the fundamental theory of strong interactions, i.e., QCD. The matching to QCD at a matching scale is therefore a crucial ingredient of the approach.

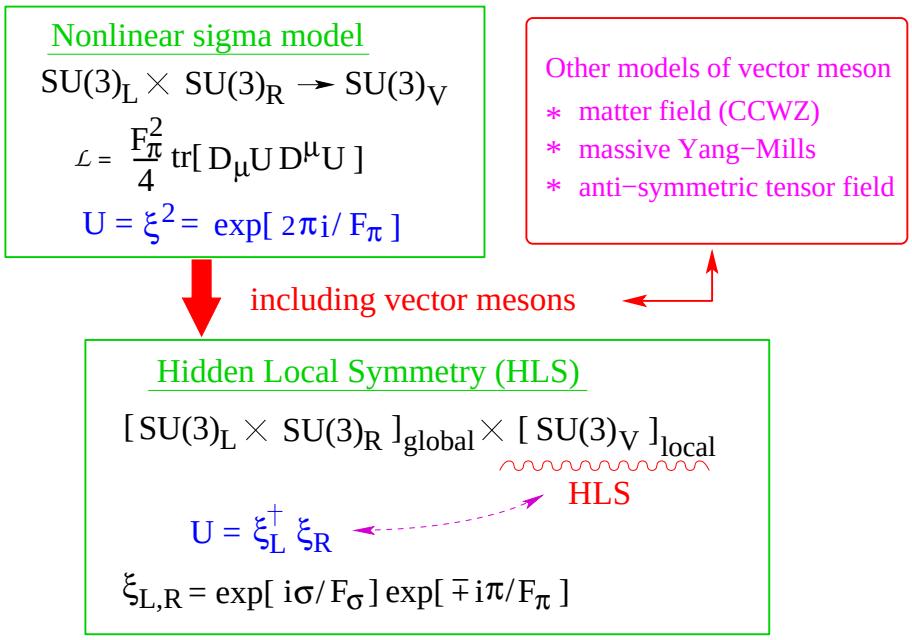

Figure 3.1: Non-linear chiral Lagrangian and the HLS theory.

boson and two matrix valued variables $\xi_L(x)$ and $\xi_R(x)$ which transform as

$$\xi_{L,R}(x) \to \xi'_{L,R}(x) = h(x)\xi_{L,R}(x)g^\dagger_{L,R} \ , \tag{3.1}$$

where $h(x) \in H_{\rm local}$ and $g_{L,R} \in [{\rm SU}(N_f)_{\rm L,R}]_{\rm global}$. These variables are parameterized as

$$\xi_{L,R}(x) = e^{i\sigma(x)/F_\sigma} e^{\mp i\pi(x)/F_\pi} \ , \tag{3.2}$$

where $\pi = \pi^a T_a$ denotes the pseudoscalar Nambu-Goldstone bosons associated with the spontaneous symmetry breaking of $G_{\rm global}$ chiral symmetry, and $\sigma = \sigma^a T_a$ denotes the Nambu-Goldstone bosons associated with the spontaneous breaking of $H_{\rm local}$ [#2]. This σ is absorbed into the HLS gauge boson through the Higgs mechanism. F_π and F_σ are the decay constants of the associated particles. The phenomenologically important parameter a is defined as

$$a = \frac{{F_\sigma}^2}{{F_\pi}^2} \ . \tag{3.3}$$

The covariant derivatives of $\xi_{L,R}$ are given by

$$\begin{aligned} D_\mu \xi_L &= \partial_\mu \xi_L - iV_\mu \xi_L + i\xi_L \mathcal{L}_\mu, \\ D_\mu \xi_R &= \partial_\mu \xi_R - iV_\mu \xi_R + i\xi_R \mathcal{R}_\mu, \end{aligned} \tag{3.4}$$

[#2]The σ is not to be confused with the scalar that figures in two-flavor linear sigma model.

where V_μ is the gauge field of $H_{\rm local}$, and $\mathcal{L}_\mu$ and $\mathcal{R}_\mu$ are the external gauge fields introduced by gauging $G_{\rm global}$ symmetry.

The basic quantities in constructing the Lagrangian are the following two 1-forms:

$$\begin{aligned}\hat{\alpha}_{\parallel\mu} &= \frac{1}{2i}\left(D_\mu\xi_{\rm R}\cdot\xi_{\rm R}^\dagger + D_\mu\xi_{\rm L}\cdot\xi_{\rm L}^\dagger\right) \ , \\ \hat{\alpha}_{\perp\mu} &= \frac{1}{2i}\left(D_\mu\xi_{\rm R}\cdot\xi_{\rm R}^\dagger - D_\mu\xi_{\rm L}\cdot\xi_{\rm L}^\dagger\right) \ . \end{aligned} \tag{3.5}$$

They transform as

$$\hat{\alpha}^\mu_{\perp,\parallel} \to h(x)\cdot\hat{\alpha}^\mu_{\perp,\parallel}\cdot h^\dagger(x) \ . \tag{3.6}$$

When HLS is gauge-fixed to the unitary gauge, $\sigma = 0$, $\xi_{\rm L}$ and $\xi_{\rm R}$ are related with each other by

$$\xi_{\rm L}^\dagger = \xi_{\rm R} \equiv \xi = e^{i\pi/F_\pi} \ . \tag{3.7}$$

This unitary gauge is not preserved under the $G_{\rm global}$ transformation, which in general has the following form

$$\begin{aligned} G_{\rm global} \ : \ \xi \ \to \ \xi' \ &= \ \xi\cdot g_{\rm R}^\dagger = g_{\rm L}\cdot\xi \\ &= \ \exp\left[i\sigma'(\pi,g_{\rm R},g_{\rm L})/F_\sigma\right]\exp\left[i\pi'/F_\pi\right] \\ &= \ \exp\left[i\pi'/F_\pi\right]\exp\left[-i\sigma'(\pi,g_{\rm R},g_{\rm L})/F_\sigma\right] \ . \end{aligned} \tag{3.8}$$

The unwanted factor $\exp\left[i\sigma'(\pi,g_{\rm R},g_{\rm L})/F_\sigma\right]$ can be eliminated if we simultaneously perform the $H_{\rm local}$ gauge transformation with

$$H_{\rm local} \ : \ h = \exp\left[i\sigma'(\pi,g_{\rm R},g_{\rm L})/F_\sigma\right] \equiv h(\pi,g_{\rm R},g_{\rm L}) \ . \tag{3.9}$$

Then the system has a global symmetry $G = SU(3)_{\rm L}\times SU(3)_{\rm R}$ under the following combined transformation:

$$G \ : \ \xi \ \to \ h(\pi,g_{\rm R},g_{\rm L})\cdot\xi\cdot g_{\rm R}^\dagger = g_{\rm L}\cdot\xi\cdot h(\pi,g_{\rm R},g_{\rm L}) \ . \tag{3.10}$$

Under this transformation the HLS gauge boson field V_μ in the unitary gauge transforms as

$$G \ : \ V_\mu \ \to \ h(\pi,g_{\rm R},g_{\rm L})\cdot V_\mu\cdot h^\dagger(\pi,g_{\rm R},g_{\rm L}) - i\partial h(\pi,g_{\rm R},g_{\rm L})\cdot h^\dagger(\pi,g_{\rm R},g_{\rm L}) \ , \tag{3.11}$$

which is nothing but the transformation property of Weinberg's "ρ meson" [55]. The two 1-forms $\hat{\alpha}^\mu_\parallel$ and $\hat{\alpha}^\mu_\perp$ transform as

$$\hat{\alpha}^\mu_{\perp,\parallel} \to h(\pi,g_{\rm R},g_{\rm L})\cdot\hat{\alpha}^\mu_{\perp,\parallel}\cdot h^\dagger(\pi,g_{\rm R},g_{\rm L}) \ . \tag{3.12}$$

Then, we can regard these 1-forms as the fields belonging to the chiral representations $(1,8)+(8,1)$ and $(1,8)-(8,1)$ under $SU(3)_{\rm L}\times SU(3)_{\rm R}$.

The HLS Lagrangian with lowest derivative terms at the chiral limit is given by [11, 12]

$$\mathcal{L}_{(2)} = {F_\pi}^2 {\rm tr}[\hat{\alpha}_{\perp\mu}\hat{\alpha}_\perp^\mu] + {F_\sigma}^2 {\rm tr}[\hat{\alpha}_{\parallel\mu}\hat{\alpha}_\parallel^\mu] - \frac{1}{2g^2}{\rm tr}[V_{\mu\nu}V^{\mu\nu}] \ , \tag{3.13}$$

where g is the HLS gauge coupling, $V_{\mu\nu}$ is the field strength of V_μ and

$$\begin{aligned} \hat{\alpha}_\perp^\mu &= \frac{1}{2i}[D^\mu\xi_R\cdot\xi_R^\dagger - D^\mu\xi_L\cdot\xi_L^\dagger] \ , \\ \hat{\alpha}_\parallel^\mu &= \frac{1}{2i}[D^\mu\xi_R\cdot\xi_R^\dagger + D^\mu\xi_L\cdot\xi_L^\dagger] \ . \end{aligned} \tag{3.14}$$

We expand the Lagrangian (3.13) in terms of the π field taking the unitary gauge of the HLS ($\sigma=0$) to obtain

$$\begin{aligned} \mathcal{L}_{(2)} &= {\rm tr}\left[\partial_\mu\pi\partial^\mu\pi\right] + ag^2F_\pi^2\,{\rm tr}\left[\rho_\mu\rho^\mu\right] + 2i\left(\frac{1}{2}ag\right)\,{\rm tr}\left[\rho^\mu\left[\partial_\mu\pi\,,\,\pi\right]\right] \\ &\quad - 2\left(agF_\pi^2\right)\,{\rm tr}\left[\rho_\mu\mathcal{V}^\mu\right] + 2i\left(1-\frac{a}{2}\right){\rm tr}\left[\mathcal{V}^\mu\left[\partial_\mu\pi\,,\,\pi\right]\right] + \cdots \ , \end{aligned} \tag{3.15}$$

where the vector meson field ρ_μ is introduced by

$$V_\mu = g\rho_\mu \ , \tag{3.16}$$

and vector external gauge field $\mathcal{V}_\mu$ is defined as [#3]

$$\mathcal{V}_\mu \equiv \frac{1}{2}\left(\mathcal{R}_\mu + \mathcal{L}_\mu\right) \ . \tag{3.17}$$

From the expansion in Eq. (3.15) we find the following expressions for the mass of vector meson M_ρ, the $\rho\pi\pi$ coupling $g_{\rho\pi\pi}$, the ρ-γ mixing strength g_ρ and the direct $\gamma\pi\pi$ coupling $g_{\gamma\pi\pi}$:

$$\begin{aligned} {M_\rho}^2 &= ag^2{F_\pi}^2, & (3.18)\\ g_{\rho\pi\pi} &= \frac{1}{2}ag, & (3.19)\\ g_\rho &= ag{F_\pi}^2, & (3.20)\\ g_{\gamma\pi\pi} &= e(1-\frac{1}{2}a). & (3.21) \end{aligned}$$

By taking the parameter choice $a=2$ at tree level, the HLS reproduces the following phenomenological facts [11]:

[#3] Note that the photon field A_μ for $N_f=3$ is embedded into $\mathcal{V}_\mu$ as

$$\mathcal{V}_\mu = eA_\mu Q, \quad Q = \begin{pmatrix} 2/3 & & \\ & -1/3 & \\ & & -1/3 \end{pmatrix} \ ,$$

with e being the electromagnetic coupling constant.

1. $g_{\rho\pi\pi} = g$ (universality of the ρ coupling) [56];
2. ${M_\rho}^2 = 2g_{\rho\pi\pi}^2 {F_\pi}^2$ (the KSRF relation, version II) [57];
3. $g_{\gamma\pi\pi} = 0$ (vector dominance of the electromagnetic form factor of the pion) [56].

Moreover, the KSRF relation (version I) [57] is predicted as a low-energy theorem of the HLS [58]:

$$g_\rho = 2{F_\pi}^2 g_{\rho\pi\pi}, \tag{3.22}$$

which is independent of the parameter a. This relation was first proved at tree level [59] and at one-loop level [60] and then at any loop order [61].

Chiral perturbation theory with HLS

In the HLS theory it is possible to perform the derivative expansion systematically owing to the gauge invariance [13, 62, 63]. In this ChPT with HLS the vector meson mass is considered as small compared with the chiral symmetry breaking scale Λ_χ, by assigning $\mathcal{O}(p)$ to the HLS gauge coupling [62, 63]:

$$g \sim \mathcal{O}(p). \tag{3.23}$$

According to the entire list shown in Ref. [63], there are 35 counter terms at $\mathcal{O}(p^4)$ for general N_f. However, only three terms are relevant when we consider two-point functions at chiral limit:

$$\mathcal{L}_{(4)} = z_1 \mathrm{tr}[\hat{\mathcal{V}}_{\mu\nu}\hat{\mathcal{V}}^{\mu\nu}] + z_2 \mathrm{tr}[\hat{\mathcal{A}}_{\mu\nu}\hat{\mathcal{A}}^{\mu\nu}] + z_3 \mathrm{tr}[\hat{\mathcal{V}}_{\mu\nu}V^{\mu\nu}], \tag{3.24}$$

where

$$\hat{\mathcal{A}}_{\mu\nu} = \frac{1}{2}[\xi_R \mathcal{R}_{\mu\nu}\xi_R^\dagger - \xi_L \mathcal{L}_{\mu\nu}\xi_L^\dagger] \ , \tag{3.25}$$

$$\hat{\mathcal{V}}_{\mu\nu} = \frac{1}{2}[\xi_R \mathcal{R}_{\mu\nu}\xi_R^\dagger + \xi_L \mathcal{L}_{\mu\nu}\xi_L^\dagger] \ , \tag{3.26}$$

with $\mathcal{R}_{\mu\nu}$ and $\mathcal{L}_{\mu\nu}$ being the field strengths of $\mathcal{R}_\mu$ and $\mathcal{L}_\mu$.

There is a limit that the vector meson mass is small, in large N_f QCD as shown in Ref. [13]. Then it can be justified to perform the derivative expansion by m_ρ^2/Λ_χ^2 under such an extreme condition. We obtain physical quantities in the real world with $N_f = 2$ or 3 by extrapolating the results in large N_f. Numerically the expansion parameter is not very small, $m_\rho^2/\Lambda_\chi^2 \sim 0.5$. However, the Wilsonian matching at $T = 0$ with $N_f = 3$, through which the parameters of the HLS Lagrangian are determined by the underlying QCD at the matching scale Λ (see chapter 4), was shown to give several predictions in remarkable agreement with experiments

[64, 13], where the validity of the ChPT with HLS is essential. This strongly suggests that the extrapolation mentioned above is valid even numerically.

As discussed in Ref. [13], $\Lambda \ll \Lambda_\chi$ can be justified in the N_c limit of QCD [#4]: In this limit, $F_\pi^2(\Lambda)$ scales as N_c, which implies that Λ_χ becomes large in the large N_c limit. On the other hand, the meson masses do not scale with N_c, so that we can introduce the Λ which has no large N_c scaling property. Thus the quadratic divergent at n-th loop order is suppressed by $[\Lambda^2/\Lambda_\chi^2]^n \sim [1/N_c]^n$. As a result, we can perform the loop expansion with quadratic divergences in the large N_c limit, and extrapolate the results to the real QCD with $N_c = 3$.

In the following, we will apply the ChPT with HLS combined with the Wilsonian matching to finite temperature. There the expansion parameter is $T/F_\pi(\Lambda)$ instead of $T/F_\pi(0)$ used in the standard ChPT. Since $F_\pi(\Lambda) > F_\pi(0)$, the present formalism can be applied in the higher temperature region than the standard ChPT.

3.2 Two-Point Functions in Background Field Gauge

In the present approach hadronic thermal effects are included by calculating pseudoscalar and vector meson loop contributions. In this section we show details of the calculation of the hadronic thermal corrections as well as the quantum corrections to the two-point functions in the background field gauge.

3.2.1 Background field gauge

In this subsection we briefly review the background field gauge following Ref. [63, 64, 13]. We introduce the background fields $\overline{\xi}_{L,R}$ as

$$\xi_{L,R} = \check{\xi}_{L,R}\overline{\xi}_{L,R}, \tag{3.27}$$

where $\check{\xi}_{L,R}$ are the quantum fields. It is convenient to write

$$\begin{aligned} \check{\xi}_{\rm L} = \check{\xi}_{\rm S}\cdot\check{\xi}_{\rm P}^\dagger\ , \qquad \check{\xi}_{\rm R} = \check{\xi}_{\rm S}\cdot\check{\xi}_{\rm P}\ , \\ \check{\xi}_{\rm P} = \exp\left[i\,\check{\pi}^a T_a/F_\pi\right]\ , \quad \check{\xi}_{\rm S} = \exp\left[i\,\check{\sigma}^a T_a/F_\sigma\right]\ , \end{aligned} \tag{3.28}$$

with $\check{\pi}$ and $\check{\sigma}$ being the quantum fields corresponding to the pseudoscalar NG boson π and the would-be NG boson σ. The background gauge field $\overline{V}_\mu$ for the HLS gauge boson is introduced as

$$V_\mu = \overline{V}_\mu + g\check{\rho}_\mu, \tag{3.29}$$

[#4] We consider that the scale at which the HLS theory breaks down is the same order as Λ_χ since the chiral symmetry is non-linearly realized.

where $\check{\rho}_\mu$ is the quantum field. It is convenient to introduce the following fields corresponding to $\hat{\alpha}_{\perp\mu}$ and $\hat{\alpha}_{\parallel\mu} + V_\mu$:

$$\begin{aligned}
\overline{\mathcal{A}}_\mu &= \frac{1}{2i}[\partial_\mu \overline{\xi}_R \cdot \overline{\xi}_R^\dagger - \partial_\mu \overline{\xi}_L \cdot \overline{\xi}_L^\dagger] + \frac{1}{2}[\overline{\xi}_R \mathcal{R}_\mu \overline{\xi}_R^\dagger - \overline{\xi}_L \mathcal{L}_\mu \overline{\xi}_L^\dagger] \ , \\
\overline{\mathcal{V}}_\mu &= \frac{1}{2i}[\partial_\mu \overline{\xi}_R \cdot \overline{\xi}_R^\dagger + \partial_\mu \overline{\xi}_L \cdot \overline{\xi}_L^\dagger] + \frac{1}{2}[\overline{\xi}_R \mathcal{R}_\mu \overline{\xi}_R^\dagger + \overline{\xi}_L \mathcal{L}_\mu \overline{\xi}_L^\dagger] \ .
\end{aligned} \tag{3.30}$$

The field strengths of $\overline{\mathcal{A}}_\mu$ and $\overline{\mathcal{V}}_\mu$ are defined as

$$\begin{aligned}
\overline{\mathcal{A}}_{\mu\nu} &= \partial_\mu \overline{\mathcal{A}}_\nu - \partial_\nu \overline{\mathcal{A}}_\mu - i\Big[\overline{\mathcal{V}}_\mu, \overline{\mathcal{A}}_\nu\Big] - i\Big[\overline{\mathcal{A}}_\mu, \overline{\mathcal{V}}_\nu\Big] \ , \\
\overline{\mathcal{V}}_{\mu\nu} &= \partial_\mu \overline{\mathcal{V}}_\nu - \partial_\nu \overline{\mathcal{V}}_\mu - i\Big[\overline{\mathcal{V}}_\mu, \overline{\mathcal{V}}_\nu\Big] - i\Big[\overline{\mathcal{A}}_\mu, \overline{\mathcal{A}}_\nu\Big] \ .
\end{aligned} \tag{3.31}$$

Note that both $\overline{\mathcal{A}}_{\mu\nu}$ and $\overline{\mathcal{V}}_{\mu\nu}$ do not include any derivatives of the background fields $\overline{\xi}_{\rm R}$ and $\overline{\xi}_{\rm L}$:

$$\begin{aligned}
\overline{\mathcal{V}}_{\mu\nu} &= \frac{1}{2}\left[\overline{\xi}_{\rm R} \mathcal{R}_{\mu\nu} \overline{\xi}_{\rm R}^\dagger + \overline{\xi}_{\rm L} \mathcal{L}_{\mu\nu} \overline{\xi}_{\rm L}^\dagger\right] \ , \\
\overline{\mathcal{A}}_{\mu\nu} &= \frac{1}{2}\left[\overline{\xi}_{\rm R} \mathcal{R}_{\mu\nu} \overline{\xi}_{\rm R}^\dagger - \overline{\xi}_{\rm L} \mathcal{L}_{\mu\nu} \overline{\xi}_{\rm L}^\dagger\right] \ .
\end{aligned} \tag{3.32}$$

Then $\overline{\mathcal{A}}_{\mu\nu}$ and $\overline{\mathcal{V}}_{\mu\nu}$ correspond to $\hat{A}_{\mu\nu}$ and $\hat{V}_{\mu\nu}$ in Eqs. (3.25) and (3.26), respectively.

In the background field gauge the quantum fields as well as the background fields $\overline{\xi}_{\rm R,L}$ transform homogeneously under the background gauge transformation, while the background gauge field $\overline{V}_\mu$ transforms inhomogeneously:

$$\begin{aligned}
\overline{\xi}_{\rm R,L} &\to h(x) \cdot \overline{\xi}_{\rm R,L} \cdot g_{\rm R,L}^\dagger \ , \\
\overline{V}_\mu &\to h(x) \cdot \overline{V}_\mu \cdot h^\dagger(x) + i h(x) \cdot \partial_\mu h^\dagger(x) \ , \\
\check{\xi}_{\rm L,R} &\to h(x) \cdot \check{\xi}_{\rm L,R} \cdot h^\dagger(x) \ , \\
\check{\pi} &\to h(x) \cdot \check{\pi} \cdot h^\dagger(x) \ , \\
\check{\sigma} &\to h(x) \cdot \check{\sigma} \cdot h^\dagger(x) \ , \\
\check{\rho}_\mu &\to h(x) \cdot \check{\rho}_\mu \cdot h^\dagger(x) \ .
\end{aligned} \tag{3.33}$$

Then the expansion of the Lagrangian in terms of the quantum field manifestly keeps the HLS of the background field $\overline{V}_\mu$ [63] and thus the gauge invariance of the result is manifest. We fix the background field gauge in 't Hooft-Feynman gauge as [63]

$$\mathcal{L}_{\rm GF} = -{\rm tr}\Big[(\overline{D}^\mu \check{\rho}_\mu + g F_\sigma \check{\sigma})^2\Big], \tag{3.34}$$

where $\overline{D}^\mu$ denotes the covariant derivative with respect to the background fields:

$$\overline{D}^\mu \check{\rho}_\nu = \partial^\mu \check{\rho}_\nu - i[\overline{V}^\mu, \check{\rho}_\nu]. \tag{3.35}$$

The FP ghost associated with $\mathcal{L}_{GF}$ is given by [63]

$$\mathcal{L}_{\rm FP} = 2i\,{\rm tr}\Big[\overline{C}(\overline{D}^\mu\overline{D}_\mu + (gF_\sigma)^2)C\Big] + \cdots \ , \tag{3.36}$$

where ellipses stand for the terms including at least three quantum fields.

Now the $\mathcal{O}(p^2)$ Lagrangian, $\mathcal{L}_{(2)} + \mathcal{L}_{\rm GF} + \mathcal{L}_{\rm FP}$, is expanded in terms of the quantum fields, $\check{\pi}$, $\check{\sigma}$, $\check{\rho}$, C and $\overline{C}$. The terms which do not include the quantum fields are nothing but the original $\mathcal{O}(p^2)$ Lagrangian with the fields replaced by the corresponding background fields. The terms which are of first order in the quantum fields lead to the equations of motions for the background fields: [64, 13]

$$\overline{D}_\mu\overline{\mathcal{A}}^\mu = -i\,(a-1)\left[\overline{\mathcal{V}}_\mu - \overline{V}_\mu\,,\,\overline{\mathcal{A}}^\mu\right] + \mathcal{O}(p^4)\ , \tag{3.37}$$

$$\overline{D}_\mu\left(\overline{\mathcal{V}}^\mu - \overline{V}^\mu\right) = \mathcal{O}(p^4)\ , \tag{3.38}$$

$$\overline{D}_\nu\overline{V}^{\nu\mu} = g^2F_\sigma^2\left(\overline{\mathcal{V}}^\mu - \overline{V}^\mu\right) + \mathcal{O}(p^4)\ . \tag{3.39}$$

The quantum correction as well as the hadronic thermal corrections are calculated from the terms of quadratic order in the quantum fields. The explicit forms of the terms as well as the Feynman rules obtained from them are shown in Ref. [13].

3.2.2 Two-point functions at $T = 0$

In this subsection, we calculate the quantum corrections from pseudoscalar and vector mesons to the two-point functions of $\overline{\mathcal{A}}_\mu$, $\overline{\mathcal{V}}_\mu$ and $\overline{V}_\mu$ at zero temperature. In the present analysis, as was done in Ref. [15] (see also subsection 4.2), we neglect possible Lorenz symmetry violating effects caused by the intrinsic temperature dependences of the bare parameters, and use the bare HLS Lagrangian with Lorenz invariance even at non-zero temperature. Then the results obtained in this subsection are identified with the quantum corrections from pseudoscalar and vector mesons at non-zero temperature by taking the intrinsic temperature dependences of the parameters into account. [#5] In the following, we write the two-point functions of $\overline{\mathcal{A}}_\mu$-$\overline{\mathcal{A}}_\nu$, $\overline{\mathcal{V}}_\mu$-$\overline{\mathcal{V}}_\nu$, $\overline{V}_\mu$-$\overline{V}_\nu$ and $\overline{V}_\mu$-$\overline{\mathcal{V}}_\nu$ as $\Pi_\perp^{\mu\nu}$, $\Pi_\parallel^{\mu\nu}$, $\Pi_V^{\mu\nu}$ and $\Pi_{V\parallel}^{\mu\nu}$, respectively.

In the present analysis, it is important to include the quadratic divergences to obtain the RGEs in the Wilsonian sense. Here, following Ref. [65, 64, 13], we adopt the dimensional regularization and identify the quadratic divergences with the presence of poles of ultraviolet origin at $n = 2$ [66]. This can be done by the following replacement in the Feynman integrals:

$$\int\frac{d^nk}{i(2\pi)^n}\frac{1}{-k^2} \to \frac{\Lambda^2}{(4\pi)^2}\ , \qquad \int\frac{d^nk}{i(2\pi)^n}\frac{k_\mu k_\nu}{[-k^2]^2} \to -\frac{\Lambda^2}{2(4\pi)^2}g_{\mu\nu}\ . \tag{3.40}$$

[#5] See next subsection for dividing the quantum corrections from the hadronic thermal corrections.

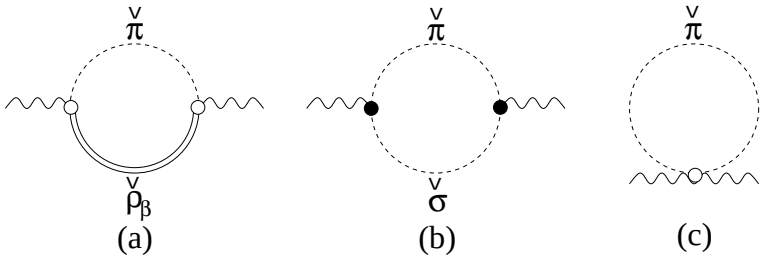

Figure 3.2: Diagrams for contributions to $\Pi_\perp^{\mu\nu}$ at one-loop level. The circle ($\circ$) denotes the momentum-independent vertex and the dot ($\bullet$) denotes the momentum-dependent vertex.

On the other hand, the logarithmic divergence is identified with the pole at $n = 4$:

$$\frac{1}{\bar{\epsilon}} + 1 \to \ln \Lambda^2 \ , \tag{3.41}$$

where

$$\frac{1}{\bar{\epsilon}} \equiv \frac{2}{4-n} - \gamma_E + \ln(4\pi) \ , \tag{3.42}$$

with γ_E being the Euler constant.

Let us start from the one-loop corrections to the two-point function of $\overline{\mathcal{A}}_\mu$-$\overline{\mathcal{A}}_\nu$ denoted by $\Pi_\perp^{\mu\nu}$. We show the diagrams for contributions to $\Pi_\perp^{\mu\nu}$ at one-loop level in Fig. 3.2. We obtain these contributions as [#6]

$$\Pi_\perp^{(a)\mu\nu}(p) = -N_f a {M_\rho}^2 g^{\mu\nu} B_0^{(\mathrm{vac})}(p; M_\rho, 0) \ , \tag{3.43}$$

$$\Pi_\perp^{(b)\mu\nu}(p) = N_f \frac{a}{4} B^{(\mathrm{vac})\mu\nu}(p; M_\rho, 0) \ , \tag{3.44}$$

$$\Pi_\perp^{(c)\mu\nu}(p) = N_f (a-1) g^{\mu\nu} A_0^{(\mathrm{vac})}(0) \ , \tag{3.45}$$

where the functions $B_0^{(\mathrm{vac})}$, $B^{(\mathrm{vac})\mu\nu}$ and $A_0^{(\mathrm{vac})}$ are defined by the following integrals [13]:

$$A_0^{(\mathrm{vac})}(M) = \int \frac{d^n k}{i(2\pi)^4} \frac{1}{M^2 - k^2} \ , \tag{3.46}$$

$$B_0^{(\mathrm{vac})}(p; M_1, M_2) = \int \frac{d^n k}{i(2\pi)^4} \frac{1}{[M_1^2 - k^2][M_2^2 - (k-p)^2]} \ , \tag{3.47}$$

$$B^{(\mathrm{vac})\mu\nu}(p; M_1, M_2) = \int \frac{d^n k}{i(2\pi)^4} \frac{(2k-p)^\mu (2k-p)^\nu}{[M_1^2 - k^2][M_2^2 - (k-p)^2]} \ . \tag{3.48}$$

Next we calculate the one-loop corrections to the $\overline{\mathcal{V}}_\mu$-$\overline{\mathcal{V}}_\nu$ two-point function denoted by $\Pi_\parallel^{\mu\nu}$. We show the diagrams for contributions to $\Pi_\parallel^{\mu\nu}$ at one-loop level in Fig. 3.3. We obtain

[#6] Here we put the superscript (vac) in the functions in the right-hand-side to distinguish them from the functions expressing the hadronic thermal corrections [see next subsection].

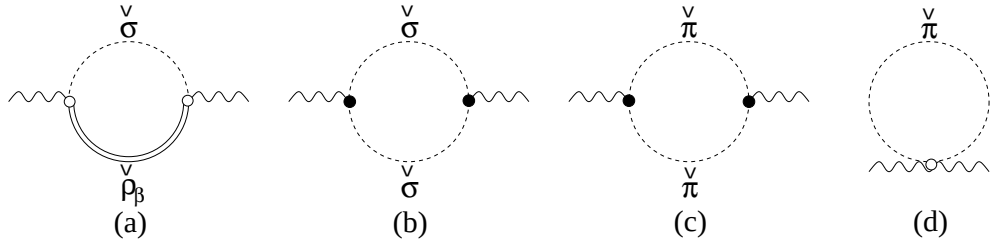

Figure 3.3: Diagrams for contributions to $\Pi_{\parallel}^{\mu\nu}$ at one-loop level.

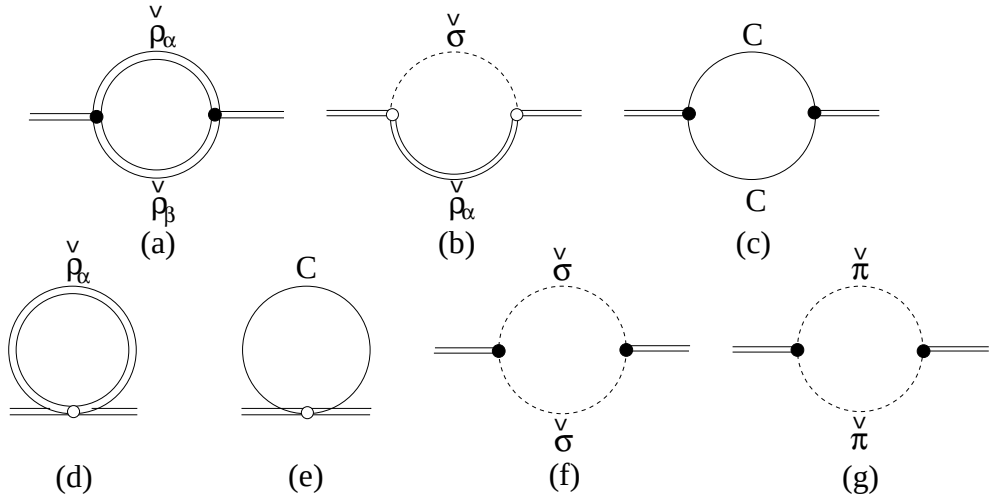

Figure 3.4: Diagrams for contributions to $\Pi_{V}^{\mu\nu}$ at one-loop level.

these contributions as

$$\Pi_{\parallel}^{(a)\mu\nu}(p) = -N_f {M_\rho}^2 g^{\mu\nu} B_0^{(\mathrm{vac})}(p; M_\rho, M_\rho), \tag{3.49}$$

$$\Pi_{\parallel}^{(b)\mu\nu}(p) = \frac{1}{8} N_f B^{(\mathrm{vac})\mu\nu}(p; M_\rho, M_\rho), \tag{3.50}$$

$$\Pi_{\parallel}^{(c)\mu\nu}(p) = \frac{(2-a)^2}{8} N_f B^{(\mathrm{vac})\mu\nu}(p; 0, 0), \tag{3.51}$$

$$\Pi_{\parallel}^{(d)\mu\nu}(p) = -(a-1) N_f g^{\mu\nu} A_0^{(\mathrm{vac})}(0). \tag{3.52}$$

The one-loop corrections to $\Pi_V^{\mu\nu}$, the diagrams for contributions to which are shown in Fig. 3.4, are evaluated as

$$\Pi_V^{(a)\mu\nu}(p) = \frac{n}{2} N_f B^{(\mathrm{vac})\mu\nu}(p; M_\rho, M_\rho) + 4N_f (g^{\mu\nu} p^2 - p^\mu p^\nu) B_0^{(\mathrm{vac})}(p; M_\rho, M_\rho), \tag{3.53}$$

$$\Pi_V^{(b)\mu\nu}(p) = -N_f {M_\rho}^2 g^{\mu\nu} B_0^{(\mathrm{vac})}(p; M_\rho, M_\rho), \tag{3.54}$$

$$\Pi_V^{(c)\mu\nu}(p) = -N_f B^{(\mathrm{vac})\mu\nu}(p; M_\rho, M_\rho), \tag{3.55}$$

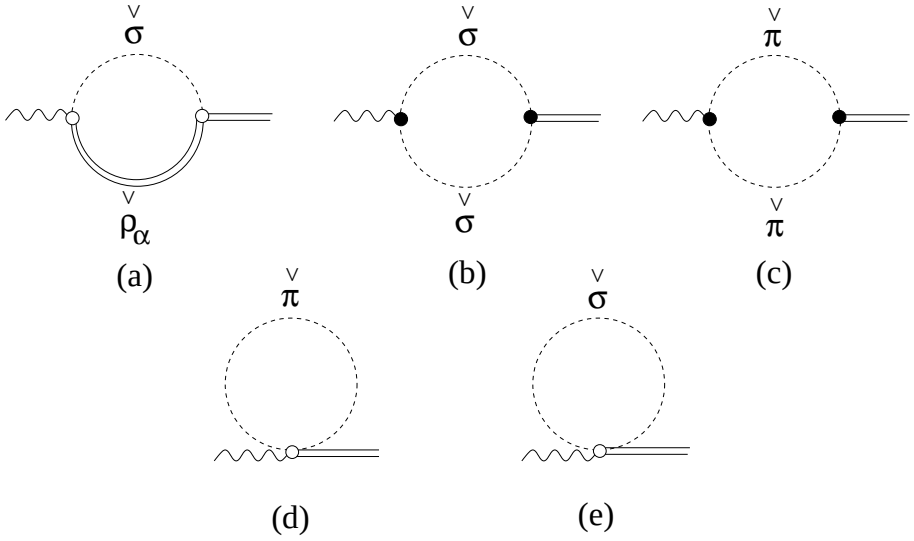

Figure 3.5: Diagrams for contributions to $\Pi_{V\parallel}^{\mu\nu}$ at one-loop level.

$$\Pi_V^{(d)\mu\nu}(p) = nN_f g^{\mu\nu} A_0^{(\mathrm{vac})}(M_\rho), \tag{3.56}$$
$$\Pi_V^{(e)\mu\nu}(p) = -2N_f g^{\mu\nu} A_0^{(\mathrm{vac})}(M_\rho), \tag{3.57}$$
$$\Pi_V^{(f)\mu\nu}(p) = \frac{1}{8} N_f B^{(\mathrm{vac})\mu\nu}(p; M_\rho, M_\rho), \tag{3.58}$$
$$\Pi_V^{(g)\mu\nu}(p) = \frac{a^2}{8} N_f B^{(\mathrm{vac})\mu\nu}(p; 0, 0), \tag{3.59}$$

where n denotes the dimension of the spacetime.

We also show the one-loop diagrams for contributions to $\Pi_{V\parallel}^{\mu\nu}$ in Fig. 3.5. These are given by

$$\Pi_{V\parallel}^{(a)\mu\nu}(p) = N_f M_\rho^2 g^{\mu\nu} B_0^{(\mathrm{vac})}(p; M_\rho, M_\rho), \tag{3.60}$$
$$\Pi_{V\parallel}^{(b)\mu\nu}(p) = \frac{1}{8} N_f B^{(\mathrm{vac})\mu\nu}(p; M_\rho, M_\rho), \tag{3.61}$$
$$\Pi_{V\parallel}^{(c)\mu\nu}(p) = \frac{a(2-a)}{8} N_f B^{(\mathrm{vac})\mu\nu}(p; 0, 0), \tag{3.62}$$
$$\Pi_{V\parallel}^{(d)\mu\nu}(p) = \frac{a}{2} N_f g^{\mu\nu} A_0^{(\mathrm{vac})}(0), \tag{3.63}$$
$$\Pi_{V\parallel}^{(e)\mu\nu}(p) = \frac{1}{2} N_f g^{\mu\nu} A_0^{(\mathrm{vac})}(M_\rho). \tag{3.64}$$

At tree level the two-point functions of $\overline{\mathcal{A}}_\mu$, $\overline{\mathcal{V}}_\mu$ and $\overline{V}_\mu$ are

$$\Pi_\perp^{(\mathrm{tree})\mu\nu}(p) = F_{\pi,\mathrm{bare}}^2 g^{\mu\nu} + 2z_{2,\mathrm{bare}}(p^2 g^{\mu\nu} - p^\mu p^\nu) \ ,$$
$$\Pi_\parallel^{(\mathrm{tree})\mu\nu}(p) = F_{\sigma,\mathrm{bare}}^2 g^{\mu\nu} + 2z_{1,\mathrm{bare}}(p^2 g^{\mu\nu} - p^\mu p^\nu) \ ,$$

$$\begin{aligned}\Pi_V^{(\mathrm{tree})\mu\nu}(p) &= F_{\sigma,\mathrm{bare}}^2 g^{\mu\nu} - \frac{1}{g_{\mathrm{bare}}^2}(p^2 g^{\mu\nu} - p^\mu p^\nu) \ , \\ \Pi_{V\parallel}^{(\mathrm{tree})\mu\nu}(p) &= -F_{\sigma,\mathrm{bare}}^2 g^{\mu\nu} + z_{3,\mathrm{bare}}(p^2 g^{\mu\nu} - p^\mu p^\nu) \ . \end{aligned} \tag{3.65}$$

Thus the one-loop contributions to $\Pi_\perp^{\mu\nu}$ give the quantum corrections to F_π^2 and z_2. Similarly, each of the one-loop contributions to $\Pi_\parallel^{\mu\nu}$, $\Pi_V^{\mu\nu}$ and $\Pi_{V\parallel}^{\mu\nu}$ includes the quantum corrections to two parameters shown above. For distinguishing the quantum corrections to two parameters included in the two-point function, it is convenient to decompose each two-point function as

$$\Pi^{\mu\nu}(p) = \Pi^S(p) g^{\mu\nu} + \Pi^{LT}(p)(g^{\mu\nu}p^2 - p^\mu p^\nu). \tag{3.66}$$

Using the above decomposition, we identify $\Pi_\perp^{S(\text{1-loop})}(p^2)$ with the quantum correction to F_π^2, $\Pi_\perp^{LT(\text{1-loop})}(p^2)$ with that to z_2, and so on. It should be noticed that the following relation is satisfied [64, 13]:

$$\Pi_V^S(p^2) = \Pi_\parallel^S(p^2) = -\Pi_{V\parallel}^S(p^2) \ . \tag{3.67}$$

Then the quantum correction to F_σ^2 can be extracted from any of $\Pi_\parallel^{\mu\nu}$, $\Pi_V^{\mu\nu}$ and $\Pi_{V\parallel}^{\mu\nu}$. The divergent contributions coming from the diagrams shown in Figs. 3.2-3.5 are listed in Refs. [64, 13]. We list them in Appendix C for convenience.

3.2.3 Two-point functions at $T \neq 0$

Let us consider the loop corrections to the two-point functions at non-zero temperature. For this purpose it is convenient to introduce the following functions:

$$A_0(M^2;T) \equiv T\sum_{n=-\infty}^{\infty}\int\frac{d^3k}{(2\pi)^3}\frac{1}{M^2-k^2} \ , \tag{3.68}$$

$$B_0(p_0,\bar{p};M_1,M_2;T) \equiv T\sum_{n=-\infty}^{\infty}\int\frac{d^3k}{(2\pi)^3}\frac{1}{[M_1^2-k^2][M_2^2-(k-p)^2]} \ , \tag{3.69}$$

$$B^{\mu\nu}(p_0,\bar{p};M_1,M_2;T) \equiv T\sum_{n=-\infty}^{\infty}\int\frac{d^3k}{(2\pi)^3}\frac{(2k-p)^\mu(2k-p)^\nu}{[M_1^2-k^2][M_2^2-(k-p)^2]} \ , \tag{3.70}$$

where $\bar{p} = |\vec{p}|$ and the 0th component of the loop momentum is taken as $k^0 = i2n\pi T$, while that of the external momentum is taken as $p^0 = i2n'\pi T$ [n, n': integer]. Using the standard formula (see, e.g., Ref. [67]), these functions are divided into two parts as

$$A_0(M;T) = A_0^{(\mathrm{vac})}(M) + \bar{A}_0(M;T) \ , \tag{3.71}$$

$$B_0(p_0,\bar{p};M_1,M_2;T) = B_0^{(\mathrm{vac})}(p;M_1,M_2) + \bar{B}_0(p_0,\bar{p};M_1,M_2;T) \ , \tag{3.72}$$

$$B^{\mu\nu}(p_0,\bar{p};M_1,M_2;T) = B^{(\mathrm{vac})\mu\nu}(p;M_1,M_2) + \bar{B}^{\mu\nu}(p_0,\bar{p};M_1,M_2;T) \ , \tag{3.73}$$

where $A_0^{(\rm vac)}$, $B_0^{(\rm vac)}$ and $B^{(\rm vac)\mu\nu}$ express the quantum corrections given in Eqs. (3.46)–(3.48), and $\bar{A}_0$, $\bar{B}_0$ and $\bar{B}^{\mu\nu}$ the hadronic thermal corrections. We summarize the explicit forms of the functions $\bar{A}_0$, $\bar{B}_0$ and $\bar{B}^{\mu\nu}$ in various limits relevant to the present analysis in Appendix B. Note that the 0th component of the momentum p_0 in the right-hand-sides of the above expressions is analytically continued to the Minkowsky variable: p_0 is understood as $p_0 + i\epsilon$ ($\epsilon \to +0$) for the retarded function and $p_0 - i\epsilon$ for the advanced function. Then, $A_0^{(\rm vac)}$, $B_0^{(\rm vac)}$ and $B^{(\rm vac)\mu\nu}$ have no explicit temperature dependence, while they have intrinsic temperature dependence which is introduced through the Wilsonian matching as we will see later.

Now, the contributions to the two-point functions at non-zero temperature are obtained by replacing, in the expressions listed in the previous subsection, the functions $A_0^{(\rm vac)}$, $B_0^{(\rm vac)}$ and $B^{(\rm vac)\mu\nu}$ defined in Eqs. (3.46)–(3.48) with A_0, B_0 and $B^{\mu\nu}$ defined in Eqs. (3.68)–(3.70).

At non-zero temperature there are four independent polarization tensors, which we choose as defined in Appendix A. We decompose the two-point functions $\Pi_\perp^{\mu\nu}$, $\Pi_V^{\mu\nu}$ $\Pi_{V\parallel}^{\mu\nu}$ and $\Pi_\parallel^{\mu\nu}$ as

$$\Pi^{\mu\nu} = u^\mu u^\nu \Pi^t + (g^{\mu\nu} - u^\mu u^\nu)\Pi^s + P_L^{\mu\nu}\Pi^L + P_T^{\mu\nu}\Pi^T \ , \tag{3.74}$$

where $u^\mu = (1, \vec{0})$ and $P_L^{\mu\nu}$ and $P_T^{\mu\nu}$ are defined in Eq. (A.1). Similarly, we decompose the function $B^{\mu\nu}$ as

$$B^{\mu\nu} = u^\mu u^\nu B^t + (g^{\mu\nu} - u^\mu u^\nu)B^s + P_L^{\mu\nu}B^L + P_T^{\mu\nu}B^T \ . \tag{3.75}$$

Furthermore, similarly to the division of the functions into one part for expressing the quantum correction and another for the hadronic thermal correction done in Eqs. (3.71)–(3.73), we divide the two-point functions into two parts as

$$\Pi^{\mu\nu}(p_0, \bar{p}; T) = \Pi^{(\rm vac)\mu\nu}(p_0, \bar{p}) + \overline{\Pi}^{\mu\nu}(p_0, \bar{p}; T) \ . \tag{3.76}$$

Accordingly each of four components of the two-point functions defined in Eqs. (3.74) is divided into the one part for the quantum correction and another for the hadronic thermal correction. We note that all the divergences are included in zero temperature part $\Pi^{(\rm vac)}$.

From the contributions in Eqs. (3.43)-(3.45), the temperature dependent parts are obtained as

$$\begin{aligned}
\overline{\Pi}_\perp^t(p_0, \bar{p}; T) &= -N_f a M_\rho^2 \overline{B}_0(p_0, \bar{p}; M_\rho, 0; T) + N_f \frac{a}{4}\overline{B}^t(p_0, \bar{p}; M_\rho, 0; T) \\
&\quad + N_f(a-1)\overline{A}_0(0; T), \qquad (3.77) \\
\overline{\Pi}_\perp^s(p_0, \bar{p}; T) &= -N_f a M_\rho^2 \overline{B}_0(p_0, \bar{p}; M_\rho, 0; T) + N_f \frac{a}{4}\overline{B}^s(p_0, \bar{p}; M_\rho, 0; T) \\
&\quad + N_f(a-1)\overline{A}_0(0; T), \qquad (3.78) \\
\overline{\Pi}_\perp^L(p_0, \bar{p}; T) &= N_f \frac{a}{4}\overline{B}^L(p_0, \bar{p}; M_\rho, 0; T), \qquad (3.79) \\
\overline{\Pi}_\perp^T(p_0, \bar{p}; T) &= N_f \frac{a}{4}\overline{B}^T(p_0, \bar{p}; M_\rho, 0; T). \qquad (3.80)
\end{aligned}$$

As we will see later in subsection 3.4.1, we define the vector meson mass as the pole of longitudinal or transverse component of the vector meson propagator. From the contributions in Eqs. (3.53)-(3.59), we obtain the hadronic thermal corrections to $\overline{\Pi}_V^{\mu\nu}$ as

$$\begin{aligned}
\overline{\Pi}_V^t(p_0,\bar{p};T) &= 2N_f\overline{A}_0(M_\rho;T) - M_\rho^2 N_f\overline{B}_0(p_0,\bar{p};M_\rho,M_\rho;T) \\
&\quad + \frac{a^2}{8}N_f\overline{B}^t(p_0,\bar{p};0,0;T) + \frac{9}{8}N_f\overline{B}^t(p_0,\bar{p};M_\rho,M_\rho;T)\ , \qquad (3.81)\\
\overline{\Pi}_V^s(p_0,\bar{p};T) &= 2N_f\overline{A}_0(M_\rho;T) - M_\rho^2 N_f\overline{B}_0(p_0,\bar{p};M_\rho,M_\rho;T) \\
&\quad + \frac{a^2}{8}N_f\overline{B}^s(p_0,\bar{p};0,0;T) + \frac{9}{8}N_f\overline{B}^s(p_0,\bar{p};M_\rho,M_\rho;T)\ , \qquad (3.82)\\
\overline{\Pi}_V^L(p_0,\bar{p};T) &= -4p^2 N_f\overline{B}_0(p_0,\bar{p};M_\rho,M_\rho;T) \\
&\quad + \frac{a^2}{8}N_f\overline{B}^L(p_0,\bar{p};0,0;T) + \frac{9}{8}N_f\overline{B}^L(p_0,\bar{p};M_\rho,M_\rho;T), \qquad (3.83)\\
\overline{\Pi}_V^T(p_0,\bar{p};T) &= -4p^2 N_f\overline{B}_0(p_0,\bar{p};M_\rho,M_\rho;T) \\
&\quad + \frac{a^2}{8}N_f\overline{B}^T(p_0,\bar{p};0,0;T) + \frac{9}{8}N_f\overline{B}^T(p_0,\bar{p};M_\rho,M_\rho;T). \qquad (3.84)
\end{aligned}$$

Another two-point function associated with the vector current correlator is $\Pi_{V\parallel}^{\mu\nu}$. From the corrections in Eqs. (3.60)-(3.64), we get the temperature dependent parts as

$$\begin{aligned}
\overline{\Pi}_{V\parallel}^t(p_0,\bar{p};T) &= \frac{a}{2}N_f\overline{A}_0(0;T) + \frac{1}{2}N_f\overline{A}_0(M_\rho;T) + N_f M_\rho^2\overline{B}_0(p_0,\bar{p};M_\rho,M_\rho;T) \\
&\quad + \frac{1}{8}N_f\overline{B}^t(p_0,\bar{p};M_\rho,M_\rho;T) + \frac{a(2-a)}{8}N_f\overline{B}^t(p_0,\bar{p};0,0;T), \qquad (3.85)\\
\overline{\Pi}_{V\parallel}^s(p_0,\bar{p};T) &= \frac{a}{2}N_f\overline{A}_0(0;T) + \frac{1}{2}N_f\overline{A}_0(M_\rho;T) + N_f M_\rho^2\overline{B}_0(p_0,\bar{p};M_\rho,M_\rho;T) \\
&\quad + \frac{1}{8}N_f\overline{B}^s(p_0,\bar{p};M_\rho,M_\rho;T) + \frac{a(2-a)}{8}N_f\overline{B}^s(p_0,\bar{p};0,0;T), \qquad (3.86)\\
\overline{\Pi}_{V\parallel}^L(p_0,\bar{p};T) &= \frac{1}{8}N_f\overline{B}^L(p_0,\bar{p};M_\rho,M_\rho;T) + \frac{a(2-a)}{8}N_f\overline{B}^L(p_0,\bar{p};0,0;T), \qquad (3.87)\\
\overline{\Pi}_{V\parallel}^T(p_0,\bar{p};T) &= \frac{1}{8}N_f\overline{B}^T(p_0,\bar{p};M_\rho,M_\rho;T) + \frac{a(2-a)}{8}N_f\overline{B}^T(p_0,\bar{p};0,0;T). \qquad (3.88)
\end{aligned}$$

In subsection 3.4.2, we will define the parameter a from the direct $\gamma\pi\pi$ coupling using the two-point function $\Pi_\parallel^{\mu\nu}$. From the corrections in Eqs. (3.49)-(3.52), we get the temperature dependent parts as

$$\begin{aligned}
\overline{\Pi}_\parallel^t(p_0,\bar{p};T) &= -(a-1)N_f\overline{A}_0(0;T) - N_f M_\rho^2\overline{B}_0(p_0,\bar{p};M_\rho,M_\rho;T) \\
&\quad + \frac{1}{8}N_f\overline{B}^t(p_0,\bar{p};M_\rho,M_\rho;T) + \frac{(2-a)^2}{8}N_f\overline{B}^t(p_0,\bar{p};0,0;T)\ , \qquad (3.89)\\
\overline{\Pi}_\parallel^s(p_0,\bar{p};T) &= -(a-1)N_f\overline{A}_0(0;T) - N_f M_\rho^2\overline{B}_0(p_0,\bar{p};M_\rho,M_\rho;T) \\
&\quad + \frac{1}{8}N_f\overline{B}^s(p_0,\bar{p};M_\rho,M_\rho;T) + \frac{(2-a)^2}{8}N_f\overline{B}^s(p_0,\bar{p};0,0;T)\ , \qquad (3.90)
\end{aligned}$$

$$\overline{\Pi}^L_{\parallel}(p_0,\bar{p};T) = \frac{1}{8}N_f\overline{B}^L(p_0,\bar{p};M_\rho,M_\rho;T)+\frac{(2-a)^2}{8}N_f\overline{B}^L(p_0,\bar{p};0,0;T), \tag{3.91}$$

$$\overline{\Pi}^T_{\parallel}(p_0,\bar{p};T) = \frac{1}{8}N_f\overline{B}^T(p_0,\bar{p};M_\rho,M_\rho;T)+\frac{(2-a)^2}{8}N_f\overline{B}^T(p_0,\bar{p};0,0;T). \tag{3.92}$$

At the end of this subsection, we note that, using the relations shown in Eq. (B.14), we obtain

$$\begin{aligned}\overline{\Pi}^t_V &= -\overline{\Pi}^t_{V\parallel} = \overline{\Pi}^t_{\parallel}\\ &= \overline{\Pi}^s_V = -\overline{\Pi}^s_{V\parallel} = \overline{\Pi}^s_{\parallel}\\ &= -N_f\frac{1}{4}\left[\overline{A}_0(M_\rho;T)+\overline{A}_0(0;T)\right]-N_fM_\rho^2\overline{B}_0(p_0,\bar{p};M_\rho,M_\rho;T)\ .\end{aligned} \tag{3.93}$$

Since the quantum corrections to the corresponding components are identical as we have shown in Eq. (3.67), the above relation implies that the components Π^t_V, $\Pi^t_{V\parallel}$, $\Pi^t_{\parallel}$, Π^s_V, $\Pi^s_{V\parallel}$ and $\Pi^t_{\parallel}$ agree:

$$\Pi^t_V = -\Pi^t_{V\parallel} = \Pi^t_{\parallel} = \Pi^s_V = -\Pi^s_{V\parallel} = \Pi^s_{\parallel}\ . \tag{3.94}$$

This relation is important to prove the conservation of the vector current correlator as we will show in subsection 3.3.2. [#7]

3.3 Current Correlators

In this section, following Ref. [15], we review how to construct the axial-vector and vector current correlators from the two-point functions calculated in the previous section. The correlators are defined by

$$\begin{aligned}G^{\mu\nu}_A(p_0=i\omega_n,\vec{p};T)\delta_{ab} &= \int_0^{1/T}d\tau\int d^3\vec{x}e^{-i(\vec{p}\cdot\vec{x}+\omega_n\tau)}\left\langle J^\mu_{5a}(\tau,\vec{x})J^\nu_{5b}(0,\vec{0})\right\rangle_\beta\ ,\\ G^{\mu\nu}_V(p_0=i\omega_n,\vec{p};T)\delta_{ab} &= \int_0^{1/T}d\tau\int d^3\vec{x}e^{-i(\vec{p}\cdot\vec{x}+\omega_n\tau)}\left\langle J^\mu_{a}(\tau,\vec{x})J^\nu_{b}(0,\vec{0})\right\rangle_\beta\ ,\end{aligned} \tag{3.95}$$

where J^μ_{5a} and J^μ_a are, respectively, the axial-vector and vector currents, $\omega_n = 2n\pi T$ is the Matsubara frequency, $(a,b) = 1,\ldots,N_f^2-1$ denotes the flavor index and $\langle\ \rangle_\beta$ the thermal average. The correlators for Minkowski momentum are obtained by the analytic continuation of p_0.

[#7] Actually, for the conservation of the vector current correlator, $\Pi^t_V = -\Pi^t_{V\parallel} = \Pi^t_{\parallel}$ and $\Pi^s_V = -\Pi^s_{V\parallel} = \Pi^s_{\parallel}$ are enough, and Π^t_V and Π^s_V can be generally different.

3.3.1 Axial-vector current correlator

Let us consider the axial-vector current correlator $G_A^{\mu\nu}$. For constructing it, we first parameterize the background field $\bar{\xi}_{\rm R}$ and $\bar{\xi}_{\rm L}$. It is convenient to take the unitary gauge of the background HLS. Then, $\bar{\xi}_{\rm R}$ and $\bar{\xi}_{\rm L}$ are parameterized

$$\bar{\xi}_{\rm L} = e^{-\bar{\phi}} \ , \quad \bar{\xi}_{\rm R} = e^{\bar{\phi}} \ , \quad \bar{\phi} = \bar{\phi}_a T_a \ , \tag{3.96}$$

where $\bar{\phi}$ is the interpolating background field corresponding to the pion field. In terms of $\bar{\phi}$, the background $\overline{\mathcal{A}}_\mu$ is expanded as

$$\overline{\mathcal{A}}_\mu = \mathcal{A}_\mu + i\partial_\mu \bar{\phi} + \cdots \ , \tag{3.97}$$

where ellipses denote the terms including two or more fields and the axial-vector external gauge field $\mathcal{A}_\mu$ is defined as

$$\mathcal{A}_\mu \equiv \frac{1}{2}\left(\mathcal{R}_\mu - \mathcal{L}_\mu\right) \ . \tag{3.98}$$

There are two contributions to the axial-vector current correlator $G_A^{\mu\nu}$: one from the $\bar{\phi}$-exchange diagram and another from the one-particle-irreducible (1PI) diagram of $\mathcal{A}_\mu$-$\mathcal{A}_\nu$ interaction. By adding these two contributions, $G_A^{\mu\nu}$ is expressed as

$$G_A^{\mu\nu} = \frac{p_\alpha p_\beta \Pi_\perp^{\mu\alpha}\Pi_\perp^{\nu\beta}}{-p_{\bar{\mu}} p_{\bar{\nu}} \Pi_\perp^{\bar{\mu}\bar{\nu}}} + \Pi_\perp^{\mu\nu} \ . \tag{3.99}$$

Substituting the decomposition of $\Pi_\perp^{\mu\nu}$ in Eq. (5.17) into the above $G_A^{\mu\nu}$, we obtain

$$G_A^{\mu\nu} = P_L^{\mu\nu} G_A^L + P_T^{\mu\nu} G_A^T, \tag{3.100}$$

where

$$\begin{aligned} G_A^L &= \frac{p^2 \Pi_\perp^t \Pi_\perp^s}{-[p_0^2 \Pi_\perp^t - \bar{p}^2 \Pi_\perp^s]} + \Pi_\perp^L, \\ G_A^T &= -\Pi_\perp^s + \Pi_\perp^T. \end{aligned} \tag{3.101}$$

From this form we can easily see that the current conservation $p_\mu G_A^{\mu\nu} = 0$ is satisfied, and the pion couples only to the longitudinal part G_A^L.

3.3.2 Vector current correlator

In the background field gauge the vector meson inverse propagator is related to the two-point function of the background field $\overline{V}_\mu$, $\Pi_V^{\mu\nu}$ as

$$i(D^{-1})^{\mu\nu} = \Pi_V^{\mu\nu} = u^\mu u^\nu \Pi_V^t + (g^{\mu\nu} - u^\mu u^\nu)\Pi_V^s + P_L^{\mu\nu}\Pi_V^L + P_T^{\mu\nu}\Pi_V^T \ . \tag{3.102}$$

It is convenient to decompose the full propagator in a same way:

$$-iD^{\mu\nu} = u^\mu u^\nu D_V^t + (g^{\mu\nu} - u^\mu u^\nu) D_V^s + P_L^{\mu\nu} D_V^L + P_T^{\mu\nu} D_V^T \ . \tag{3.103}$$

After some algebra, these four components are expressed as

$$\begin{aligned}
D_V^t &= \frac{p^2(\Pi_V^L - \Pi_V^s)}{p_0^2\Pi_V^t(\Pi_V^L - \Pi_V^s) - \bar{p}^2\Pi_V^s(\Pi_V^L - \Pi_V^t)}, \\
D_V^s &= \frac{p^2(\Pi_V^L - \Pi_V^t)}{p_0^2\Pi_V^t(\Pi_V^L - \Pi_V^s) - \bar{p}^2\Pi_V^s(\Pi_V^L - \Pi_V^t)}, \\
D_V^L &= \frac{p^2\Pi_V^L}{p_0^2\Pi_V^t(\Pi_V^L - \Pi_V^s) - \bar{p}^2\Pi_V^s(\Pi_V^L - \Pi_V^t)}, \\
D_V^T &= D_V^s + \frac{1}{\Pi_V^T - \Pi_V^s},
\end{aligned} \tag{3.104}$$

where we define $\bar{p} = |\vec{p}|$. By using the above vector meson propagator $-iD^{\mu\nu}$ and the two-point functions $\Pi_\parallel^{\mu\nu}$ and $\Pi_{V\parallel}^{\mu\nu}$, the vector current correlator $G_V^{\mu\nu}$, which consists of the contributions from the vector meson exchange and 1PI diagrams, is obtained as

$$G_V^{\mu\nu} = \Pi_{V\parallel}^{\mu\alpha} iD_{\alpha\beta} \Pi_{V\parallel}^{\beta\nu} + \Pi_\parallel^{\mu\nu} \ . \tag{3.105}$$

Substituting Eq. (3.103) together with Eqs. (3.74) into Eq. (3.105), we obtain $G_V^{\mu\nu}$ as

$$G_V^{\mu\nu} = u^\mu u^\nu G_V^t + (g^{\mu\nu} - u^\mu u^\nu) G_V^s + P_L^{\mu\nu} G_V^L + P_T^{\mu\nu} G_V^T, \tag{3.106}$$

where each component is expressed as

$$\begin{aligned}
G_V^t &= \frac{D_V^L}{\Pi_V^L}\Big[\frac{\bar{p}^2}{p^2}\Pi_{V\parallel}^L\{\Pi_V^s\Pi_{V\parallel}^t - \Pi_V^t\Pi_{V\parallel}^s\} \\
&\quad - \frac{\Pi_{V\parallel}^t}{p^2}\{-p_0^2\Pi_{V\parallel}^t(\Pi_V^s - \Pi_V^L) + p^2(\Pi_{V\parallel}^t\Pi_V^s - \Pi_{V\parallel}\Pi_V^L)\}\Big] + \Pi_\parallel^t, \\
G_V^s &= \frac{D_V^L}{\Pi_V^L}\Big[\frac{p_0^2}{p^2}\Pi_{V\parallel}^L\{\Pi_V^s\Pi_{V\parallel}^t - \Pi_V^t\Pi_{V\parallel}^s\} \\
&\quad - \frac{\Pi_{V\parallel}^s}{p^2}\{-p_0^2(\Pi_V^t\Pi_{V\parallel}^s - \Pi_{V\parallel}^t\Pi_V^L) + \bar{p}^2\Pi_{V\parallel}^s(\Pi_V^t - \Pi_V^s)\}\Big] + \Pi_\parallel^s, \\
G_V^L &= \frac{D_V^L}{\Pi_V^L}\Big[-\Pi_V^L\Pi_{V\parallel}^t + \Pi_{V\parallel}^L(\Pi_{V\parallel}^t\Pi_V^s + \Pi_{V\parallel}^s\Pi_V^t) \\
&\quad - \frac{1}{p^2}(p_0^2\Pi_V^t - \bar{p}^2\Pi_V^s)(\Pi_{V\parallel}^L)^2\Big] + \Pi_\parallel^L, \\
G_V^T &= \frac{D_V^L}{\Pi_V^L}\Big[-\frac{p_0^2}{p^2}\Pi_{V\parallel}^L\{\Pi_V^t\Pi_{V\parallel}^s - \Pi_V^s\Pi_{V\parallel}^t\} \\
&\quad - \frac{\Pi_{V\parallel}^s}{p^2}\{-p_0^2(\Pi_V^t\Pi_{V\parallel}^s - \Pi_{V\parallel}^t\Pi_V^L) + \bar{p}^2\Pi_{V\parallel}^s(\Pi_V^t - \Pi_V^L)\}\Big] \\
&\quad + \frac{(\Pi_{V\parallel}^s - \Pi_{V\parallel}^T)^2}{\Pi_V^s - \Pi_V^T} + \Pi_\parallel^T.
\end{aligned} \tag{3.107}$$

One might worry that the above form does not satisfy the current conservation $p_\mu G_V^{\mu\nu} = 0$. However, since the following equalities are satisfied [see Eq. (3.94)],

$$\begin{aligned} \Pi_V^t &= -\Pi_{V\parallel}^t = \Pi_\parallel^t, \\ \Pi_V^s &= -\Pi_{V\parallel}^s = \Pi_\parallel^s, \end{aligned} \tag{3.108}$$

each component of the above $G_V^{\mu\nu}$ is rewritten as

$$\begin{aligned} G_V^t &= G_V^s = 0, \\ G_V^L &= -\frac{D_V^L}{\Pi_V^L}\Big[\Pi_V^t\Pi_V^s(\Pi_V^L + 2\Pi_{V\parallel}^L) + \frac{p_0^2\Pi_V^t - \vec{p}^2\Pi_V^s}{p^2}(\Pi_{V\parallel}^L)^2\Big] + \Pi_\parallel^L, \\ G_V^T &= \frac{\Pi_V^s(\Pi_V^T + 2\Pi_{V\parallel}^T) + (\Pi_{V\parallel}^T)^2}{\Pi_V^s - \Pi_V^T} + \Pi_\parallel^T. \end{aligned} \tag{3.109}$$

Now we can easily see that the current conservation $p_\mu G_V^{\mu\nu} = 0$ is satisfied since $p_\mu P_L^{\mu\nu} = p_\mu P_T^{\mu\nu} = 0$. In the present analysis we further have $\Pi_V^t = \Pi_V^s$ as can be seen from Eq. (3.94). Finally we obtain the following $G_V^{\mu\nu}$:

$$G_V^{\mu\nu} = P_L^{\mu\nu} G_V^L + P_T^{\mu\nu} G_V^T, \tag{3.110}$$

where

$$\begin{aligned} G_V^L &= \frac{\Pi_V^s(\Pi_V^L + 2\Pi_{V\parallel}^L)}{\Pi_V^s - \Pi_V^L} + \Pi_\parallel^L, \\ G_V^T &= \frac{\Pi_V^s(\Pi_V^T + 2\Pi_{V\parallel}^T)}{\Pi_V^s - \Pi_V^T} + \Pi_\parallel^T. \end{aligned} \tag{3.111}$$

Here we have dropped the terms $(\Pi_{V\parallel}^L)^2$ and $(\Pi_{V\parallel}^T)^2$ since they are of higher order.

3.4 Thermal Properties of π-ρ Parameters

In this section, we briefly summarize the temperature dependences of several parameters of pions and vector mesons in hot medium following Refs. [14, 15, 16].

3.4.1 Vector meson mass

In this subsection, we first define the vector meson pole masses of both the longitudinal and transverse modes at non-zero temperature from the vector current correlator in the background field gauge and show the explicit forms of the hadronic thermal corrections from the vector and pseudoscalar meson loop.

Let us define pole masses of longitudinal and transverse modes of the vector meson from the poles of longitudinal and transverse components of the vector current correlator in the rest frame, which are given by Eqs. (3.110) and (3.111). Then, the pole masses are obtained as the solutions of the following on-shell conditions:

$$\begin{aligned} 0 &= \mathrm{Re}\left[\Pi_V^s(p_0 = m_\rho^L(T), 0; T) - \Pi_V^L(p_0 = m_\rho^L(T), 0; T)\right] \ , \\ 0 &= \mathrm{Re}\left[\Pi_V^s(p_0 = m_\rho^T(T), 0; T) - \Pi_V^T(p_0 = m_\rho^T(T), 0; T)\right] \ , \end{aligned} \tag{3.112}$$

where $m_\rho^L(T)$ and $m_\rho^T(T)$ denote the pole masses of the longitudinal and transverse modes, respectively. As we have calculated in section 3.2, $\Pi_V^s(p_0, \bar{p}; T)$, $\Pi_V^L(p_0, \bar{p}; T)$ and $\Pi_V^T(p_0, \bar{p}; T)$ in the HLS at one-loop level are expressed as

$$\begin{aligned} \Pi_V^s(p_0, \bar{p}; T) &= F_\sigma^2(M_\rho) + \widetilde{\Pi}_V^S(p^2) + \overline{\Pi}_V^s(p_0, \bar{p}; T) \ , \\ \Pi_V^L(p_0, \bar{p}; T) &= \frac{p^2}{g^2(M_\rho)} + \widetilde{\Pi}_V^{LT}(p^2) + \overline{\Pi}_V^L(p_0, \bar{p}; T) \ , \\ \Pi_V^T(p_0, \bar{p}; T) &= \frac{p^2}{g^2(M_\rho)} + \widetilde{\Pi}_V^{LT}(p^2) + \overline{\Pi}_V^T(p_0, \bar{p}; T) \ , \end{aligned} \tag{3.113}$$

where the explicit forms of the finite renormalization effects $\widetilde{\Pi}_V^S(p^2)$ and $\widetilde{\Pi}_V^{LT}(p^2)$ are given in Eqs. (C.31) and (C.32), and those of the hadronic thermal effects $\overline{\Pi}_V^s(p_0, \bar{p}; T)$, $\overline{\Pi}_V^L(p_0, \bar{p}; T)$ and $\overline{\Pi}_V^T(p_0, \bar{p}; T)$ are given in Eqs. (3.93), (3.83) and (3.84). Substituting Eq. (3.113) into Eq. (3.112), we obtain

$$\begin{aligned} \left[m_\rho^L(T)\right]^2 &= M_\rho^2 + g^2(M_\rho) \Big[\mathrm{Re}\,\widetilde{\Pi}_V^S(p_0^2) + \mathrm{Re}\,\overline{\Pi}_V^s(p_0, 0; T) \\ &\qquad - \mathrm{Re}\,\widetilde{\Pi}_V^T(p_0^2) - \mathrm{Re}\,\overline{\Pi}_V^L(p_0, 0; T) \Big]_{p_0 = m_\rho^L(T)} \ , \\ \left[m_\rho^T(T)\right]^2 &= M_\rho^2 + g^2(M_\rho) \Big[\mathrm{Re}\,\widetilde{\Pi}_V^S(p_0^2) + \mathrm{Re}\,\overline{\Pi}_V^s(p_0, 0; T) \\ &\qquad - \mathrm{Re}\,\widetilde{\Pi}_V^T(p_0^2) - \mathrm{Re}\,\overline{\Pi}_V^T(p_0, 0; T) \Big]_{p_0 = m_\rho^T(T)} \ . \end{aligned} \tag{3.114}$$

We can replace $m_\rho^L(T)$ and $m_\rho^T(T)$ with M_ρ in the hadronic thermal effects as well as in the finite renormalization effect, since the difference is of higher order. Then, noting that $\mathrm{Re}\,\widetilde{\Pi}_V^S(p^2 = M_\rho^2) = \mathrm{Re}\,\widetilde{\Pi}_V^{LT}(p^2 = M_\rho^2) = 0$ as shown in Eq. (C.19), we obtain

$$\left[m_\rho^L(T)\right]^2 = M_\rho^2 - g^2(M_\rho)\,\mathrm{Re}\left[\overline{\Pi}_V^L(M_\rho; 0; T) - \overline{\Pi}_V^s(M_\rho; 0; T)\right] \ , \tag{3.115}$$

$$\left[m_\rho^T(T)\right]^2 = M_\rho^2 - g^2(M_\rho)\,\mathrm{Re}\left[\overline{\Pi}_V^T(M_\rho; 0; T) - \overline{\Pi}_V^s(M_\rho; 0; T)\right] \ . \tag{3.116}$$

Let us calculate the explicit form of the pole mass using the expression of $\overline{\Pi}_V^s$, $\overline{\Pi}_V^L$ and $\overline{\Pi}_V^T$ obtained in section 3.2. Here we note that Eqs. (B.24) and (B.25) imply that $\overline{B}^L - \overline{B}^s$ agrees with $\overline{B}^T - \overline{B}^s$ in the rest frame. Then in the rest frame $\overline{\Pi}_V^L - \overline{\Pi}_V^s$ agrees with $\overline{\Pi}_V^T - \overline{\Pi}_V^s$. Thus the longitudinal pole mass is the same as the transverse one:

$$m_\rho^L(T) = m_\rho^T(T) \equiv m_\rho(T) \ . \tag{3.117}$$

By using the low momentum limits of the functions shown in Eqs. (B.23) and (B.24), $\overline{\Pi}_V^L - \overline{\Pi}_V^s$ in the rest frame is expressed as

$$\begin{aligned} &\overline{\Pi}_V^L(p_0, \bar{p} = 0; T) - \overline{\Pi}_V^s(p_0, \bar{p} = 0; T) \\ &= N_f \Big[\frac{a^2}{24} \tilde{G}_2(p_0; T) - \tilde{J}_1^2(M_\rho; T) + (\frac{M_\rho^2}{4} - p_0^2) \tilde{F}_3^2(p_0; M_\rho; T) + \frac{3}{8} \tilde{F}_3^4(p_0; M_\rho; T) \Big] \end{aligned} \tag{3.118}$$

where the functions $\tilde{I}_n$, $\tilde{J}_m^n$, $\tilde{F}_m^n$ and $\tilde{G}_m^n$ are defined in Appendix D. Substituting the above expression into Eq. (3.115) and using the relation

$$-\frac{1}{3M_\rho^2} \tilde{F}_3^4(M_\rho; M_\rho; T) \ = \ \frac{1}{4} \tilde{F}_3^2(M_\rho; M_\rho; T) - \frac{1}{3M_\rho^2} \tilde{J}_1^2(M_\rho; T) \ , \tag{3.119}$$

we find that the vector meson pole mass is expressed as

$$m_\rho^2(T) \ = \ {M_\rho}^2 + N_f \, g^2 \left[-\frac{a^2}{12} \tilde{G}_2(M_\rho; T) + \frac{4}{5} \tilde{J}_1^2(M_\rho; T) + \frac{33}{16} M_\rho^2 \tilde{F}_3^2(M_\rho; M_\rho; T) \right] . \tag{3.120}$$

The contribution in this expression agrees with the result in Ref. [14] which is derived from the hadronic thermal correction calculated in the Landau gauge in Ref. [68] by taking the on-shell condition (3.115). [#8]

We study the behavior of the pole mass in the low temperature region, $T \ll M_\rho$. In this region the functions F_m^n and J_m^n are suppressed by $e^{-M_\rho/T}$, and thus give negligible contributions. Since $G_2 \approx -\frac{\pi^4}{15} \frac{T^4}{{M_\rho}^2}$, the vector meson pole mass increases as T^4 in the low temperature region, dominated by the π-loop effects:

$${m_\rho}^2(T) \approx {M_\rho}^2 + \frac{N_f \pi^2 a}{360 {F_\pi}^2} T^4 \qquad \text{for} \quad T \ll M_\rho. \tag{3.121}$$

Note that the lack of T^2-term in the above expression is consistent with the result by the current algebra analysis [69].

[#8] The functions used in this paper are related to the ones used in Ref. [14] as $\tilde{J}_1^2 = \frac{1}{2\pi^2} J_1^2$, $\tilde{G}_2 = \frac{1}{2\pi^2} \bar{G}_2$, and so on.

3.4.2 Pion parameters

First we study the on-shell structure of the pion. For this, we look at the pole of the longitudinal component G_A^L in Eq. (3.101). Since both $\Pi_\perp^t$ and $\Pi_\perp^s$ have imaginary parts, we choose to determine the pion energy E from the real part by solving the dispersion formula

$$0 \;=\; \left[p_0^2\,\mathrm{Re}\Pi_\perp^t(p_0,\bar{p};T) - \bar{p}^2\,\mathrm{Re}\Pi_\perp^s(p_0,\bar{p};T)\right]_{p_0=E}\ , \tag{3.122}$$

where $\bar{p} \equiv |\vec{p}|$. As remarked in section 3.2, in HLS at one-loop level, $\Pi_\perp^t(p_0,\bar{p};T)$ and $\Pi_\perp^s(p_0,\bar{p};T)$ are of the form

$$\begin{aligned}\Pi_\perp^t(p_0,\bar{p};T) &= F_\pi^2(0) + \widetilde{\Pi}_\perp^S(p^2) + \bar{\Pi}_\perp^t(p_0,\bar{p};T)\ ,\\ \Pi_\perp^s(p_0,\bar{p};T) &= F_\pi^2(0) + \widetilde{\Pi}_\perp^S(p^2) + \bar{\Pi}_\perp^s(p_0,\bar{p};T)\ ,\end{aligned} \tag{3.123}$$

where $\widetilde{\Pi}_\perp^S(p^2)$ is the finite renormalization contribution, and $\bar{\Pi}_\perp^t(p_0,\bar{p};T)$ and $\bar{\Pi}_\perp^s(p_0,\bar{p};T)$ are the hadronic thermal contributions. Substituting Eq. (3.123) into Eq. (3.122), we obtain

$$\begin{aligned}0 = \left(E^2-\bar{p}^2\right)\left[F_\pi^2(0) + \mathrm{Re}\,\widetilde{\Pi}_\perp^S(p^2=E^2-\bar{p}^2)\right]\\ + E^2\mathrm{Re}\,\bar{\Pi}_\perp^t(E,\bar{p};T) - \bar{p}^2\mathrm{Re}\,\bar{\Pi}_\perp^s(E,\bar{p};T)\ .\end{aligned} \tag{3.124}$$

The pion velocity $v_\pi(\bar{p}) \equiv E/\bar{p}$ is then obtained by solving

$$v_\pi^2(\bar{p}) \;=\; \frac{F_\pi^2(0) + \mathrm{Re}\,\bar{\Pi}_\perp^s(\bar{p},\bar{p};T)}{F_\pi^2(0) + \mathrm{Re}\,\bar{\Pi}_\perp^t(\bar{p},\bar{p};T)}\ . \tag{3.125}$$

Here we replaced E by $\bar{p}$ in the hadronic thermal terms $\bar{\Pi}_\perp^t(E,\vec{p})$ and $\bar{\Pi}_\perp^s(E,\vec{p})$ as well as in the finite renormalization contribution $\widetilde{\Pi}_\perp^S(p^2=E^2-\bar{p}^2)$, since the difference is of higher order. [Note that $\widetilde{\Pi}_\perp^S(p^2=0)=0$.]

Next we determine the wave function renormalization of the pion field, which relates the background field $\bar{\phi}$ to the pion field $\bar{\pi}$ in the momentum space as

$$\bar{\phi} = \bar{\pi}/\widetilde{F}(\bar{p};T). \tag{3.126}$$

We follow the analysis in Ref. [70] to obtain

$$\widetilde{F}^2(\bar{p};T) = \mathrm{Re}\Pi_\perp^t(E,\bar{p};T) = F_\pi^2(0) + \mathrm{Re}\,\bar{\Pi}_\perp^t(\bar{p},\bar{p};T)\ . \tag{3.127}$$

Using this wave function renormalization and the velocity in Eq. (3.125), we can rewrite the longitudinal part of the axial-vector current correlator as

$$G_A^L(p_0,\vec{p}) \;=\; \frac{p^2\Pi_\perp^t(p_0,\bar{p};T)\Pi_\perp^s(p_0,\bar{p};T)/\widetilde{F}^2(\bar{p};T)}{-\left[p_0^2 - v_\pi^2(\bar{p})\bar{p}^2 + \Pi_\pi(p_0,\bar{p};T)\right]} + \Pi_\perp^L(p_0,\bar{p};T)\ , \tag{3.128}$$

where the pion self energy $\Pi_\pi(p_0, \bar{p}; T)$ is given by

$$\Pi_\pi(p_0, \bar{p}; T) = \frac{1}{\mathrm{Re}\,\Pi_\perp^t(E, \bar{p}; T)} \times \left[p_0^2 \left\{ \Pi_\perp^t(p_0, \bar{p}; T) - \mathrm{Re}\,\Pi_\perp^t(E, \bar{p}; T) \right\} - \bar{p}^2 \left\{ \Pi_\perp^s(p_0, \bar{p}; T) - \mathrm{Re}\,\Pi_\perp^s(E, \bar{p}; T) \right\} \right] \quad (3.129)$$

Let us now define the pion decay constant. A natural procedure is to define the pion decay constant from the pole residue of the axial-vector current correlator. From Eq. (3.128), the pion decay constant is given by

$$\begin{aligned} f_\pi^2(\bar{p}; T) &= \frac{\Pi_\perp^t(E, \bar{p}; T)\Pi_\perp^s(E, \bar{p}; T)}{\widetilde{F}^2(\bar{p}; T)} \\ &= \frac{\left[F_\pi^2(0) + \bar{\Pi}_\perp^t(\bar{p}, \bar{p}; T)\right]\left[F_\pi^2(0) + \bar{\Pi}_\perp^s(\bar{p}, \bar{p}; T)\right]}{\widetilde{F}^2(\bar{p}; T)} \ . \end{aligned} \quad (3.130)$$

We now address how $f_\pi^2(\bar{p}; T)$ is related to the temporal and spatial components of the pion decay constant introduced in Ref. [20]. Following their notation, let f_π^t denote the decay constant associated with the temporal component of the axial-vector current and f_π^s the one with the spatial component. In the present analysis, they can be read off from the coupling of the $\bar{\pi}$ field to the axial-vector external field $\mathcal{A}_\mu$:

$$f_\pi^t(\bar{p}; T) \equiv \frac{\Pi_\perp^t(E, \bar{p}; T)}{\widetilde{F}(\bar{p}; T)} = \frac{F_\pi^2(0) + \bar{\Pi}_\perp^t(\bar{p}, \bar{p}; T)}{\widetilde{F}(\bar{p}; T)} \ , \quad (3.131)$$

$$f_\pi^s(\bar{p}; T) \equiv \frac{\Pi_\perp^s(\tilde{E}, \bar{p}; T)}{\widetilde{F}(\bar{p}; T)} = \frac{F_\pi^2(0) + \bar{\Pi}_\perp^s(\bar{p}, \bar{p}; T)}{\widetilde{F}(\bar{p}; T)} \ . \quad (3.132)$$

Comparing Eqs. (3.131) and (3.132) with Eqs. (3.125), (3.127) and (3.130), we have [20, 70]

$$\widetilde{F}(\bar{p}; T) = \mathrm{Re}\, f_\pi^t(\bar{p}; T) \ , \quad (3.133)$$

$$f_\pi^2(\bar{p}; T) = f_\pi^t(\bar{p}; T) f_\pi^s(\bar{p}; T) \ . \quad (3.134)$$

By using the above decay constants, the pion velocity at one-loop level is expressed as [20, 15] #9

$$v_\pi^2(\bar{p}; T) = 1 + \frac{\tilde{F}(\bar{p}; T)}{F_\pi^2}\Big[\mathrm{Re} f_\pi^s(\bar{p}; T) - \mathrm{Re} f_\pi^t(\bar{p}; T)\Big]. \quad (3.135)$$

Substituting Eqs. (B.1) and (B.2) into Eqs. (3.77) and (3.78), we obtain $\overline{\Pi}_\perp^t$ and $\overline{\Pi}_\perp^s$ for the on-shell pion as

$$\overline{\Pi}_\perp^t(p_0 = \bar{p} + i\epsilon, \bar{p}; T) = N_f(a-1)\tilde{I}_2(T)$$

#9 This form of the pion velocity looks slightly different from Eq. (3.125). However, Eq. (3.135) is actually equivalent to Eq. (3.125) at one-loop order, and more convenient to study the temperature dependence of the pion velocity in the low temperature region.

$$+\frac{N_f}{2}a\left[\frac{1}{2}\overline{B}^t(\bar{p}+i\epsilon,\bar{p};M_\rho,0;T)-2M_\rho^2\overline{B}_0(\bar{p}+i\epsilon,\bar{p};M_\rho,0;T)\right]\,, \tag{3.136}$$

$$\overline{\Pi}^s_\perp(p_0=\bar{p}+i\epsilon,\bar{p};T)=N_f(a-1)\tilde{I}_2(T)$$
$$+\frac{N_f}{2}a\left[\frac{1}{2}\overline{B}^s(\bar{p}+i\epsilon,\bar{p};M_\rho,0;T)-2M_\rho^2\overline{B}_0(\bar{p}+i\epsilon,\bar{p};M_\rho,0;T)\right]\,, \tag{3.137}$$

where we put $\epsilon\to+0$ to make the analytic continuation for the frequency $p_0=i2\pi nT$ to the Minkowski variable. We show the explicit forms of the functions $\overline{B}^t$, $\overline{B}^s$ and $\overline{B}_0$ in Eqs. (B.3), (B.5) and (B.6).

In general the pion velocity in medium does not agree with the value at $T=0$ due to the interaction with the heat bath. Below T_c, since the temporal component does not agree with the spatial one due to the thermal vector meson effect, $\overline{\Pi}^t_\perp\neq\overline{\Pi}^s_\perp$, the pion velocity $v_\pi(\bar{p};T)$ is not the speed of light. As we will see below, in the framework of HLS the pion velocity receives a change from the ρ-loop effect for $0<T<T_c$. When we take the low temperature limit ($T\ll M_\rho$) and the soft pion limit ($\bar{p}\ll M_\rho$ and $\bar{p}\ll T$), the real parts of $\overline{\Pi}^t_\perp$ and $\overline{\Pi}^s_\perp$ are approximated as

$$\mathrm{Re}\overline{\Pi}^t_\perp(p_0=\bar{p}+i\epsilon,\bar{p};T)\ \simeq\ -N_f\tilde{I}_2(T)+N_f\frac{a}{M_\rho^2}\tilde{I}_4(T)-N_f\,a\sqrt{\frac{M_\rho}{8\pi^3}}\,e^{-M_\rho/T}T^{3/2}, \tag{3.138}$$

$$\mathrm{Re}\overline{\Pi}^s_\perp(p_0=\bar{p}+i\epsilon,\bar{p};T)\ \simeq\ -N_f\tilde{I}_2(T)-N_f\frac{a}{M_\rho^2}\tilde{I}_4(T)+N_f\,a\sqrt{\frac{M_\rho}{8\pi^3}}\,e^{-M_\rho/T}T^{3/2}, \tag{3.139}$$

By using Eqs. (3.138) and (3.139) and neglecting the terms proportional to the suppression factor $e^{-M_\rho/T}$, the pion velocity is expressed as

$$\begin{aligned}v_\pi^2(\bar{p};T)\ &\simeq\ 1-N_f\frac{2a}{F_\pi^2M_\rho^2}\tilde{I}_4(T)\\ &=\ 1-\frac{N_f}{15}\,a\pi^2\frac{T^4}{F_\pi^2M_\rho^2}\ <1\,.\end{aligned} \tag{3.140}$$

This shows that the pion velocity is smaller than the speed of light already at one-loop level in the HLS due to the ρ-loop effect. This is different from the result obtained in the ordinary ChPT including only the pion at one-loop [see for example, Ref. [20] and references therein]. Generally, the longitudinal ρ contribution to $\overline{\Pi}^t_\perp$ expressed by $\overline{B}^t$ in Eq. (3.136) differs from that to $\overline{\Pi}^s_\perp$ by $\overline{B}^s$ in Eq. (3.137), which implies that, below the critical temperature, there always exists a deviation of the pion velocity from the speed of light due to the longitudinal ρ-loop effect:

$$v_\pi^2(\bar{p};T)<1\qquad\text{for}\quad 0<T<T_c\,. \tag{3.141}$$

Next, we study the temporal and spatial pion decay constants in hot matter defined by Eqs. (3.131) and (3.132). The imaginary parts of $\overline{\Pi}^t_\perp$ and $\overline{\Pi}^s_\perp$ in the low temperature region

are given by

$$\begin{aligned}
\mathrm{Im}\overline{\Pi}^t_\perp(p_0=\bar{p}+i\epsilon,\bar{p};M_\rho,0;T) &\overset{\bar{p}\ll T}{\simeq} \frac{N_f}{4}\,a\,\mathrm{Im}\overline{B}^t(p_0=\bar{p}+i\epsilon,\bar{p};M_\rho,0;T) \\
&\overset{T\ll M_\rho}{\simeq} \frac{N_f}{8\pi}\,a\,M_\rho^2 e^{-M_\rho/T}, \qquad (3.142)\\
\mathrm{Im}\overline{\Pi}^s_\perp(p_0=\bar{p}+i\epsilon,\bar{p};M_\rho,0;T) &\overset{\bar{p}\ll T}{\simeq} \frac{N_f}{4}\,a\,\mathrm{Im}\overline{B}^s(p_0=\bar{p}+i\epsilon,\bar{p};M_\rho,0;T) \\
&\overset{T\ll M_\rho}{\simeq} -\frac{N_f}{8\pi}\,a\,M_\rho^2 e^{-M_\rho/T}. \qquad (3.143)
\end{aligned}$$

Thus the contributions from the imaginary parts $\mathrm{Im}\overline{\Pi}^{t,s}_\perp$ are small because of the suppression factor $e^{-M_\rho/T}$. From Eqs. (3.138) and (3.139) with $\tilde{I}_2(T)=T^2/12$ and $\tilde{I}_4(T)=\pi^2T^4/30$, we obtain the following results for the real parts of f_π^t and f_π^s:

$$\begin{aligned}
[\mathrm{Re}f_\pi^t]\tilde{F} &\simeq F_\pi^2 - N_f\left[\frac{T^2}{12}-\frac{a\,\pi^2}{30M_\rho^2}T^4+a\sqrt{\frac{M_\rho}{8\pi^3}}\,e^{-M_\rho/T}T^{3/2}\right],\\
[\mathrm{Re}f_\pi^s]\tilde{F} &\simeq F_\pi^2 - N_f\left[\frac{T^2}{12}+\frac{a\,\pi^2}{30M_\rho^2}T^4-a\sqrt{\frac{M_\rho}{8\pi^3}}\,e^{-M_\rho/T}T^{3/2}\right]. \qquad (3.144)
\end{aligned}$$

We note that $\tilde{F}=\mathrm{Re}f_\pi^t$ as shown in Eq. (3.133). Then, neglecting the terms suppressed by $e^{-M_\rho/T}$, we obtain the difference between $(f_\pi^t)^2$ and $f_\pi^t f_\pi^s$ as

$$(f_\pi^t)^2 - f_\pi^t f_\pi^s \simeq \frac{N_f}{15}\,a\pi^2\frac{T^4}{M_\rho^2} > 0. \qquad (3.145)$$

This implies that the contribution from the ρ-loop (the second and third terms in the brackets) generates a difference between the temporal and spatial pion decay constants in the low temperature region. Similarly, at general temperature below T_c, there exists a difference between $f_\pi^t\tilde{F}$ and $f_\pi^s\tilde{F}$ due to the ρ-loop effects: $[\mathrm{Re}f_\pi^t]\tilde{F} > [\mathrm{Re}f_\pi^s]\tilde{F}$. Since we can always take $\tilde{F}$ to be positive, we find that $\mathrm{Re}f_\pi^t$ is larger than $\mathrm{Re}f_\pi^s$:

$$\mathrm{Re}f_\pi^t(\bar{p};T) > \mathrm{Re}f_\pi^s(\bar{p};T) \qquad \text{for} \quad 0<T<T_c\,. \qquad (3.146)$$

This result is consistent with Eq. (3.141) because $v_\pi^2-1=(\tilde{F}/F_\pi^2)[\mathrm{Re}f_\pi^s-\mathrm{Re}f_\pi^t]$ by definition. The difference between $(f_\pi^t)^2$ and $f_\pi^t f_\pi^s$ shown in Eq. (3.145) is tiny, and the hadronic thermal corrections to them are dominated by the first term $(T^2/12)$ in the bracket in Eq. (3.144). Then, in the very low temperature region, the above expressions are further reduced to

$$f_\pi^2=(f_\pi^t)(f_\pi^s)\sim(f_\pi^t)^2\sim {F_\pi}^2-\frac{N_f}{12}T^2, \qquad (3.147)$$

which is consistent with the result obtained in Ref. [71].

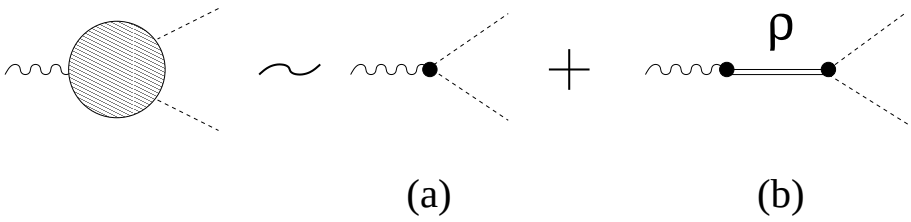

Figure 3.6: Leading contributions to the $\gamma\pi\pi$ interaction.

3.4.3 Vector meson dominance

As shown in section 3.1, the HLS theory can reproduce the vector dominance (VD) of the electromagnetic form factor of pion, which is phenomenologically successful in mesonic system. In this subsection, we study the validity of the VD in hot matter.

We first study the direct $\gamma\pi\pi$ interaction at zero temperature. We expand the Lagrangian (3.13) in terms of the π field with taking the unitary gauge of the HLS ($\sigma = 0$) to obtain

$$\begin{aligned}\mathcal{L}_{(2)} &= \mathrm{tr}\left[\partial_\mu\pi\partial^\mu\pi\right] + ag^2F_\pi^2\,\mathrm{tr}\left[\rho_\mu\rho^\mu\right] + 2i\left(\frac{1}{2}ag\right)\,\mathrm{tr}\left[\rho^\mu\left[\partial_\mu\pi\,,\,\pi\right]\right] \\ &\quad - 2\left(agF_\pi^2\right)\,\mathrm{tr}\left[\rho_\mu\mathcal{V}^\mu\right] + 2i\left(1-\frac{a}{2}\right)\mathrm{tr}\left[\mathcal{V}^\mu\left[\partial_\mu\pi\,,\,\pi\right]\right] + \cdots\,, \end{aligned} \tag{3.148}$$

where the vector meson field ρ_μ is introduced by

$$V_\mu = g\rho_\mu\ , \tag{3.149}$$

and vector external gauge field $\mathcal{V}_\mu$ is defined as

$$\mathcal{V}_\mu \equiv \frac{1}{2}\left(\mathcal{R}_\mu + \mathcal{L}_\mu\right)\ . \tag{3.150}$$

At the leading order of the derivative expansion in the HLS, there are two contributions shown in Fig. 3.6, i.e., the direct $\gamma\pi\pi$ interaction [Fig. 3.6 (a)] and the ρ-mediated interaction [Fig. 3.6 (b)]. The form of the direct $\gamma\pi\pi$ interaction is easily read from Eq. (3.148) as

$$\Gamma^{(\mathrm{a})\mu}_{\gamma\pi\pi(\mathrm{tree})} = e(q-k)^\mu\left(1-\frac{a}{2}\right)\,, \tag{3.151}$$

where e is the electromagnetic coupling constant and q and k denote outgoing momenta of the pions. This shows that, for the parameter choice $a = 2$, the direct $\gamma\pi\pi$ coupling vanishes (the VD of the electromagnetic form factor of the pion).

At the next order there exist quantum corrections. In the background field gauge adopted in the present analysis the background fields $\overline{\mathcal{A}}_\mu$ and $\overline{\mathcal{V}}_\mu$ include the photon field A_μ and the

background pion field $\bar{\pi}$ as

$$\begin{aligned} \overline{\mathcal{A}}_\mu &= \frac{1}{F_\pi(0)}\partial_\mu\bar{\pi} + \frac{i\,e}{F_\pi(0)}A_\mu\,[Q\,,\,\bar{\pi}] + \cdots\,, \\ \overline{\mathcal{V}}_\mu &= e\,QA_\mu - \frac{i}{2F_\pi^2(0)}\,[\partial_\mu\bar{\pi}\,,\,\bar{\pi}] + \cdots\,, \end{aligned} \tag{3.152}$$

where $F_\pi(0)$ is the on-shell pion decay constant (residue of the pion pole) in order to identify the field $\bar{\pi}$ with the on-shell pion field, and the charge matrix Q is given by

$$Q = \begin{pmatrix} 2/3 & & \\ & -1/3 & \\ & & -1/3 \end{pmatrix}\,. \tag{3.153}$$

The direct $\gamma\pi\pi$ interaction including the next order correction is determined from the two-point functions of $\overline{\mathcal{V}}_\mu$-$\overline{\mathcal{V}}_\nu$ and $\overline{\mathcal{A}}_\mu$-$\overline{\mathcal{A}}_\nu$ and three-point function of $\overline{\mathcal{V}}_\mu$-$\overline{\mathcal{A}}_\alpha$-$\overline{\mathcal{A}}_\beta$. We can easily show that contribution from the three-point function vanishes in the low energy limit as follows: Let $\Gamma^{\mu\alpha\beta}_{\overline{\mathcal{V}}\overline{\mathcal{A}}\overline{\mathcal{A}}}$ denote the $\overline{\mathcal{V}}_\mu$-$\overline{\mathcal{A}}_\alpha$-$\overline{\mathcal{A}}_\beta$ three-point function. Then the direct $\gamma\pi\pi$ coupling derived from this three-point function is proportional to $q_\alpha k_\beta\Gamma^{\mu\alpha\beta}_{\overline{\mathcal{V}}\overline{\mathcal{A}}\overline{\mathcal{A}}}$. Since the legs α and β of $\Gamma^{\mu\alpha\beta}_{\overline{\mathcal{V}}\overline{\mathcal{A}}\overline{\mathcal{A}}}$ are carried by q or k, $q_\alpha k_\beta\Gamma^{\mu\alpha\beta}_{\overline{\mathcal{V}}\overline{\mathcal{A}}\overline{\mathcal{A}}}$ is generally proportional to two of q^2, k^2 and $q\cdot k$. Since the loop integral does not generate any massless poles, this implies that $q_\alpha k_\beta\Gamma^{\mu\alpha\beta}_{\overline{\mathcal{V}}\overline{\mathcal{A}}\overline{\mathcal{A}}}$ vanishes in the low energy limit $q^2 = k^2 = q\cdot k = 0$. Thus, the direct $\gamma\pi\pi$ interaction in the low energy limit can be read from the two-point functions of $\overline{\mathcal{V}}_\mu$-$\overline{\mathcal{V}}_\nu$ and $\overline{\mathcal{A}}_\mu$-$\overline{\mathcal{A}}_\nu$ as

$$\Gamma^\mu_{\gamma\pi\pi} = e\frac{1}{F_\pi^2(0)}\left[q_\nu\Pi_\perp^{\mu\nu}(q) - k_\nu\Pi_\perp^{\mu\nu}(k) - \frac{1}{2}(q-k)_\nu\Pi_\parallel^{\mu\nu}(p)\right]\,, \tag{3.154}$$

where $p_\nu = (q+k)_\nu$ is the photon momentum. Substituting the decomposition of the two-point function given in Eq. (3.66) and taking the low-energy limit $q^2 = k^2 = p^2 = 0$, we obtain

$$\Gamma^\mu_{\gamma\pi\pi} = e(q-k)^\mu\left[1 - \frac{1}{2}\frac{\Pi_\parallel^{(\mathrm{vac})S}(p^2=0)}{F_\pi^2(0)}\right]\,, \tag{3.155}$$

where we used $\Pi_\perp^{(\mathrm{vac})S}(q^2=0) = F_\pi^2(0)$. Comparing the above expression with the one in Eq. (3.151), we define the parameter $a(0)$ at one-loop level as

$$a(0) = \frac{\Pi_\parallel^{(\mathrm{vac})S}(p^2=0)}{F_\pi^2(0)}\,. \tag{3.156}$$

We note that, in Ref. [21], $a(0)$ is defined by the ratio $F_\sigma^2(M_\rho)/F_\pi^2(0)$ by neglecting the finite renormalization effect which depends on the details of the renormalization condition. While

the above $a(0)$ in Eq. (3.156) defined from the direct $\gamma\pi\pi$ interaction is equivalent to the one used in Ref. [15]. In the present renormalization condition (C.16), $\Pi_{\parallel}^{(\mathrm{vac})S}(p^2=0)$ is given by

$$\Pi_{\parallel}^{(\mathrm{vac})S}(p^2=0) = F_\sigma^2(M_\rho) + \frac{N_f}{(4\pi)^2} M_\rho^2 (2 - \sqrt{3}\tan^{-1}\sqrt{3}) \ . \tag{3.157}$$

By adding this, the parameter $a(0)$ is expressed as

$$a(0) = \frac{F_\sigma^2(M_\rho)}{F_\pi^2(0)} + \frac{N_f}{(4\pi)^2}\frac{M_\rho^2}{F_\pi^2(0)} (2 - \sqrt{3}\tan^{-1}\sqrt{3}) \ . \tag{3.158}$$

Using $M_\rho = 771.1\,\mathrm{MeV}$, $F_\pi(\mu=0) = 86.4\,\mathrm{MeV}$ estimated in the chiral limit [38, 40, 39] [#10] and $F_\sigma^2(M_\rho)/F_\pi^2(0) = 2.03$ obtained through the Wilsonian matching for $\Lambda_{\mathrm{QCD}} = 400\,\mathrm{MeV}$ and the matching scale $\Lambda = 1.1\,\mathrm{GeV}$ in Ref. [13], we estimate the value of $a(0)$ at zero temperature as

$$a(0) \simeq 2.31 \ . \tag{3.159}$$

This implies that the VD is well satisfied at $T=0$ even though the value of the parameter a at the scale M_ρ is close to one [72].

Now, let us study the direct $\gamma\pi\pi$ coupling in hot matter. In general, the electric mode and the magnetic mode of the photon couple to the pions differently in hot matter, so that there are two parameters as extensions of the parameter a. Similarly to the one obtained at $T=0$ in Eq. (3.154), in the low energy limit the direct $\gamma\pi\pi$ interaction derived from $\overline{\mathcal{A}}_\mu$-$\overline{\mathcal{A}}_\nu$ and $\overline{\mathcal{V}}_\mu$-$\overline{\mathcal{V}}_\nu$ two-point functions is expressed as

$$\begin{aligned}
&\Gamma^\mu_{\gamma\pi\pi}(p;q,k) \\
&\quad = \frac{1}{\widetilde{F}(\bar{q};T)\widetilde{F}(\bar{k};T)} \Big[q_\nu \, \Pi_\perp^{\mu\nu}(q_0,\bar{q};T) - k_\nu \, \Pi_\perp^{\mu\nu}(k_0,\bar{k};T) \\
&\qquad\qquad - \frac{1}{2}(q-k)_\nu \, \Pi_\parallel^{\mu\nu}(p_0,\bar{p};T) \Big] \ ,
\end{aligned} \tag{3.160}$$

where q and k denote outgoing momenta of the pions and $p=(q+k)$ is the photon momentum. $\widetilde{F}$ is the wave function renormalization of the background $\bar{\pi}$ field given in Eq. (3.133). Note that each pion is on its mass shell, so that $q_0 = v_\pi(\bar{q})\bar{q}$ and $k_0 = v_\pi(\bar{k})\bar{k}$. To define extensions of the parameter a, we consider the soft limit of the photon: $p_0 \to 0$ and $\bar{p} \to 0$. [#11] Then the pion momenta become

$$q_0 = -k_0 \ , \quad \bar{q} = -\bar{k} \ . \tag{3.161}$$

[#10] In Ref. [13], it was assumed that the scale dependent $F_\pi(\mu)$ agrees with the scale-independent parameter F_π in the ChPT at $\mu=0$ to obtain $F_\pi(\mu=0) = 86.4 \pm 9.7\,\mathrm{MeV}$. Here, we simply use this value to get a rough estimate of the value of the parameter $a(0)$ as done in Ref. [13].

[#11] Note that we take the $p_0 \to 0$ limit first and then take the $\bar{p} \to 0$ limit for definiteness. This is natural since the form factor in the vacuum is defined for space-like momentum of the photon.

Note that while only two components $\Pi_\perp^t$ and $\Pi_\perp^s$ appear in $q_\nu\,\Pi_\perp^{\mu\nu}$ or $k_\nu\,\Pi_\perp^{\mu\nu}$, $(q-k)_\nu\,\Pi_\parallel^{\mu\nu}$ includes all four components $\Pi_\parallel^t$, $\Pi_\parallel^s$, $\Pi_\parallel^L$ and $\Pi_\parallel^T$. Since the tree part of $\Pi_\parallel^L$ and $\Pi_\parallel^T$ is $-2z_2\,p^2$ which vanishes at $p^2=0$, it is natural to use only $\Pi_\parallel^t$ and $\Pi_\parallel^s$ to define the extensions of the parameter a. By including these two parts only, the temporal and the spatial components of $\Gamma^\mu_{\gamma\pi\pi}$ are given by

$$\begin{aligned}
\Gamma^0_{\gamma\pi\pi}(0;q,-q) &= \frac{2q_0}{\widetilde{F}^2(\bar{q};T)}\Big[\Pi_\perp^t(q_0,\bar{q};T)-\frac{1}{2}\Pi_\parallel^t(0,0;T)\Big],\\
\Gamma^i_{\gamma\pi\pi}(0;q,-q) &= \frac{-2q_i}{\widetilde{F}^2(\bar{q};T)}\Big[\Pi_\perp^s(q_0,\bar{q};T)-\frac{1}{2}\Pi_\parallel^s(0,0;T)\Big].
\end{aligned}\tag{3.162}$$

Thus we define $a^t(T)$ and $a^s(T)$ as

$$\begin{aligned}
a^t(\bar{q};T) &= \frac{\Pi_\parallel^t(0,0;T)}{\Pi_\perp^t(q_0,\bar{q};T)}\ ,\\
a^s(\bar{q};T) &= \frac{\Pi_\parallel^s(0,0;T)}{\Pi_\perp^s(q_0,\bar{q};T)}\ .
\end{aligned}\tag{3.163}$$

Here we should stress again that the pion momentum q_μ is on mass-shell: $q_0=v_\pi(\bar{q})\bar{q}$.

In the HLS at one-loop level the above $a^t(\bar{q};T)$ and $a^s(\bar{q};T)$ are expressed as

$$a^t(\bar{q};T) = a(0)\left[1+\frac{\overline{\Pi}_\parallel^t(0,0;T)-a(0)\overline{\Pi}_\perp^t(\bar{q},\bar{q};T)}{a(0)F_\pi^2(0;T)}\right],\tag{3.164}$$

$$a^s(\bar{q};T) = a(0)\left[1+\frac{\overline{\Pi}_\parallel^s(0,0;T)-a(0)\overline{\Pi}_\perp^s(\bar{q},\bar{q};T)}{a(0)F_\pi^2(0;T)}\right],\tag{3.165}$$

where $a(0)$ is defined in Eq. (3.156). From Eq. (3.93) together with Eq. (B.9) we obtain $\overline{\Pi}_\parallel^t$ and $\overline{\Pi}_\parallel^s$ in Eqs. (3.164) and (3.165) as

$$\begin{aligned}
\overline{\Pi}_\parallel^t(0,0;T) &= \overline{\Pi}_\parallel^s(0,0;T)\\
&= -\frac{N_f}{4}\left[a^2\tilde{I}_2(T)-\tilde{J}_1^2(M_\rho;T)+2\tilde{J}^0_{-1}(M_\rho;T)\right].
\end{aligned}\tag{3.166}$$

Let us study the temperature dependence of the parameters $a^t(\bar{q};T)$ and $a^s(\bar{q};T)$ in the low temperature region. At low temperature $T\ll M_\rho$ the functions $\tilde{J}_1^2(M_\rho;T)$ and $\tilde{J}^0_{-1}(M_\rho;T)$ are suppressed by $e^{-M_\rho/T}$. Then the dominant contribution is given by $\tilde{I}_2(T)=T^2/12$. Combining this with Eq. (3.138) and (3.139), we obtain

$$a^t\simeq a^s\simeq a(0)\left[1+\frac{N_f}{12}\left(1-\frac{a^2}{4a(0)}\right)\frac{T^2}{F_\pi^2(0;T)}\right],\tag{3.167}$$

where a is the parameter renormalized at the scale $\mu=M_\rho$, while $a(0)$ is defined in Eq. (3.156). We expect that the temperature dependences of the parameters are small in the low temperature region, so that we use the values of parameters at $T=0$ to estimate the hadronic thermal

corrections to $a^{t,s}(T)$. By using $F_\pi(0) = 86.4\,\mathrm{MeV}$, $a(0) \simeq 2.31$ given in Eq. (3.159) and $a(M_\rho) = 1.38$ obtained through the Wilsonian matching for $(\Lambda_{\rm QCD}\,,\,\Lambda) = (0.4\,,\,1.1)\,\mathrm{GeV}$ and $N_f = 3$ [13], a^t and a^s in Eq. (3.167) are evaluated as

$$a^t \simeq a^s \simeq a(0)\left[1 + 0.066\left(\frac{T}{50\,\mathrm{MeV}}\right)^2\right] . \tag{3.168}$$

This implies that the parameters a^t and a^s increase with temperature in the low temperature region. However, since the correction is small, we conclude that the vector dominance is well satisfied in the low temperature region.

3.5 Lorentz Non-invariance at Bare Level

As stressed in section 2.3, the Lorentz non-invariance appears in the bare HLS theory as a result of including the intrinsic temperature dependence. Once the temperature dependence of the bare parameters is determined through the matching with QCD mentioned above, the parameters appearing in the hadronic corrections pick up the intrinsic thermal effects through the RGEs. Then the HLS Lagrangian in hot and/or dense matter is generically Lorentz non-invariant. Its explicit form was presented in Ref. [22]. In this section, we show the HLS Lagrangian at leading order including the effects of Lorentz non-invariance.

Two matrix valued variables $\xi_L(x)$ and $\xi_R(x)$ are now parameterized as [#12]

$$\xi_{L,R}(x) = e^{i\sigma(x)/F_\sigma^t} e^{\mp i\pi(x)/F_\pi^t}, \tag{3.169}$$

where F_π^t and F_σ^t denote the temporal components of the decay constant of π and σ, respectively. The leading order Lagrangian with Lorentz non-invariance can be written as [22]

$$\begin{aligned}\mathcal{L} = &\left[(F_\pi^t)^2 u_\mu u_\nu + F_\pi^t F_\pi^s\,(g_{\mu\nu} - u_\mu u_\nu)\right]\mathrm{tr}\,[\hat\alpha_\perp^\mu \hat\alpha_\perp^\nu] \\ &+ \left[(F_\sigma^t)^2 u_\mu u_\nu + F_\sigma^t F_\sigma^s\,(g_{\mu\nu} - u_\mu u_\nu)\right]\mathrm{tr}\left[\hat\alpha_\parallel^\mu \hat\alpha_\parallel^\nu\right] \\ &+ \left[-\frac{1}{g_L^2}\,u_\mu u_\alpha g_{\nu\beta} - \frac{1}{2g_T^2}\,(g_{\mu\alpha}g_{\nu\beta} - 2u_\mu u_\alpha g_{\nu\beta})\right]\mathrm{tr}\left[V^{\mu\nu}V^{\alpha\beta}\right] .\end{aligned} \tag{3.170}$$

Here F_π^s denote the spatial pion decay constant and similarly F_σ^s for the σ. The rest frame of the medium is specified by $u^\mu = (1, \vec{0})$ and $V_{\mu\nu}$ is the field strength of V_μ. g_L and g_T correspond in medium to the HLS gauge coupling g. The parametric π and σ velocities are defined by [20]

$$V_\pi^2 = F_\pi^s/F_\pi^t, \qquad V_\sigma^2 = F_\sigma^s/F_\sigma^t. \tag{3.171}$$

[#12] The wave function renormalization constant of the pion field is given by the temporal component of the pion decay constant [70]. Thus we normalize π and σ by F_π^t and F_σ^t respectively.

The axial-vector and vector current correlators at bare level are constructed in terms of bare parameters and are divided into the longitudinal and transverse components:

$$G^{\mu\nu}_{A,V} = P^{\mu\nu}_L G^L_{A,V} + P^{\mu\nu}_T G^T_{A,V}, \tag{3.172}$$

where $P^{\mu\nu}_{L,T}$ are the longitudinal and transverse projection operators, respectively. The axial-vector current correlator in the HLS around the matching scale Λ is well described by the following forms with the bare parameters [22, 15]:

$$\begin{aligned} G^L_{A(\mathrm{HLS})}(p_0,\bar{p}) &= \frac{p^2 F^t_{\pi,\mathrm{bare}} F^s_{\pi,\mathrm{bare}}}{-[p_0^2 - V^2_{\pi,\mathrm{bare}}\bar{p}^2]} - 2p^2 z^L_{2,\mathrm{bare}}, \\ G^T_{A(\mathrm{HLS})}(p_0,\bar{p}) &= -F^t_{\pi,\mathrm{bare}} F^s_{\pi,\mathrm{bare}} - 2\left(p_0^2 z^L_{2,\mathrm{bare}} - \bar{p}^2 z^T_{2,\mathrm{bare}}\right) \ , \end{aligned} \tag{3.173}$$

where $z^L_{2,\mathrm{bare}}$ and $z^T_{2,\mathrm{bare}}$ are the coefficients of the higher order terms, and $V_{\pi,\mathrm{bare}}$ is the bare pion velocity related to $F^t_{\pi,\mathrm{bare}}$ and $F^s_{\pi,\mathrm{bare}}$ as

$$V^2_{\pi,\mathrm{bare}} = \frac{F^s_{\pi,\mathrm{bare}}}{F^t_{\pi,\mathrm{bare}}} \ . \tag{3.174}$$

Similarly, two components of the vector current correlator have the following forms:

$$\begin{aligned} &G^L_{V(\mathrm{HLS})}(p_0,\bar{p}) \\ &= \frac{p^2\, F^t_{\sigma,\mathrm{bare}} F^s_{\sigma,\mathrm{bare}} \left(1 - 2g^2_{L,\mathrm{bare}} z^L_{3,\mathrm{bare}}\right)}{-\left[p_0^2 - V^2_{\sigma,\mathrm{bare}}\bar{p}^2 - M^2_{\rho,\mathrm{bare}}\right]} - 2p^2 z^L_{1,\mathrm{bare}} + \mathcal{O}(p^4) \ , \\ &G^T_{V(\mathrm{HLS})}(p_0,\bar{p}) \\ &= \frac{F^t_{\sigma,\mathrm{bare}} F^s_{\sigma,\mathrm{bare}}}{-\left[p_0^2 - V^2_{T,\mathrm{bare}}\bar{p}^2 - M^2_{\rho,\mathrm{bare}}\right]} \\ &\qquad \times \left[p_0^2\left(1 - 2g^2_{L,\mathrm{bare}} z^L_{3,\mathrm{bare}}\right) - V^2_{T,\mathrm{bare}}\bar{p}^2\left(1 - 2g^2_{T,\mathrm{bare}} z^T_{3,\mathrm{bare}}\right)\right] \\ &\quad - 2\left(p_0^2 z^L_{1,\mathrm{bare}} - \bar{p}^2 z^T_{1,\mathrm{bare}}\right) + \mathcal{O}(p^4) \ , \end{aligned} \tag{3.175}$$

where $z^L_{1,2,\mathrm{bare}}$ and $z^T_{1,2,\mathrm{bare}}$ denote the coefficients of the higher order terms. In the above expressions, the bare vector meson mass in the rest frame, $M_{\rho,\mathrm{bare}}$, is

$$M^2_{\rho,\mathrm{bare}} \equiv g^2_{L,\mathrm{bare}} F^t_{\sigma,\mathrm{bare}} F^s_{\sigma,\mathrm{bare}} \ . \tag{3.176}$$

We define the bare parameters a^t_{bare} and a^s_{bare} as

$$a^t_{\mathrm{bare}} = \left(\frac{F^t_{\sigma,\mathrm{bare}}}{F^t_{\pi,\mathrm{bare}}}\right)^2, \quad a^s_{\mathrm{bare}} = \left(\frac{F^s_{\sigma,\mathrm{bare}}}{F^s_{\pi,\mathrm{bare}}}\right)^2, \tag{3.177}$$

and the bare σ and transverse ρ velocities as

$$V^2_{\sigma,\mathrm{bare}} = \frac{F^s_{\sigma,\mathrm{bare}}}{F^t_{\sigma,\mathrm{bare}}}, \quad V^2_{T,\mathrm{bare}} = \frac{g^2_{L,\mathrm{bare}}}{g^2_{T,\mathrm{bare}}}. \tag{3.178}$$

Chapter 4

Wilsonian Matching at Finite Temperature

In order to fix full temperature dependences of physical quantities, parameters of the EFT should be determined through the matching to QCD. In this chapter, we perform the matching in the Wilsonian sense discussed in section 2.2. The bare parameters of HLS theory at zero temperature were originally determined in Ref. [64], where they matched the bare HLS theory to the operator product expansion (OPE). The Wilsonian matching well describes the real world (for details, see Ref. [13]). Applying this scheme to QCD in hot/dense matter, we obtain the bare parameters in terms of the OPE variables like expectation value of an operator. The intrinsic thermal effects of bare parameters are caused by the temperature dependences of such condensations at a matching scale, which are evaluated in the *thermal* vacuum.

In this chapter, we briefly review the Wilsonian matching proposed at zero temperature. Next we extend the Wilsonian matching to the version at non-zero temperature in order to incorporate the intrinsic thermal effect into the bare parameters of the HLS Lagrangian following Refs. [14, 15, 16, 17, 18]. There we also discuss the effect of Lorentz symmetry violation at bare level.

4.1 Wilsonian Matching Conditions at $T = 0$

The Wilsonian matching proposed in Ref. [64] is done by matching the axial-vector and vector current correlators derived from the HLS with those by the operator product expansion (OPE)

in QCD at the matching scale Λ. [#1] The axial-vector and vector current correlators in the OPE up until $\mathcal{O}(1/Q^6)$ at $T=0$ are expressed as [73]

$$\begin{aligned} G_A^{(\mathrm{QCD})}(Q^2) &= \frac{1}{8\pi^2}\left(\frac{N_c}{3}\right)\left[-\left(1+\frac{3(N_c^2-1)}{8N_c}\,\frac{\alpha_s}{\pi}\right)\ln\frac{Q^2}{\mu^2}\right. \\ &\quad \left. +\frac{\pi^2}{N_c}\frac{\left\langle\frac{\alpha_s}{\pi}G_{\mu\nu}G^{\mu\nu}\right\rangle}{Q^4}+\frac{\pi^3}{N_c}\frac{96(N_c^2-1)}{N_c^2}\left(\frac{1}{2}+\frac{1}{3N_c}\right)\frac{\alpha_s\left\langle\bar{q}q\right\rangle^2}{Q^6}\right], \quad (4.1) \\ G_V^{(\mathrm{QCD})}(Q^2) &= \frac{1}{8\pi^2}\left(\frac{N_c}{3}\right)\left[-\left(1+\frac{3(N_c^2-1)}{8N_c}\,\frac{\alpha_s}{\pi}\right)\ln\frac{Q^2}{\mu^2}\right. \\ &\quad \left. +\frac{\pi^2}{N_c}\frac{\left\langle\frac{\alpha_s}{\pi}G_{\mu\nu}G^{\mu\nu}\right\rangle}{Q^4}-\frac{\pi^3}{N_c}\frac{96(N_c^2-1)}{N_c^2}\left(\frac{1}{2}-\frac{1}{3N_c}\right)\frac{\alpha_s\left\langle\bar{q}q\right\rangle^2}{Q^6}\right], \quad (4.2) \end{aligned}$$

where μ is the renormalization scale of QCD and we wrote the N_c-dependences explicitly (see, e.g., Ref. [74]). In the HLS the same correlators are well described by the tree contributions with including $\mathcal{O}(p^4)$ terms when the momentum is around the matching scale, $Q^2\sim\Lambda^2$:

$$\begin{aligned} G_A^{(\mathrm{HLS})}(Q^2) &= \frac{F_\pi^2(\Lambda)}{Q^2}-2z_2(\Lambda)\,, \quad (4.3) \\ G_V^{(\mathrm{HLS})}(Q^2) &= \frac{F_\sigma^2(\Lambda)}{M_\rho^2(\Lambda)+Q^2}\left[1-2g^2(\Lambda)z_3(\Lambda)\right]-2z_1(\Lambda)\,, \quad (4.4) \end{aligned}$$

where we defined the bare ρ mass $M_\rho(\Lambda)$ as

$$M_\rho^2(\Lambda)\equiv g^2(\Lambda)F_\sigma^2(\Lambda)\,. \quad (4.5)$$

We require that current correlators in the HLS in Eqs. (4.3) and (4.4) can be matched with those in QCD in Eqs. (4.1) and (4.2). Of course, this matching cannot be made for any value of Q^2, since the Q^2-dependences of the current correlators in the HLS are completely different from those in the OPE: In the HLS the derivative expansion (in *positive* power of Q) is used, and the expressions for the current correlators are valid in the low energy region. The OPE, on the other hand, is an asymptotic expansion (in *negative* power of Q), and it is valid in the high energy region. Since we calculate the current correlators in the HLS including the first non-leading order [$\mathcal{O}(p^4)$], we expect that we can match the correlators with those in the OPE up until the first derivative [#2]. Then we obtain the following Wilsonian matching

[#1] For the validity of the expansion in the HLS the matching scale Λ must be smaller than the chiral symmetry breaking scale Λ_χ as we stressed in chapter 2.

[#2] If there exists an overlapping area around a scale $\widetilde{\Lambda}$, we can require the matching condition at that $\widetilde{\Lambda}$. In fact, the Wilsonian matching at $T=0$ in three flavor QCD was shown to give several predictions in remarkable agreement with experiments [64, 13]. This strongly suggests that there exists such an overlapping region. As discussed in Ref. [13], $\Lambda\ll\Lambda_{\mathrm{HLS}}$ can be justified in the large N_c limit, where Λ_{HLS} denotes the scale at

conditions [64, 13] [#3]

$$\frac{F_\pi^2(\Lambda)}{\Lambda^2} = \frac{1}{8\pi^2}\left(\frac{N_c}{3}\right)\left[1 + \frac{3(N_c^2-1)}{8N_c}\frac{\alpha_s}{\pi} + \frac{2\pi^2}{N_c}\frac{\left\langle \frac{\alpha_s}{\pi} G_{\mu\nu}G^{\mu\nu}\right\rangle}{\Lambda^4} + \frac{288\pi(N_c^2-1)}{N_c^3}\left(\frac{1}{2}+\frac{1}{3N_c}\right)\frac{\alpha_s\left\langle\bar{q}q\right\rangle^2}{\Lambda^6}\right], \tag{4.6}$$

$$\frac{F_\sigma^2(\Lambda)}{\Lambda^2}\frac{\Lambda^4[1-2g^2(\Lambda)z_3(\Lambda)]}{({M_\rho}^2(\Lambda)+\Lambda^2)^2} = \frac{1}{8\pi^2}\left(\frac{N_c}{3}\right)\left[1 + \frac{3(N_c^2-1)}{8N_c}\frac{\alpha_s}{\pi} + \frac{2\pi^2}{N_c}\frac{\left\langle \frac{\alpha_s}{\pi} G_{\mu\nu}G^{\mu\nu}\right\rangle}{\Lambda^4} - \frac{288\pi(N_c^2-1)}{N_c^3}\left(\frac{1}{2}-\frac{1}{3N_c}\right)\frac{\alpha_s\left\langle\bar{q}q\right\rangle^2}{\Lambda^6}\right], \tag{4.7}$$

$$\frac{F_\pi^2(\Lambda)}{\Lambda^2} - \frac{F_\sigma^2(\Lambda)[1-2g^2(\Lambda)z_3(\Lambda)]}{{M_\rho}^2(\Lambda)+\Lambda^2} - 2[z_2(\Lambda)-z_1(\Lambda)] = \frac{4\pi(N_c^2-1)}{N_c^2}\frac{\alpha_s\left\langle\bar{q}q\right\rangle^2}{\Lambda^6}\ . \tag{4.8}$$

The above three equations (4.8), (4.6) and (4.7) are the Wilsonian matching conditions proposed in Ref. [64]. They determine several bare parameters of the HLS without much ambiguity. Especially, the first condition (4.6) determines the ratio $F_\pi(\Lambda)/\Lambda$ directly from QCD.

4.2 Wilsonian Matching Conditions at $T \neq 0$

Next we consider the extension of the matching conditions at $T = 0$ to the analysis in hot matter. We present the matching conditions to determine the bare pion decay constants including the effect of Lorentz symmetry breaking at the bare level which is caused by the intrinsic thermal effect.

Case neglecting Lorentz non-invariance

Before going to study the matching conditions taking into account the possible Lorentz non-invariance, we consider a naive extension of the matching to the one in hot matter: Strictly speaking, inclusion of intrinsic effects generates Lorentz non-invariance in bare theory. Then

which the HLS theory breaks down (see also section 3.1). We obtain the matching conditions in $N_c = 3$ by extrapolating the conditions in large N_c. As we mentioned above, the success of the Wilsonian matching at $T = 0$ with taking the matching scale as $\Lambda = 1.1\,\mathrm{GeV}$ shows that this extrapolation is valid.

[#3] One might think that there appear corrections from ρ and/or π loops in the left-hand-sides of Eqs. (4.6) and (4.7). However, such corrections are of higher order in the present counting scheme, and thus we neglect them here at $Q^2 \sim \Lambda^2$. In the low-energy scale we incorporate the loop effects into the correlators.

we should include the Lorentz non-scalar operators such as $\bar{q}\gamma_\mu D_\nu q$ into the form of the current correlators derived from the OPE [75], which leads to a difference between the temporal and spatial bare pion decay constants. However, we neglect the contributions from these operators since they give a small correction compared with the main term $1+\frac{\alpha_s}{\pi}$ as discussed in Ref. [14]. This implies that the Lorentz symmetry breaking effect in the bare pion decay constant is small, $F^t_{\pi,\mathrm{bare}} \simeq F^s_{\pi,\mathrm{bare}}$ [15]. In fact, we will see below that the difference between them is caused by an existence of a higher spin operator in the OPE side of the Wilsonian matching condition. Thus to a good approximation we determine the pion decay constant at non-zero temperature through the matching condition at zero temperature, putting possible temperature dependences into the gluonic and quark condensates [14, 15]:

$$\frac{F_\pi^2(\Lambda;T)}{\Lambda^2} = \frac{1}{8\pi^2}\Big[1+\frac{\alpha_s}{\pi}+\frac{2\pi^2}{3}\frac{\langle\frac{\alpha_s}{\pi}G_{\mu\nu}G^{\mu\nu}\rangle_T}{\Lambda^4}+\pi^3\frac{1408}{27}\frac{\alpha_s\langle\bar{q}q\rangle_T^2}{\Lambda^6}\Big]\ . \tag{4.9}$$

Through this condition the temperature dependences of the quark and gluonic condensates determine the intrinsic temperature dependences of the bare parameter $F_\pi(\Lambda;T)$, which is then converted into those of the on-shell parameter $F_\pi(\mu=0;T)$ through the Wilsonian RGEs.

Case taking into account Lorentz non-invariance

Now we study the Wilsonian matching conditions for the bare pion decay constants without Lorentz invariance. From the bare Lagrangian with replacement of the parameters by the bare ones in Eq. (3.170), the current correlator at the matching scale is constructed as Eq. (3.173):

$$\begin{aligned} G^L_{A(\mathrm{HLS})}(q_0,\bar{q}) &= \frac{F^t_{\pi,\mathrm{bare}}F^s_{\pi,\mathrm{bare}}}{-[q_0^2-V^2_{\pi,\mathrm{bare}}\bar{q}^2]}-2z^L_{2,\mathrm{bare}}\ , \\ G^T_{A(\mathrm{HLS})}(q_0,\bar{q}) &= -\frac{F^t_{\pi,\mathrm{bare}}F^s_{\pi,\mathrm{bare}}}{q^2}-2\frac{q_0^2z^L_{2,\mathrm{bare}}-\bar{q}^2z^T_{2,\mathrm{bare}}}{q^2}\ , \end{aligned} \tag{4.10}$$

where $V_{\pi,\mathrm{bare}} = F^s_{\pi,\mathrm{bare}}/F^t_{\pi,\mathrm{bare}}$ is the bare pion velocity. To perform the matching, we regard $G_A^{L,T}$ as functions of $-q^2$ and $\bar{q}^2$ instead of q_0 and $\bar{q}$, and expand $G_A^{L,T}$ in a Taylor series around $\bar{q}=|\vec{q}|=0$ in $\bar{q}^2/(-q^2)$ as follows:

$$\begin{aligned} G^L_A(-q^2,\bar{q}^2) &= G^{L(0)}_A(-q^2)+G^{L(1)}_A(-q^2)\bar{q}^2+\cdots, \\ G^T_A(-q^2,\bar{q}^2) &= G^{T(0)}_A(-q^2)+G^{T(1)}_A(-q^2)\bar{q}^2+\cdots. \end{aligned} \tag{4.11}$$

In the following, we determine the bare pion velocity $V_{\pi,\mathrm{bare}}$ from $G_A^{L(0)}$ and $G_A^{L(1)}$ via the matching.

Expanding $G_A^{(\mathrm{HLS})L}$ in Eq. (4.10) in terms of $\bar{q}^2/(-q^2)$, we obtain

$$G_A^{(\mathrm{HLS})L(0)}(-q^2) = \frac{F^t_{\pi,\mathrm{bare}} F^s_{\pi,\mathrm{bare}}}{-q^2} - 2z^L_{2,\mathrm{bare}} \ , \tag{4.12}$$

$$G_A^{(\mathrm{HLS})L(1)}(-q^2) = \frac{F^t_{\pi,\mathrm{bare}} F^s_{\pi,\mathrm{bare}}(1 - V^2_{\pi,\mathrm{bare}})}{(-q^2)^2}. \tag{4.13}$$

On the other hand, the correlator $G_A^{\mu\nu}$ in the QCD sector to be given in OPE is more involved. Our strategy goes as follows. Since the effect of Lorentz non-invariance in medium has been more extensively studied in dense matter, we first examine the form of the relevant correlator in dense matter following Refs. [76, 77]. The current correlator $\tilde{G}^{\mu\nu}$ constructed from the current defined by

$$J^{(q)}_\mu = \bar{q}\gamma_\mu q, \quad \text{or} \quad J^{(q)}_{5\mu} = \bar{q}\gamma_5\gamma_\mu q, \tag{4.14}$$

is given by

$$\begin{aligned}
\tilde{G}^{\mu\nu}(q_0, \bar{q}) = (q^\mu q^\nu - g^{\mu\nu}q^2)\Big[-c_0 \ln|Q^2| + \sum_n \frac{1}{Q^n} A^{n,n}\Big] \\
+ \sum_{\tau=2}\sum_{k=1} [-g^{\mu\nu} q^{\mu_1} q^{\mu_2} + g^{\mu\mu_1} q^\nu q^{\mu_2} + q^\mu q^{\mu_1} g^{\nu\mu_2} + g^{\mu\mu_1} g^{\nu\mu_2} Q^2] \\
\times q^{\mu_3} \cdots q^{\mu_{2k}} \frac{2^{2k}}{Q^{4k+\tau-2}} A^{2k+\tau,\tau}_{\mu_1\cdots\mu_{2k}} \\
+ \sum_{\tau=2}\sum_{k=1} \Big[g^{\mu\nu} - \frac{q^\mu q^\nu}{q^2}\Big] q^{\mu_1} \cdots q^{\mu_{2k}} \frac{2^{2k}}{Q^{4k+\tau-2}} C^{2k+\tau,\tau}_{\mu_1\cdots\mu_{2k}},
\end{aligned} \tag{4.15}$$

where $Q^2 = -q^2$. $\tau = d - s$ denotes the twist, and $s = 2k$ is the number of spin indices of the operator of dimension d. Here $A^{n,n}$ represents the contribution from the Lorentz invariant operators such as $A^{4,4} = \frac{1}{6}\left\langle \frac{\alpha_s}{\pi} G^2 \right\rangle_\rho$. $A^{2k+\tau,\tau}_{\mu_1\cdots\mu_{2k}}$ and $C^{2k+\tau,\tau}_{\mu_1\cdots\mu_{2k}}$ are the residual Wilson coefficient times matrix element of dimension d and twist τ; e.g., $A^{6,2}_{\mu_1\mu_2\mu_3\mu_4}$ is given by

$$A^{6,2}_{\mu_1\mu_2\mu_3\mu_4} = i\left\langle \mathcal{S}T\left(\bar{q}\gamma_{\mu_1} D_{\mu_2} D_{\mu_3} D_{\mu_4} q\right)\right\rangle_\rho \ , \tag{4.16}$$

where we have introduced the symbol $\mathcal{S}T$ which makes the operators symmetric and traceless with respect to the Lorentz indices. The general tensor structure of the matrix element of $A^{2k+\tau,\tau}_{\mu_1\cdots\mu_{2k}}$ is given in Ref. [75]. For $k = 2$, it takes the following form:

$$\begin{aligned}
A_{\alpha\beta\lambda\sigma} = \Big[p_\alpha p_\beta p_\lambda p_\sigma - \frac{p^2}{8}(p_\alpha p_\beta g_{\lambda\sigma} + p_\alpha p_\lambda g_{\beta\sigma} + p_\alpha p_\sigma g_{\lambda\beta} + p_\beta p_\lambda g_{\alpha\sigma} \\
+ p_\beta p_\sigma g_{\alpha\lambda} + p_\lambda p_\sigma g_{\alpha\beta}) + \frac{p^4}{48}(g_{\alpha\beta} g_{\lambda\sigma} + g_{\alpha\lambda} g_{\beta\sigma} + g_{\alpha\sigma} g_{\beta\lambda})\Big] A_4
\end{aligned} \tag{4.17}$$

For $\tau = 2$ with arbitrary k, we have [76]:

$$\begin{aligned}
A^{2k+2,2}_{2k} &= C^q_{2,2k} A^q_{2k} + C^{\mathrm{G}}_{2,2k} A^{\mathrm{G}}_{2k} \\
C^{2k+2,2}_{2k} &= C^q_{L,2k} A^q_{2k} + C^{\mathrm{G}}_{L,2k} A^{\mathrm{G}}_{2k} \ ,
\end{aligned} \tag{4.18}$$

where $C^q_{2,2k} = 1 + \mathcal{O}(\alpha_s)$, $C^{q,\mathrm{G}}_{L,2k} \sim \mathcal{O}(\alpha_s)$ and $C^{\mathrm{G}}_{2,2k} \sim \mathcal{O}(\alpha_s)$ (with the superscripts q and G standing respectively for quark and gluon) are the Wilson coefficients in the OPE [76]. The quantities A^q_n and A^{G}_n are defined by

$$\begin{aligned} A^q_n(\mu) &= 2\int_0^1 dx\ x^{n-1}[q(x,\mu) + \bar{q}(x,\mu)] \\ A^{\mathrm{G}}_n(\mu) &= 2\int_0^1 dx\ x^{n-1}G(x,\mu)\ , \end{aligned} \tag{4.19}$$

where $q(x,\mu)$ and $G(x,\mu)$ are quark and gluon distribution functions respectively. We observe that (4.15) consists of three classes of terms: One is independent of the background, i.e., density in this case, the second consists of scalar operators with various condensates $\langle\mathcal{O}\rangle_\rho$ and the third is made up of non-scalar operators whose matrix elements in dense matter could not be simply expressed in terms of various condensates $\langle\mathcal{O}\rangle_\rho$.

It is clear that Eq. (4.15) is a general expression that can be applied equally well to heat-bath systems. Thus we can simply transcribe (4.15) to the temperature case by replacing the condensates $\langle\mathcal{O}\rangle_\rho$ by $\langle\mathcal{O}\rangle_T$ and the quantities $A^{2k+\tau,\tau}_{\mu_1\cdots\mu_{2k}}$ and $C^{2k+\tau,\tau}_{\mu_1\cdots\mu_{2k}}$ by the corresponding quantities in heat bath. (We show the matching condition on the bare pion velocity at finite density in Appendix F.) The higher the twist of operators becomes, the more these operators are suppressed since the dimensions of such operators become higher and the power of $1/Q^2$ appear. Thus in the following, we restrict ourselves to contributions from the twist 2 ($\tau = 2$) operators. Then the temperature-dependent correlator can be written as

$$\begin{aligned} G^{\mu\nu}_A(q_0,\bar{q}) = (q^\mu q^\nu - g^{\mu\nu}q^2)\frac{-1}{4}\Bigg[&\frac{1}{2\pi^2}\left(1+\frac{\alpha_s}{\pi}\right)\ln\left(\frac{Q^2}{\mu^2}\right) + \frac{1}{6Q^4}\left\langle\frac{\alpha_s}{\pi}G^2\right\rangle_T \\ &- \frac{2\pi\alpha_s}{Q^6}\left\langle\left(\bar{u}\gamma_\mu\gamma_5\lambda^a u - \bar{d}\gamma_\mu\gamma_5\lambda^a d\right)^2\right\rangle_T \\ &- \frac{4\pi\alpha_s}{9Q^6}\left\langle\left(\bar{u}\gamma_\mu\lambda^a u + \bar{d}\gamma_\mu\lambda^a d\right)\sum_q^{u,d,s}\bar{q}\gamma^\mu\lambda^a q\right\rangle_T\Bigg] \\ &+ [-g^{\mu\nu}q^{\mu_1}q^{\mu_2} + g^{\mu\mu_1}q^\nu q^{\mu_2} + q^\mu q^{\mu_1}g^{\nu\mu_2} + g^{\mu\mu_1}g^{\nu\mu_2}Q^2] \\ &\times [\frac{4}{Q^4}A^{4,2}_{\mu_1\mu_2} + \frac{16}{Q^8}q^{\mu_3}q^{\mu_4}A^{6,2}_{\mu_1\mu_2\mu_3\mu_4}]\ , \end{aligned} \tag{4.20}$$

where $G^{\mu\nu}_A$ is constructed from the axial-vector current associated with the iso-triplet channel defined by

$$J_{5\mu} = \frac{1}{2}(\bar{u}\gamma_5\gamma_\mu u - \bar{d}\gamma_5\gamma_\mu d), \tag{4.21}$$

and we keep terms only up to the order of $1/Q^8$ for $A^{2k+2,2}_{\mu_1\cdots\mu_{2k}}$. The λ^a denote the $SU(3)$ color matrices normalized as $\mathrm{tr}[\lambda^a\lambda^b] = 2\delta^{ab}$. Here we have dropped the terms with $C^{2k+2,2}_{\mu_1\cdots\mu_{2k}}$ in the

non-scalar operators since they are of higher order in both $1/(Q^2)^n$ and α_s compared to the terms in the first line of Eq. (4.20). The temperature dependence of $A^{4,2}_{\mu_1\mu_2}$ and $A^{6,2}_{\mu_1\mu_2\mu_3\mu_4}$, implicit in Eq. (4.20), will be specified below.

In order to effectuate the Wilsonian matching, we should in principle evaluate the condensates and temperature-dependent matrix elements of the non-scalar operators in Eq.(4.20) at the given scale Λ and temperature T in terms of QCD variables only. This can presumably be done on lattice. However no complete information is as yet available from model-independent QCD calculations. We are therefore compelled to resort to indirect methods and we adopt here an approach borrowed from QCD sum-rule calculations.

Let us first evaluate the quantities that figure in Eq.(4.20) at low temperature. In low temperature regime, only the pions are expected to be thermally excited. In the dilute pion-gas approximation, $\langle\mathcal{O}\rangle_T$ is evaluated as

$$\langle\mathcal{O}\rangle_T \simeq \langle\mathcal{O}\rangle_0 + \sum_{a=1}^{3}\int \frac{d^3p}{2\epsilon(2\pi)^3}\langle\pi^a(\vec{p})|\mathcal{O}|\pi^a(\vec{p})\rangle n_B(\epsilon/T), \tag{4.22}$$

where $\epsilon = \sqrt{\vec{p}^2 + m_\pi^2}$ and n_B is the Bose-Einstein distribution. As an example, we consider the operator of $(\tau, s) = (2, 4)$ that contributes to both $G_A^{L(0)}$ and $G_A^{L(1)}$. Noting that $G_A^L(q_0, \bar{q}) = G_{A00}/\bar{q}^2$, we evaluate $G_{A00}(q_0, \bar{q})$.

$$\begin{aligned} G_{\rm A00}^{(\tau=2,s=4)}(q_0,\bar{q}) &= \frac{3}{4}\int \frac{d^3p}{2\epsilon(2\pi)^3}\frac{16}{Q^8}[-q^\alpha q^\beta + g^{0\alpha}q^0q^\beta + q^0q^\alpha g^{0\beta} + g^{0\alpha}g^{0\beta}Q^2] \\ &\quad \times q^\lambda q^\sigma A^{6,2(\pi)}_{\alpha\beta\lambda\sigma} n_B(\epsilon/T), \end{aligned} \tag{4.23}$$

where $A^{6,2(\pi)}_{\alpha\beta\lambda\sigma}$ is given by [#4]

$$\begin{aligned} A^{6,2(\pi)}_{\alpha\beta\lambda\sigma} = \Big[& p_\alpha p_\beta p_\lambda p_\sigma - \frac{p^2}{8}(p_\alpha p_\beta g_{\lambda\sigma} + p_\alpha p_\lambda g_{\beta\sigma} + p_\alpha p_\sigma g_{\lambda\beta} + p_\beta p_\lambda g_{\alpha\sigma} \\ & + p_\beta p_\sigma g_{\alpha\lambda} + p_\lambda p_\sigma g_{\alpha\beta}) + \frac{p^4}{48}(g_{\alpha\beta}g_{\lambda\sigma} + g_{\alpha\lambda}g_{\beta\sigma} + g_{\alpha\sigma}g_{\beta\lambda})\Big] A_4^\pi \ , \end{aligned} \tag{4.24}$$

where A_4^π carries the temperature dependence. Taking $m_\pi^2 = 0$, we see that the terms with p^2 and p^4 in Eq. (4.24) are zero.

From Eqs. (4.20), (4.22) and (4.23), we obtain

$$\begin{aligned} G_A^{({\rm OPE})L(0)}(-q^2) &= \frac{-1}{3}g^{\mu\nu}G^{({\rm OPE})(0)}_{A,\mu\nu} \\ &= \frac{-1}{4}\left[\frac{1}{2\pi^2}\left(1+\frac{\alpha_s}{\pi}\right)\ln\left(\frac{Q^2}{\mu^2}\right) + \frac{1}{6Q^4}\left\langle\frac{\alpha_s}{\pi}G^2\right\rangle_T\right. \end{aligned}$$

[#4] For the general tensor structure of the matrix elements with a polarized spin-one target, say, along the beam direction in scattering process, see Ref. [78].

$$
\begin{aligned}
&- \frac{2\pi\alpha_s}{Q^6}\left\langle\left(\bar{u}\gamma_\mu\gamma_5\lambda^a u - \bar{d}\gamma_\mu\gamma_5\lambda^a d\right)^2\right\rangle_T \\
&- \frac{4\pi\alpha_s}{9Q^6}\left\langle\left(\bar{u}\gamma_\mu\lambda^a u + \bar{d}\gamma_\mu\lambda^a d\right)\sum_q^{u,d,s}\bar{q}\gamma^\mu\lambda^a q\right\rangle_T\Bigg] \\
&+ \frac{\pi^2}{30}\frac{T^4}{Q^4}A_2^{\pi(u+d)} - \frac{16\pi^4}{63}\frac{T^6}{Q^6}A_4^{\pi(u+d)}. \qquad (4.25)
\end{aligned}
$$

$G_A^{(\mathrm{OPE})L(1)}$ takes the following form

$$
G_A^{(\mathrm{OPE})L(1)} = \frac{32}{105}\pi^4\frac{T^6}{Q^8}A_4^{\pi(u+d)}. \qquad (4.26)
$$

We now proceed to estimate the pion velocity by matching to QCD.

First we consider the matching between $G_A^{(\mathrm{HLS})L(0)}$ and $G_A^{(\mathrm{OPE})L(0)}$. From Eqs. (4.12) and (4.25), we obtain

$$
\begin{aligned}
(-q^2)\frac{d}{d(-q^2)}G_A^{(\mathrm{HLS})L(0)} &= -\frac{F^t_{\pi,\mathrm{bare}}F^s_{\pi,\mathrm{bare}}}{Q^2}, \\
(-q^2)\frac{d}{d(-q^2)}G_A^{(\mathrm{OPE})L(0)} &= \frac{-1}{8\pi^2}\left[\left(1+\frac{\alpha_s}{\pi}\right) + \frac{2\pi^2}{3}\frac{\langle\frac{\alpha_s}{\pi}G^2\rangle_T}{Q^4} + \pi^3\frac{1408}{27}\frac{\alpha_s\langle\bar{q}q\rangle_T^2}{Q^6}\right] \\
&\quad - \frac{\pi^2}{15}\frac{T^4}{Q^4}A_2^{\pi(u+d)} + \frac{16\pi^4}{21}\frac{T^6}{Q^6}A_4^{\pi(u+d)}. \qquad (4.27)
\end{aligned}
$$

Matching them at $Q^2 = \Lambda^2$, we obtain

$$
\begin{aligned}
\frac{F^t_{\pi,\mathrm{bare}}F^s_{\pi,\mathrm{bare}}}{\Lambda^2} &= \frac{1}{8\pi^2}\left[\left(1+\frac{\alpha_s}{\pi}\right) + \frac{2\pi^2}{3}\frac{\langle\frac{\alpha_s}{\pi}G^2\rangle_T}{\Lambda^4} + \pi^3\frac{1408}{27}\frac{\alpha_s\langle\bar{q}q\rangle_T^2}{\Lambda^6}\right] \\
&\quad + \frac{\pi^2}{15}\frac{T^4}{\Lambda^4}A_2^{\pi(u+d)} - \frac{16\pi^4}{21}\frac{T^6}{\Lambda^6}A_4^{\pi(u+d)} \\
&\equiv G_0. \qquad (4.28)
\end{aligned}
$$

Next we consider the matching between $G_A^{(\mathrm{HLS})L(1)}$ and $G_A^{(\mathrm{OPE})L(1)}$. From Eqs. (4.13) and (4.26), we have

$$
\frac{F^t_{\pi,\mathrm{bare}}F^s_{\pi,\mathrm{bare}}(1-V^2_{\pi,\mathrm{bare}})}{\Lambda^2} = \frac{32}{105}\pi^4\frac{T^6}{\Lambda^6}A_4^{\pi(u+d)}. \qquad (4.29)
$$

Noting that the right-hand-side of this expression is positive, we verify that

$$
V_{\pi,\mathrm{bare}} < 1 \qquad (4.30)
$$

which is consistent with the causality.

The bare pion velocity can be obtained by dividing Eq. (4.29) with Eq. (4.28). What we obtain is the deviation from the speed of light:

$$
\delta_{\mathrm{bare}} \equiv 1 - V^2_{\pi,\mathrm{bare}} = \frac{1}{G_0}\frac{32}{105}\pi^4\frac{T^6}{\Lambda^6}A_4^{\pi(u+d)}. \qquad (4.31)
$$

This should be valid at low temperature. We note that the Lorentz non-invariance does not appear when we consider the operator with $s = 2$, and that the operator with $s = 4$ generates the Lorentz non-invariance. This is consistent with the fact that G_A^L including up to the operator with $s = 2$ is expressed as the function of only Q^2 [79]. Equation (4.31) implies that the intrinsic temperature dependence starts from the $\mathcal{O}(T^6)$ contribution. On the other hand, the hadronic thermal correction to the pion velocity starts from the $\mathcal{O}(T^4)$. [There are $\mathcal{O}(T^2)$ corrections to $[f_\pi^t]^2$ and $[f_\pi^t f_\pi^s]$, but they are canceled with each other in the pion velocity. See subsection 3.4.2.] Thus the hadronic thermal effect is dominant in low temperature region.

Chapter 5

Vector Manifestation in Hot Matter

The vector manifestation (VM) is a new pattern for Wigner realization of chiral symmetry, in sharp contrast to the standard scenario of chiral symmetry restoration. In order to clarify the difference between the standard scenario and the VM, we consider the chiral representations of the low-lying mesons.

In the broken phase, the eigenstate of the chiral representation under $SU(3)_L \times SU(3)_R$ does not generally agree with the mass eigenstate due to the existence of the Nambu-Goldstone bosons: There exists a representation mixing. Then the scalar, pseudoscalar, vector and axial-vector mesons belong to the following representations [80, 81]:

$$\begin{aligned} |s\rangle &= |(3,3^*) \oplus (3^*,3)\rangle, \\ |\pi\rangle &= |(3,3^*) \oplus (3^*,3)\rangle \sin\psi + |(1,8) \oplus (8,1)\rangle \cos\psi, \\ |\rho\rangle &= |(1,8) \oplus (8,1)\rangle, \\ |A_1\rangle &= |(3,3^*) \oplus (3^*,3)\rangle \cos\psi - |(1,8) \oplus (8,1)\rangle \sin\psi, \end{aligned} \tag{5.1}$$

where ψ denotes the mixing angle and is determined as $\psi \simeq 45\,^\circ$.

Now we consider the chiral symmetry restoration, where it is expected that the above representation mixing is dissolved. From Eq. (5.1), one can easily see that there are two possibilities for pattern of chiral symmetry restoration. One possible pattern is the case where $\cos\psi \to 0$ when we approach the critical point. In this case, the pion belongs to $|(3,3^*)\oplus(3^*,3)\rangle$ and becomes the chiral partner of the scalar meson:

$$\begin{aligned} |\pi\rangle &= |(3,3^*) \oplus (3^*,3)\rangle, \\ |s\rangle &= |(3,3^*) \oplus (3^*,3)\rangle \qquad \text{for} \quad \cos\psi \to 0. \end{aligned} \tag{5.2}$$

The vector and axial-vector mesons are in the same multiplet $|(1,8) \oplus (8,1)\rangle$. This is the standard scenario of chiral symmetry restoration.

Another possibility is the case where $\sin\psi \to 0$ when we approach the critical point [21]. In this case, the pion belongs to pure $|(1,8)\oplus(8,1)\rangle$ and so its chiral partner is the vector meson:

$$\begin{aligned} |\pi\rangle &= |(1,8)\oplus(8,1)\rangle, \\ |\rho\rangle &= |(1,8)\oplus(8,1)\rangle \qquad \text{for} \quad \sin\psi \to 0. \end{aligned} \tag{5.3}$$

The scalar meson joins with the axial-vector meson in the same representation $|(3,3^*)\oplus(3^*,3)\rangle$. This is nothing but the VM of chiral symmetry.

In order to formulate the VM, we need a theory including both pions and vector mesons. One of such theories is the one based on the hidden local symmetry (HLS). In the following sections, we will show how the VM is formulated at the critical point in the framework of the HLS theory. We also study the predictions of the VM in hot matter.

5.1 Conditions for Bare Parameters

In this section, we summarize the conditions for the bare parameters obtained in Ref. [14] through the Wilsonian matching at the critical temperature.

5.1.1 Case with Lorentz invariance

We consider the Wilsonian matching near the chiral symmetry restoration point. Here we assume that the order of the chiral phase transition is second or weakly first order, and thus the quark condensate becomes zero continuously for $T \to T_c$. First, note that the Wilsonian matching condition (4.9) provides

$$\frac{F_\pi^2(\Lambda;T_c)}{\Lambda^2} = \frac{1}{8\pi^2}\Big[1+\frac{\alpha_s}{\pi}+\frac{2\pi^2}{3}\frac{\langle\frac{\alpha_s}{\pi}G_{\mu\nu}G^{\mu\nu}\rangle_{T_c}}{\Lambda^4}\Big] \neq 0\ , \tag{5.4}$$

which implies that the matching with QCD dictates

$$F_\pi^2(\Lambda;T_c) \neq 0 \tag{5.5}$$

even at the critical temperature where the on-shell pion decay constant vanishes by adding the quantum corrections through the RGE including the quadratic divergence [64] and hadronic thermal corrections, as we will show in section 5.3. As was shown in Ref. [22] for the VM in dense matter, the Lorentz non-invariant version of the VM conditions for the bare parameters

are obtained by the requirement of the equality between the axial-vector and vector current correlators in the HLS, which is valid also in hot matter (see next subsection):

$$a^t_{\rm bare} \equiv \left(\frac{F^t_{\sigma,\rm bare}}{F^t_{\pi,\rm bare}}\right)^2 \overset{T\to T_c}{\to} 1, \quad a^s_{\rm bare} \equiv \left(\frac{F^s_{\sigma,\rm bare}}{F^s_{\pi,\rm bare}}\right)^2 \overset{T\to T_c}{\to} 1, \tag{5.6}$$

$$g_{T,\rm bare} \overset{T\to T_c}{\to} 0, \quad g_{L,\rm bare} \overset{T\to T_c}{\to} 0, \tag{5.7}$$

where $a^t_{\rm bare}, a^s_{\rm bare}, g_{T,\rm bare}$ and $g_{L,\rm bare}$ are the extensions of the parameters $a_{\rm bare}$ and $g_{\rm bare}$ in the bare Lagrangian with the Lorentz symmetry breaking effect included as in Appendix A of Ref. [22].

When we use the conditions for the parameters $a^{t,s}$ in Eq. (5.6) and the above result that the Lorentz symmetry violation between the bare pion decay constants $F^{t,s}_{\pi,\rm bare}$ is small, we can easily show that the Lorentz symmetry breaking effect between the temporal and spatial bare sigma decay constants is also small, $F^t_{\sigma,\rm bare} \simeq F^s_{\sigma,\rm bare}$. While we cannot determine the ratio $g_{L,\rm bare}/g_{T,\rm bare}$ through the Wilsonian matching since the transverse mode of vector meson decouples near the critical temperature. [#1] However this implies that the transverse mode is irrelevant for the quantities studied in this thesis. Therefore in the present analysis, we set $g_{L,\rm bare} = g_{T,\rm bare}$ for simplicity and use the Lorentz invariant Lagrangian at bare level. In the low temperature region, the intrinsic temperature dependences are negligible, so that we also use the Lorentz invariant Lagrangian at bare level as in the analysis by the ordinary chiral Lagrangian in Ref. [71].

At the critical temperature, the axial-vector and vector current correlators derived in the OPE agree with each other for any value of Q^2. Thus we require that these current correlators in the HLS are equal at the critical temperature for any value of Q^2 around Λ^2. As we discussed above, we start from the Lorentz invariant bare Lagrangian even in hot matter, and then the axial-vector current correlator $G^{(\rm HLS)}_A$ and the vector current correlator $G^{(\rm HLS)}_V$ are expressed by the same forms as those at zero temperature with the bare parameters having the intrinsic temperature dependences:

$$G^{(\rm HLS)}_A(Q^2;T) \;=\; \frac{F^2_\pi(\Lambda;T)}{Q^2} - 2z_2(\Lambda;T),$$

[#1] In Ref. [22], the analysis including the Lorentz non-invariance at bare HLS theory was carried out. Due to the equality between axial-vector and vector current correlators, $(g_{L,\rm bare}, g_{T,\rm bare}) \to (0,0)$ is satisfied when we approach the critical point. This implies that at the bare level the longitudinal mode becomes the real NG boson and couples to the vector current correlator, while the transverse mode decouples. Furthermore $g_L \to 0$ is a fixed point for the RGE [17]. Thus in any energy scale the transverse mode decouples from the vector current correlator. For details, see next subsection.

$$G_V^{(\mathrm{HLS})}(Q^2;T) \;=\; \frac{F_\sigma^2(\Lambda;T)[1-2g^2(\Lambda;T)z_3(\Lambda;T)]}{{M_\rho}^2(\Lambda;T)+Q^2} - 2z_1(\Lambda;T). \tag{5.8}$$

By taking account of the fact $F_\pi^2(\Lambda;T_c)\neq 0$ derived from the Wilsonian matching condition given in Eq. (5.4), the requirement $G_A^{(\mathrm{HLS})}=G_V^{(\mathrm{HLS})}$ is satisfied only if the following conditions are met [14]:

$$g(\Lambda;T) \;\overset{T\to T_c}{\to}\; 0, \tag{5.9}$$

$$a(\Lambda;T)=F_\sigma^2(\Lambda;T)/F_\pi^2(\Lambda;T) \;\overset{T\to T_c}{\to}\; 1, \tag{5.10}$$

$$z_1(\Lambda;T)-z_2(\Lambda;T) \;\overset{T\to T_c}{\to}\; 0. \tag{5.11}$$

Note that the intrinsic thermal effects act on the parameters in such a way that they become the values of Eqs. (5.9)-(5.11).

Through the Wilsonian matching at non-zero temperature mentioned above, the parameters appearing in the hadronic thermal corrections calculated in section 3.2 have the intrinsic temperature dependences: F_π, a and g appearing there should be regarded as

$$\begin{aligned} F_\pi &\equiv F_\pi(\mu=0;T)\ , \\ a &\equiv a\left(\mu=M_\rho(T);T\right)\ , \\ g &\equiv g\left(\mu=M_\rho(T);T\right)\ , \end{aligned} \tag{5.12}$$

where M_ρ is determined from the on-shell condition:

$$M_\rho^2\equiv M_\rho^2(T)=a(\mu=M_\rho;T)g^2(\mu=M_\rho;T)F_\pi^2(\mu=M_\rho;T)\ . \tag{5.13}$$

From the RGEs for g and a in Eqs.(C.29) and (C.28), we find that $(g,a)=(0,1)$ is the fixed point. Therefore, Eqs. (5.9) and (5.10) imply that g and a at the on-shell of the vector meson take the same values:

$$\begin{aligned} a\left(\mu=M_\rho(T);T\right) &\overset{T\to T_c}{\longrightarrow} 1\ , \\ g\left(\mu=M_\rho(T);T\right) &\overset{T\to T_c}{\longrightarrow} 0\ , \end{aligned} \tag{5.14}$$

where the parametric vector meson mass $M_\rho(T)$ is determined from the condition (5.13). The above conditions with Eq. (5.13) imply that $M_\rho(T)$ also vanishes:

$$M_\rho(T) \;\overset{T\to T_c}{\longrightarrow}\; 0\ . \tag{5.15}$$

5.1.2 Case without Lorentz invariance

In this subsection, we start from the Lagrangian with Lorentz non-invariance, and requiring that the axial-vector current correlator be equal to the vector current correlator at the critical point, we obtain the conditions for the bare parameters. Then we show that the conditions are satisfied in any energy scale, which is protected by the fixed point of the RGEs.

First we show the Lorentz non-invariant version of the conditions satisfied at the critical temperature for the bare parameters, following Ref. [22] where the conditions for the current correlators with the bare parameters in dense matter were presented. We consider the matching near the critical temperature. At the chiral phase transition point, the axial-vector and vector current correlators must agree with each other: $G^L_{A(\mathrm{HLS})} = G^L_{V(\mathrm{HLS})}$ and $G^T_{A(\mathrm{HLS})} = G^T_{V(\mathrm{HLS})}$. These equalities are satisfied for any values of p_0 and $\bar{p}$ around the matching scale only if the following conditions are met:

$$\begin{aligned} &a^t_{\mathrm{bare}} \to 1, \quad a^s_{\mathrm{bare}} \to 1, \\ &g_{L,\mathrm{bare}} \to 0, \quad g_{T,\mathrm{bare}} \to 0 \quad \text{for } T \to T_c. \end{aligned} \tag{5.16}$$

This implies that at bare level the longitudinal mode of the vector meson becomes the real NG boson and couples to the vector current correlator, while the transverse mode decouples.

Next, we show that the conditions for the bare parameters for $T \to T_c$ are satisfied in any energy scale and that this is protected by the fixed point of the RGEs.

It was shown that the HLS gauge coupling $g = 0$ is a fixed point of the RGE for g at one-loop level [60, 64]. The existence of the fixed point $g = 0$ is guaranteed by the gauge invariance. This is easily understood from the fact that the gauge field is normalized as $V_\mu = g\rho_\mu$. In the present case without Lorentz symmetry, the gauge field is normalized by g_L as $V_\mu = g_L\rho_\mu$ and thus $g_L = 0$ becomes a fixed point of the RGE for g_L.

Provided that $g_L = 0$ is a fixed point, we can show that $a^t = a^s = 1$ is also a fixed point of the coupled RGEs for a^t and a^s as follows: We start from the bare theory defined at a scale Λ with $a^t_{\mathrm{bare}} = a^s_{\mathrm{bare}} = 1$ (and $g_L = 0$). The parameters a^t and a^s at $(\Lambda - \delta\Lambda)$ are calculated by integrating out the modes in $[\Lambda - \delta\Lambda, \Lambda]$. They are obtained from the two-point functions of $\mathcal{A}_\mu$ and $\mathcal{V}_\mu$, denoted by $\Pi^{\mu\nu}_\perp$ and $\Pi^{\mu\nu}_\parallel$. We decompose these functions into

$$\Pi^{\mu\nu}_{\perp,\parallel} = u^\mu u^\nu \Pi^t_{\perp,\parallel} + (g^{\mu\nu} - u^\mu u^\nu)\Pi^s_{\perp,\parallel} + P^{\mu\nu}_L \Pi^L_{\perp,\parallel} + P^{\mu\nu}_T \Pi^T_{\perp,\parallel}, \tag{5.17}$$

where $u^\mu u^\nu$, $(g^{\mu\nu} - u^\mu u^\nu)$, $P^{\mu\nu}_L$ and $P^{\mu\nu}_T$ denote the temporal, spatial, longitudinal and transverse projection operators, respectively. The parameters a^t and a^s are defined by $a^t = \Pi^t_\parallel/\Pi^t_\perp$, $a^s =$

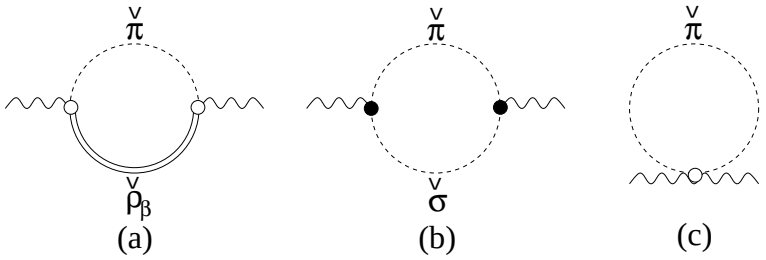

Figure 5.1: Diagrams for contributions to $\Pi_\perp^{\mu\nu}$ at one-loop level.

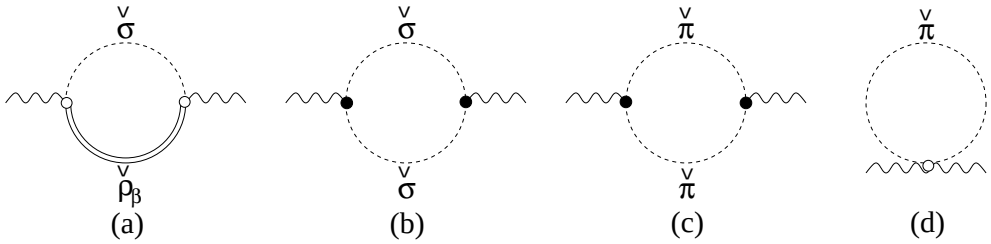

Figure 5.2: Diagrams for contributions to $\Pi_\parallel^{\mu\nu}$ at one-loop level.

$\Pi_\parallel^s/\Pi_\perp^s$ [16]. These expressions are further reduced to

$$a^t(\Lambda-\delta\Lambda) = a^t_{\rm bare} + \frac{1}{(F^t_{\pi,{\rm bare}})^2}\Big[\Pi^t_\parallel(\Lambda;\Lambda-\delta\Lambda) - a^t_{\rm bare}\Pi^t_\perp(\Lambda;\Lambda-\delta\Lambda)\Big],$$
$$a^s(\Lambda-\delta\Lambda) = a^s_{\rm bare} + \frac{1}{F^t_{\pi,{\rm bare}}F^s_{\pi,{\rm bare}}}\Big[\Pi^s_\parallel(\Lambda;\Lambda-\delta\Lambda) - a^s_{\rm bare}\Pi^s_\perp(\Lambda;\Lambda-\delta\Lambda)\Big], \quad (5.18)$$

where $\Pi^{t,s}_{\perp,\parallel}(\Lambda;\Lambda-\delta\Lambda)$ denotes the quantum correction obtained by integrating the modes out between $[\Lambda-\delta\Lambda,\Lambda]$. We show the diagrams for contributions to $\Pi_\perp^{\mu\nu}$ and $\Pi_\parallel^{\mu\nu}$ at one-loop level in Figs. 5.1 and 5.2. The contributions (a) in Fig. 5.1 and (a) in Fig. 5.2 are proportional to $g^2_{L,{\rm bare}}$. The contributions (c) in Fig. 5.1 and (d) in Fig. 5.2 are proportional to $(a^t_{\rm bare}-1)$. Taking $g_{L,{\rm bare}}=0$ and $a^t_{\rm bare}=a^s_{\rm bare}=1$, these contributions vanish. We note that σ (i.e., longitudinal vector meson) is massless and the chiral partner of pion at the critical temperature. Then the contributions (b) and (c) in Fig. 5.2 have a symmetry factor 1/2 respectively and are obviously equal to the contribution (b) in Fig. 5.1, i.e., $\Pi_\perp^{(b)\mu\nu} = \Pi_\parallel^{(b)+(c)\mu\nu}$. Thus from Eq. (5.18), we obtain

$$a^t(\Lambda-\delta\Lambda) = a^t_{\rm bare} = 1,$$
$$a^s(\Lambda-\delta\Lambda) = a^s_{\rm bare} = 1. \quad (5.19)$$

This implies that a^t and a^s are not renormalized at the scale $(\Lambda-\delta\Lambda)$. Similarly, we include the corrections below the scale $(\Lambda-\delta\Lambda)$ in turn, and find that a^t and a^s do not receive the

quantum corrections. Eventually we conclude that $a^t = a^s = 1$ is a fixed point of the RGEs for a^t and a^s.

From the above, we find that $(g_L, a^t, a^s) = (0, 1, 1)$ is a fixed point of the combined RGEs for g_L, a^t and a^s. Thus the VM condition is given by

$$\begin{aligned} g_L &\to 0, \\ a^t \to 1, \quad a^s &\to 1 \qquad \text{for } T \to T_c. \end{aligned} \tag{5.20}$$

The vector meson mass is never generated at the critical temperature since the quantum correction to M_ρ^2 is proportional to g_L^2. Because of $g_L \to 0$, the transverse vector meson at the critical point, in any energy scale, decouples from the vector current correlator. The VM condition for a^t and a^s leads to the equality between the π and σ (i.e., longitudinal vector meson) velocities:

$$\begin{aligned} (V_\pi/V_\sigma)^4 &= (F_\pi^s F_\sigma^t / F_\sigma^s F_\pi^t)^2 \\ &= a^t/a^s \overset{T\to T_c}{\to} 1. \end{aligned} \tag{5.21}$$

This is easily understood from a point of view of the VM since the longitudinal vector meson becomes the chiral partner of pion. We note that this condition $V_\sigma = V_\pi$ holds independently of the value of the bare pion velocity which is to be determined through the Wilsonian matching.

5.2 Vector Meson Mass

In this section, we briefly review that the vector manifestation (VM) in hot matter can be formulated following Ref. [16]. Including the intrinsic temperature dependences of the parameters near the critical temperature determined in the previous section, we show that the vector meson mass vanishes at the critical temperature.

Let us study the vector meson pole mass near the critical temperature. As shown in section 5.1, the parametric vector meson mass M_ρ vanishes at the critical temperature, which is driven by the intrinsic effects. Then, near the critical temperature we should take $M_\rho \ll T$ in Eq. (3.120) instead of $T \ll M_\rho$ which was taken to reach the expression in Eq. (3.121) in the low temperature region. Thus, by noting that

$$\begin{aligned} \tilde{G}_2(M_\rho; T) &\overset{M_\rho\to 0}{\to} \tilde{I}_2(T), \\ \tilde{J}_1^2(M_\rho; T) &\overset{M_\rho\to 0}{\to} \tilde{I}_2(T), \\ {M_\rho}^2 \tilde{F}_3^2(M_\rho; M_\rho; T) &\overset{M_\rho\to 0}{\to} 0, \end{aligned} \tag{5.22}$$

the pole mass of the vector meson at $T \lesssim T_c$ becomes

$$\begin{aligned} {m_\rho}^2(T) &= {M_\rho}^2 + N_f\, g^2 \frac{15-a^2}{12}\tilde{I}_2(T) \\ &= {M_\rho}^2 + N_f\, g^2 \frac{15-a^2}{144} T^2. \end{aligned} \tag{5.23}$$

In the vicinity of $a \simeq 1$ the hadronic thermal effect gives a positive correction, and then the vector meson pole mass is actually larger than the parametric mass M_ρ. However, the intrinsic temperature dependences of the parameters obtained in section 5.1 lead to $g \to 0$ and $M_\rho \to 0$ for $T \to T_c$. Then, from Eq. (5.23) we conclude that the pole mass of the vector meson m_ρ also vanishes at the critical temperature:

$$m_\rho(T) \to 0 \quad \text{for } T \to T_c\ . \tag{5.24}$$

This implies that the VM is formulated at the critical temperature in the framework of the HLS theory, which is consistent with the picture shown in Refs. [10, 3, 82, 4].

5.3 Pion Decay Constants

In this section, we show how the two decay constants, f_π^t and f_π^s, vanish at the critical temperature following Ref. [15].

As we discussed around Eq. (5.14), at the critical temperature the intrinsic thermal effects lead to $(g, a) \to (0, 1)$ which is a fixed point of the coupled RGEs. Then the RGE for F_π becomes

$$\mu \frac{d{F_\pi}^2}{d\mu} = \frac{N_f}{(4\pi)^2}\mu^2. \tag{5.25}$$

This RGE is easily solved and the relation between $F_\pi(\Lambda; T_c)$ and $F_\pi(0; T_c)$ is given by

$$F_\pi^2(0; T_c) = F_\pi^2(\Lambda; T_c) - \frac{N_f}{2(4\pi)^2}\Lambda^2. \tag{5.26}$$

Finally we obtain the pion decay constants as follows:

$$\begin{aligned} f_\pi^t \tilde{F} &= F_\pi^2(0; T) + \overline{\Pi}_\perp^t(\bar{p}, \bar{p}; T), \\ f_\pi^s \tilde{F} &= F_\pi^2(0; T) + \overline{\Pi}_\perp^s(\bar{p}, \bar{p}; T), \end{aligned} \tag{5.27}$$

where the second terms are the hadronic thermal effects. In the VM limit $(g, a) \to (0, 1)$ the temperature dependent parts become

$$\overline{\Pi}_\perp^t(\bar{p}, \bar{p}; T) \overset{T \to T_c}{\to} -\frac{N_f}{24}{T_c}^2, \quad \overline{\Pi}_\perp^s(\bar{p}, \bar{p}; T) \overset{T \to T_c}{\to} -\frac{N_f}{24}{T_c}^2. \tag{5.28}$$

From Eqs. (3.134), (5.27) and (5.28), the order parameter f_π becomes

$$f_\pi^2(\bar{p};T) \overset{T\to T_c}{\to} f_\pi^2(\bar{p};T_c) = F_\pi^2(0;T_c) - \frac{N_f}{24}T_c^2. \tag{5.29}$$

Since the order parameter f_π vanishes at the critical temperature, this implies

$$F_\pi^2(0;T) \overset{T\to T_c}{\to} F_\pi^2(0;T_c) = \frac{N_f}{24}T_c^2. \tag{5.30}$$

Thus we obtain

$$(f_\pi^t)^2 \overset{T\to T_c}{\to} 0, \quad f_\pi^t f_\pi^s \overset{T\to T_c}{\to} 0. \tag{5.31}$$

From Eq. (3.146) or equivalently Eq. (3.141), the above results imply that the temporal and spatial pion decay constants vanish simultaneously at the critical temperature [15]:

$$f_\pi^t(T_c) = f_\pi^s(T_c) = 0. \tag{5.32}$$

Comparing Eq. (5.29) with the expression in the low temperature region in Eq. (3.147) where the vector meson is decoupled, we find that the coefficient of ${T_c}^2$ is different by the factor $\frac{1}{2}$. This is the contribution from the σ-loop (longitudinal ρ-loop). In the low temperature region the π-loop effects give the dominant contributions to $f_\pi(T)$ and the ρ-loop effects are negligible. However *by the vector manifestation the ρ contributions become essentially equal to the one of π*, are then incorporated into $f_\pi(T)$ near the critical temperature.

5.4 Predictions of the Vector Manifestation

In this section, we summarize the predictions of the VM in hot matter studied in Refs. [14, 15, 16, 17, 18].

5.4.1 Critical temperature

In this subsection we estimate the value of the critical temperature T_c where the order parameter f_π^2 vanishes.

We first determine T_c by naively extending the expression (3.147) to the higher temperature region to get $T_c^{(\mathrm{hadron})} = 180\,\mathrm{MeV}$ for $N_f = 3$. However this naive extension is inconsistent with the chiral restoration in QCD since the axial vector and vector current correlators do not agree with each other at that temperature. As is stressed in Ref. [14], the disagreement between two correlators is cured by including the intrinsic thermal effect. As can be seen from Eq. (4.9), the intrinsic temperature dependence of the parameter F_π is determined from $\langle \frac{\alpha_s}{\pi} G_{\mu\nu} G^{\mu\nu} \rangle_T$

$\Lambda_{\rm QCD}$				0.30				0.35
Λ	0.8	0.9	1.0	1.1	0.8	0.9	1.0	1.1
T_c	0.20	0.20	0.22	0.23	0.20	0.21	0.22	0.24
$\Lambda_{\rm QCD}$				0.40				0.45
Λ	0.8	0.9	1.0	1.1	0.8	0.9	1.0	1.1
T_c	0.21	0.22	0.23	0.25	0.22	0.23	0.24	0.25

Table 5.1: Values of the critical temperature for several choices of $\Lambda_{\rm QCD}$ and Λ. The units of $\Lambda_{\rm QCD}, \Lambda$ and T_c are GeV.

and $\langle\bar{q}q\rangle_T$, and gives only a small contribution compared with the main term $1+\frac{\alpha_s}{\pi}$. However it is important that the parameters in the hadronic corrections have the intrinsic temperature dependences as $(a, g) \to (1, 0)$ for $T \to T_c$, which carry the information of QCD. Actually the inclusion of the intrinsic thermal effects provides the formula (5.29) for the pion decay constant at the critical temperature, in which the second term has an extra factor of $1/2$ compared with the one in Eq. (3.147).

In Ref. [14] we determined the critical temperature from $f_\pi(T_c) = 0$ and estimated the value which is dependent on the matching scale Λ: From Eq. (5.30) we obtain

$$T_c = \sqrt{\frac{24}{N_f}} F_\pi(0; T_c). \tag{5.33}$$

Using Eqs.(5.4) and (5.26) we get [14]

$$\frac{T_c}{\Lambda} = \sqrt{\frac{3}{N_f\pi^2}}\Big[1 + \frac{\alpha_s}{\pi} + \frac{2\pi^2}{3}\frac{\langle\frac{\alpha_s}{\pi}G_{\mu\nu}G^{\mu\nu}\rangle_{T_c}}{\Lambda^4} - \frac{N_f}{4}\Big]^{\frac{1}{2}}. \tag{5.34}$$

We would like to stress that the critical temperature is expressed in terms of the parameters appearing in the OPE. We evaluate the critical temperature for $N_f = 3$. The gluonic condensate at T_c is about half of the value at $T = 0$ [83, 4] and we use $\langle\frac{\alpha_s}{\pi}G_{\mu\nu}G^{\mu\nu}\rangle_{T_c} = 0.006\,\text{GeV}^4$. We show the predicted values of T_c for several choices of $\Lambda_{\rm QCD}$ and Λ in Table 5.1. Note that the Wilsonian matching describes the experimental results very well for $\Lambda_{QCD} = 0.4\,\text{GeV}$ and $\Lambda = 1.1\,\text{GeV}$ at $T = 0$ [13]. At non-zero temperature, however, the matching scale Λ may be dependent on temperature. The smallest Λ in Table 5.1 is determined by requiring $(2\pi^2/3)\,\langle\frac{\alpha_s}{\pi}G_{\mu\nu}G^{\mu\nu}\rangle/\Lambda^4 < 0.1$.

We should note that the above values may be changed when we adopt a different way to estimate the matrix elements of operators in the OPE side, e.g., an estimation with the dilute

pion gas approximation [75] or that by the lattice QCD calculation [84]. Even when we choose one way to estimate the matrix elements in the OPE, some temperature effects are supposed to be left out due to the truncation of the OPE to neglect higher order operators, inclusion of which will cause a small change of the above values of the critical temperature. The important point is that as a result of the Wilsonian matching, T_c is obtained as in Eq. (5.34) in terms of the quark and gluonic condensates, not hadronic degrees of freedom. It is expected that the value of T_c may become smaller than that obtained in this paper by including the higher order corrections.

5.4.2 Axial-vector and vector charge susceptibilities

In this subsection, we address the issue of what the relevant degrees of freedom can be at the chiral transition induced by high temperature and their possible implications on observables in heavy-ion physics. In doing this, we focus on the vector and axial-vector susceptibilities very near the critical temperature T_c. The issue of what happens at high density is discussed in [85].

Susceptibility is related with the fluctuation of a conserved quantity. The statistical expectation value of a conserved operator $\mathcal{O}$ is given by

$$\langle \mathcal{O} \rangle = \frac{\mathrm{Tr}[\mathcal{O} e^{-(\mathcal{H}-\mu\mathcal{O})/T}]}{Z}, \tag{5.35}$$

where $\mathcal{H}$ denotes the Hamiltonian of system and μ is the chemical potential associated with $\mathcal{O}$ and we define the partition function Z as

$$Z = \mathrm{Tr}[e^{-(\mathcal{H}-\mu\mathcal{O})/T}]. \tag{5.36}$$

The mean square deviation of $\mathcal{O}$ is

$$\begin{aligned} (\delta\mathcal{O})^2 &\equiv \langle \mathcal{O}^2 \rangle - \langle \mathcal{O} \rangle^2 \\ &= T\frac{\partial \langle \mathcal{O} \rangle}{\partial \mu}. \end{aligned} \tag{5.37}$$

Then we define the susceptibility of $\mathcal{O}$ as follows:

$$\begin{aligned} \chi(T) &\equiv \frac{\partial \langle \mathcal{O} \rangle}{\partial \mu}|_{\mu=0} \\ &= \int_0^{1/T} d\tau \int d^3\vec{x} \langle \mathcal{O}(\tau, \vec{x}) \mathcal{O}(0, \vec{0}) \rangle. \end{aligned} \tag{5.38}$$

Consider the vector isospin susceptibility (VSUS) χ_V and the axial-vector isospin susceptibility (ASUS) χ_A defined in terms of the vector charge density $V_0^a(x)$ and the axial-vector

charge density $A_0^a(x)$ by the Euclidean correlators:

$$\delta^{ab}\chi_V = \int_0^{1/T} d\tau \int d^3\vec{x}\langle V_0^a(\tau,\vec{x})V_0^b(0,\vec{0})\rangle_\beta, \tag{5.39}$$

$$\delta^{ab}\chi_A = \int_0^{1/T} d\tau \int d^3\vec{x}\langle A_0^a(\tau,\vec{x})A_0^b(0,\vec{0})\rangle_\beta \tag{5.40}$$

where $\langle\ \rangle_\beta$ denotes thermal average and

$$V_0^a \equiv \bar{\psi}\gamma^0\frac{\tau^a}{2}\psi, \quad A_0^a \equiv \bar{\psi}\gamma^0\gamma^5\frac{\tau^a}{2}\psi \tag{5.41}$$

with the quark field ψ and the τ^a Pauli matrix the generator of the flavor $SU(2)$.

The axial-vector susceptibility $\chi_A(T)$ and the vector susceptibility $\chi_V(T)$ for non-singlet currents [#2] are given by the 00-component of the axial-vector and vector current correlators in the static–low-momentum limit:

$$\begin{aligned}\chi_A(T) &= 2N_f \lim_{\vec{p}\to 0}\lim_{p_0\to 0}\left[G_A^{00}(p_0,\vec{p};T)\right] \ , \\ \chi_V(T) &= 2N_f \lim_{\vec{p}\to 0}\lim_{p_0\to 0}\left[G_V^{00}(p_0,\vec{p};T)\right] \ ,\end{aligned} \tag{5.42}$$

where we have included the normalization factor of $2N_f$. Using the current correlators given in Eqs. (3.100) and (3.110) and noting that $\lim_{p_0\to 0} P_L^{00} = \lim_{p_0\to 0}\vec{p}^2/p^2 = -1$, we can express $\chi_A(T)$ and $\chi_V(T)$ as

$$\begin{aligned}\chi_A(T) &= -2N_f \lim_{\vec{p}\to 0}\lim_{p_0\to 0}\left[\Pi_\perp^L(p_0,\vec{p};T) - \Pi_\perp^t(p_0,\vec{p};T)\right] \ , \\ \chi_V(T) &= -2N_f \lim_{\vec{p}\to 0}\lim_{p_0\to 0}\left[\frac{\Pi_V^t\left(\Pi_V^L + 2\Pi_{V\|}^L\right)}{\Pi_V^t - \Pi_V^L} + \Pi_\|^L\right] \ ,\end{aligned} \tag{5.43}$$

where for simplicity of notation, we have suppressed the argument $(p_0,\vec{p};T)$ in the right-hand-side of the expression for $\chi_V(T)$. In HLS theory at one-loop level, the susceptibilities read

$$\begin{aligned}\chi_A(T) &= 2N_f\left[F_\pi^2(0) + \lim_{\vec{p}\to 0}\lim_{p_0\to 0}\left\{\bar{\Pi}_\perp^t(p_0,\vec{p};T) - \bar{\Pi}_\perp^L(p_0,\vec{p};T)\right\}\right] \ , \\ \chi_V(T) &= -2N_f \lim_{\vec{p}\to 0}\lim_{p_0\to 0}\left[\frac{\left(a(0)F_\pi^2(0) + \bar{\Pi}_V^t\right)\left(\bar{\Pi}_V^L + 2\bar{\Pi}_{V\|}^L\right)}{a(0)F_\pi^2(0) + \bar{\Pi}_V^t - \bar{\Pi}_V^L} + \Pi_\|^L\right] \ ,\end{aligned} \tag{5.44}$$

where the parameter $a(0)$ is defined by (see section 5.4.3)

$$a(0) = \frac{\Pi_V^{(\mathrm{vac})t}(p_0=0,\bar{p}=0)}{F_\pi^2(0)} = \frac{\Pi_V^{(\mathrm{vac})s}(p_0=0,\bar{p}=0)}{F_\pi^2(0)} \ . \tag{5.45}$$

We show the tree and one-loop contributions to χ_A and χ_V in Figs. 5.3 and 5.4 It follows

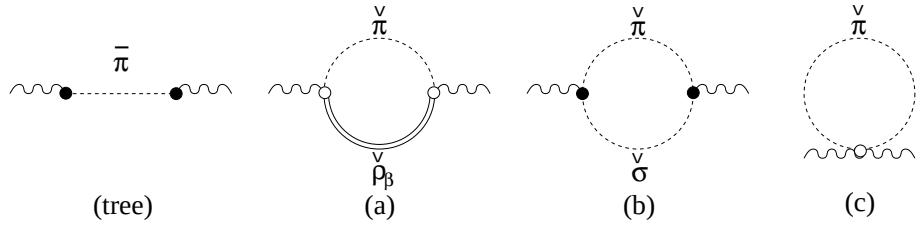

Figure 5.3: Diagrams for contributions to χ_A.

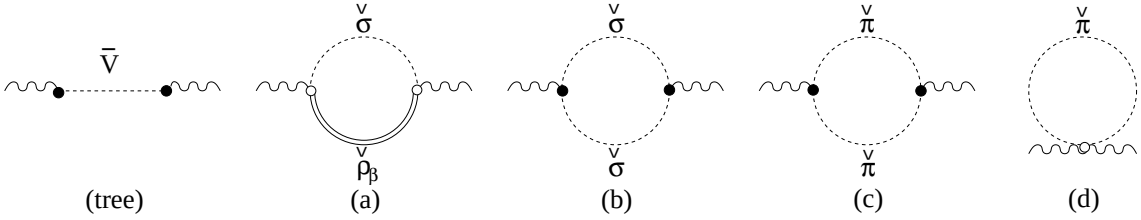

Figure 5.4: Diagrams for contributions to χ_V.

from the static–low-momentum limit of $(\bar{\Pi}^t_\perp - \bar{\Pi}^L_\perp)$ given in Eq. (G.8) that the axial-vector susceptibility $\chi_A(T)$ takes the form

$$\begin{aligned}\chi_A(T) &= 2N_f\Big[F_\pi^2(0) - N_f\widetilde{J}_1^2(0;T) + N_f a\,\widetilde{J}_1^2(M_\rho;T) \\ &\qquad - N_f\frac{a}{M_\rho^2}\left\{\widetilde{J}_{-1}^2(M_\rho;T) - \widetilde{J}_{-1}^2(0;T)\right\}\Big]\ . \end{aligned} \tag{5.46}$$

Near the critical temperature ($T \to T_c$), we have $M_\rho \to 0$, $a \to 1$ due to the intrinsic temperature dependence in the VM in hot matter [14]. Furthermore, from Eq. (5.30), we see that the parameter $F_\pi^2(0)$ approaches $\frac{N_f}{24}T_c^2$ for $T \to T_c$. Substituting these conditions into Eq. (5.46) and noting that

$$\lim_{M_\rho\to 0}\left[-\frac{1}{M_\rho^2}\left\{\widetilde{J}_{-1}^2(M_\rho;T) - \widetilde{J}_{-1}^2(0;T)\right\}\right] = \frac{1}{2}\widetilde{J}_1^2(0;T) = \frac{1}{24}T^2\ , \tag{5.47}$$

we obtain

$$\chi_A(T_c) = \frac{N_f^2}{6}T_c^2\ . \tag{5.48}$$

To obtain the vector susceptibility near the critical temperature, we first consider $a(0)F_\pi^2(0) + \bar{\Pi}^t_V$ appearing in the numerator of the first term in the right-hand-side of Eq. (5.44). Using

[#2]We will confine ourselves to non-singlet (that is, isovector) susceptibilities, so we won't specify the isospin structure from here on.

Eq. (G.9), we get for the static–low-momentum limit of $a(0)F_\pi^2(0) + \bar{\Pi}_V^t$ as

$$\lim_{\bar{p}\to 0}\lim_{p_0\to 0}\left[a(0)F_\pi^2(0) + \bar{\Pi}_V^t(p_0,\bar{p};T)\right] = a(0)F_\pi^2(0) - \frac{N_f}{4}\left[2\widetilde{J}^0_{-1}(M_\rho;T) - \widetilde{J}_1^2(M_\rho;T) + a^2\,\widetilde{J}_1^2(0;T)\right] . \tag{5.49}$$

From Eq. (3.158) we can see that $a(0) \to 1$ as $T \to T_c$ since $F_\sigma^2(M_\rho) \to F_\pi^2(0)$ and $M_\rho \to 0$. Furthermore, $F_\pi^2(0) \to \frac{N_f}{24}T_c^2$ as we have shown in Eq. (5.30). Then, the first term of Eq. (5.49) approaches $\frac{N_f}{24}T_c^2$. The second term, on the other hand, approaches $-\frac{N_f}{24}T_c^2$ as $M_\rho \to 0$ and $a \to 1$ for $T \to T_c$. Thus, we have

$$\lim_{\bar{p}\to 0}\lim_{p_0\to 0}\left[a(0)F_\pi^2(0) + \bar{\Pi}_V^t(p_0,\bar{p};T)\right] \underset{T\to T_c}{\longrightarrow} 0 . \tag{5.50}$$

This implies that only the second term $\Pi_\parallel^L$ in the right-hand-side of Eq. (5.44) contributes to the vector susceptibility near the critical temperature. Thus, taking $M_\rho \to 0$ and $a \to 1$, in Eq. (G.10), we obtain

$$\chi_V(T_c) = \frac{N_f^2}{6}T_c^2 , \tag{5.51}$$

which agrees with the axial-vector susceptibility in Eq. (5.48). This is a prediction, not an input condition, of the theory. For $N_f = 2$, we have

$$\chi_A(T_c) = \chi_V(T_c) = \frac{2}{3}T_c^2 . \tag{5.52}$$

The result $\chi_V(T_c) = \frac{2}{3}T_c^2$ is consistent with the lattice result as interpreted in [3]. It is interesting to note that the RPA result obtained in [3] in NJL model in terms of a quasi-quark-quasi-antiquark bubble is reproduced quantitatively by the one-loop graphs in HLS with the VM.

One might think that the VSUS diverges at T_c because of the massless ρ meson pole. However the resultant VSUS is finite, and it will imply that the screening mass of ρ meson is also finite.

It should be noticed that the pion pole effect does not contribute to the ASUS in Eq. (5.48) since the pion decay constant f_π^t vanishes at the critical temperature as we have shown in section 5.3, and that the contribution to the ASUS comes from the non-pole contribution expressed in Fig. 5.3. In three diagrams, the third diagram in Fig. 5.3(c) is proportional to $(1-a)$ and then it vanishes at the critical temperature due to the VM. Similarly, since the transverse ρ decouples at the critical point in the VM [21, 14], the first diagram in Fig. 5.3(a) does not contribute. Thus, the above result for the ASUS in Eq. (5.48) comes from only the contribution generated via the (longitudinal) vector meson plus pion loop [see Fig. 5.3(b)]. Similarly,

the vector meson pole effect to the VSUS vanishes at the critical temperature as shown in Eq. (5.50), and the contribution to the VSUS is generated via the pion loop [Fig. 5.4(c)] and the longitudinal vector meson loop [Fig. 5.4(b)]. [#3] Since the longitudinal vector meson becomes massless, degenerate with the pion as the chiral partner in the VM, loop contribution to the ASUS becomes identical to that to the VSUS. Thus, the massless vector meson predicted by the VM fixed point plays an essential role to obtain the above equality between the ASUS and the VSUS.

In the present analysis, our aim is to show the qualitative structure of the ASUS and the VSUS in the VM, i.e., *the equality between them is predicted by the VM*. In order to compare our qualitative results with the lattice result, we need to go beyond the one-loop approximation. We note here that there is a result from a hard thermal loop calculation which gives $\chi_V(T_c) \approx 1.3T_c^2$ [86]. However this result cannot be compared to ours for two reasons. First we need to sum higher loops in our formalism which may be done in random phase approximation as in [87]. Second, the perturbative QCD with a hard thermal loop approximation may not be valid in the temperature regime we are considering. Even at $T \gg T_c$, the situation is not clear as pointed out in Ref. [88].

5.4.3 Violation of vector dominance

In this subsection, we shed some light on the validity of the vector dominance (VD) of electromagnetic form factor of the pion near the critical temperature. In several analyses such as the one on the dilepton spectra in hot matter carried out in Ref. [6], the VD is assumed to be held even in the high temperature region. There are several analyses resulting in the dropping mass consistent with the VD, as shown in Refs. [89, 90]. On the other hand, the analysis done in Ref. [91] shows that the thermal vector meson mass goes up if the VD holds. Thus, it is interesting to study what the VM predicts on the VD. In the present analysis we present a new prediction of the VM in hot matter on the direct photon-π-π coupling which measures the validity of the VD of the electromagnetic form factor of the pion. We find that *the VM predicts a large violation of the VD at the critical temperature*. This indicates that the assumption of the VD may need to be weakened, at least in some amounts, for consistently including the effect of the dropping mass of the vector meson.

In Ref. [72] it has been shown that VD is accidentally satisfied in $N_f = 3$ QCD at zero temperature and zero density, and that it is largely violated in large N_f QCD when the

[#3] Note that the contribution from Fig. 5.4(a) vanishes since the transverse ρ decouples and that the one from Fig. 5.4(d) also vanishes since it is proportional to $(1 - a)$.

VM occurs. At non-zero temperature there exists the hadronic thermal correction to the parameters. Thus it is nontrivial whether or not the VD is realized in hot matter, especially near the critical temperature. Here we will show that the intrinsic temperature dependences of the parameters of the HLS Lagrangian play essential roles, and then the VD is largely violated near the critical temperature.

Let us study the validity of the VD near the critical temperature. As we have shown in section 5.3, near the critical temperature $\Pi_\perp^t$ and $\Pi_\perp^s$ in Eqs. (3.164) and (3.165) approach the following expressions:

$$\begin{aligned}\overline{\Pi}_\perp^t(\bar{q},\bar{q};T) &\overset{T\to T_c}{\to} -\frac{N_f}{24}T^2,\\ \overline{\Pi}_\perp^s(\bar{q},\bar{q};T) &\overset{T\to T_c}{\to} -\frac{N_f}{24}T^2.\end{aligned} \tag{5.53}$$

On the other hand, the functions $\Pi_\parallel^t$ and $\Pi_\parallel^s$ in Eq. (3.166) in the limit of $M_\rho/T \to 0$ and $a \to 1$ become

$$\bar{\Pi}_\parallel^t(0,0;T) = \bar{\Pi}_\parallel^s(0,0;T) \to -\frac{N_f}{2}\tilde{I}_2(T) = -\frac{N_f}{24}T^2 \ . \tag{5.54}$$

Furthermore, from Eq. (3.158), the parameter $a(0)$ approaches 1 in the limit of $M_\rho \to 0$ and $F_\sigma^2(M_\rho)/F_\pi^2(0) \to 1$:

$$a(0) \to 1 \ . \tag{5.55}$$

From the above limits in Eqs. (5.53), (5.54) and (5.55), the numerators of $a^t(\bar{q};T)$ and $a^s(\bar{q};T)$ in Eqs. (3.164) and (3.165) behave as

$$\begin{aligned}\overline{\Pi}_\parallel^t(0,0;T) - a(0)\overline{\Pi}_\perp^t(\bar{q},\bar{q};T) &\to 0,\\ \overline{\Pi}_\parallel^s(0,0;T) - a(0)\overline{\Pi}_\perp^s(\bar{q},\bar{q};T) &\to 0.\end{aligned} \tag{5.56}$$

Thus we obtain

$$a^t(\bar{q};T), a^s(\bar{q};T) \overset{T\to T_c}{\to} 1 \ , \tag{5.57}$$

namely, the vector dominance is largely violated near the critical temperature.

5.4.4 Pion velocity

In this subsection, we focus on the pion velocity at the critical temperature and study the quantum and hadronic thermal effects based on the VM. The pion velocity is one of the important quantities since it is a dynamical object, which controls the pion propagation in medium through the dispersion relation.

Non-renormalization theorem on pion velocity at T_c

As we mentioned in chapter 2, the intrinsic temperature dependence generates the effect of Lorentz symmetry breaking at bare level. Then how does the Lorentz non-invariance at bare level influence physical quantities? In order to make it clear, in this section we study the pion decay constants and the pion velocity near the critical temperature.

Following subsection 3.4.2, we define the on-shell of the pion from the pole of the longitudinal component G_A^L of the axial-vector current correlator. This pole structure is expressed by temporal and spatial components of the two-point function $\Pi_\perp^{\mu\nu}$. The temporal and spatial pion decay constants are expressed as follows [15, 16]:

$$\begin{aligned}(f_\pi^t(\bar{p};T))^2 &= \Pi_\perp^t(V_\pi\bar{p},\bar{p};T),\\ f_\pi^t(\bar{p};T)f_\pi^s(\bar{p};T) &= \Pi_\perp^s(V_\pi\bar{p},\bar{p};T),\end{aligned} \tag{5.58}$$

where the on-shell condition $p_0 \to V_\pi\bar{p}$ was taken. We divide the two-point function $\Pi_\perp^{\mu\nu}$ into two parts, zero temperature (vacuum) and non-zero temperature parts, as $\Pi_\perp^{\mu\nu} = \Pi_\perp^{(\mathrm{vac})\mu\nu} + \bar{\Pi}_\perp^{\mu\nu}$. The quantum correction is included in the vacuum part $\Pi_\perp^{(\mathrm{vac})\mu\nu}$, and the hadronic thermal correction is in $\bar{\Pi}_\perp^{\mu\nu}$. In the present perturbative analysis, we obtain the pion velocity as [16]

$$\begin{aligned}v_\pi^2(\bar{p};T) &= \frac{f_\pi^s(\bar{p};T)}{f_\pi^t(\bar{p};T)}\\ &= V_\pi^2 + \widetilde{\Pi}_\perp(V_\pi\bar{p},\bar{p}) + \frac{\bar{\Pi}_\perp^s(V_\pi\bar{p},\bar{p};T) - V_\pi^2\bar{\Pi}_\perp^t(V_\pi\bar{p},\bar{p};T)}{(F_\pi^t)^2},\end{aligned} \tag{5.59}$$

where $\widetilde{\Pi}_\perp(V_\pi\bar{p},\bar{p})$ denotes a possible finite renormalization effect. Note that the renormalization condition on V_π is determined as $\widetilde{\Pi}_\perp(V_\pi\bar{p},\bar{p})|_{\bar{p}=0} = 0$.

In the following, we study the quantum and hadronic corrections to the pion velocity for $T \to T_c$, on the assumption of the VM conditions (5.20). As we defined above, the two-point function associated with the pion velocity $v_\pi(\bar{p};T)$ is $\Pi_\perp^{\mu\nu}(p_0,\bar{p};T)$. The diagrams contributing to $\Pi_\perp^{\mu\nu}$ are shown in Fig. 5.1. As mentioned in subsection 5.1.2, diagram (a) is proportional to g_L and diagram (c) has the factor $(a^t - 1)$. Then these contributions vanish at the critical point. We consider the contribution from diagram (b) only.

Quantum correction at T_c

First we evaluate the quantum correction to the vacuum part $\Pi_\perp^{(\mathrm{vac})(\mathrm{b})\mu\nu}$. This is expressed as

$$\Pi_\perp^{(\mathrm{vac})(\mathrm{b})\mu\nu}(p_0,\bar{p}) = N_f\int\frac{d^nk}{i(2\pi)^n}\frac{\Gamma^\mu(k;p)\Gamma^\nu(-k;-p)}{[-k_0^2+V_\pi^2\bar{k}^2][M_\rho^2-(k_0-p_0)^2+V_\sigma^2|\vec{k}-\vec{p}|^2]}, \tag{5.60}$$

where Γ^μ denotes the $\bar{\mathcal{A}}\check{\pi}\check{\sigma}$ vertex as

$$\Gamma^\mu(k;p) = \frac{i}{2}\sqrt{a^t}\, g^\mu_{\bar{\mu}}[u^{\bar{\mu}}u^{\bar{\nu}} + V_\sigma^2(g^{\bar{\mu}\bar{\nu}} - u^{\bar{\mu}}u^{\bar{\nu}})](2k-p)_{\bar{\nu}}. \tag{5.61}$$

We note that the spatial component of this vertex Γ^i has an extra-factor V_σ^2 as compared with the temporal one. In the present analysis it is important to include the quadratic divergences to obtain the RGEs in the Wilsonian sense as we have already seen in chapter 4 and 5. In this section, when we evaluate four dimensional integral, we first integrate over k_0 from $-\infty$ to ∞. Then we carry out the integral over three-dimensional momentum $\vec{k}$ with three-dimensional cutoff Λ_3. In order to be consistent with ordinary regularization in four dimension [65, 64, 13], we use the following replacement associated with quadratic divergence:

$$\Lambda_3 \;\to\; \frac{1}{\sqrt{2}}\Lambda_4 = \frac{1}{\sqrt{2}}\Lambda, \tag{5.62}$$

$$\int \frac{d^{n-1}\bar{k}}{(2\pi)^{n-1}}\frac{1}{\bar{k}} \to \frac{\Lambda^2}{8\pi^2}, \qquad \int \frac{d^{n-1}\bar{k}}{(2\pi)^{n-1}}\frac{\bar{k}^i\bar{k}^j}{\bar{k}^3} \to -\delta^{ij}\frac{\Lambda^2}{8\pi^2}. \tag{5.63}$$

When we make these replacement, the present method of integral preserves chiral symmetry.

As shown in Appendix A, $\Pi_\perp^{(\mathrm{vac})t}$ and $\Pi_\perp^{(\mathrm{vac})s}$ are independent of the external momentum. Accordingly, the finite renormalization effect $\widetilde{\Pi}_\perp$ is also independent of the external momentum and then vanishes:

$$\widetilde{\Pi}_\perp(V_\pi\bar{p},\bar{p}) = 0. \tag{5.64}$$

Thus in the following, we take the external momentum as zero. In that case, the temporal and spatial components of $\Pi_\perp^{(\mathrm{vac})\mu\nu}$ are expressed as $\Pi_\perp^{(\mathrm{vac})\mathrm{t}} = \Pi_\perp^{(\mathrm{vac})00}$ and $\Pi_\perp^{(\mathrm{vac})\mathrm{s}} = -(\delta^{ij}/3)\Pi_\perp^{(\mathrm{vac})ij}$. Taking the VM limit ($M_\rho \to 0$ and $V_\sigma \to V_\pi$), these components become

$$\begin{aligned}
\lim_{\mathrm{VM}} \Pi_\perp^{(\mathrm{vac})00}(p_0=\bar{p}=0) &= \frac{N_f}{4}\int \frac{dk_0 d^{n-1}\bar{k}}{i(2\pi)^n}\frac{4k_0^2}{[-k_0^2+V_\pi^2\bar{k}^2]^2} \\
&= -\frac{N_f}{4}\int \frac{d^{n-1}\bar{k}}{(2\pi)^{n-1}}\frac{1}{V_\pi\bar{k}} \\
&= -\frac{N_f}{4}\frac{1}{V_\pi}\frac{\Lambda^2}{8\pi^2}, \\
\lim_{\mathrm{VM}} \Pi_\perp^{(\mathrm{vac})\mathrm{ij}}(p_0=\bar{p}=0) &= -\frac{N_f}{4}(V_\pi^2)^2\int \frac{dk_0 d^{n-1}\bar{k}}{i(2\pi)^n}\frac{4\bar{k}^i\bar{k}^j}{[-k_0^2+V_\pi^2\bar{k}^2]^2} \\
&= -\frac{N_f}{4}V_\pi^4\int \frac{d^{n-1}\bar{k}}{(2\pi)^{n-1}}\frac{\bar{k}^i\bar{k}^j}{(V_\pi\bar{k})^3} \\
&= \frac{N_f}{4}V_\pi\,\delta^{ij}\,\frac{\Lambda^2}{8\pi^2}.
\end{aligned} \tag{5.65}$$

Thus we obtain the temporal and spatial parts as

$$\lim_{\mathrm{VM}} \Pi_\perp^{(\mathrm{vac})\mathrm{t}}(p_0=\bar{p}=0) = -\frac{N_f}{4}\frac{1}{V_\pi}\frac{\Lambda^2}{8\pi^2},$$

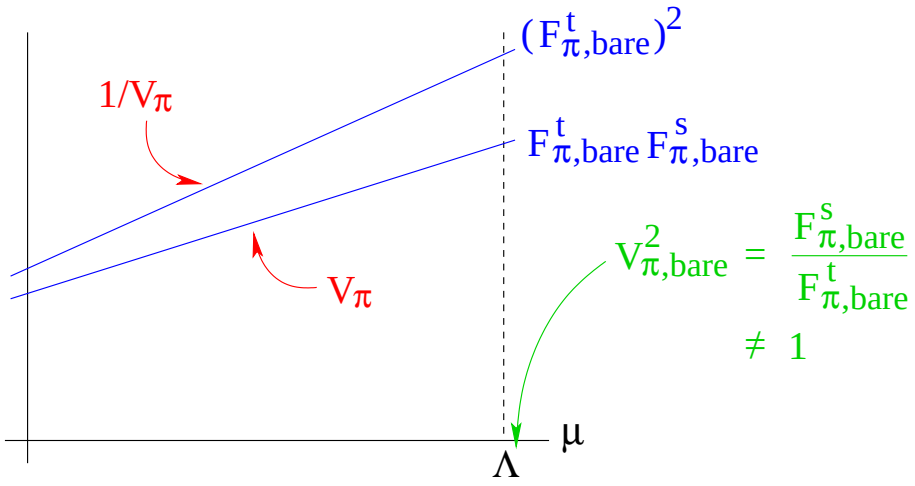

Figure 5.5: Quadratic running of $(F^t_\pi)^2$ and $F^t_\pi F^s_\pi$ at T_c.

$$\lim_{\mathrm{VM}} \Pi_\perp^{(\mathrm{vac})\mathrm{s}}(p_0 = \bar{p} = 0) = -\frac{N_f}{4} V_\pi \frac{\Lambda^2}{8\pi^2}. \tag{5.66}$$

These quadratic divergences are renormalized by $(F^t_{\pi,\mathrm{bare}})^2$ and $F^t_{\pi,\mathrm{bare}}F^s_{\pi,\mathrm{bare}}$, respectively. Then RGEs for the parameters $(F^t_\pi)^2$ and $F^t_\pi F^s_\pi$ are expressed as

$$\mu\frac{d(F^t_\pi)^2}{d\mu} = \frac{N_f}{(4\pi)^2}\frac{1}{V_\pi}\mu^2, \tag{5.67}$$

$$\mu\frac{d(F^t_\pi F^s_\pi)}{d\mu} = \frac{N_f}{(4\pi)^2} V_\pi\, \mu^2. \tag{5.68}$$

Both $(F^t_\pi)^2$ and $F^t_\pi F^s_\pi$ scale following the quadratic running μ^2. However, the coefficient of μ^2 in the RGE for $(F^t_\pi)^2$ is different from that for $F^t_\pi F^s_\pi$ (see Fig. 5.5).

When we use these RGEs, the scale dependence of the parametric pion velocity is

$$\begin{aligned}
\mu\frac{dV_\pi^2}{d\mu} &= \mu\frac{d(F^t_\pi F^s_\pi/(F^t_\pi)^2)}{d\mu} \\
&= \frac{1}{(F^t_\pi)^4}\frac{N_f}{(4\pi)^2}\left[V_\pi (F^t_\pi)^2 - F^t_\pi F^s_\pi \frac{1}{V_\pi}\right]\mu^2 \\
&= 0\,.
\end{aligned} \tag{5.69}$$

This implies that *the parametric pion velocity at the critical temperature does not scale.* In other words, the Lorentz non-invariance at bare level is not enhanced through the RGEs as long as we consider the pion velocity. As we noted below Eq. (5.61), the factor V_σ^2 is in the spatial component of the vertex Γ^μ. If V_σ were not equal to V_π, the coefficients of running in the right-hand-side of Eqs. (5.67) and (5.68) would change. However, since the VM conditions do guarantee $V_\sigma = V_\pi$, the quadratic running caused from Λ^2 in $(F^t_\pi)^2$ and $F^t_\pi F^s_\pi$ are exactly canceled in the second line of Eq. (5.69).

Hadronic thermal correction at T_c

Next we study the hadronic thermal correction to the pion velocity at the critical temperature. The temporal and spatial parts of the hadronic thermal correction $\bar{\Pi}_\perp^{\mu\nu}$ contribute to the pion velocity, which have the same structure as those of the quantum correction $\Pi_\perp^{(\mathrm{vac})\mu\nu}$, except for a Bose-Einstein distribution function. Thus by the replacement of $\Lambda^2/(4\pi)^2$ with $T^2/12$ in $\Pi_\perp^{(\mathrm{vac})\mathrm{t,s}}$, hadronic corrections to the temporal and spatial parts of $\bar{\Pi}_\perp^{\mu\nu}$ are obtained as follows:

$$\begin{aligned}\lim_{\mathrm{VM}} \bar{\Pi}_\perp^t(p_0,\bar{p};T) &= -\frac{N_f}{24}\frac{1}{V_\pi}T_c^2,\\ \lim_{\mathrm{VM}} \bar{\Pi}_\perp^s(p_0,\bar{p};T) &= -\frac{N_f}{24}V_\pi\, T_c^2.\end{aligned} \tag{5.70}$$

Substituting Eq. (5.70) into Eq. (5.59) with $\widetilde{\Pi}_\perp = 0$ as shown in Eq. (5.64), we obtain the physical pion velocity in the VM as

$$\begin{aligned} v_\pi^2(\bar{p};T) &\overset{T\to T_c}{\to} V_\pi^2 + \frac{\bar{\Pi}_\perp^s(V_\pi\bar{p},\bar{p};T_c) - V_\pi^2\bar{\Pi}_\perp^t(V_\pi\bar{p},\bar{p};T_c)}{(F_\pi^t)^2}\\ &= V_\pi^2. \end{aligned} \tag{5.71}$$

Since the parametric pion velocity in the VM does not scale with energy [see Eq. (5.69)], V_π in the above expression is equivalent to the bare pion velocity:

$$v_\pi(\bar{p};T) = V_{\pi,\mathrm{bare}}(T) \qquad \text{for}\, T\to T_c. \tag{5.72}$$

This implies that *the pion velocity in the limit $T\to T_c$ receives neither hadronic nor quantum corrections due to the protection by the VM.*

In order to clarify the reason of this non-renormalization property, let us recall the fact that only the diagram (b) in Fig. 5.1 contributes to the pion velocity at the critical temperature. Away from the critical temperature, the contribution of the massive σ (i.e., the longitudinal mode of massive vector meson) is suppressed owing to the Boltzmann factor $\exp[-M_\rho/T]$, and then only the pion loop contributes to the pion velocity. Then there exists the $\mathcal{O}(T^4)$ correction to the pion velocity [16] (see subsection 3.4.2). Near the critical temperature, on the other hand, σ becomes massless due to the VM since σ (i.e., the longitudinal vector meson) becomes the chiral partner of the pion. Thus the absence of the hadronic corrections in the pion velocity at the critical temperature is due to the exact cancellation between the contribution of pion and that of its chiral partner σ. Similarly the quantum correction generated from the pion loop is exactly canceled by that from the σ loop.

Non-renormalization property

Now we consider the meaning of our result (5.72). Based on the point of view that the bare HLS theory is defined from QCD, we presented the VM conditions realizing the chiral symmetry in QCD consistently, i.e, $(g_L, a^t, a^s) \to (0, 1, 1)$ for $T \to T_c$. This is the fixed point of the RGEs for the parameters g_L, a^t and a^s. Although both pion decay constants $(F_\pi^t)^2$ and $F_\pi^t F_\pi^s$ scale following the quadratic running, $(F_\pi^t)^2$ and $F_\pi^t F_\pi^s$ show a different running since the coefficient of μ^2 in Eq. (5.67) is different from that in Eq. (5.68). Nevertheless in the pion velocity at the critical temperature, the quadratic running in $(F_\pi^t)^2$ is exactly canceled by that in $F_\pi^t F_\pi^s$ [see second line of Eq. (5.69)]. There it was crucial for intricate cancellation of the quadratic running that the velocity of σ (i.e., longitudinal vector meson) is equal to its chiral partner, i.e., $V_\sigma \to V_\pi$ for $T \to T_c$. Note that this is not an extra condition but a consequence from the VM conditions for a^t and a^s; we started simply from the VM conditions alone and found that V_π does not receive quantum corrections at the restoration point. As we showed in Eq. (5.70), the hadronic correction to $(F_\pi^t)^2$ is different from that to $F_\pi^t F_\pi^s$. In the pion velocity, however, the hadronic correction from $(F_\pi^t)^2$ is exactly cancelled by that from $F_\pi^t F_\pi^s$ [see second line of Eq. (5.71)]. The VM conditions guarantee these exact cancellations of the quantum and hadronic corrections. This implies that $(g_L, a^t, a^s, V_\pi) = (0, 1, 1, \text{any})$ forms a fixed line for four RGEs of g_L, a^t, a^s and V_π. When one point on this fixed line is selected through the matching procedure as done in Ref. [18], namely the value of $V_{\pi,\text{bare}}$ is fixed, the present result implies that the point does not move in a subspace of the parameters. This is likely the manifestation of a new fixed point in the Lorentz non-invariant formulation of the VM. Approaching the restoration point of chiral symmetry, the physical pion velocity itself would flow into the fixed point.

We should distinguish the consequences within HLS/VM from those beyond HLS/VM. Clearly the determination of the definite value of the bare pion velocity is done outside HLS/VM. On the other hand, our main result (5.72) holds independently of the value of the bare pion velocity itself. Applying this result to the case where one starts from the bare HLS theory with Lorentz invariance, i.e., $V_{\pi,\text{bare}} = 1$, one finds that the pion velocity at T_c becomes the speed of light since $v_\pi = V_{\pi,\text{bare}} = 1$, as obtained in Ref. [15].

As a consequence of the relation (5.72), we can determine the temporal and spatial pion decay constants at the critical temperature when we take the bare pion velocity as finite. In the following, we study these decay constants and discuss their determinations based on Eq. (5.72). Using Eq. (5.69), we solve the RGEs (5.67) and (5.68) and obtain a relation between two parametric pion decay constants as $F_\pi^t(0; T_c) F_\pi^s(0; T_c) = V_\pi^2 (F_\pi^t(0; T))^2$. From

this and (5.70), the temporal and spatial pion decay constants with the quantum and hadronic corrections are obtained as

$$\begin{aligned}(f_\pi^t)^2 &= \Big(F_\pi^t(0;T_c)\Big)^2 - \frac{N_f}{24}\frac{1}{V_\pi}T_c^2, \\ f_\pi^t\, f_\pi^s &= F_\pi^t(0;T_c)F_\pi^s(0;T_c) - \frac{N_f}{24}V_\pi\, T_c^2 \\ &= V_\pi^2(f_\pi^t)^2. \end{aligned} \tag{5.73}$$

Since the order parameter $(f_\pi^t f_\pi^s)$ vanishes as expected at the critical temperature, we find that $f_\pi^t f_\pi^s = V_\pi^2(f_\pi^t)^2 = 0$. Multiplying both side by $v_\pi^2 = V_\pi^2$, the above expression is reduced to

$$(f_\pi^s)^2 = V_\pi^4(f_\pi^t)^2 = 0. \tag{5.74}$$

Now, the spatial pion decay constant vanishes at the critical temperature, $f_\pi^s(T_c) = 0$. In the case of a vanishing pion velocity, f_π^t can be finite at the restoration point. On the other hand, when V_π is finite, Eq. (5.74) leads to $f_\pi^t(T_c) = 0$. Thus we find that both temporal and spatial pion decay constants vanish simultaneously at the critical temperature when the bare pion velocity is determined as finite.

In order to know the value of the (bare) pion velocity, we need to specify a method that determines the bare parameters.

As we will show below, the analysis performed on the basis of a Wilsonian matching gives the finie bare pion velocity at the critical temperature, i.e., $V_{\pi,\mathrm{bare}} \neq 0$. Thus, by combining Eq. (5.72) with estimation of $V_{\pi,\mathrm{bare}}$, the value of the physical pion velocity $v_\pi(T)$ at the critical temperature is obtained to be finite [18].

Estimation

Now we evaluate the physical pion velocity at the critical temperature T_c starting from the Lorentz non-invariant bare Lagrangian. According to the non-renormalization theorem, the *bare* velocity so calculated should correspond to the *physical* pion velocity *at* the chiral transition point. Now, in the VM, bare parameters are determined by matching the HLS to QCD at the matching scale Λ and at temperature $T = T_c$.

We begin with a summary of the pion velocity found in the HLS/VM theory with Lorentz invariance [15, 17, 16]. The pion velocity is given by Eq. (3.135):

$$v_\pi^2(\bar{p};T) = 1 + \frac{\tilde{F}(\bar{p};T)}{F_\pi^2}\Big[\mathrm{Re}f_\pi^s(\bar{p};T) - \mathrm{Re}f_\pi^t(\bar{p};T)\Big]. \tag{5.75}$$

The VM dictates that if one ignores Lorentz non-invariance in the bare Lagrangian in medium, the pion velocity approaches the speed of light as $T \to T_c$ [15, 16].

In the following, we extend the matching condition valid at low temperature, Eq. (4.31), to near the critical temperature, and determine the bare pion velocity at T_c. We should in principle evaluate the matrix elements in terms of QCD variables only in order for performing the Wilsonian matching, which is as yet unavailable from model-independent QCD calculations. Therefore, we make an estimation by extending the dilute gas approximation adopted in the QCD sum-rule analysis in the low-temperature region to the critical temperature with including all the light degrees of freedom expected in the VM. In the HLS/VM theory, both the longitudinal and transverse ρ mesons become massless at the critical temperature since the HLS gauge coupling constant g vanishes. At the critical point, the longitudinal ρ meson which becomes the NG boson σ couples to the vector current whereas the transverse ρ mesons decouple from the theory because of the vanishing g. Thus we assume that thermal fluctuations of the system are dominated near T_c not only by the pions but also by the longitudinal ρ mesons. In evaluating the thermal matrix elements of the non-scalar operators in the OPE, we extend the thermal pion gas approximation employed in Ref. [75] to the longitudinal ρ mesons that figure in our approach [18]. This is feasible since at the critical temperature, we expect the equality $A_4^\rho(T_c) = A_4^\pi(T_c)$ to hold as the massless ρ meson is the chiral partner of the pion in the VM [#4]. It should be noted that, although we use the dilute gas approximation, the treatment here is already beyond the low-temperature approximation adopted in Eq. (4.22) because the contribution from ρ meson is negligible in the low-temperature region. Since we treat the pion as a massless particle in the present analysis, it is reasonable to take $A_4^\pi(T) \simeq A_4^\pi(T=0)$. We therefore use

$$A_4^\rho(T) \simeq A_4^\pi(T) \simeq A_4^\pi(T=0) \quad \text{for} \quad T \simeq T_c. \tag{5.76}$$

The properties of the scalar operators giving rise to the condensates are fairly well understood at chiral restoration. We know that the quark condensate must be zero at the critical temperature. Furthermore the value of the gluon condensate at the phase transition is known from lattice calculations to be roughly half of the one in the free space [83]. We therefore can use in what follows the following values at $T = T_c$:

$$\langle \bar{q}q \rangle_T = 0, \quad \langle \frac{\alpha_s}{\pi} G^2 \rangle_T \sim 0.006 \text{GeV}^4 \ . \tag{5.77}$$

Including the contributions from both pions and massless ρ mesons, Eq. (4.26) can be expressed as

$$G_A^{(\text{OPE})L(1)} = \frac{32}{105}\pi^4 \frac{T^6}{Q^8}\left[A_4^{\pi(u+d)} + A_4^{\rho(u+d)} \right]. \tag{5.78}$$

[#4] We observe from Refs. [92, 93] that $A_4^{\pi(u+d)}(\mu = 2.4 \text{ GeV}) \sim A_4^{\rho(u+d)}(\mu = 2.4 \text{ GeV})$ even at zero temperature.

Therefore from Eq. (4.31), we obtain the deviation $\delta_{\rm bare}$ as

$$\delta_{\rm bare} = 1 - V^2_{\pi,{\rm bare}} = \frac{1}{G_0}\frac{32}{105}\pi^4\frac{T^6}{\Lambda^6}\left[A_4^{\pi(u+d)} + A_4^{\rho(u+d)}\right]. \tag{5.79}$$

This is the matching condition to be used for determining the value of the bare pion velocity near the critical temperature.

To make a rough estimate of $\delta_{\rm bare}$, we use $A_4^{\pi(u+d)}(\mu = 1\ {\rm GeV}) = 0.255$ [75]. This value is arrived at by following Appendix B of [75]. $A_n^{\pi(q)}$ is defined by

$$\langle\pi|\bar{q}\gamma_{\mu_1}D_{\mu_2}...D_{\mu_n}q(\mu)|\pi\rangle = (-i)^{n-1}(p_{\mu_1}...p_{\mu_n} - {\rm traces})A_n^{\pi(q)}(\mu)\ , \tag{5.80}$$

where

$$A_n^{\pi(q)}(\mu) = 2\int_0^1 dx x^{n-1}[q(x,\mu) + (-1)^n\bar{q}(x,\mu)]\ . \tag{5.81}$$

For any charge state of the pion (π^0, π^+, π^-), $A_n^{\pi(u+d)}$ $(n = 2, 4)$ can be written in terms of the nth moment of valence quark distribution $V_n^\pi(\mu)$ and sea quark distribution $S_n^\pi(\mu)$ [75],

$$A_n^{\pi(u+d)}(\mu) = 4V_n^\pi(\mu) + 8S_n^\pi(\mu)\ , \tag{5.82}$$

where

$$\begin{aligned} V_n^\pi &= \int_0^1 dx x^{n-1}v^\pi(x,\mu), \\ S_n^\pi &= \int_0^1 dx x^{n-1}s^\pi(x,\mu). \end{aligned} \tag{5.83}$$

Simple parameterizations of the valence distribution $v^\pi(x,\mu)$ and the sea distribution $s^\pi(x,\mu)$ can be found in Ref. [94]– see Ref. [95] for the updated results – where the parton distributions in the pions are determined through the π-N Drell-Yan and direct photon production processes. With the leading-order parton distribution functions given in [94], we obtain $A_4^{\pi(u+d)} = 0.255$ at $\mu = 1$ GeV [75]. For the purpose of comparison with the lattice QCD result [92], we need to calculate the value at $\mu = 2.4$ GeV; it comes out to be $A_4^{\pi(u+d)} = 0.18$. The value $A_4^{\pi(u+d)} = 0.18$ is slightly bigger than the ~ 0.13 calculated by the lattice QCD [92], while it is a bit smaller than the ~ 0.22 of Ref. [93]. Note that the value ~ 0.18 agrees with the one determined by lattice QCD [92] within quoted errors. Using $A_2^{\pi(u+d)} = 0.972$ and $A_4^{\pi(u+d)} = 0.255$ and for the range of matching scale $(\Lambda = 0.8 - 1.1\,{\rm GeV})$, that of QCD scale $(\Lambda_{QCD} = 0.30 - 0.45\,{\rm GeV})$ and critical temperature $(T_c = 0.15 - 0.20\,{\rm GeV})$, we get

$$\delta_{\rm bare}(T_c) = 0.0061 - 0.29\,, \tag{5.84}$$

where the Λ dependence of $A_{2,4}^{\pi(u+d)}$ is ignored as it is expected to be suppressed by more than $1/\Lambda^6$. Thus we find the *bare* pion velocity to be close to the speed of light:

$$V_{\pi,\mathrm{bare}}(T_c) = 0.83 - 0.99\,. \tag{5.85}$$

Thanks to the non-renormalization theorem, i.e., $v_\pi(T_c) = V_{\pi,\mathrm{bare}}(T_c)$, we arrive at the physical pion velocity at chiral restoration [18]:

$$v_\pi(T_c) = 0.83 - 0.99\,. \tag{5.86}$$

This is in contrast to the result obtained from the chiral theory [96], where the relevant degree of freedom near T_c is only the pion. Their result is that the pion velocity becomes zero for $T \to T_c$. Therefore by experiment and lattice analysis, we may be able to distinguish which theory is appropriate to describe the chiral phase transition.

5.5 Critical Behavior of Vector Meson Mass

We showed that the vector meson pole mass $m_\rho(T)$ goes to zero in the limit $T \to T_c$ and the chiral symmetry is restored as the VM in the framework of the HLS theory. In this section, we study how $m_\rho(T)$ falls in the limit $T \to T_c$.

We expand the vector current correlator $G_V^{(\mathrm{HLS})}$ at the matching scale around T_c taking the limits $g(\Lambda;T) \ll 1$, $a(\Lambda;T) - 1 \ll 1$ and $M_\rho(\Lambda;T)/\Lambda \ll 1$. Then the quantity $G_A - G_V$ in the HLS sector is obtained as

$$\begin{aligned} &G_A^{(\mathrm{HLS})}(\Lambda;T) - G_V^{(\mathrm{HLS})}(\Lambda;T) \\ &\qquad \sim g^2(\Lambda;T)\left(\frac{F_\pi^2(\Lambda;T)}{\Lambda^2}\right)^2 - \Big(a(\Lambda;T)-1\Big)\frac{F_\pi^2(\Lambda;T)}{\Lambda^2}\,, \end{aligned} \tag{5.87}$$

where we neglected the higher order coefficients. The same quantity using the OPE has the following form:

$$G_A^{(\mathrm{OPE})}(\Lambda;T) - G_V^{(\mathrm{OPE})}(\Lambda;T) = \frac{4\pi(N_c^2-1)}{N_c^2}\frac{\alpha_s\langle\bar{q}q\rangle_T^2}{\Lambda^6}\,. \tag{5.88}$$

Here we assume that all the terms of Eq. (5.87) have same scaling behaviors near T_c. From Eqs. (5.87) and (5.88), we obtain the scaling behavior on the gauge coupling constant as

$$g(\Lambda;T) \sim \langle\bar{q}q\rangle_T\,. \tag{5.89}$$

As shown in section 5.2, the vector meson pole mass $m_\rho(T)$ near T_c is

$$m_\rho^2(T) \simeq g^2(T)\Big(a(T)F_\pi^2 + \delta T^2\Big)\,, \tag{5.90}$$

where δT^2 denotes the hadronic thermal correction and gives a positive contribution [see Eq. (5.23)]. Thus $m_\rho(T)$ vanishes as $\langle\bar{q}q\rangle_T$:

$$m_\rho(T) \sim \langle\bar{q}q\rangle_T \,. \tag{5.91}$$

If $\langle\bar{q}q\rangle_T^2$ falls as $f_\pi^2(T)$ near T_c, then the ρ pole mass $m_\rho^2(T)$ vanishes as $f_\pi^2(T)$. In such a case the scaling property in the VM may be consistent with the Brown-Rho scaling $m_\rho(T)/m_\rho(0) \sim f_\pi(T)/f_\pi(0)$ [10].

Chapter 6

Chiral Doubling of Heavy-Light Mesons

Based on the manifestation of chiral symmetry à la linear sigma model, it was predicted a decade ago [97, 98] that the mass splitting ΔM between the $\mathcal{M}(0^-, 1^-)$ and $\tilde{\mathcal{M}}(0^+, 1^+)$ mesons where $\mathcal{M}$ denotes a heavy-light meson consisting of heavy quark Q and light antiquark $\bar{q}$ should be of the size of the constituent quark mass. Recently, BaBar [34], CLEO [35] and subsequently the Belle collaboration [36], discovered new D mesons with $Q = c$, c being charm quark, which most likely have spin-party 0^+ and 1^+ and the mass difference to the $D(0^-, 1^-)$ is in fair agreement with the prediction of [97, 98]. In Ref. [99], it was proposed that the splitting of $\mathcal{M}$ and $\tilde{\mathcal{M}}$ mesons could carry direct information on the property of chiral symmetry at some critical density or temperature at which the symmetry is restored [#1]. In this chapter, we pick up this idea and make a first step in consolidating the proposal of Ref. [99] following Ref. [33]. In doing this, we shall take the reverse direction: Instead of starting with a Lagrangian defined in the chiral-symmetry broken phase and then driving the system to the chiral symmetry restoration point by an external disturbance, we will start from an assumed structure of chiral symmetry at its restoration point and then make a prediction as to what happens to the splitting in the broken phase. We find that the splitting is directly proportional to the light-quark condensate and comes out to be of the size of the constituent quark mass consistent with the prediction of Refs. [97, 98]. We shall associate this result as giving a link between the assumed structure of the chiral restoration point and the broken phase.

Our procedure is following: We assume that the heavy-light hadrons are described by a VM-

[#1] In what follows, unless otherwise specified, we will refer to heavy-light mesons generically as D but the arguments should apply better to heavier-quark mesons. Numerical estimates will however be made solely for the (open charm) D mesons.

fixed point theory at the chiral restoration point generically denoted C_χ (critical temperature T_c [14] or density n_c [22] or number of flavors N_f^c [21]) and by introducing the simplest form of the VM breaking terms, we compute the mass splitting of the chiral doublers in matter-free space in terms of the quantities that figure in the QCD correlators [#2].

6.1 Heavy Quark Symmetry

Like the approximate light quark flavor symmetry (chiral symmetry) in the light quark sector of QCD, the heavy quark symmetry is also approximate in the situation where the heavy quark mass m_Q is much larger than $\Lambda_{\rm QCD}$, $\Lambda_{\rm QCD}/m_Q \ll 1$. The heavy quark symmetry arises in the limit of QCD where the heavy quark, charm and bottom, masses m_Q are taken to be infinity. In this limit, dynamics of the heavy quark Q is independent of its mass and spin [100]. In this section, we give a brief review of the heavy quark symmetry and the multiplet of hadrons containing a single heavy quark.

In the limit where the heavy quark mass goes to infinity, $m_Q \to \infty$, the four velocity of the heavy quark v_μ is fixed. The size of the meson is of order $1/\Lambda_{\rm QCD}$, and then the typical momentum scale of the light degrees of freedom is of order $\Lambda_{\rm QCD}$. We decompose the four momentum of the heavy quark into

$$p_\mu = m_Q v_\mu + k_\mu \,, \tag{6.1}$$

where k_μ is called the residual momentum and is of order $\Lambda_{\rm QCD}$. The propagator of the heavy quark is given by

$$\frac{-(p_\mu \gamma^\mu + m_Q)}{p^2 - m_Q^2 + i\epsilon} \,. \tag{6.2}$$

Substituting Eq. (6.1) into the propagator, we obtain the leading form as follows:

$$\frac{-1}{v \cdot k + i\epsilon} \,, \tag{6.3}$$

where we moved the projection operator $(v_\mu \gamma^\mu + 1)/2$ taking out of the large component. We should note that it is independent of the heavy quark mass m_Q and the gamma matrices are completely disappeared. Similarly the vertices are also independent of m_Q and gamma matrices. The heavy quark is sitting with infinite mass $m_Q \to \infty$, and thus the spin of the heavy quark does not flip at all by the interaction of the light degrees of freedom which is of order $\Lambda_{\rm QCD}$. Thus the absence of gamma matrices indicates that the spin of heavy quark is

[#2] Introducing vector mesons in the light-quark sector of heavy-light mesons was considered in Ref. [97] but without the matching to QCD and hence without the VM fixed point.

conserved. Hence if there are N_f heavy quarks with the same four velocity, the effective heavy quark theory has a $SU(2N_f)$ spin-flavor symmetry [100].

Let us consider the heavy-light meson multiplet. For the hadrons containing a single heavy quark Q, there is a $SU(2)$ spin symmetry between Q with up-spin, $Q(\uparrow)$ and Q with down-spin, $Q(\downarrow)$. Thus the hadrons with the spin combined $\uparrow$ and $\downarrow$ with the spin of the light degrees of freedom $s_{\rm light}$ are the spin partners each other. In general for each $s_{\rm light}$, there is a degenerate doublet with the total spin s_+ and s_-:

$$s_\pm = s_{\rm light} \pm \frac{1}{2}\,. \tag{6.4}$$

Hadron in the ground state has $s_{\rm light} = 1/2$ and negative parity and then the hadron with $J^P = 0^-$ is the spin partner of the one with $J^P = 1^-$.

6.2 An Effective Field Theory

In this section we give our reasoning that leads to the Lagrangian that defines our approach. Here we construct the Lagrangian using the approximate chiral $SU(3)_{\rm L} \times SU(3)_{\rm R}$ symmetry in the light-quark sector and the heavy quark symmetry in the heavy-quark sector. We will start from the Lagrangian given at the vector manifestation (VM) fixed point. We first describe how to construct the fixed point Lagrangian based on the VM. Then, we account for the effect of spontaneous chiral symmetry breaking by adding a *bare* parameter for the mass splitting in the heavy sector and including the deviation of the HLS parameters from the values at the VM fixed point. The explicit form of the Lagrangian so constructed is shown in subsection 6.2.3.

6.2.1 The fixed point Lagrangian

Let us consider the VM at the point at which chiral symmetry is restored (in the chiral limit). At the VM at its fixed point characterized by $(g, a) = (0, 1)$, the two 1-forms become

$$\begin{aligned}
\alpha_{\parallel\mu} &= \frac{1}{2i}\left(\partial_\mu \xi_{\rm R}\cdot\xi_{\rm R}^\dagger + \partial_\mu \xi_{\rm L}\cdot\xi_{\rm L}^\dagger\right)\ , \\
\alpha_{\perp\mu} &= \frac{1}{2i}\left(\partial_\mu \xi_{\rm R}\cdot\xi_{\rm R}^\dagger - \partial_\mu \xi_{\rm L}\cdot\xi_{\rm L}^\dagger\right)\ .
\end{aligned} \tag{6.5}$$

Note that the above $\alpha_{\parallel\mu}$ and $\alpha_{\perp\mu}$ do not contain the HLS gauge field since the gauge coupling g vanishes at the VM fixed point. It is convenient to define the (L,R) 1-forms:

$$\begin{aligned}
\alpha_{R\mu} &= \alpha_{\parallel\mu} + \alpha_{\perp\mu} = \frac{1}{i}\partial_\mu \xi_{\rm R}\cdot\xi_{\rm R}^\dagger\ , \\
\alpha_{L\mu} &= \alpha_{\parallel\mu} - \alpha_{\perp\mu} = \frac{1}{i}\partial_\mu \xi_{\rm L}\cdot\xi_{\rm L}^\dagger\ ,
\end{aligned} \tag{6.6}$$

which can be regarded as belonging to the chiral representation $(1,8)$ and $(8,1)$, respectively, transforming under chiral $SU(3)_{\rm L} \times SU(3)_{\rm R}$ as

$$\begin{aligned} \alpha_{R\mu} &\to g_{\rm R} \alpha_{R\mu} g_{\rm R}^\dagger \ , \\ \alpha_{L\mu} &\to g_{\rm L} \alpha_{L\mu} g_{\rm L}^\dagger \ . \end{aligned} \tag{6.7}$$

By using these 1-forms, the HLS Lagrangian at the VM fixed point can be written as [13]

$$\mathcal{L}^*_{\rm light} = \frac{1}{2} F_\pi^2 \, {\rm tr} \left[\alpha_{R\mu} \alpha_R^\mu \right] + \frac{1}{2} F_\pi^2 \, {\rm tr} \left[\alpha_{L\mu} \alpha_L^\mu \right] \ , \tag{6.8}$$

where the $*$ affixed to the Lagrangian denotes that it is a fixed-point Lagrangian, and F_π denotes the bare pion decay constant. Note that the physical pion decay constant f_π vanishes at the VM fixed point by the quadratic divergence although the bare one is non-zero [13]. It should be stressed that the above fixed point Lagrangian is approached only as a limit of chiral symmetry restoration [13].

Next we consider the fixed-point Lagrangian of the heavy meson sector at the chiral restoration point identified with the VM fixed point. Let us introduce two heavy-meson fields $\mathcal{H}_R$ and $\mathcal{H}_L$ transforming under chiral ${\rm SU}(3)_{\rm R} \times {\rm SU}(3)_{\rm L}$ as

$$\mathcal{H}_R \to \mathcal{H}_R \, g_{\rm R}^\dagger \ , \quad \mathcal{H}_L \to \mathcal{H}_L \, g_{\rm L}^\dagger \ . \tag{6.9}$$

By using these fields together with the light-meson 1-forms $\alpha^\mu_{L,R}$, the fixed point Lagrangian of the heavy mesons is expressed as [#3]

$$\begin{aligned} \mathcal{L}^*_{\rm heavy} \ = \ & -{\rm tr} \left[\mathcal{H}_R i v_\mu \partial^\mu \bar{\mathcal{H}}_R \right] - {\rm tr} \left[\mathcal{H}_L i v_\mu \partial^\mu \bar{\mathcal{H}}_L \right] \\ & + m_0 \, {\rm tr} \left[\mathcal{H}_R \bar{\mathcal{H}}_R + \mathcal{H}_L \bar{\mathcal{H}}_L \right] \\ & + 2k \, {\rm tr} \left[\mathcal{H}_R \alpha_{R\mu} \gamma^\mu \frac{1+\gamma_5}{2} \bar{\mathcal{H}}_R + \mathcal{H}_L \alpha_{L\mu} \gamma^\mu \frac{1-\gamma_5}{2} \bar{\mathcal{H}}_L \right] \ , \end{aligned} \tag{6.10}$$

where v_μ is the velocity of heavy meson, m_0 represents the mass generated by the interaction between heavy quark and the "pion cloud" surrounding the heavy quark, and k is a real constant to be determined.

6.2.2 Effects of spontaneous chiral symmetry breaking

Next we consider what happens in the broken phase of chiral symmetry. In the real world at low temperature and low density, chiral symmetry is spontaneously broken by the non-vanishing

[#3] We assign the right chirality to $\mathcal{H}_R$, and the left chirality to $\mathcal{H}_L$. Then the interaction term has the right and left projection operators. Note that the insertion of $(1 \pm \gamma_5)$ to kinetic and mass termes does not cause any difference.

quark condensate. In the scenario of chiral-symmetry manifestation à la linear sigma model, the effect of spontaneous chiral symmetry breaking is expressed by the vacuum expectation value (VEV) of the scalar fields. In the VM, on the other hand, it is signaled by the HLS Lagrangian departing from the VM fixed point: There the gauge coupling constant $g \neq 0$ [#4] and we have the kinetic term of the HLS gauge bosons $\mathcal{L}_{\rho\text{kin}} = -\frac{1}{2}\text{tr}\,[\rho_{\mu\nu}\rho^{\mu\nu}]$. The derivatives in the HLS 1-forms become the covariant derivatives and then $\alpha_{L\mu}$ and $\alpha_{R\mu}$ are covariantized:

$$\begin{aligned}\partial_\mu &\to D_\mu = \partial_\mu - ig\rho_\mu,\\ \alpha_{R\mu} &\to \hat{\alpha}_{R\mu} = \alpha_{R\mu} - g\rho_\mu,\\ \alpha_{L\mu} &\to \hat{\alpha}_{L\mu} = \alpha_{L\mu} - g\rho_\mu.\end{aligned} \tag{6.11}$$

These 1-forms transform as $\hat{\alpha}_{R(L)\mu} \to h\,\hat{\alpha}_{R(L)\mu}h^\dagger$ with $h \in [SU(3)_{\text{V}}]_{\text{local}}$ as shown in Eq. (3.6).

Although $a = 1$ at the VM fixed point, generally $a \neq 1$ in the broken phase. We therefore expect to have a term of the form $\frac{1}{2}(a-1)F_\pi^2\text{tr}[\hat{\alpha}_{L\mu}\hat{\alpha}_R^\mu]$. Thus the Lagrangian for the light mesons takes the following form:

$$\begin{aligned}\mathcal{L}_{\text{light}} &= \frac{a+1}{4}F_\pi^2\text{tr}[\hat{\alpha}_{R\mu}\hat{\alpha}_R^\mu + \hat{\alpha}_{L\mu}\hat{\alpha}_L^\mu]\\ &\quad + \frac{a-1}{2}F_\pi^2\text{tr}[\hat{\alpha}_{R\mu}\hat{\alpha}_L^\mu] + \mathcal{L}_{\rho\text{kin}}.\end{aligned} \tag{6.12}$$

By using $\hat{\alpha}_{\parallel\mu}$ and $\hat{\alpha}_{\perp\mu}$ given in Eq. (3.5), this Lagrangian is rewritten as

$$\mathcal{L}_{\text{light}} = F_\pi^2\text{tr}[\hat{\alpha}_{\perp\mu}\hat{\alpha}_\perp^\mu] + F_\sigma^2\text{tr}[\hat{\alpha}_{\parallel\mu}\hat{\alpha}_\parallel^\mu] + \mathcal{L}_{\rho\text{kin}}, \tag{6.13}$$

which is nothing but the general HLS Lagrangian.

We next consider the spontaneous breaking of chiral symmetry in the heavy-meson sector. One of the most important effects of the symmetry breaking is to generate the mass splitting between the odd parity multiplet and the even parity multiplet [97]. This effect can be represented by the Lagrangian of the form:

$$\mathcal{L}_{\chi\text{SB}} = \frac{1}{2}\Delta M\,\text{tr}\left[\mathcal{H}_L\bar{\mathcal{H}}_R + \mathcal{H}_R\bar{\mathcal{H}}_L\right]\ , \tag{6.14}$$

where $\mathcal{H}_{R(L)}$ transforms under the HLS as $\mathcal{H}_{R(L)} \to \mathcal{H}_{R(L)}\,h^\dagger$. Here ΔM is the *bare* parameter corresponding to the mass splitting between the two multiplets. An important point of our work is that the bare ΔM can be determined by matching the EFT with QCD as we will show in section 6.5: The matching actually shows that ΔM is proportional to the quark condensate:

$$\Delta M \sim \langle\bar{q}q\rangle. \tag{6.15}$$

[#4] Actually, near the chiral restoration point, the Wilsonian matching between HLS and QCD dictates [13] that (in the chiral limit) the HLS gauge coupling be proportional to the quark condensate: $g \sim \langle\bar{q}q\rangle$. See section 5.5.

6.2.3 Lagrangian in parity eigenfields

In order to compute the mass splitting between $\mathcal{M}$ and $\tilde{\mathcal{M}}$, it is convenient to go to the corresponding fields in parity eigenstate, H (odd-parity) and G (even-parity) as defined, e.g., in Ref. [99];

$$\begin{aligned} \mathcal{H}_R &= \frac{1}{\sqrt{2}}\left[G - iH\gamma_5\right] \ , \\ \mathcal{H}_L &= \frac{1}{\sqrt{2}}\left[G + iH\gamma_5\right] \ . \end{aligned} \tag{6.16}$$

Here, the pseudoscalar meson P and the vector meson P^*_μ are included in the H field as

$$H = \frac{1+v_\mu\gamma^\mu}{2}\left[i\gamma_5 P + \gamma^\mu P^*_\mu\right] \ , \tag{6.17}$$

and the scalar meson Q^* and the axial-vector meson Q_μ are in G as

$$G = \frac{1+v_\mu\gamma^\mu}{2}\left[Q^* - i\gamma^\mu\gamma_5 Q_\mu\right] \ . \tag{6.18}$$

In terms of the H and G fields, the heavy-meson Lagrangian *off* the VM fixed point is of the form

$$\mathcal{L}_{\rm heavy} = \mathcal{L}_{\rm kin} + \mathcal{L}_{\rm int} \ , \tag{6.19}$$

with

$$\mathcal{L}_{\rm kin} = {\rm tr}\left[H\ (iv_\mu D^\mu - M_H)\,\bar{H}\right] - {\rm tr}\left[G\ (iv_\mu D^\mu - M_G)\,\bar{G}\right] \ , \tag{6.20}$$

$$\begin{aligned} \mathcal{L}_{\rm int} = k\Big[& {\rm tr}[H\gamma_\mu\gamma_5\hat{\alpha}^\mu_\perp\bar{H}] - {\rm tr}[Hv_\mu\hat{\alpha}^\mu_\parallel\bar{H}] \\ & + {\rm tr}[G\gamma_\mu\gamma_5\hat{\alpha}^\mu_\perp\bar{G}] + {\rm tr}[Gv_\mu\hat{\alpha}^\mu_\parallel\bar{G}] \\ & - i{\rm tr}[G\hat{\alpha}_{\perp\mu}\gamma^\mu\gamma_5\bar{H}] + i{\rm tr}[H\hat{\alpha}_{\perp\mu}\gamma^\mu\gamma_5\bar{G}] \\ & - i{\rm tr}[G\hat{\alpha}_{\parallel\mu}\gamma^\mu\bar{H}] + i{\rm tr}[H\hat{\alpha}_{\parallel\mu}\gamma^\mu\bar{G}]\Big], \end{aligned} \tag{6.21}$$

where the covariant derivatives acting on $\bar{H}$ and $\bar{G}$ are defined as

$$D_\mu\bar{H} = (\partial_\mu - ig\rho_\mu)\,\bar{H} \ , \quad D_\mu\bar{G} = (\partial_\mu - ig\rho_\mu)\,\bar{G} \ . \tag{6.22}$$

In the above expression, M_H and M_G denote the masses of the parity-odd multiplet H and the parity-even multiplet G, respectively. They are related to m_0 and ΔM as

$$\begin{aligned} M_H &= -m_0 - \frac{1}{2}\Delta M \ , \\ M_G &= -m_0 + \frac{1}{2}\Delta M \ . \end{aligned} \tag{6.23}$$

The mass splitting between G and H is therefore given by

$$M_G - M_H = \Delta M \ . \tag{6.24}$$

6.3 Matching to the Operator Product Expansion

The bare parameter $\Delta M_{\rm bare}$ which carries information on QCD should be determined by matching the EFT correltators to QCD ones. We are concerned with the pseudoscalar correlator G_P and the scalar correlator G_S. In the EFT sector, the correlators at the matching scale are of the form [#5]

$$\begin{aligned} G_P(Q^2) &= \frac{F_D^2 M_D^4}{M_D^2 + Q^2}, \\ G_S(Q^2) &= \frac{F_{\tilde{D}}^2 M_{\tilde{D}}^4}{M_{\tilde{D}}^2 + Q^2}, \end{aligned} \tag{6.25}$$

where F_D ($F_{\tilde{D}}$) denotes the D-meson ($\tilde{D}$-meson) decay constant and the space-like momentum $Q^2 = (M_D + \Lambda_M)^2$ with Λ_M being the matching scale. We note that the heavy quark limit $M_D \to \infty$ should be taken with Λ_M kept fixed since Λ_M must be smaller than the chiral symmetry breaking scale characterized by $\Lambda_\chi \sim 4\pi f_\pi$. Then, Q^2 should be regarded as $Q^2 \simeq M_D^2$ in the present framework based on the chiral and heavy quark symmetries. If we ignore the difference between F_D and $F_{\tilde{D}}$ which can be justified by the QCD sum rule analysis [101], then we get

$$\Delta_{SP}(Q^2) \equiv G_S(Q^2) - G_P(Q^2) \simeq \frac{3F_D^2 M_D^3}{M_D^2 + Q^2} \Delta M_D. \tag{6.26}$$

In the QCD sector, the correlators G_S and G_P are given by the operator product expansion (OPE) as [102]

$$\begin{aligned} G_S(Q^2) &= G(Q^2)\big|_{\rm pert} \\ &+ \frac{m_H^2}{m_H^2 + Q^2}\left[- m_H \langle \bar{q}q \rangle + \frac{\alpha_s}{12\pi} \langle G^{\mu\nu} G_{\mu\nu} \rangle \right], \\ G_P(Q^2) &= G(Q^2)\big|_{\rm pert} \\ &+ \frac{m_H^2}{m_H^2 + Q^2}\left[m_H \langle \bar{q}q \rangle + \frac{\alpha_s}{12\pi} \langle G^{\mu\nu} G_{\mu\nu} \rangle \right], \end{aligned} \tag{6.27}$$

where m_H is the heavy-quark mass. To the accuracy we are aiming at, the OPE can be truncated at $\mathcal{O}(1/Q^2)$. The explicit expression for the perturbative contribution $G(Q^2)|_{\rm pert}$ is available in the literature but we do not need it since it drops out in the difference. From these correlators, the Δ_{SP} becomes

$$\Delta_{SP}(Q^2) = -\frac{2m_H^3}{m_H^2 + Q^2} \langle \bar{q}q \rangle. \tag{6.28}$$

[#5] Here and in the rest of this chapter, the heavy meson is denoted D with the open charm heavy meson in mind. However the arguments (except for the numerical values) are generic for all heavy mesons $\mathcal{M}$.

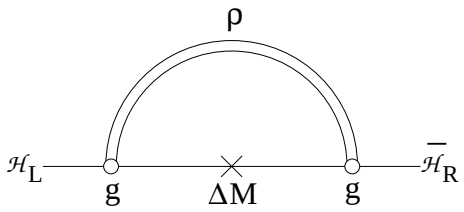

Figure 6.1: Diagram contributing to the mass difference.

Equating Eq. (6.26) to Eq. (6.28) and neglecting the difference $(m_H - M_D)$, we obtain the following matching condition:

$$3F_D^2\,\Delta M \simeq -2\langle\bar{q}q\rangle. \tag{6.29}$$

Thus at the matching scale, the splitting is

$$\Delta M_{\rm bare} \simeq -\frac{2}{3}\frac{\langle\bar{q}q\rangle}{F_D^2}. \tag{6.30}$$

As announced, the *bare* splitting is indeed proportional to the light-quark condensate. The quantum corrections do not change the dependence on the quark condensate [see section 6.4].

6.4 Quantum Corrections and RGE

Given the bare Lagrangian whose parameters are fixed at the matching scale Λ_M, the next step is to decimate the theory à la Wilson to the scale at which ΔM is measured. This amounts to calculating quantum corrections to the mass difference ΔM in the framework of the present EFT.

This calculation turns out to be surprisingly simple for $a \approx 1$. If one sets $a = 1$ which is the approximation we are adopting here, α_L does not mix with α_R in the light sector, and then α_L couples to only $\mathcal{H}_L$ and α_R to only $\mathcal{H}_R$. As a result $\mathcal{H}_{L(R)}$ cannot connect to $\mathcal{H}_{R(L)}$ by the exchange of α_L or α_R. Only the ρ-loop links between the fields with different chiralities as shown in Fig. 6.1. We have verified this approximation to be reliable since corrections to the result with $a = 1$ come only at higher loop orders [see the next paragraph]. The diagram shown in Fig. 6.1 contributes to the two-point function as

$$\Pi_{LR}\Big|_{\rm div} = -\frac{1}{2}\Delta M\,\mathcal{C}_2(N_f)\,\frac{g^2}{2\pi^2}\Big(1-2k-k^2\Big)\ln\Lambda, \tag{6.31}$$

where $\mathcal{C}_2(N_f)$ is the second Casimir defined by $(T_a)_{ij}(T_a)_{jl} = \mathcal{C}_2(N_f)\delta_{il}$ with i, j and l denoting the flavor indices of the light quarks. This divergence is renormalized by the bare contribution

of the form $\Pi_{LR,\mathrm{bare}} = \frac{1}{2}\Delta M_{\mathrm{bare}}$. Thus the renormalization-group equation (RGE) takes the form

$$\mu\frac{d\,\Delta M}{d\mu} = \mathcal{C}_2(N_f)\,\frac{g^2}{2\pi^2}\Big(1-2k-k^2\Big)\Delta M. \tag{6.32}$$

For an approximate estimate that we are interested in at this point, it seems reasonable to ignore the scale dependence in g and k. Then the solution is simple:

$$\Delta M = \Delta M_{\mathrm{bare}} \times C_{\mathrm{quantum}}\ , \tag{6.33}$$

where we define C_{quantum} by

$$C_{\mathrm{quantum}} = \exp\Big[-\mathcal{C}_2(N_f)\,\frac{g^2}{2\pi^2}\Big(1-2k-k^2\Big)\ln\frac{\Lambda}{\mu}\Big]\ . \tag{6.34}$$

This shows unequivocally that the mass splitting is dictated by the "bare" splitting ΔM_{bare} proportional to $\langle\bar{q}q\rangle$ corrected by the quantum effect C_{quantum}.

Next we lift the condition $a = 1$ made in the above analysis. For this purpose, we compute the quantum effects to the masses of 0^- (P) and 0^+ (Q^*) D-mesons by calculating the one-loop corrections to the two-point functions of P and Q^* denoted by Π_{PP} and $\Pi_{Q^*Q^*}$ [for the explicit calculation, see Appendix H]. We find that amazingly, the resultant form of the quantum correction exactly agrees with the previous one which was obtained by taking $a = 1$. To arrive at this result, it is essential that P (or P^*_μ) be the chiral partner of Q^* (or Q_μ) as follows: The loop diagrams shown in Fig. H.1 and Fig. H.2 in Appendix H have power and logarithmic divergences. However all the divergences of the diagrams with pion loop are exactly canceled among themselves since the internal (or external) particles are chiral partners. In a similar way, the exact cancellation takes place in the diagrams with σ loop. Finally, the logarithmic divergence from the ρ loop does contribute to the mass difference. This shows that the effect of spontaneous chiral symmetry breaking introduced as the deviation of a from 1 does not get transferred to the heavy sector. Thus even in the case of $a \neq 1$, the bare mass splitting is enhanced by only the vector meson loop, with the pions not figuring in the quantum corrections at least at one-loop order. Solving the RGE (H.11), which is exactly same as Eq. (6.32), we obtain exactly the same mass splitting as the one given in Eq. (6.33).

6.5 Mass Splitting

In this section we make a numerical estimation of the mass splitting for the chiral doublers in the open charm system. (Here D denotes the open charm meson.) Since we are considering the chiral limit, strictly speaking, a precise comparison with experiments is not feasible particularly

if the light quark is strange, so what we obtain should be considered as semi-quantitative at best. This caveat should be kept in mind in what follows.

Determining the bare mass splitting from the matching condition (6.30) requires the quark condensate at that scale and the D-meson decay constant F_D. For the quark condensate, we shall use the so-called "standard value" [103] $\langle\bar{q}q\rangle = -(225 \pm 25\,\mathrm{MeV})^3$ at 1 GeV. Extrapolated to the scale $\Lambda_M = 1.1$ GeV we shall adopt here, this gives

$$\langle\bar{q}q\rangle_{\Lambda_M} = -(228 \pm 25\,\mathrm{MeV})^3. \tag{6.35}$$

Unfortunately this value is not firmly established, there being no consensus on it. The values found in the literature vary widely, even by a factor of ~ 2, some higher [104] and some lower [105]. (We will study the dependence on the values of the mass splitting of those of the quark condensate later.) Here we take the standard value as a median [#6]. As for the D-meson decay constant, we take as a typical value $F_D = 0.205 \pm 0.020\,\mathrm{GeV}$ obtained from the QCD sum rule analysis [101]. Plugging the above input values into Eq. (6.30) we obtain

$$\Delta M_{\mathrm{bare}} \simeq 0.19\,\mathrm{GeV}\ . \tag{6.36}$$

By taking $\mu = m_\rho = 771\,\mathrm{MeV}$, $\Lambda = \Lambda_M = 1.1\,\mathrm{GeV}$, $g = g(m_\rho) = 6.27$ determined via the Wilsonian matching for $(\Lambda_M, \Lambda_{\mathrm{QCD}}) = (1.1, 0.4)\,\mathrm{GeV}$ in Ref. [13] and $k \simeq 0.59$ extracted from the $D^* \to D\pi$ decay [see section 6.6.1] in Eq. (6.34), we find for $N_f = 3$

$$C_{\mathrm{quantum}} = 1.6\ . \tag{6.37}$$

This is a sizable quantum correction involving only the vector meson. If one takes into account the uncertainties involved in the condensate and the decay constant, the quantum-corrected splitting ΔM comes out to be

$$\Delta M \approx 0.31 \pm 0.12\,\mathrm{GeV}\ . \tag{6.38}$$

Despite the uncertainty involved, (6.38) is a pleasing result. It shows that the splitting is indeed of the size of the constituent quark mass of a chiral quark $\Sigma \sim m_p/3 \sim 310$ MeV and is directly proportional to the quark condensate.

[#6] It was shown in Ref. [105] that there is a strong N_f dependence on the quark condensate and the value of the quark condensate for QCD with three massless quarks is smaller than the value used in estimating the value of the mass splitting in section 6.5. In the present analysis, we extract the value of the coupling constant k from the experiment. To be consistent, we need to use the quark condensate together with other parameters involved determined at the same scale from experimental and/or lattice data. This corresponds to the standard value of the condensate we are using here.

We emphasized in the above analysis that there is a great deal of uncertainty on the value of the quark condensate at the relevant matching scale Λ_M. Here we list a few examples to show what sort of uncertainty we are faced with. We took $\langle\bar{q}q\rangle_{1\,\mathrm{GeV}} = -(225\pm 25\,\mathrm{MeV})^3$ in the above analysis as a "standard value." For comparison, we shall take two other values quoted in Ref. [104] (without making any judgments on their validity). Consider therefore

$$\begin{aligned}\langle\bar{q}q\rangle_{1\,\mathrm{GeV}} &= -(225\pm 25\,\mathrm{MeV})^3\ ,\\ \langle\bar{q}q\rangle_{2\,\mathrm{GeV}} &= \begin{cases} -(273\pm 19\,\mathrm{MeV})^3\ , \\ -(316\pm 24\,\mathrm{MeV})^3\ . \end{cases}\end{aligned} \tag{6.39}$$

Brought by RGE to the scale we are working at, $\Lambda_M = 1.1$ GeV, and substituted into our formula for ΔM, we get the corresponding quantum corrected splitting

$$\Delta M = \begin{cases} 0.31\pm 0.12\,\mathrm{GeV}\ , \\ 0.43\pm 0.12\,\mathrm{GeV}\ , \\ 0.67\pm 0.20\,\mathrm{GeV}\ . \end{cases} \tag{6.40}$$

This result clearly shows that the splitting cannot be pinned down unless one has a confirmed quark condensate.

We should stress other several caveats associated with (6.38). Apart from the sensitivity to the quark condensate, if one naively plugs in the matching scale Λ_M into the RGE solution, one finds the splitting is not insensitive as it should be to the scale change. This is neither surprising nor too disturbing since our RGE solution is obtained with the scale dependence in both g and k ignored. In order to eliminate this dependence on the matching scale, it will be necessary to solve the RGE with the full scale dependence taken into account – which is at the moment beyond our scope here. The best we can do within the scheme adopted is to pick the optimal Λ_M determined phenomenologically from elsewhere [13] and this is what we have done above.

6.6 Hadronic Decay Modes

In this section we turn to the hadronic decay processes of the $\tilde{D}$ mesons and make predictions of our scenario based on the vector manifestation (VM) of chiral symmetry. Here we adopt the notations $D_{u,d}$ and $\tilde{D}_{u,d}$ for the heavy ground-state mesons and heavy excited mesons composed of $c\bar{u}$ and $c\bar{d}$, and D_s and $\tilde{D}_s$ for those composed of $c\bar{s}$. The spin-parity quantum numbers will be explicitly written as $D_{u,d}(0^-)$. For the heavy vector meson, we follow the notation adopted by the Particle Data Group (PDG) [26] and write $D^*_{u,d}(1^-)$ and $D^*_s(1^-)$.

Unless otherwise noted, the masses of the ground-state heavy mesons will be denoted as M_D and those of the excited states as $M_{\tilde{D}}$.

6.6.1 $D^* \to D + \pi$

Before studying the decay processes of the excited heavy mesons, we first calculate the decay width of $D^*_{u,d} \to D_{u,d} + \pi$ so as to determine the coupling constant k. The decay widths of the π^0 and the $\pi^\pm$ modes are given by

$$\begin{aligned}\Gamma(D^*_{u,d}(1^-) \to D_{u,d}(0^-) + \pi^0) &= \frac{\bar{p}_\pi^3}{24\pi M_{D^*}^2}\left(M_Q\,\frac{k}{F_\pi}\right)^2 , \\ \Gamma(D^*_{u,d}(1^-) \to D_{u,d}(0^-) + \pi^\pm) &= \frac{\bar{p}_\pi^3}{12\pi M_{D^*}^2}\left(M_Q\,\frac{k}{F_\pi}\right)^2 , \end{aligned} \tag{6.41}$$

where $\bar{p}_\pi \equiv |\vec{p}_\pi|$ denotes the three-momentum of the pion in the rest frame of the decaying particle $D^*_{u,d}(1^-)$, and M_Q the "heavy quark mass" introduced for correctly normalizing the heavy meson field. In the present analysis we use the following reduced mass for definiteness:

$$M_Q \equiv \frac{1}{4}\Big(M_{D(0^-)} + 3M_{D^*(1^-)}\Big) = 1974\,\mathrm{MeV} . \tag{6.42}$$

The total width is not determined for $D^*_u(1^-)$, although the branching fractions for both the π^0 and the π^+ decay modes are known experimentally. For $D^*_d(1^-)$ meson, on the other hand, the total width is also determined. Using the values listed in PDG table [26], the partial decay widths are estimated to be

$$\begin{aligned}&\Gamma(D^*_d(1^-) \to D_d(0^-) + \pi^0) = 29.5 \pm 6.8\,\mathrm{keV} , \\ &\Gamma(D^*_d(1^-) \to D_u(0^-) + \pi^+) = 65 \pm 15\,\mathrm{keV} . \end{aligned} \tag{6.43}$$

Here the π^0 mode will be used as an input to fix k. From the experimental masses $M_{D^*_u(1^-)} = 2010.1\,\mathrm{MeV}$, $M_{D_d(0^-)} = 1869.4\,\mathrm{MeV}$ and $M_{\pi^0} = 134.9766\,\mathrm{MeV}$ together with the value of the pion decay constant $F_\pi = 92.42 \pm 0.26\,\mathrm{MeV}$, we obtain

$$k = 0.59 \pm 0.07 . \tag{6.44}$$

Note that the error is mainly from that of the $D^*_d(1^-) \to D_d(0^-) + \pi^0$ decay width.

In the following analysis, we shall use the central value of k to make predictions for the decay widths of $\tilde{D}$ mesons. Each prediction includes at least about 25% error from the value of k. For the masses of excited D mesons, we use $M_{\tilde{D}_s(0^+)} = 2317\,\mathrm{MeV}$ determined by BaBar [34], $M_{\tilde{D}_s(1^+)} = 2460\,\mathrm{MeV}$ by CLEO [35] and $(M_{\tilde{D}_{u,d}(0^+)}, M_{\tilde{D}_{u,d}(1^+)}) = (2308, 2427)\,\mathrm{MeV}$ by Belle [36]. Table 6.1 summarizes the input parameters used in the present analysis.

$D_{u,d}$ meson masses	$M_{\tilde{D}_{u,d}(1^+)}$	$M_{\tilde{D}_{u,d}(0^+)}$	$M_{D^*_{u,d}(1^-)}$	$M_{D_{u,d}(0^-)}$
(MeV)	2427	2308	2010	1865
D_s meson masses	$M_{\tilde{D}_s(1^+)}$	$M_{\tilde{D}_s(0^+)}$	$M_{D^*_s(1^-)}$	$M_{D_s(0^-)}$
(MeV)	2460	2317	2112	1969
Light meson masses	M_π	M_ρ	M_η	M_ϕ
(MeV)	138.039	771.1	547.30	1019.456
π^0-η mixing	A_{11}	A_{21}	$\Pi_{\pi^0\eta}\,(\mathrm{MeV})^2$	$K_{\pi^0\eta}$
	0.71	-0.52	-4.25×10^3	-1.06×10^{-2}
ϕ-ρ mixing	$\Gamma_{\phi\to\pi^+\pi^-}$ (MeV)	$\Gamma_{\rho\to\pi^+\pi^-}$ (MeV)		
	3.11×10^{-4}	149.2		

Table 6.1: The values of input parameters. We use the values of $M_{\tilde{D}_s(0^+)}$ [34], $M_{\tilde{D}_s(1^+)}$ [35] and $M_{\tilde{D}_{u,d}(0^+,1^+)}$ [36]. The D mesons in the ground state, light mesons and decay widths $\Gamma(\phi,\rho)$ are the values listed by the PDG table [26]. As for the parameters associated with the π^0-η mixing, we use the values given in Refs. [106, 107].

6.6.2 $\tilde{D}\to D+\pi$

For the systems of $c\bar{u}$ and $c\bar{d}$, the following decay processes of the $\tilde{D}_{u,d}$ meson into the $D_{u,d}$ meson and one pion are allowed by the spin and parity:

$$\tilde{D}_{u,d}(0^+)\to D_{u,d}(0^-)+\pi \qquad \tilde{D}_{u,d}(1^+)\to D^*_{u,d}(1^-)+\pi. \tag{6.45}$$

Their partial decay widths are given by

$$\begin{aligned}\Gamma(\tilde{D}_{u,d}\to D_{u,d}+\pi^\pm)&=\frac{\bar{p}_\pi}{4\pi}\left(\frac{k}{F_\pi}\frac{M_Q}{M_{\tilde{D}}}E_\pi\right)^2,\\ \Gamma(\tilde{D}_{u,d}\to D_{u,d}+\pi^0)&=\frac{\bar{p}_\pi}{8\pi}\left(\frac{k}{F_\pi}\frac{M_Q}{M_{\tilde{D}}}E_\pi\right)^2,\end{aligned} \tag{6.46}$$

where E_π is the energy of the pion, and the reduced mass M_Q is defined in Eq. (6.42). With the input parameters given in Table 6.1, these decay widths come out to be

$$\begin{aligned}\Gamma(\tilde{D}_{u,d}(0^+)\to D_{u,d}(0^-)+\pi^0)&=74\pm18\,\mathrm{MeV}\ ,\\ \Gamma(\tilde{D}_{u,d}(0^+)\to D_{u,d}(0^-)+\pi^\pm)&=147\pm37\,\mathrm{MeV}\ ,\\ \Gamma(\tilde{D}_{u,d}(1^+)\to D^*_{u,d}(1^-)+\pi^0)&=57\pm14\,\mathrm{MeV}\ ,\\ \Gamma(\tilde{D}_{u,d}(1^+)\to D^*_{u,d}(1^-)+\pi^\pm)&=114\pm29\,\mathrm{MeV}\ ,\end{aligned} \tag{6.47}$$

Here we have put the 25% error from the value of k, which we expect the dominant one.

For the system of $c\bar{s}$ there are two decay processes of the $\tilde{D}_s$ meson into the D_s meson and one pion:

$$\tilde{D}_s(0^+) \to D_s(0^-) + \pi^0 \qquad \tilde{D}_s(1^+) \to D_s^*(1^-) + \pi^0. \tag{6.48}$$

These processes violate the isospin invariance, and hence are suppressed. In the present analysis we assume as in Ref. [108] that the isospin violation occurs dominantly through the π^0-η mixing. In other words, we assume that the $\tilde{D}_s$ meson decays into the D_s meson and the virtual η meson which mixes with the π^0 through the π^0-η mixing. Then, the decay width is given by

$$\Gamma(\tilde{D}_s \to D_s + \pi^0) = \frac{\bar{p}_\pi}{2\pi}\left(\frac{k}{F_\pi}\frac{M_Q}{M_{\tilde{D}}}E_\pi \Delta_{\pi^0\eta}\right)^2, \tag{6.49}$$

where $\Delta_{\pi^0\eta}$ denotes the π^0-η mixing and takes the following form [106, 107]:

$$\Delta_{\pi^0\eta} = -\frac{A_{11}A_{21}}{M_\eta^2 - M_{\pi^0}^2}(\Pi_{\pi^0\eta} - K_{\pi^0\eta}M_{\pi^0}^2) \tag{6.50}$$

with $\Pi_{\pi^0\eta}$ and $K_{\pi^0\eta}$ being the mass-type and kinetic-type π^0-η mixing, respectively. A_{11} and A_{21} are the components of the η-η' mixing matrix in the two-mixing-angle scheme [106]. By using the values listed in Table 6.1, the π^0-η mixing is estimated as

$$\Delta_{\pi^0\eta} = -5.3 \times 10^{-3}. \tag{6.51}$$

From this value, the predicted decay widths are estimated as

$$\begin{aligned}\Gamma(\tilde{D}_s(0^+) \to D_s(0^-) + \pi^0) &\sim 4\,\mathrm{keV}\ , \\ \Gamma(\tilde{D}_s(1^+) \to D_s^*(1^-) + \pi^0) &\sim 4\,\mathrm{keV}\ .\end{aligned} \tag{6.52}$$

6.6.3 $\tilde{D}(1^+) \to \tilde{D}(0^+) + \pi$

With the masses of $\tilde{D}_{u,d}(1^+)$ and $\tilde{D}_{u,d}(0^+)$ listed in Table 6.1, the intra-multiplet decay $\tilde{D}_{u,d}(1^+) \to \tilde{D}_{u,d}(0^+) + \pi$ is not allowed kinematically. Since the experimental errors for the masses are large [#7], this decay mode may still turn out to be possible. To show how large the possible decay width is, we use $M_{\tilde{D}_{u,d}(0^+)} = 2272\,\mathrm{MeV}$ and $M_{\tilde{D}_{u,d}(1^+)} = 2464\,\mathrm{MeV}$ together with the formulas

$$\begin{aligned}\Gamma(\tilde{D}_{u,d}(1^+) \to \tilde{D}_{u,d}(0^+) + \pi^0) &= \frac{\bar{p}_\pi^3}{24\pi}\left(\frac{M_Q}{M_{\tilde{D}(1^+)}}\frac{k}{F_\pi}\right)^2\ , \\ \Gamma(\tilde{D}_{u,d}(1^+) \to \tilde{D}_{u,d}(0^+) + \pi^+) &= \frac{\bar{p}_\pi^3}{12\pi}\left(\frac{M_Q}{M_{\tilde{D}(1^+)}}\frac{k}{F_\pi}\right)^2\ .\end{aligned} \tag{6.53}$$

[#7] The Belle collaboration [109, 110, 111] gives $M_{\tilde{D}_{u,d}(1^+)} = 2427 \pm 26 \pm 20 \pm 17\,\mathrm{MeV}$ and $M_{\tilde{D}_{u,d}(0^+)} = 2308 \pm 17 \pm 15 \pm 28\,\mathrm{MeV}$.

The resultant decay widths are given by

$$\Gamma(\tilde{D}_{u,d}(1^+) \to \tilde{D}_{u,d}(0^+) + \pi^0) = 0.7 \pm 0.2\,\mathrm{MeV}\ ,$$
$$\Gamma(\tilde{D}_{u,d}(1^+) \to \tilde{D}_{u,d}(0^+) + \pi^+) = 1.5 \pm 0.4\,\mathrm{MeV}\ , \tag{6.54}$$

where we put 25% error coming from the value of k. We expect that this is the main source of the entire error. They are smaller by the order of 10^{-2} than other one-pion modes [see Table 6.2]. This is caused by the suppression from the phase space.

With the present input values of $\tilde{D}$ masses, the process $\tilde{D}_s(1^+) \to \tilde{D}_s(0^+) + \pi^0$ is kinematically allowed. Similarly to the $\tilde{D}_s \to D_s + \pi^0$ decay, we assume that this decay is dominated by the process through the π^0-η mixing. Then, the decay width is estimated as

$$\begin{aligned}\Gamma(\tilde{D}_s(1^+) \to \tilde{D}_s(0^+) + \pi^0) &= \frac{\bar{p}_\pi^3}{6\pi}\left(\frac{k}{F_\pi}\frac{M_Q}{M_{\tilde{D}(1^+)}}\Delta_{\pi^0\eta}\right)^2 \\ &\sim 2 \times 10^{-3}\,\mathrm{keV}.\end{aligned} \tag{6.55}$$

This is very tiny due to the isospin violation and the phase-space suppression.

6.6.4 $\tilde{D} \to D + 2\pi$

There are several processes such as $\tilde{D} \to D + \pi^\pm\pi^\mp$ to which the light scalar mesons could give important contributions. In models based on the standard scenario of the chiral symmetry restoration in the light quark sector, the scalar-meson coupling to the heavy-quark system is related to the pion coupling, enabling one to compute the decay width. In our model based on the VM of the chiral symmetry restoration, on the other hand, it is the coupling constant of the vector meson to the heavy system that is related to the pion coupling constant: Here coupling of the scalar meson is not directly connected, at least in the present framework which contains no explicit scalar fields [#8], to do that of the pion. So, while we cannot make firm predictions to processes for which scalar mesons might contribute, we can make definite predictions on certain decay widths for which scalar mesons do not figure. If one ignores isospin violation, the two-pion decay processes $\tilde{D}_{u,d} \to D_{u,d} + \pi^\pm\pi^0$ receive no contributions from scalar mesons. We give predictions for these processes below. As for the two-pion decay modes of the $\tilde{D}_s$ meson, the scalar mesons could give a contribution. To have an idea, we shall also compute the vector-meson contribution to this process.

[#8] Scalar excitations can of course be generated at high loop level to assure unitarity or with the account of QCD trace anomaly but we shall not attempt this extension in this paper.

First, consider $\tilde{D}_{u,d}(0^+) \to D^*_{u,d}(1^-) + \pi^\pm\pi^0$. In this process, there are two contributions:

$$\begin{aligned} \tilde{D}_{u,d}(0^+) \;\; &\to \;\; D^*_{u,d}(1^-) + \pi^\pm\pi^0 \qquad\qquad \text{(direct)} \\ &\qquad\; D^*_{u,d}(1^-) + (\rho^\pm \to \pi^\pm\pi^0) \qquad \text{(ρ-mediation)} \; . \end{aligned} \tag{6.56}$$

The decay width is given by

$$\begin{aligned} &\Gamma(\tilde{D}_{u,d}(0^+) \to D^*_{u,d}(1^-) + \pi^\pm\pi^0) \\ &\quad = \frac{M_Q^2}{64(2\pi)^3 M_{\tilde{D}}^3} \frac{k^2}{F_\pi^4} \int dm_{D\pi}^2 \int dm_{\pi\pi}^2 |F_{\tilde{D}D}|^2 \\ &\qquad \times \left[m_{\pi\pi}^2 - 4M_\pi^2 + \frac{1}{4M_D^2}(m_{\pi\pi}^2 - M_{\tilde{D}}^2 - M_D^2 - 2M_\pi^2 + 2m_{D\pi}^2)^2 \right], \end{aligned} \tag{6.57}$$

with $m_{D\pi}^2 = (p_D + p_\pi)^2$ and $m_{\pi\pi}^2 = (p_{1\pi} + p_{2\pi})^2$. The form factor $F_{\tilde{D}D}$ is taken to be of the form

$$F_{\tilde{D}D} = 1 + \frac{M_\rho^2}{m_{\pi\pi}^2 - M_\rho^2} \; . \tag{6.58}$$

The first term of the form factor comes from the direct contribution and the second from the ρ-mediation. Here we have neglected the ρ meson width in the propagator, since the maximum value of $m_{\pi\pi}$ is about 300 MeV with the input values listed in Table 6.1. We can see that the form factor $F_{\tilde{D}D}$ vanishes in the limit of $m_{\pi\pi} \to 0$, which is a consequence of chiral symmetry [#9]. We note that $m_{\pi\pi}|_{\max} \simeq 300\,\text{MeV}$ makes this decay width strongly suppressed due to the large cancellation between the direct and ρ-mediated contributions. Furthermore, since 300 MeV is close to the two-pion threshold, additional suppression comes from the phase space. Due to these two types of suppressions the predicted decay width is predicted to be very small, of the order of 10^{-2} keV. [#10]

Next we consider the process $\tilde{D}_{u,d}(1^+) \to D^*_{u,d}(1^-) + \pi\pi$. Again there are two contributions, direct and a ρ-mediated:

$$\begin{aligned} \tilde{D}_{u,d}(1^+) \;\; &\to \;\; D^*_{u,d}(1^-) + \pi^\pm\pi^0 \qquad\qquad \text{(direct)} \\ &\qquad\; D^*_{u,d}(1^-) + (\rho^\pm \to \pi^\pm\pi^0) \qquad \text{(ρ-mediation)} \end{aligned} \tag{6.59}$$

[#9] It should be stressed that this cancellation occurs because the vector meson is included consistently with chiral symmetry, and that it is *not* a specific feature of the VM. The chiral symmetry restoration based on the VM implies that the coupling constant of the vector meson to the heavy system is equal to that of the pion.

[#10] Note that the prediction on the decay width is very sensitive to the precise value of the mass of $\tilde{D}(0^+)$ meson.

The resultant decay width is given by

$$\begin{aligned}
&\Gamma(\tilde{D}_{u,d}(1^+) \to D^*_{u,d}(1^-) + \pi^\pm\pi^0) \\
&= \frac{M_Q^2}{96(2\pi)^3 M_{\tilde{D}}^3}\frac{k^2}{F_\pi^4}\int dm_{D\pi}^2 \int dm_{\pi\pi}^2 |F_{\tilde{D}D}|^2 \\
&\quad\times\left[m_{\pi\pi}^2 - 4M_\pi^2 + \frac{1}{4M_{\tilde{D}}^2}(m_{\pi\pi}^2 - M_{\tilde{D}}^2 - M_D^2 - 2M_\pi^2 + 2m_{D\pi}^2)^2\right].
\end{aligned} \tag{6.60}$$

Similarly to $\Gamma(\tilde{D}_{u,d}(0^+) \to D^*_{u,d}(1^-) + \pi^\pm\pi^0)$, the width is again suppressed due to the large cancellation between the direct and ρ-mediated contributions. The suppression from the phase space, on the other hand, is not so large since $m_{\pi\pi}|_{\rm max} \simeq 420\,{\rm MeV}$ is not so close to the two-pion threshold. The resulting decay width is

$$\Gamma(\tilde{D}_{u,d}(1^+) \to D^*_{u,d}(1^-) + \pi^\pm\pi^0) = 12 \pm 3\,{\rm keV}\ , \tag{6.61}$$

where the error comes from the value of k.

The decay width of the process

$$\begin{aligned}
\tilde{D}_{u,d}(1^+) \ &\to\ D_{u,d}(0^-) + \pi^\pm\pi^0 \qquad\qquad \text{(direct)} \\
&\quad\ D_{u,d}(0^-) + (\rho^\pm \to \pi^\pm\pi^0) \qquad \text{(ρ-mediation)}
\end{aligned} \tag{6.62}$$

is given by

$$\begin{aligned}
&\Gamma(\tilde{D}_{u,d}(1^+) \to D_{u,d}(0^-) + \pi^\pm\pi^0) \\
&= \frac{M_Q^2}{192(2\pi)^3 M_{\tilde{D}}^3}\frac{k^2}{F_\pi^4}\int dm_{D\pi}^2 \int dm_{\pi\pi}^2 |F_{\tilde{D}D}|^2 \\
&\quad\times\left[m_{\pi\pi}^2 - 4M_\pi^2 + \frac{1}{4M_{\tilde{D}}^2}(m_{\pi\pi}^2 - M_{\tilde{D}}^2 - M_D^2 - 2M_\pi^2 + 2m_{D\pi}^2)^2\right].
\end{aligned} \tag{6.63}$$

In the present case, $m_{\pi\pi}|_{\rm max} \simeq 560\,{\rm MeV}$ is much larger than the two-pion threshold and hence the width becomes larger than other two-pion processes. We find

$$\Gamma(\tilde{D}_{u,d}(1^+) \to D_{u,d}(0^-) + \pi^\pm\pi^0) = 310 \pm 80\,{\rm keV}, \tag{6.64}$$

where the error comes from the value of k.

Finally we turn to the decay $\tilde{D}_s(1^+) \to D_s(0^-) + \pi^+\pi^-$ which as mentioned could receive direct contributions from scalar excitations. Since we have not incorporated scalar degrees of freedom in the theory, we might not be able to make a reliable estimate even if were to go to higher-loop orders. Just to have an idea as to how important the vector meson contribution can be, we calculate the decay width in which the $\tilde{D}_s$ meson decays into two pions through

the ϕ meson. This isospin violating decay can occur through the direct ϕ-π-π coupling and the ϕ-ρ mixing:

$$\begin{aligned} \tilde{D}_s(1^+) \;\; &\rightarrow \;\; D_s(0^-) + (\phi \rightarrow \pi^+\pi^-) \qquad\qquad \text{(direct)} \\ &\qquad\;\; D_s(0^-) + (\phi \rightarrow \rho^0 \rightarrow \pi^+\pi^-) \qquad \text{(ϕ-ρ mixing)} \end{aligned} \tag{6.65}$$

Since the main contribution to the $\phi \rightarrow \pi\pi$ is expected to be given by the ϕ-ρ mixing, we shall neglect the direct ϕ-π-π-coupling contribution in the following. Then the decay width is given by

$$\begin{aligned} &\Gamma(\tilde{D}_s(1^+) \rightarrow D_s(0^-) + \pi^+\pi^-) \\ &\quad = \frac{M_Q^2}{192(2\pi)^3 M_{\tilde{D}}^3}\frac{k^2}{F_\pi^4}\int dm_{D\pi}^2 \int dm_{\pi\pi}^2 \left[\frac{M_\rho^2 \Pi_{\phi\rho}}{(m_{\pi\pi}^2 - M_\phi^2)(m_{\pi\pi}^2 - M_\rho^2)}\right]^2 \\ &\qquad \times \left[m_{\pi\pi}^2 - 4M_\pi^2 + \frac{1}{4M_{\tilde{D}}^2}(m_{\pi\pi}^2 - M_{\tilde{D}}^2 - M_D^2 - 2M_\pi^2 + 2m_{D\pi}^2)^2\right], \end{aligned} \tag{6.66}$$

where $\Pi_{\phi\rho}$ denotes the ϕ-ρ mixing given by

$$\Pi_{\phi\rho}^2 = (M_\phi^2 - M_\rho^2)^2 \left(\frac{\bar{p}_\pi(\rho)}{\bar{p}_\pi(\phi)}\right)^3 \frac{M_\phi^2}{M_\rho^2}\frac{\Gamma(\phi \rightarrow \pi^+\pi^-)}{\Gamma(\rho \rightarrow \pi^+\pi^-)}, \tag{6.67}$$

with $\bar{p}_\pi(X)$ being the three-momentum of pion in the rest frame of the decaying particle $X = \phi, \rho$. Using the values listed in Table 6.1, we have

$$\Pi_{\phi\rho} = 530\,(\text{MeV})^2 \tag{6.68}$$

so the decay width is predicted to be

$$\Gamma(\tilde{D}_s(1^+) \rightarrow D_s(0^-) + \pi^+\pi^-) \sim 2 \times 10^{-4}\,\text{keV}\ . \tag{6.69}$$

The ϕ-ρ mixing is caused by the isospin violation, and this process is highly suppressed. We conclude that should a measured width come out to be substantially greater than what we found here, it would mean that either scalars must figure importantly or the VM is invalid in its present form.

6.6.5 Summary of hadronic decay modes

Our predictions of the decay widths are summarized in Table 6.2. It should be stressed that the values obtained in this paper on the one-pion reflect only that the $\tilde{D}$ meson is the chiral partner of the D meson. They are *not* specific to the VM. We therefore expect that as

Decaying particle	Process	Width (MeV)
$\tilde{D}_{u,d}$	$0^+ \to 0^- + \pi^0$	$(7.4 \pm 1.8) \times 10^1$
	$0^+ \to 0^- + \pi^\pm$	$(1.5 \pm 0.4) \times 10^2$
	$0^+ \to 1^- + \pi^\pm\pi^0$	$\sim 2 \times 10^{-5}$
	$1^+ \to 1^- + \pi^0$	$(5.7 \pm 1.4) \times 10^1$
	$1^+ \to 1^- + \pi^\pm$	$(1.1 \pm 0.3) \times 10^2$
	$1^+ \to 0^- + \pi^\pm\pi^0$	$(3.1 \pm 0.8) \times 10^{-1}$
	$1^+ \to 1^- + \pi^\pm\pi^0$	$(1.2 \pm 0.3) \times 10^{-2}$
$\tilde{D}_s$	$0^+ \to 0^- + \pi^0$	$\sim 4 \times 10^{-3}$
	$1^+ \to 0^+ + \pi^0$	$\sim 2 \times 10^{-6}$
	$1^+ \to 1^- + \pi^0$	$\sim 4 \times 10^{-3}$
	$1^+ \to 0^- + \pi^+\pi^-$ (through $\phi \to \rho^0 \to \pi^+\pi^-$)	$\sim 2 \times 10^{-7}$

Table 6.2: The predicted values of the hadronic decay processes. 25% error comes from the value of k. "$\sim$" implies that the precise value also depends on parameters other than k, and we can give only the order estimation.

far as the one-pion processes are concerned, there will be no essential differences between our predictions and those in Ref. [108]. However, in the two-pion decay processes in which the scalar meson does not mediate, our scenario based on the VM can make definite predictions which might be distinguished from that based on the standard picture. Especially for $\tilde{D}_{u,d}(1^+) \to D_{u,d}(0^-) + \pi^\pm\pi^0$, we obtain a larger width than for other two-pion modes. Although the predicted width is still small – perhaps too small to be detected experimentally, it is important because of the following reason. In our approach, since the excited heavy meson multiplets of $\tilde{D}(0^+)$ and $\tilde{D}(1^+)$ denoted by G are the chiral partners to the ground-state multiplets denote by H, the G-$\bar{H}$-π coupling is the same as the H-$\bar{H}$-π coupling [see the fifth and first terms of Eq. (6.21)]. Thus the width which is dependent on the strength of k is a good probe to test our scenario. The common k is also essential for the ratio of the widths of the two-pion modes to those of the one-pion modes, which has no k dependence. These are therefore are definite predictions of our scenario. From the values listed in Table 6.2, we obtain

$$\frac{\Gamma(\tilde{D}_{u,d}(1^+) \to D_{u,d}(0^-) + \pi^\pm\pi^0)}{\Gamma^{(\mathrm{had})}_{\pi+2\pi}} \simeq 2 \times 10^{-3}, \tag{6.70}$$

where $\Gamma^{(\mathrm{had})}_{\pi+2\pi}$ is the sum of the widths of the one-pion and two-pion modes of the decaying $\tilde{D}_{u,d}(1^+)$.

Chapter 7

Summary and Discussions

In this thesis, we first showed the details of the hidden local symmetry (HLS) theory at finite temperature. Then in order to determine the parameters of the theory, we presented the extension of the Wilsonian matching at zero temperature to the version in hot matter. Next we showed the formulation of the vector manifestation (VM) in hot matter using the HLS theory. Based on the VM, we gave several predictions which are testable by experiments and lattice analysis. In the following, we summarize them and give discussions.

HLS theory at finite temperature

In chapter 3, we applied the HLS theory developed in Ref. [13] to QCD at finite temperature. Both pions and vector mesons are introduced as the relevant degrees of freedom into the theory, and thus the HLS theory has a wider range of the validity than the ordinary chiral perturbation theory (ChPT) including only pions. Especially we can see it in studying the pion decay constants which was carried out in section 3.4: Two kinds of pion decay constants, temporal and spatial components (f_π^t and f_π^s), appear due to the lack of Lorentz invariance in medium and in general they do not agree with each other. The splitting between f_π^t and f_π^s appears at one-loop level in the HLS theory, which is generated by the thermal loop contribution of the vector meson. [The non-zero splitting also implies that the pion velocity is not equal to the speed of light.] On the other hand, the splitting of the pion decay constant is not generated at one-loop level in the ordinary ChPT.

Further by using the Wilsonian matching studied in chapter 4, the intrinsic temperature dependences of the bare parameters are included. We in fact determined the intrinsic thermal effects to the bare pion decay constants by performing the matching to the operator product expansion (OPE) in section 4.2.

Formulation of the VM in hot matter

In chapter 5, we first presented the formulation of the VM in hot matter using the HLS theory combined with the Wilsonian matching. Throughout this thesis, we assume that the chiral phase transition is of second or weakly first order so that the axial-vector and vector current correlators agree with each other at the critical temperature. Thus the Wilsonian matching leads to the following conditions on the parameters of the bare HLS Lagrangian:

$$\begin{aligned} &g_{\rm bare}(T) \overset{T\to T_c}{\to} 0 \qquad (\text{ or } \quad M_{\rho,\rm bare}(T) \overset{T\to T_c}{\to} 0)\,, \\ &a_{\rm bare}(T) = \left(F_{\sigma,\rm bare}(T)/F_{\pi,\rm bare}(T)\right)^2 \overset{T\to T_c}{\to} 1\,. \end{aligned} \tag{7.1}$$

We should stress the following features: (i) The above conditions for the bare parameters are realized by the intrinsic thermal effect only. (ii) $(g, a) = (0, 1)$ is a fixed point of RGEs. The agreement of both current correlators is satisfied only in the case that we take into account the intrinsic thermal effects as well as the hadronic ones.

Vector meson mass : Near T_c, the vector meson mass has a positive thermal contribution, which is proportional to the square of the HLS gauge coupling g, as studied in section 5.2. When we take the limit $T \to T_c$, both the parametric mass M_ρ and hadronic thermal correction go to zero following Eq. (7.1). Thus we showed that the vector meson mass vanishes:

$$m_\rho^2(T) \overset{T\lesssim T_c}{\to} g^2(T)\Big[a(T)F_\pi^2(\mu=0;T) + \delta T^2\Big] \overset{T\to T_c}{\to} 0\,,$$

where δT^2 denotes the thermal contribution and $F_\pi(\mu = 0; T)$ is the on-shell parametric pion decay constant obtained in Eq. (5.30) to be non-zero.

Order parameter : If we write explicitly the quantum and hadronic thermal corrections to the parameter F_π, the pion decay constant at T_c takes the following form as studied in section 5.3:

$$f_\pi^2(T) \overset{T\to T_c}{\to} F_\pi^2(\Lambda; T_c) - \frac{N_f}{2(4\pi)^2}\Lambda^2 - \frac{N_f}{24}T_c^2 \;=\; 0\,.$$

This implies that the order parameter goes to zero by the cancellation among the non-zero bare pion decay constant, the quantum correction and the leading contribution of matter effect to F_π^2. Here we should note that both the above quantum and hadronic contributions include the contribution of the massless vector meson in the same footing as the pion.

The conditions for the bare parameters (7.1), which we call "the VM conditions in hot matter", are essential for the VM to take place in hot matter. Further even when we take into account the Lorentz non-invariance in the bare HLS theory, we obtained the similar conditions to Eq. (7.1) and showed that the conditions are still non-renormalized: There are no quantum corrections to the conditions. In section 5.5 we studied the critical behavior of m_ρ and showed that $m_\rho(T)$ falls as the quark condensate in the limit $T \to T_c$:

$$m_\rho(T) \sim \langle \bar{q}q \rangle_T \, .$$

At present, there are no clear lattice data for the ρ pole mass in hot matter. Our result here will be checked by lattice analyses in future. [112]

Predictions

In section 5.4, we gave the following predictions of the VM in hot matter:

- **Critical temperature :** From the order parameter f_π including the intrinsic thermal effect as well as the hadronic correction, we obtained $T_c = 200$ - 250 MeV for several choices of the matching scale ($\Lambda = 0.8$ - $1.1\,\mathrm{GeV}$) and the scale of QCD ($\Lambda_{\mathrm{QCD}} = 0.30$ -$0.45\,\mathrm{GeV}$).

- **Axial-vector and vector charge susceptibilities (ASUS and VSUS):** The masslss vector meson becomes a relevant degree of freedom near T_c and it contributes to the VSUS. The equality between ASUS and VSUS is predicted by the VM.

- **Violation of vector dominance :** We showed that the vector dominance (VD) of the electromagnetic form factor of the pion is largely violated near T_c. This indicates that the assumption of the VD may need to be weakened, at least in some amounts, for consistently including the effect of the dropping mass of the vector meson.

- **Pion velocity :** We first showed that the pion velocity at T_c never receive any quantum and hadronic thermal corrections protected by the VM. Using the non-renormalization property, we next performed the Wilsonian matching to the OPE and then obtained that the pion velocity is close to the speed of light.

  This is in contrast to the result obtained from the chiral theory [96], where the relevant degree of freedom near T_c is only the pion. Their result is that the pion velocity becomes zero for $T \to T_c$. Therefore by experiment and lattice analysis, we may be able to distinguish which theory is appropriate to describe the chiral phase transition.

We note that the above estimated values may be changed by including higher order effects. On the other hand, it is expected that the VM is governed by the fixed point and not changed by such higher order effects.

Remnant of the VM in the real world

In chapter 6, we studied the heavy meson system which consists of one heavy quark and one light anti-quark, which was motivated by the recent discovery of new D mesons ($J^P = 0^+$ and 1^+) in Babar, CLEO and Belle [34, 35, 36]. We showed that the mass splitting between new D mesons (denoted by $\tilde{D}$ in the text) and the existing D mesons ($J^P = 0^-$ and 1^-) is directly proportional to the light quark condensate. The estimated value was in good agreement with the experiments. We also gave the predictions on the decay widths and the branching ratios for the characteristic processes. In the two-pion decay processes in which the scalar meson does not mediate, our scenario gives definite predictions, since the vector meson coupling to the heavy system is equivalent to the pion coupling due to the VM. Although the predicted values of widths are small, we hope that they are clarified in future experiment.

One of the significant results of the analysis, is that the vector meson plays an important role in accounting for the splitting in the D and $\tilde{D}$ mesons: The *bare* mass splitting determined through the matching is estimated as about 190 MeV, too small to explain the observed mass difference. However by including the quantum corrections through the hadronic loop, the bare mass splitting is enhanced by $\sim 60\%$, where only the loop effect of the vector meson contributes to the running of the mass splitting. The contributions from the pion loop are completely canceled among themselves. This implies that the observed mass difference can not be understood if one takes only the pion as the relevant degree of freedom and that we need other degrees of freedom. In the VM, it is nothing but the vector meson. The situation here is much like in the calculation of pion velocity at the chiral restoration point: The pion velocity is zero if the pion is the only effective degree of freedom but approaches 1 if the vector meson with the VM is included [15, 18].

In the construction of the EFT, we assumed the VM as the chiral symmetry restoration of QCD in the light sector, and then we introduced the effects of the spontaneous chiral symmetry breaking by putting the mass term as soft breaking term. In the analysis, we assumed that the coefficients of the interaction such as $DD\pi$ and $DD\rho$ denoted by k are universal, which are the remnant of the VM. Strictly speaking, each interaction term may have its own coefficient different from others. However, we expect that the effect of these interaction terms is suppressed by the factor $1/\Lambda$ and as a result the contribution to ΔM is

small since the dimension of them is higher than that of the mass term.

Furthermore, the result is independent of the deviation of a from the fixed point value 1, at least at one-loop level. This implies that the deviation of a from 1 which reflects the effect of spontaneous chiral symmetry breaking in the light quark sector does not get transmitted to the heavy sector. This strongly suggests that the deviation from $a = 1$ involves physics that is not as primary as the non-vanishing gauge coupling $g \neq 0$ in the description of the broken phase: The deviation seems to be a "secondary" phenomenon, which is generated from $g \neq 0$ as expected in Refs. [62]. [Although $a = 1$ is the fixed point of the RGE at one-loop level, the deviation of a from 1 is generated by the finite renormalization part once we allow the deviation of the gauge coupling g from 0 (see Appendix C).] In fact, even when we start from the bare HLS theory with $g \neq 0$ and $a = 1$, the physical quantities obtained through the Wilsonian matching are in good agreement with experimental results as discussed in [13]. This observation supports the above argument.

The consistency of the physics taking $a_{\rm bare} = 1$ and the universal coupling k with the one in the real world remarkably indicates that the VM is realized as the chiral symmetry restoration in QCD.

Several comments are in order:

Although we concentrated on the hot matter calculation in this thesis, the present approach can be applied to the general hot and/or dense matter calculation. As mentioned in chapter 1, the vector meson is one of the most important degrees of freedom in hot and/or dense matter since it will be lighter in medium than in the vacuum due to the (partial) chiral symmetry restoration. The HLS theory is an efficient implement to study hadron properties in hot and/or dense matter as well as the chiral phase transition.

One might think that the VM is same as the Georgi's vector realization [62], in which the order parameter f_π is non-zero although the chiral symmetry is unbroken. However in the VM the order parameter certainly becomes zero and the chiral symmetry is restored accompanied by massless vector meson. Therefore the VM is consistent with the Ward-Takahashi identity since it is the Wigner realization [113].

As shown in Ref. [21], in the VM only the longitudinal ρ couples to the vector current near the critical point, and the transverse ρ is decoupled from it. The A_1 in the VM is resolved and/or decoupled from the axial-vector current near T_c since there is no contribution in the vector current correlator to be matched with the axial-vector correlator. We expect that the scalar meson is also resolved and/or decoupled near T_c since it in the VM is in the same representation as the A_1 is in. We also expect that excited mesons are also resolved and/or

decoupled.

The VSUS was obtained to be finite, which will imply that the screening mass of the vector meson is also finite at T_c.

In this thesis, we performed our analysis at the chiral limit. We need to include the explicit chiral symmetry breaking effect from the current quark masses when we apply the present analysis to the real QCD. In such a case, we need the Wilsonian matching conditions with including non-zero quark mass which have not yet been established. Here we expect that the qualitative structure obtained in the present analysis will not be changed by the inclusion of the current quark masses.

Acknowledgment

The author is sincerely grateful to Professor Masayasu Harada, who is her adviser, and Professor Mannque Rho for plenty of useful discussions and continuous encouragements throughout her research. She would like to thank Professor Koichi Yamawaki for valuable discussions and encouragement. She would like to express her thanks to Doctor Youngman Kim, who is a collaborator, for many fruitful discussions and exchange of their opinions.

She would like to express her sincere gratitude for all the helps and encouragements she has received. She would never complete this thesis without their helps.

Support by the 21st Century COE Program of Nagoya University provided by Japan Society for the Promotion of Science (15COEG01) is much appreciated.

Appendix A

Polarization Tensors at Finite Temperature

At non-zero temperature there exist four independent polarization tensors, $u^\mu u^\nu$, $(g^{\mu\nu} - u^\mu u^\nu)$, $P_L^{\mu\nu}$ and $P_T^{\mu\nu}$. The rest frame of medium is shown by $u^\mu = (1, \vec{0})$. $P_L^{\mu\nu}$ and $P_T^{\mu\nu}$ are given by [67]

$$\begin{aligned} P_{T\mu\nu} &= g_{\mu i}\Big(\delta_{ij} - \frac{\vec{p_i}\vec{p_j}}{\vec{p}^2}\Big)g_{j\nu}, \\ P_{L\mu\nu} &= -\Big(g_{\mu\nu} - \frac{p_\mu p_\nu}{p^2}\Big) - P_{T\mu\nu}, \end{aligned} \tag{A.1}$$

where we define $p^\mu = (p_0\,,\,\vec{p})$ and $\bar{p} = |\vec{p}|$. They have the following properties:

$$\begin{gathered} P_{L\mu}^{\mu} = -1,\ P_{T\mu}^{\mu} = -2, \\ P_{L\mu\alpha}P_L^{\alpha\nu} = -P_{L\mu}{}^{\nu},\ P_{T\mu\alpha}P_T^{\alpha\nu} = -P_{T\mu}{}^{\nu}, \\ P_{L\mu\alpha}P_T^{\alpha\nu} = 0. \end{gathered} \tag{A.2}$$

Let us decompose a tensor $\Pi^{\mu\nu}(p_0, \bar{p})$ into

$$\Pi^{\mu\nu} = u^\mu u^\nu \Pi^t + (g^{\mu\nu} - u^\mu u^\nu)\Pi^s + P_L^{\mu\nu}\Pi^L + P_T^{\mu\nu}\Pi^T. \tag{A.3}$$

Each component is obtained as

$$\begin{aligned} \Pi^t &= \Pi^{00} + \frac{\vec{p_i}}{p_0}\Pi^{i0}, \\ \Pi^s &= -\frac{\vec{p_i}}{\bar{p}}\Pi^{ij}\frac{\vec{p_j}}{\bar{p}} - \frac{p_0\vec{p_i}}{\vec{p}^2}\Pi^{i0}, \\ \Pi^L - \Pi^s &= \frac{\vec{p_i}}{\bar{p}}\Pi^{ij}\frac{\vec{p_j}}{\bar{p}} + \frac{\vec{p_i}}{p_0}\Pi^{i0}, \\ \Pi^T - \Pi^s &= \frac{1}{2}P_{T\mu\nu}\Pi^{\mu\nu}. \end{aligned} \tag{A.4}$$

Appendix B

Loop Integrals at Finite Temperature

In this appendix we list the explicit forms of the functions appearing in the hadronic thermal corrections, $\overline{A}_0$, $\overline{B}_0$ and $\overline{B}^{\mu\nu}$ [see Eqs. (3.68)–(3.73) for definitions] in various limits relevant to the present analysis.

The functions $\overline{A}_0$, which are independent of external momentum p_μ, is given by

$$\overline{A}_0(M_\rho;T) = \tilde{J}_1^2(M_\rho;T) \ , \tag{B.1}$$

$$\overline{A}_0(0;T) = \tilde{I}_2(T) \ , \tag{B.2}$$

where $\tilde{J}_1^2$ and $\tilde{I}_2$ are defined in Eqs. (D.1) and (D.2).

We list the relevant limits of the functions $\overline{B}_0(p_0,\bar{p};M_\rho,0;T)$ and $\overline{B}^{\mu\nu}(p_0,\bar{p};M_\rho,0;T)$ which appear in the two-point function of $\overline{\mathcal{A}}_\mu$. When the pion momentum is taken as its on-shell, the function $\overline{B}_0$ becomes

$$\begin{aligned}
&\overline{B}_0(p_0=\bar{p}+i\epsilon,\bar{p};M_\rho,0;T) \\
&= \int \frac{d^3k}{(2\pi)^3}\left[\frac{-1}{2\omega_\rho}\frac{1}{e^{\omega_\rho/T}-1}\left\{\frac{1}{(\omega_\rho-\bar{p})^2-(\omega_\pi^p)^2-2i\epsilon(\omega_\rho-\bar{p})}+\frac{1}{(\omega_\rho+\bar{p})^2-(\omega_\pi^p)^2+2i\epsilon(\omega_\rho+\bar{p})}\right\}\right. \\
&\quad \left.+\frac{-1}{2\omega_\pi^p}\frac{1}{e^{\omega_\pi^p/T}-1}\left\{\frac{1}{(\omega_\pi^p-\bar{p})^2-\omega_\rho^2-2i\epsilon(\omega_\pi^p-\bar{p})}+\frac{1}{(\omega_\pi^p+\bar{p})^2-\omega_\rho^2+2i\epsilon(\omega_\pi^p+\bar{p})}\right\}\right] ,
\end{aligned} \tag{B.3}$$

where we put $\epsilon \to +0$ to make the analytic continuation of the frequency $p_0 = i2\pi nT$ to the Minkowski variable, and we defined

$$\omega_\rho = \sqrt{|\vec{k}|^2+M_\rho^2} \ , \quad \omega_\pi^p = |\vec{k}-\vec{p}| \ . \tag{B.4}$$

Two components $\overline{B}^t$ and $\overline{B}^s$ of $\overline{B}^{\mu\nu}$ in the same limit are given by

$$\overline{B}^t(p_0=\bar{p}+i\epsilon,\bar{p};M_\rho,0;T)$$

$$
\begin{aligned}
= & \int \frac{d^3k}{(2\pi)^3}\left[\frac{-1}{2\omega_\rho}\frac{1}{e^{\omega_\rho/T}-1}\left\{\frac{(2\omega_\rho-\bar{p})^2}{(\omega_\rho-\bar{p})^2-(\omega_\pi^p)^2-2i\epsilon(\omega_\rho-\bar{p})}+\frac{(2\omega_\rho+\bar{p})^2}{(\omega_\rho+\bar{p})^2-(\omega_\pi^p)^2+2i\epsilon(\omega_\rho+\bar{p})}\right.\right. \\
& \left.-\frac{\vec{p}\cdot(2\vec{k}-\vec{p})}{\bar{p}}\left(\frac{2\omega_\rho-\bar{p}}{(\omega_\rho-\bar{p})^2-(\omega_\pi^p)^2-2i\epsilon(\omega_\rho-\bar{p})}-\frac{2\omega_\rho+\bar{p}}{(\omega_\rho+\bar{p})^2-(\omega_\pi^p)^2+2i\epsilon(\omega_\rho+\bar{p})}\right)\right\} \\
& +\frac{-1}{2\omega_\pi^p}\frac{1}{e^{\omega_\pi^p/T}-1}\left\{\frac{(2\omega_\pi^p-\bar{p})^2}{(\omega_\pi^p-\bar{p})^2-\omega_\rho^2-2i\epsilon(\omega_\pi^p-\bar{p})}+\frac{(2\omega_\pi^p+\bar{p})^2}{(\omega_\pi^p+\bar{p})^2-\omega_\rho^2+2i\epsilon(\omega_\pi^p+\bar{p})}\right. \\
& \left.\left.+\frac{\vec{p}\cdot(2\vec{k}-\vec{p})}{\bar{p}}\left(\frac{2\omega_\pi^p-\bar{p}}{(\omega_\pi^p-\bar{p})^2-\omega_\rho^2-2i\epsilon(\omega_\pi^p-\bar{p})}-\frac{2\omega_\pi^p+\bar{p}}{(\omega_\pi^p+\bar{p})^2-\omega_\rho^2+2i\epsilon(\omega_\pi^p+\bar{p})}\right)\right\}\right] ,
\end{aligned}
\tag{B.5}
$$

$$
\begin{aligned}
& \overline{B}^s(p_0=\bar{p}+i\epsilon,\bar{p};M_\rho,0;T) \\
= & \int \frac{d^3k}{(2\pi)^3}\left[\frac{1}{2\omega_\rho}\frac{1}{e^{\omega_\rho/T}-1}\right. \\
& \times\left\{\frac{(2\vec{k}\cdot\vec{p}-\bar{p}^2)^2}{\bar{p}^2}\left(\frac{1}{(\omega_\rho-\bar{p})^2-(\omega_\pi^p)^2-2i\epsilon(\omega_\rho-\bar{p})}+\frac{1}{(\omega_\rho+\bar{p})^2-(\omega_\pi^p)^2+2i\epsilon(\omega_\rho+\bar{p})}\right)\right. \\
& \left.-\frac{\vec{p}\cdot(2\vec{k}-\vec{p})}{\bar{p}}\left(\frac{2\omega_\rho-\bar{p}}{(\omega_\rho-\bar{p})^2-(\omega_\pi^p)^2-2i\epsilon(\omega_\rho-\bar{p})}-\frac{2\omega_\rho+\bar{p}}{(\omega_\rho+\bar{p})^2-(\omega_\pi^p)^2+2i\epsilon(\omega_\rho+\bar{p})}\right)\right\} \\
& +\frac{1}{2\omega_\pi^p}\frac{1}{e^{\omega_\pi^p/T}-1} \\
& \times\left\{\frac{(2\vec{k}\cdot\vec{p}-\bar{p}^2)^2}{\bar{p}^2}\left(\frac{1}{(\omega_\pi^p-\bar{p})^2-\omega_\rho^2-2i\epsilon(\omega_\pi^p-\bar{p})}+\frac{1}{(\omega_\pi^p+\bar{p})^2-\omega_\rho^2+2i\epsilon(\omega_\pi^p+\bar{p})}\right)\right. \\
& \left.\left.+\frac{\vec{p}\cdot(2\vec{k}-\vec{p})}{\bar{p}}\left(\frac{2\omega_\pi^p-\bar{p}}{(\omega_\pi^p-\bar{p})^2-\omega_\rho^2-2i\epsilon(\omega_\pi^p-\bar{p})}-\frac{2\omega_\pi^p+\bar{p}}{(\omega_\pi^p+\bar{p})^2-\omega_\rho^2+2i\epsilon(\omega_\pi^p+\bar{p})}\right)\right\}\right] .
\end{aligned}
\tag{B.6}
$$

We further take the $M_\rho \to 0$ limits of the above expressions. The limit of $\overline{B}_0(p_0 = \bar{p} + i\epsilon, \bar{p}; M_\rho, 0; T)$ includes the infrared logarithmic divergence $\ln M_\rho^2$. However, it appears multiplied by M_ρ^2 in $\overline{\Pi}_\perp^t$ and $\overline{\Pi}_\perp^s$, and the product $M_\rho^2\overline{B}_0(p_0 = \bar{p}+i\epsilon, \bar{p}; M_\rho, 0; T)$ vanishes at $M_\rho \to 0$ limit:

$$
\lim_{M_\rho\to 0} M_\rho^2\overline{B}_0(p_0=\bar{p}+i\epsilon,\bar{p};M_\rho,0;T)=0 \ . \tag{B.7}
$$

As for $\overline{B}^{t,s}(p_0 = \bar{p} + i\epsilon, \bar{p}; M_\rho, 0; T)$, we obtain

$$
\begin{aligned}
\lim_{M_\rho\to 0}\overline{B}^t(p_0=\bar{p}+i\epsilon,\bar{p};M_\rho,0;T) &= -2\tilde{I}_2(T) \ , \\
\lim_{M_\rho\to 0}\overline{B}^s(p_0=\bar{p}+i\epsilon,\bar{p};M_\rho,0;T) &= -2\tilde{I}_2(T) \ .
\end{aligned}
\tag{B.8}
$$

In the static limit ($p_0 \to 0$), the functions $M_\rho^2\overline{B}_0(p_0, \bar{p}; M_\rho, 0; T)$ and $\overline{B}^t(p_0, \bar{p}; M_\rho, 0; T) - \overline{B}^L(p_0, \bar{p}; M_\rho, 0; T)$ become

$$
\lim_{p_0\to 0} M_\rho^2\overline{B}_0(p_0,\bar{p};M_\rho,0;T)
$$

$$= M_\rho^2 \int \frac{d^3k}{(2\pi)^3} \frac{-1}{\omega_\rho^2 - (\omega_\pi^p)^2} \left[\frac{1}{\omega_\rho} \frac{1}{e^{\omega_\rho/T} - 1} - \frac{1}{\omega_\pi^p} \frac{1}{e^{\omega_\pi^p/T} - 1} \right], \tag{B.9}$$

$$\lim_{p_0 \to 0} \left[\overline{B}^t(p_0, \bar{p}; M_\rho, 0; T) - \overline{B}^L(p_0, \bar{p}; M_\rho, 0; T) \right]$$
$$= \int \frac{d^3k}{(2\pi)^3} \frac{-4}{\omega_\rho^2 - (\omega_\pi^p)^2} \left[\frac{\omega_\rho}{e^{\omega_\rho/T} - 1} - \frac{\omega_\pi^p}{e^{\omega_\pi^p/T} - 1} \right]. \tag{B.10}$$

Taking the low momentum limits of these expressions, we obtain

$$\lim_{\bar{p} \to 0} M_\rho^2 \overline{B}_0(p_0 = 0, \bar{p}; M_\rho, 0; T) = \tilde{I}_2(T) - \tilde{J}_1^2(M_\rho; T), \tag{B.11}$$

$$\lim_{\bar{p} \to 0} \left[\overline{B}^t(p_0 = 0, \bar{p}; M_\rho, 0; T) - \overline{B}^L(p_0 = 0, \bar{p}; M_\rho, 0; T) \right]$$
$$= -\frac{4}{M_\rho^2} \left[\tilde{J}_{-1}^2(M_\rho; T) - \tilde{I}_4(T) \right]. \tag{B.12}$$

Moreover, in the VM limit ($M_\rho \to 0$), these are reduced to

$$\lim_{\bar{p} \to 0} M_\rho^2 \overline{B}_0(p_0 = 0, \bar{p}; M_\rho, 0; T) \overset{M_\rho \to 0}{\to} 0,$$
$$\lim_{\bar{p} \to 0} \left[\overline{B}^t(p_0 = 0, \bar{p}; M_\rho, 0; T) - \overline{B}^L(p_0 = 0, \bar{p}; M_\rho, 0; T) \right] \overset{M_\rho \to 0}{\to} 2\tilde{I}_2(T) \ . \tag{B.13}$$

We consider the functions $\overline{B}_0$ and $\overline{B}^{\mu\nu}$ appearing in the two-point functions of $\overline{\mathcal{V}}_\mu$ and $\overline{V}_\mu$. $\overline{B}^t$ and $\overline{B}^s$ are calculated as

$$\overline{B}^t(p_0, \bar{p}; 0, 0; T) = \overline{B}^s(p_0, \bar{p}; 0, 0; T) = -2\overline{A}_0(0; T) = -2\tilde{I}_2(T),$$
$$\overline{B}^t(p_0, \bar{p}; M_\rho, M_\rho; T) = \overline{B}^s(p_0, \bar{p}; M_\rho, M_\rho; T) = -2\overline{A}_0(M_\rho; T) = -2\tilde{J}_1^2(M_\rho; T). \tag{B.14}$$

The function $\overline{B}_0$ is expressed as

$$\overline{B}_0(p_0, \bar{p}; M_\rho, M_\rho; T)$$
$$= \int \frac{d^3k}{(2\pi)^3} \left[\frac{-1}{2\omega_\rho} \frac{1}{e^{\omega_\rho/T} - 1} \left\{ \frac{1}{(\omega_\rho - p_0)^2 - (\omega_\rho^p)^2} + \frac{1}{(\omega_\rho + p_0)^2 - (\omega_\rho^p)^2} \right\} \right.$$
$$\left. + \frac{-1}{2\omega_\rho^p} \frac{1}{e^{\omega_\rho^p/T} - 1} \left\{ \frac{1}{(\omega_\rho^p - p_0)^2 - \omega_\rho^2} + \frac{1}{(\omega_\rho^p + p_0)^2 - \omega_\rho^2} \right\} \right], \tag{B.15}$$

where we define

$$\omega_\rho^p = \sqrt{|\vec{k} - \vec{p}|^2 + M_\rho^2} \ . \tag{B.16}$$

In the static limit ($p_0 \to 0$), the functions $\overline{B}_0$ and $\overline{B}^L$ are expressed as

$$\lim_{p_0 \to 0} M_\rho^2 \overline{B}_0(p_0, \bar{p}; M_\rho, M_\rho; T)$$

$$= M_\rho^2 \int \frac{d^3k}{(2\pi)^3} \frac{-1}{\omega_\rho^2 - (\omega_\rho^p)^2} \left[\frac{1}{\omega_\rho} \frac{1}{e^{\omega_\rho/T} - 1} - \frac{1}{\omega_\rho^p} \frac{1}{e^{\omega_\rho^p/T} - 1} \right], \tag{B.17}$$

$$\lim_{p_0 \to 0} \overline{B}^L(p_0, \bar{p}; M_\rho, M_\rho; T)$$

$$= \int \frac{d^3k}{(2\pi)^3} \frac{1}{\vec{p} \cdot (2\vec{k} - \vec{p})} \left[\frac{1}{\omega_\rho} \frac{1}{e^{\omega_\rho/T} - 1} \left\{ 4\omega_\rho^2 - \vec{p} \cdot (2\vec{k} - \vec{p}) \right\} \right.$$

$$\left. - \frac{1}{\omega_\rho^p} \frac{1}{e^{\omega_\rho^p/T} - 1} \left\{ 4(\omega_\rho^p)^2 + \vec{p} \cdot (2\vec{k} - \vec{p}) \right\} \right]. \tag{B.18}$$

Taking the low momentum limit ($\bar{p} \to 0$), these expressions become

$$\lim_{\bar{p} \to 0} M_\rho^2 \overline{B}_0(p_0 = 0, \bar{p}; M_\rho, M_\rho; T) = \frac{1}{2} \left[\tilde{J}_{-1}^0(M_\rho; T) - \tilde{J}_1^2(M_\rho; T) \right], \tag{B.19}$$

$$\lim_{\bar{p} \to 0} \overline{B}^L(p_0 = 0, \bar{p}; M_\rho, M_\rho; T) = -2 \left[M_\rho^2 \tilde{J}_1^0(M_\rho; T) + 2\tilde{J}_1^2(M_\rho; T) \right]. \tag{B.20}$$

In the VM limit ($M_\rho \to 0$), these are reduced to

$$\lim_{\bar{p} \to 0} M_\rho^2 \overline{B}_0(p_0 = 0, \bar{p}; M_\rho, M_\rho; T) \overset{M_\rho \to 0}{\to} 0, \tag{B.21}$$

$$\lim_{\bar{p} \to 0} \overline{B}^L(p_0 = 0, \bar{p}; M_\rho, M_\rho; T) \overset{M_\rho \to 0}{\to} -4\tilde{I}_2(T). \tag{B.22}$$

On the other hand, the functions $\overline{B}_0, \overline{B}^L - \overline{B}^s$ and $\overline{B}^T - \overline{B}^s$ in the low momentum limit ($\bar{p} \to 0$) are given by

$$\lim_{\bar{p} \to 0} \overline{B}_0(p_0, \bar{p}; M_\rho, M_\rho; T) = \frac{1}{2} \tilde{F}_3^2(p_0; M_\rho; T) \ , \tag{B.23}$$

$$\lim_{\bar{p} \to 0} \left[\overline{B}^L(p_0, \bar{p}; M_\rho, M_\rho; T) - \overline{B}^s(p_0, \bar{p}; M_\rho, M_\rho; T) \right] = \frac{2}{3} \tilde{F}_3^4(p_0; M_\rho; T), \tag{B.24}$$

$$\lim_{\bar{p} \to 0} \left[\overline{B}^T(p_0, \bar{p}; M_\rho, M_\rho; T) - \overline{B}^s(p_0, \bar{p}; M_\rho, M_\rho; T) \right] = \frac{2}{3} \tilde{F}_3^4(p_0; M_\rho; T), \tag{B.25}$$

where the function $\tilde{F}_3^n$ is defined in Appendix D.

Appendix C

Quantum Corrections

In this appendix we briefly summarize the quantum corrections to the two-point functions.

Let us define the functions $B_0^{(\mathrm{vac})}$, $B^{(\mathrm{vac})\mu\nu}$ and $A_0^{(\mathrm{vac})}$ by the following integrals [13]:

$$A_0^{(\mathrm{vac})}(M) = \int \frac{d^n k}{i(2\pi)^4} \frac{1}{M^2 - k^2} \ , \tag{C.1}$$

$$B_0^{(\mathrm{vac})}(p; M_1, M_2) = \int \frac{d^n k}{i(2\pi)^4} \frac{1}{[M_1^2 - k^2][M_2^2 - (k-p)^2]} \ , \tag{C.2}$$

$$B^{(\mathrm{vac})\mu\nu}(p; M_1, M_2) = \int \frac{d^n k}{i(2\pi)^4} \frac{(2k-p)^\mu (2k-p)^\nu}{[M_1^2 - k^2][M_2^2 - (k-p)^2]} \ . \tag{C.3}$$

In the present analysis it is important to include the quadratic divergences to obtain the RGEs in the Wilsonian sense. Here, following Refs. [65, 64, 13], we adopt the dimensional regularization and identify the quadratic divergences with the presence of poles of ultraviolet origin at $n = 2$ [66]. This can be done by the following replacement in the Feynman integrals:

$$\int \frac{d^n k}{i(2\pi)^n} \frac{1}{-k^2} \to \frac{\Lambda^2}{(4\pi)^2} \ , \qquad \int \frac{d^n k}{i(2\pi)^n} \frac{k_\mu k_\nu}{[-k^2]^2} \to -\frac{\Lambda^2}{2(4\pi)^2} g_{\mu\nu} \ . \tag{C.4}$$

On the other hand, the logarithmic divergence is identified with the pole at $n = 4$:

$$\frac{1}{\bar{\epsilon}} + 1 \to \ln \Lambda^2 \ , \tag{C.5}$$

where

$$\frac{1}{\bar{\epsilon}} \equiv \frac{2}{4-n} - \gamma_E + \ln(4\pi) \ , \tag{C.6}$$

with γ_E being the Euler constant.

By using the replacements in Eqs. (C.4) and (C.5), the integrals in Eqs. (C.1), (C.2) and (C.3) are evaluated as

$$A_0^{(\mathrm{vac})}(M) = \frac{\Lambda^2}{(4\pi)^2} - \frac{M^2}{(4\pi)^2} \ln \frac{\Lambda^2}{M^2} \ , \tag{C.7}$$

$$B_0^{(\mathrm{vac})}(p^2; M_1, M_2) = \frac{1}{(4\pi)^2}\left[\ln\Lambda^2 - 1 - F_0(p^2; M_1, M_2)\right] \ , \tag{C.8}$$

$$\begin{aligned} &B^{(\mathrm{vac})\mu\nu}(p; M_1, M_2) \\ &\quad = -g^{\mu\nu}\frac{1}{(4\pi)^2}\left[2\Lambda^2 - M_1^2\ln\frac{\Lambda^2}{M_1^2} - M_2^2\ln\frac{\Lambda^2}{M_2^2} - (M_1^2 - M_2^2)F_A(p^2; M_1, M_2)\right] \\ &\qquad - \left(g^{\mu\nu}p^2 - p^\mu p^\nu\right)\frac{1}{(4\pi)^2}\left[\frac{1}{3}\ln\Lambda^2 - F_0(p^2; M_1, M_2) + 4F_3(p^2; M_1, M_2)\right] \ , \end{aligned} \tag{C.9}$$

where F_0, F_A and F_3 are defined by

$$\begin{aligned} F_0(s; M_1, M_2) &= \int_0^1 dx \ln\left[(1-x)M_1^2 + xM_2^2 - x(1-x)s\right] \ , \\ F_A(s; M_1, M_2) &= \int_0^1 dx\,(1-2x)\,\ln\left[(1-x)M_1^2 + xM_2^2 - x(1-x)s\right] \ , \\ F_3(s; M_1, M_2) &= \int_0^1 dx\, x(1-x)\ln\left[(1-x)M_1^2 + xM_2^2 - x(1-x)s\right] \ . \end{aligned} \tag{C.10}$$

We consider the quantum corrections denoted by $\Pi^{(\mathrm{vac})\mu\nu}$ [see Eq. (3.76)]. At tree level the two-point functions of $\overline{\mathcal{A}}_\mu$, $\overline{\mathcal{V}}_\mu$ and $\overline{V}_\mu$ are given by

$$\begin{aligned} \Pi_\perp^{(\mathrm{tree})\mu\nu}(p) &= F_{\pi,\mathrm{bare}}^2 g^{\mu\nu} + 2z_{2,\mathrm{bare}}(p^2 g^{\mu\nu} - p^\mu p^\nu) \ , \\ \Pi_\parallel^{(\mathrm{tree})\mu\nu}(p) &= F_{\sigma,\mathrm{bare}}^2 g^{\mu\nu} + 2z_{1,\mathrm{bare}}(p^2 g^{\mu\nu} - p^\mu p^\nu) \ , \\ \Pi_V^{(\mathrm{tree})\mu\nu}(p) &= F_{\sigma,\mathrm{bare}}^2 g^{\mu\nu} - \frac{1}{g_{\mathrm{bare}}^2}(p^2 g^{\mu\nu} - p^\mu p^\nu) \ , \\ \Pi_{V\parallel}^{(\mathrm{tree})\mu\nu}(p) &= -F_{\sigma,\mathrm{bare}}^2 g^{\mu\nu} + z_{3,\mathrm{bare}}(p^2 g^{\mu\nu} - p^\mu p^\nu) \ . \end{aligned} \tag{C.11}$$

Thus the one-loop contributions to $\Pi_\perp^{(\mathrm{vac})\mu\nu}$ give the quantum corrections to F_π^2 and z_2. Similarly, each of the one-loop contributions to $\Pi_\parallel^{(\mathrm{vac})\mu\nu}$, $\Pi_V^{(\mathrm{vac})\mu\nu}$ and $\Pi_{V\parallel}^{(\mathrm{vac})\mu\nu}$ includes the quantum corrections to two parameters shown above. For distinguishing the quantum corrections to two parameters included in the two-point function, it is convenient to decompose each two-point function as

$$\Pi^{(\mathrm{vac})\mu\nu}(p) = \Pi^{(\mathrm{vac})S}(p)g^{\mu\nu} + \Pi^{(\mathrm{vac})LT}(p)(g^{\mu\nu}p^2 - p^\mu p^\nu). \tag{C.12}$$

It should be noticed that, since we use the Lagrangian with Lorentz invariance, the form of the quantum corrections is Lorentz invariant. Then, the relation between four components given in Eq. (5.17) and two components shown above are given by

$$\begin{aligned} &\Pi^{(\mathrm{vac})t} = \Pi^{(\mathrm{vac})s} = \Pi^{(\mathrm{vac})S}, \\ &\Pi^{(\mathrm{vac})L} = \Pi^{(\mathrm{vac})T} = \Pi^{(\mathrm{vac})LT}. \end{aligned} \tag{C.13}$$

Using the decomposition in Eq. (C.12), we identify $\Pi_{\perp(\text{1-loop})}^{(\mathrm{vac})S}(p^2)$ with the quantum correction to F_π^2, $\Pi_{\perp(\text{1-loop})}^{(\mathrm{vac})LT}(p^2)$ with that to z_2, and so on. It should be noticed that the following relation

is satisfied [64, 13]:

$$\Pi_V^{(\mathrm{vac})S}(p^2) = \Pi_\parallel^{(\mathrm{vac})S}(p^2) = -\Pi_{V\parallel}^{(\mathrm{vac})S}(p^2) \ . \tag{C.14}$$

Then the quantum correction to F_σ^2 can be extracted from any of $\Pi_\parallel^{\mu\nu}$, $\Pi_V^{\mu\nu}$ and $\Pi_{V\parallel}^{\mu\nu}$.

We note that in Refs. [64, 13] the finite corrections of $\Pi_{(\text{1-loop})}^{(\mathrm{vac})\mu\nu}$ are neglected by assuming that they are small. In this paper we include these finite contributions in addition to the divergent corrections. As in Refs. [68, 14], we adopt the on-shell renormalization condition. They are expressed as [#1]:

$$\mathrm{Re}\Big[\Pi_\perp^{(\mathrm{vac})S}(p^2=0)\Big] = F_\pi^2(\mu=0) \ , \tag{C.15}$$

$$\mathrm{Re}\Big[\Pi_V^{(\mathrm{vac})S}(p^2=M_\rho^2)\Big] = F_\sigma^2(\mu=M_\rho), \tag{C.16}$$

$$\mathrm{Re}\Big[\Pi_V^{(\mathrm{vac})LT}(p^2=M_\rho^2)\Big] = -\frac{1}{g^2(\mu=M_\rho)}, \tag{C.17}$$

where μ denotes the renormalization point. Using the above renormalization conditions, we can write the two-point functions as

$$\begin{aligned}
\Pi_\perp^{(\mathrm{vac})S}(p^2) &= F_\pi^2(0) + \widetilde{\Pi}_\perp^S(p^2) \ , \\
\Pi_V^{(\mathrm{vac})S}(p^2) &= F_\sigma^2(M_\rho) + \widetilde{\Pi}_V^S(p^2) \ , \\
\Pi_V^{(\mathrm{vac})LT}(p^2) &= -\frac{1}{g^2(M_\rho)} + \widetilde{\Pi}_V^{LT}(p^2) \ ,
\end{aligned} \tag{C.18}$$

where $\widetilde{\Pi}_\perp^S(p^2)$, $\widetilde{\Pi}_V^S(p^2)$ and $\widetilde{\Pi}_V^{LT}(p^2)$ denote the finite renormalization effects. Their explicit forms are listed below. From the above renormalization conditions they satisfy

$$\widetilde{\Pi}_\perp^S(p^2=0) = \mathrm{Re}\,\widetilde{\Pi}_V^S(p^2=M_\rho^2) = \mathrm{Re}\,\widetilde{\Pi}_V^{LT}(p^2=M_\rho^2) = 0 \ . \tag{C.19}$$

Thus in the present renormalization scheme, all the quantum effects for the on-shell parameters at leading order are included through the renormalization group equations.

[#1] In the framework of the ChPT with HLS, the renormalization point μ should be taken as $\mu \geq M_\rho$ since the vector meson decouples at $\mu = M_\rho$. Below the scale M_ρ the parameter F_π, which is expressed as $F_\pi^{(\pi)}(\mu)$ in Refs. [64, 13], runs by the quantum correction from the pion loop alone. Then $F_\pi^2(\mu=0)$ in the right-hand-side of the renormalization condition Eq. (C.15) is defined by $[F_\pi^{(\pi)}(\mu=0)]^2$. Due to the presence of the quadratic divergence $F_\pi(M_\rho)$ is not connected smoothly to $F_\pi^{(\pi)}(M_\rho)$. The relation between them is expressed as [64, 13] $[F_\pi^{(\pi)}(M_\rho)]^2 = F_\pi^2(M_\rho) + [N_f/(4\pi)^2][a(M_\rho)/2]M_\rho^2$, where $a(\mu)$ for $\mu > M_\rho$ is defined as $a(\mu) \equiv F_\sigma^2(\mu)/F_\pi^2(\mu)$. By using this relation, the renormalization condition (C.15) determines the condition for $F_\pi^2(M_\rho)$. Strictly speaking, we should use $F_\pi(M_\rho)$ in the calculations in the present analysis. However, the difference between $F_\pi(0)$ and $F_\pi(M_\rho)$ inside the loop correction coming from the finite renormalization effect is of higher order, and we use $F_\pi(0)$ inside one-loop corrections in this paper.

In the following, using the above functions, we summarize the quantum corrections to two components $\Pi^{(\mathrm{vac})S}$ and $\Pi^{(\mathrm{vac})LT}$ of the two-point functions $\Pi_{\perp}^{(\mathrm{vac})\mu\nu}$, $\Pi_{\parallel}^{(\mathrm{vac})\mu\nu}$, $\Pi_{V}^{(\mathrm{vac})\mu\nu}$ and $\Pi_{V\parallel}^{(\mathrm{vac})\mu\nu}$ which are defined in Eq. (C.12). For $\overline{\mathcal{A}}_\mu$-$\overline{\mathcal{A}}_\nu$ two-point function, we obtain

$$\begin{aligned}
\Pi^{(\mathrm{vac})S}_{\perp(\text{1-loop})}(p^2) &= -\frac{N_f}{(4\pi)^2}\Big[\frac{2-a}{2}\Lambda^2 + \frac{3}{4}a\,M_\rho^2\ln\Lambda^2 + \frac{1}{4}a\,M_\rho^2\ln M_\rho^2 \\
&\qquad - a\,M_\rho^2\Big\{1 + F_0(p^2;M_\rho,0) + \frac{1}{4}F_A(p^2;M_\rho,0)\Big\}\Big], \\
\Pi^{(\mathrm{vac})LT}_{\perp(\text{1-loop})}(p^2) &= -\frac{N_f}{(4\pi)^2}\frac{a}{4}\Big[\frac{1}{3}\ln\Lambda^2 - F_0(p^2;M_\rho,0) + 4F_3(p^2;M_\rho,0)\Big].
\end{aligned} \tag{C.20}$$

Corrections to $\overline{\mathcal{V}}_\mu$-$\overline{\mathcal{V}}_\nu$ two-point function are given by

$$\begin{aligned}
\Pi^{(\mathrm{vac})S}_{\parallel(\text{1-loop})}(p^2) &= -\frac{N_f}{(4\pi)^2}\Big[\frac{a^2+1}{4}\Lambda^2 + \frac{3}{4}M_\rho^2\ln M_\rho^2 + M_\rho^2\Big\{\frac{1}{4}\ln M_\rho^2 - 1 - F_0(p^2;M_\rho,M_\rho)\Big\}\Big], \\
\Pi^{(\mathrm{vac})LT}_{\parallel(\text{1-loop})}(p^2) &= -\frac{N_f}{(4\pi)^2}\frac{1}{8}\Big[\frac{a^2-4a+5}{3}\ln\Lambda^2 - F_0(p^2;M_\rho,M_\rho) \\
&\qquad + 4F_3(p^2;M_\rho,M_\rho) - 4(2-a)^2\ln M_\rho^2\Big].
\end{aligned} \tag{C.21}$$

As for $\overline{V}_\mu$-$\overline{V}_\nu$ we have

$$\begin{aligned}
\Pi^{(\mathrm{vac})S}_{V(\text{1-loop})}(p^2) &= \Pi^{(\mathrm{vac})S}_{\parallel(\text{1-loop})}(p^2), \\
\Pi^{(\mathrm{vac})LT}_{V(\text{1-loop})}(p^2) &= -\frac{N_f}{(4\pi)^2}\Big[\frac{a^2-87}{24}\ln\Lambda^2 + 4 + \frac{23}{8}F_0(p^2;M_\rho,M_\rho) \\
&\qquad + \frac{9}{2}F_3(p^2;M_\rho,M_\rho) - \frac{a^2}{8}\Big\{F_0(p^2;0,0) - 4F_3(p^2;0,0)\Big\}\Big]
\end{aligned} \tag{C.22}$$

Finally, corrections to $\overline{V}_\mu$-$\overline{\mathcal{V}}_\nu$ two-point function are expressed as

$$\begin{aligned}
\Pi^{(\mathrm{vac})S}_{V\parallel(\text{1-loop})}(p^2) &= -\Pi^{(\mathrm{vac})S}_{\parallel(\text{1-loop})}(p^2), \\
\Pi^{(\mathrm{vac})LT}_{V\parallel(\text{1-loop})}(p^2) &= -\frac{N_f}{(4\pi)^2}\frac{1}{8}\Big[\frac{1+2a-a^2}{3}\ln\Lambda^2 - a(2-a)\ln M_\rho^2 \\
&\qquad - F_0(p^2;M_\rho,M_\rho) + 4F_3(p^2;M_\rho,M_\rho)\Big].
\end{aligned} \tag{C.23}$$

The renormalization conditions in Eqs. (C.15)- (C.17) lead to the following relations among the bare and renormalized parameters:

$$\begin{aligned}
&F^2_{\pi,\mathrm{bare}} - \frac{N_f}{4(4\pi)^2}[2(2-a)\Lambda^2 + 3aM_\rho^2\ln\Lambda^2] \\
&\quad = F_\pi^2(0) - \frac{N_f}{4(4\pi)^2}aM_\rho^2[3\ln M_\rho^2 + \frac{1}{2}], \\
&F^2_{\sigma,\mathrm{bare}} - \frac{N_f}{4(4\pi)^2}[(a^2+1)\Lambda^2 + 3M_\rho^2\ln\Lambda^2]
\end{aligned} \tag{C.24}$$

$$= F_\sigma^2(M_\rho) - \frac{N_f}{4(4\pi)^2} M_\rho^2 [3\ln M_\rho^2 - 4(1-\sqrt{3}\tan^{-1}\sqrt{3})], \tag{C.25}$$

$$\frac{1}{g_{\rm bare}^2} - \frac{N_f}{(4\pi)^2}\frac{87-a^2}{24}\ln\Lambda^2$$
$$= \frac{1}{g^2(M_\rho)} - \frac{N_f}{8(4\pi)^2}[\frac{87-a^2}{3}\ln M_\rho^2 - \frac{147-5a^2}{9} + 41\sqrt{3}\tan^{-1}\sqrt{3}]. \tag{C.26}$$

From these relations, we obtain the RGEs for the parameters F_π, g and a as [64]

$$\mu\frac{d{F_\pi}^2}{d\mu} = \frac{N_f}{2(4\pi)^2}\Big[3a^2g^2{F_\pi}^2 + 2(2-a)\mu^2\Big], \tag{C.27}$$

$$\mu\frac{da}{d\mu} = -\frac{N_f}{2(4\pi)^2}(a-1)\Big[3a(a+1)g^2 - (3a-1)\frac{\mu^2}{{F_\pi}^2}\Big], \tag{C.28}$$

$$\mu\frac{dg^2}{d\mu} = -\frac{N_f}{2(4\pi)^2}\frac{87-a^2}{6}g^4. \tag{C.29}$$

The finite renormalization effects of the two-point functions are expressed as

$$\tilde{\Pi}_\perp^S(p^2) = \frac{N_f}{(4\pi)^2}aM_\rho^2\Big[-\Big(1-\frac{M_\rho^2}{4p^2}\Big)\Big\{1-\Big(1-\frac{M_\rho^2}{p^2}\Big)\ln\Big(1-\frac{p^2}{M_\rho^2}\Big)\Big\} - \frac{1}{8}\Big], \tag{C.30}$$

$$\tilde{\Pi}_V^S(p^2) = \frac{N_f}{(4\pi)^2}M_\rho^2\Big[-\sqrt{3}\tan^{-1}\sqrt{3} + 2\sqrt{\frac{4M_\rho^2-p^2}{p^2}}\tan^{-1}\sqrt{\frac{p^2}{4M_\rho^2-p^2}}\Big], \tag{C.31}$$

$$\tilde{\Pi}_V^{LT}(p^2) = \frac{N_f}{8(4\pi)^2}\Big[\frac{a^2}{3}\ln\Big(\frac{-p^2}{M_\rho^2}\Big) - 24\Big(1-\frac{M_\rho^2}{p^2}\Big) + 41\sqrt{3}\tan^{-1}\sqrt{3}$$
$$- \frac{2(12M_\rho^2+29p^2)}{p^2}\sqrt{\frac{4M_\rho^2-p^2}{p^2}}\tan^{-1}\sqrt{\frac{p^2}{4M_\rho^2-p^2}}\Big]. \tag{C.32}$$

Appendix D

Functions

In this appendix, we list the integral forms of the functions which appear in the expressions of the physical quantities and the several limits of the loop integrals shown in Appendix B. The functions $\tilde{I}_n(T)$ and $\tilde{J}^n_m(M;T)$ (n, m: integers) are given by

$$\tilde{I}_n(T) = \int \frac{d^3k}{(2\pi)^3} \frac{|\vec{k}|^{n-3}}{e^{k/T}-1} = \frac{1}{2\pi^2}\hat{I}_n T^n \ ,$$

$$\hat{I}_2 = \frac{\pi^2}{6}, \quad \hat{I}_4 = \frac{\pi^4}{15} \ , \tag{D.1}$$

$$\tilde{J}^n_m(M;T) = \int \frac{d^3k}{(2\pi)^3} \frac{1}{e^{\omega/T}-1} \frac{|\vec{k}|^{n-2}}{\omega^m} \ , \tag{D.2}$$

where

$$\omega = \sqrt{k^2+M^2} \ . \tag{D.3}$$

The functions $\tilde{F}^n_3(p_0;M;T)$ and $\tilde{G}_n(p_0;T)$, which appear in the vector meson pole mass in section 5.2, are defined as

$$\tilde{F}^n_3(p_0;M;T) = \int \frac{d^3k}{(2\pi)^3} \frac{1}{e^{\omega/T}-1} \frac{4|\vec{k}|^{n-2}}{\omega(4\omega^2-{p_0}^2)} \ ,$$

$$\tilde{G}_n(p_0;T) = \int \frac{d^3k}{(2\pi)^3} \frac{|\vec{k}|^{n-3}}{e^{k/T}-1} \frac{4|\vec{k}|^2}{4|\vec{k}|^2-{p_0}^2} \ . \tag{D.4}$$

Appendix E

Temporal and Spatial Parts of Two-point Function

In this appendix, we show that the temporal and spatial components of the two-point function $\Pi_{\perp}^{(\mathrm{vac})\mu\nu}$ are independent of the external momentum in the VM limit.

From Eq. (5.60), $\Pi_{\perp}^{(\mathrm{vac})(\mathrm{b})\mu\nu}$ is rewritten as

$$\begin{aligned}\Pi_{\perp}^{(\mathrm{vac})(\mathrm{b})\mu\nu}(p_0,\bar{p}) &= N_f\,\frac{a^t}{4}X^{\mu}_{\bar{\mu}}X^{\nu}_{\bar{\nu}}B^{(\mathrm{vac})\bar{\mu}\bar{\nu}}(p_0,\bar{p};M_\rho,0)\\ &\equiv N_f\,\frac{a^t}{4}\tilde{B}^{(\mathrm{vac})\mu\nu}(p_0,\bar{p};M_\rho,0),\end{aligned} \tag{E.1}$$

where we define

$$X^{\mu}_{\bar{\mu}} = u^{\mu}u_{\bar{\mu}} + V_\sigma^2(g^{\mu}_{\bar{\mu}} - u^{\mu}u_{\bar{\mu}}). \tag{E.2}$$

In the above expression, we define the function $B^{(\mathrm{vac})\mu\nu}$ contributed to the diagram (b) in Fig. 5.1 as

$$\begin{aligned}&B^{(\mathrm{vac})\mu\nu}(p_0,\bar{p};M_\rho,0)\\ &\quad=\int\frac{dk_0}{i(2\pi)}\int\frac{d^3\bar{k}}{(2\pi)^3}\frac{(2k-p)^\mu(2k-p)^\nu}{[k_0^2-\omega_\pi^2][(k_0-p_0)^2-(\omega_\rho^p)^2]},\end{aligned} \tag{E.3}$$

with

$$\begin{aligned}\omega_\pi^2 &= V_\pi^2\bar{k}^2,\\ (\omega_\rho^p)^2 &= V_\sigma^2|\vec{k}-\vec{p}|^2+M_\rho^2.\end{aligned} \tag{E.4}$$

In terms of each components of $B^{(\mathrm{vac})\mu\nu}$, the temporal and spatial parts of $\tilde{B}^{\mu\nu}$ are given by

$$\tilde{B}^{(\mathrm{vac})\mathrm{t}}(p_0,\bar{p};M_\rho,0)$$

$$= \Big[B^{(\mathrm{vac})\mathrm{t}}(p_0,\bar{p};M_\rho,0) + (1-V_\sigma^2)\frac{\bar{p}^2}{p^2}B^{(\mathrm{vac})\mathrm{L}}(p_0,\bar{p};M_\rho,0)\Big],$$

$$\tilde{B}^{(\mathrm{vac})\mathrm{s}}(p_0,\bar{p};M_\rho,0)$$

$$= V_\sigma^4\Big[B^{(\mathrm{vac})\mathrm{s}}(p_0,\bar{p};M_\rho,0) + \frac{1-V_\sigma^2}{V_\sigma^2}\,\frac{p_0^2}{p^2}B^{(\mathrm{vac})\mathrm{L}}(p_0,\bar{p};M_\rho,0)\Big]. \tag{E.5}$$

By using the expressions in Appendix B, the componets $B^{(\mathrm{vac})\mathrm{t}}, B^{(\mathrm{vac})\mathrm{s}}$ and $B^{(\mathrm{vac})\mathrm{L}}$ take the following forms:

$$\begin{aligned}
&B^{(\mathrm{vac})\mathrm{t}}(p_0,\bar{p};M_\rho,0)\\
&= \int\frac{d^3k}{(2\pi)^3}\Bigg[\frac{-1}{2\omega_\pi}\frac{(2\omega_\pi-p_0)^2}{(\omega_\pi-p_0)^2-(\omega_\rho^p)^2}+\frac{-1}{2\omega_\rho^p}\frac{(2\omega_\rho^p+p_0)^2}{(\omega_\rho^p+p_0)^2-\omega_\pi^2}\\
&\quad-\frac{\vec{p}\cdot(2\vec{k}-\vec{p})}{p_0}\left\{\frac{1}{2\omega_\pi}\frac{2\omega_\pi-p_0}{(\omega_\pi-p_0)^2-(\omega_\rho^p)^2}+\frac{1}{2\omega_\rho^p}\frac{2\omega_\rho^p+p_0}{(\omega_\rho^p+p_0)^2-\omega_\pi^2}\right\}\Bigg],\\
&B^{(\mathrm{vac})\mathrm{s}}(p_0,\bar{p};M_\rho,0)\\
&= \int\frac{d^3k}{(2\pi)^3}\Bigg[\frac{(2\vec{k}\cdot\vec{p}-\bar{p}^2)^2}{\bar{p}^2}\left\{\frac{1}{2\omega_\pi}\frac{1}{(\omega_\pi-p_0)^2-(\omega_\rho^p)^2}+\frac{1}{2\omega_\rho^p}\frac{1}{(\omega_\rho^p+p_0)^2-\omega_\pi^2}\right\}\\
&\quad+\frac{p_0\vec{p}\cdot(2\vec{k}-\vec{p})}{\bar{p}^2}\left\{\frac{1}{2\omega_\pi}\frac{2\omega_\pi-p_0}{(\omega_\pi-p_0)^2-(\omega_\rho^p)^2}+\frac{1}{2\omega_\rho^p}\frac{2\omega_\rho^p+p_0}{(\omega_\rho^p+p_0)^2-\omega_\pi^2}\right\}\Bigg],\\
&B^{(\mathrm{vac})\mathrm{L}}(p_0,\bar{p};M_\rho,0)\\
&= \int\frac{d^3k}{(2\pi)^3}\frac{p^2\vec{p}\cdot(2\vec{k}-\vec{p})}{p_0\bar{p}^2}\left[\frac{1}{2\omega_\pi}\frac{2\omega_\pi-p_0}{(\omega_\pi-p_0)^2-(\omega_\rho^p)^2}+\frac{1}{2\omega_\rho^p}\frac{2\omega_\rho^p+p_0}{(\omega_\rho^p+p_0)^2-\omega_\pi^2}\right].
\end{aligned}\tag{E.6}$$

Now we take the VM limit. Note that the VM condition for a^t and a^s implies that σ velocity becomes equal to the pion velocity, $V_\sigma \to V_\pi$ for $T \to T_c$ as shown in Eq. (5.21). The components $B^{(\mathrm{vac})\mathrm{t}}, B^{(\mathrm{vac})\mathrm{s}}$ and $B^{(\mathrm{vac})\mathrm{L}}$ are calculated as follows:

$$\begin{aligned}
&\lim_{\mathrm{VM}} B^{(\mathrm{vac})\mathrm{t}}(p_0,\bar{p};M_\rho,0)\\
&\quad= \int\frac{d^3k}{(2\pi)^3}\frac{-1}{\omega_\pi}\frac{\mathcal{I}(\bar{k};p_0,\bar{p})+\vec{p}\cdot(2\vec{k}-\vec{p})\mathcal{J}(\bar{k};p_0,\bar{p})}{[(\omega_\pi-p_0)^2-(\omega_\pi^p)^2][(\omega_\pi+p_0)^2-(\omega_\pi^p)^2]},
\end{aligned}\tag{E.7}$$

$$\begin{aligned}
&\lim_{\mathrm{VM}} B^{(\mathrm{vac})\mathrm{s}}(p_0,\bar{p};M_\rho,0)\\
&\quad= \int\frac{d^3k}{(2\pi)^3}\frac{1}{\omega_\pi}\frac{1}{\bar{p}^2}\frac{1}{[(\omega_\pi-p_0)^2-(\omega_\pi^p)^2][(\omega_\pi+p_0)^2-(\omega_\pi^p)^2]}\\
&\qquad\times\Big[\Big(\vec{p}\cdot(2\vec{k}-\vec{p})\Big)^2\mathcal{K}(\bar{k};p_0,\bar{p})+p_0^2\vec{p}\cdot(2\vec{k}-\vec{p})\mathcal{J}(\bar{k};p_0,\bar{p})\Big],
\end{aligned}\tag{E.8}$$

$$\begin{aligned}
&\lim_{\mathrm{VM}} B^{(\mathrm{vac})\mathrm{L}}(p_0,\bar{p};M_\rho,0)\\
&\quad= \int\frac{d^3k}{(2\pi)^3}\frac{1}{\omega_\pi}\frac{p^2}{\bar{p}^2}\frac{\vec{p}\cdot(2\vec{k}-\vec{p})\mathcal{J}(\bar{k};p_0,\bar{p})}{[(\omega_\pi-p_0)^2-(\omega_\pi^p)^2][(\omega_\pi+p_0)^2-(\omega_\pi^p)^2]},
\end{aligned}\tag{E.9}$$

where we define the functions as

$$\mathcal{I}(\bar{k};p_0,\bar{p}) = \omega_\pi^2[4\omega_\pi^2-4(\omega_\pi^p)^2-3p_0^2]+p_0^2[p_0^2-(\omega_\pi^p)^2],$$

$$\mathcal{J}(\bar{k};p_0,\bar{p}) = -p_0[-3\omega_\pi^2 + p_0^2 - (\omega_\pi^p)^2],$$
$$\mathcal{K}(\bar{k};p_0,\bar{p}) = \omega_\pi^2 + p_0^2 - (\omega_\pi^p)^2. \tag{E.10}$$

Using Eqs. (E.7)-(E.9) with these functions, we obtain $\tilde{B}^{(\mathrm{vac})\mathrm{t,s}}$ as

$$\lim_{\mathrm{VM}} \tilde{B}^{(\mathrm{vac})\mathrm{t}}(p_0,\bar{p};M_\rho,0)$$
$$= \int \frac{d^3k}{(2\pi)^3}\frac{-1}{\omega_\pi}\frac{\mathcal{I}(\bar{k};p_0,\bar{p}) + V_\pi^2\vec{p}\cdot(2\vec{k}-\vec{p})\mathcal{J}(\bar{k};p_0,\bar{p})}{[(\omega_\pi-p_0)^2-(\omega_\pi^p)^2][(\omega_\pi+p_0)^2-(\omega_\pi^p)^2]}, \tag{E.11}$$
$$\lim_{\mathrm{VM}} \tilde{B}^{(\mathrm{vac})\mathrm{s}}(p_0,\bar{p};M_\rho,0)$$
$$= \int \frac{d^3k}{(2\pi)^3}\frac{1}{\omega_\pi}\frac{1}{V_\pi^2\bar{p}^2}\frac{1}{[(\omega_\pi-p_0)^2-(\omega_\pi^p)^2][(\omega_\pi+p_0)^2-(\omega_\pi^p)^2]}$$
$$\times\Big[\Big(V_\pi^2\vec{p}\cdot(2\vec{k}-\vec{p})\Big)^2\mathcal{K}(\bar{k};p_0,\bar{p}) + p_0^2V_\pi^2\vec{p}\cdot(2\vec{k}-\vec{p})\mathcal{J}(\bar{k};p_0,\bar{p})\Big]. \tag{E.12}$$

The integrand of the functions $\tilde{B}^{(\mathrm{vac})\mathrm{t}}$ and $\tilde{B}^{(\mathrm{vac})\mathrm{s}}$ in the VM limit are same as those of $B^{(\mathrm{vac})\mathrm{t}}$ and $B^{(\mathrm{vac})\mathrm{s}}$ with $V_\pi = 1$ when we make the following replacement in $\tilde{B}^{(\mathrm{vac})\mathrm{t,s}}$:

$$V_\pi\bar{k} \to \bar{k}, \qquad V_\pi|\vec{k}-\vec{p}| \to |\vec{k}-\vec{p}|. \tag{E.13}$$

The functions $B^{(\mathrm{vac})\mathrm{t,s}}$ with $M_\rho \to 0$ are independent of the external momentum p_0 and $\bar{p}$ [see Appendix B] [#1]. Thus we find that the functions $\tilde{B}^{(\mathrm{vac})\mathrm{t}}$ and $\tilde{B}^{(\mathrm{vac})\mathrm{s}}$ in the VM limit are obtained independently of the external momentum p_0 and $\bar{p}$:

$$\lim_{\mathrm{VM}} \tilde{B}^{(\mathrm{vac})\mathrm{t}}(p_0,\bar{p};M_\rho,0) = -\frac{1}{V_\pi}\frac{\Lambda^2}{8\pi^2},$$
$$\lim_{\mathrm{VM}} \tilde{B}^{(\mathrm{vac})\mathrm{s}}(p_0,\bar{p};M_\rho,0) = -V_\pi\frac{\Lambda^2}{8\pi^2}. \tag{E.14}$$

[#1] In Ref. [15] where $V_\pi = 1$ was taken, it was shown that the hadronic corrections $\bar{\Pi}_\perp^{t,s}(p_0,\bar{p};T)$ at the VM limit are independent of the external momentum p_0 and $\bar{p}$. The structure of the integrand in the vacuum part is the same as that in the hadronic part except for the absence of the Bose-Einstein distribution function. Thus the vacuum part is also independent of p_0 and $\bar{p}$.

Appendix F

Current Correlator in Operator Product Expansion

In this appendix, following Ref. [76] where the current correlator is discussed using the OPE in dense matter, we determine the Lorentz non-invariant effect in bare pion velocity $V_{\pi,\mathrm{bare}}$ through the Wilsonian matching. The tensor structure of the current correlator with Lorentz non-scalar operators in dense matter is same as that in hot matter. Thus in order to obtain the current correlator in terms of OPE variables, we simply make a replacement of the matrix element in dense matter with the one in hot matter.

The axial-vector current correlator $G_A^{\mu\nu}$ obtained from the OPE in dense matter is given by [76]

$$\begin{aligned}
G_A^{\mu\nu}(q_0,\bar{q}) = (q^\mu q^\nu - g^{\mu\nu}q^2)\frac{-1}{4}\Bigg[&\frac{1}{2\pi^2}\left(1+\frac{\alpha_s}{\pi}\right)\ln\left(\frac{Q^2}{\mu^2}\right) + \frac{1}{6Q^4}\left\langle\frac{\alpha_s}{\pi}G^2\right\rangle_\rho \\
&- \frac{2\pi\alpha_s}{Q^6}\left\langle\left(\bar{u}\gamma_\mu\gamma_5\lambda^a u - \bar{d}\gamma_\mu\gamma_5\lambda^a d\right)^2\right\rangle_\rho \\
&- \frac{4\pi\alpha_s}{9Q^6}\left\langle\left(\bar{u}\gamma_\mu\lambda^a u + \bar{d}\gamma_\mu\lambda^a d\right)\sum_q^{u,d,s}\bar{q}\gamma_\mu\lambda^a q\right\rangle_\rho\Bigg] \\
&+ \sum_{\tau=2}\sum_{k=1}[-g^{\mu\nu}q^{\mu_1}q^{\mu_2} + g^{\mu\mu_1}q^\nu q^{\mu_2} + q^\mu q^{\mu_1}g^{\nu\mu_2} + g^{\mu\mu_1}g^{\nu\mu_2}Q^2] \\
&\quad\times q^{\mu_3}\cdots q^{\mu_{2k}}\frac{2^{2k}}{Q^{4k+\tau-2}}A^{2k+\tau,\tau}_{\mu_1\cdots\mu_{2k}} \\
&+ \sum_{\tau=2}\sum_{k=1}\left[g^{\mu\nu} - \frac{q^\mu q^\nu}{q^2}\right]q^{\mu_1}\cdots q^{\mu_{2k}}\frac{2^{2k}}{Q^{4k+\tau-2}}C^{2k+\tau,\tau}_{\mu_1\cdots\mu_{2k}}.
\end{aligned} \tag{F.1}$$

with $Q^2 = -q^2$. $\tau = d - s$ denotes the twist, where $s = 2k$ is the number of spin indices of the operator of dimension d. When we consider the operators of $(\tau, s) = (2, 2)$ and $(2, 4)$, $G_A^{\mu\nu}$ has

$A^{4,2}_{\alpha\beta}$ and $A^{6,2}_{\alpha\beta\lambda\sigma}$ defined by [#1]

$$
\begin{aligned}
A^{4,2}_{\alpha\beta} &= \Big(p_\alpha p_\beta - \frac{1}{4} g_{\alpha\beta} p^2\Big) \frac{\rho}{2m} A^{4,2}_2, \\
A^{6,2}_{\alpha\beta\lambda\sigma} &= \Big[p_\alpha p_\beta p_\lambda p_\sigma - \frac{p^2}{8}(p_\alpha p_\beta g_{\lambda\sigma} + p_\alpha p_\lambda g_{\beta\sigma} + p_\alpha p_\sigma g_{\lambda\beta} + p_\beta p_\lambda g_{\alpha\sigma} \\
&\quad + p_\beta p_\sigma g_{\alpha\lambda} + p_\lambda p_\sigma g_{\alpha\beta}) + \frac{p^4}{48}(g_{\alpha\beta} g_{\lambda\sigma} + g_{\alpha\lambda} g_{\beta\sigma} + g_{\alpha\sigma} g_{\beta\lambda})\Big] \frac{\rho}{2m} A^{6,2}_4, \qquad \text{(F.2)}
\end{aligned}
$$

where ρ denotes the nuclear density and m the nucleon mass, and p^μ is the nucleon momentum and we take $p^\mu = mu^\mu = m(1, \vec{0})$. From Eq. (F.2), we have the following expressions of $G_A^{L(0)}$ and $G_A^{L(1)}$ [76] [#2]:

$$
\begin{aligned}
G_A^{(\mathrm{OPE})L(0)}(-q^2) &= \frac{-1}{3} g^{\mu\nu} G^{(\mathrm{OPE})(0)}_{A,\mu\nu} \\
&= \frac{-1}{4}\Bigg[\frac{1}{2\pi^2}\left(1 + \frac{\alpha_s}{\pi}\right)\ln\left(\frac{Q^2}{\mu^2}\right) + \frac{1}{6Q^4}\left\langle \frac{\alpha_s}{\pi} G^2 \right\rangle_\rho \\
&\quad - \frac{2\pi\alpha_s}{Q^6}\left\langle \left(\bar{u}\gamma_\mu\gamma_5\lambda^a u - \bar{d}\gamma_\mu\gamma_5\lambda^a d\right)^2 \right\rangle_\rho \\
&\quad - \frac{4\pi\alpha_s}{9Q^6}\left\langle \left(\bar{u}\gamma_\mu\lambda^a u + \bar{d}\gamma_\mu\lambda^a d\right) \sum_q^{u,d,s} \bar{q}\gamma_\mu\lambda^a q \right\rangle_\rho\Bigg] \\
&\quad + \frac{\rho m}{(-q^2)^2} A_2^{\mathrm{u+d}} - \frac{5}{3}\frac{\rho m^3}{(-q^2)^3} A_4^{\mathrm{u+d}}, \qquad \text{(F.3)} \\
G_A^{(\mathrm{OPE})L(1)}(-p^2) &= 2\rho m^3 \frac{A_4^{u+d}}{q^8}. \qquad \text{(F.4)}
\end{aligned}
$$

Following the same procedure done in section 4.2, we obtain the matching condition on the bare pion velocity:

$$
1 - V^2_{\pi,\mathrm{bare}} = \frac{1}{G_0}\frac{2\rho m^3}{\Lambda^6} A_4^{\mathrm{u+d}}, \qquad \text{(F.5)}
$$

where we define G_0 as

$$
G_0 \equiv \frac{1}{8\pi^2}\left[\left(1 + \frac{\alpha_s}{\pi}\right) + \frac{2\pi^2}{3}\frac{\langle \frac{\alpha_s}{\pi} G^2\rangle_\rho}{\Lambda^4} + \pi^3 \frac{1408}{27}\frac{\alpha_s \langle \bar{q}q\rangle^2_\rho}{\Lambda^6}\right]
$$

[#1] Eq. (8) in Ref. [76] does not have the factor $\frac{\rho}{2m}$. In the following, we explain the reason why this factor $\frac{\rho}{2m}$ appears in Eq. (F.2): In the linear density approximation, the matrix element of an operator $\hat{A}$ is expressed as $\langle G|\hat{A}|G\rangle = \langle 0|\hat{A}|0\rangle + \frac{\rho}{2m}\langle p|\hat{A}|p\rangle$ where $|G\rangle$ denotes the ground state of nuclear matter [76]. The first term on the right-hand-side is the vacuum expectation value, which vanishes for operators with spin. In the second term $|p\rangle$ denotes a nucleon state with momentum p. In the present analysis, we consider the operators with spin 2 and spin 4 which are dominant to the Lorentz non-invariant effect. The matrix elements of these operators with spin s are expressed as $\tilde{A}_s \equiv \langle G|\hat{A}_s|G\rangle = \frac{\rho}{2m}\langle p|\hat{A}_s|p\rangle \equiv \frac{\rho}{2m} A_s$. $A_{2,4}$ in Eq. (8) in Ref. [76] correspond to $\tilde{A}_{2,4}$. In terms of A_s, $A_{\alpha\beta}$ is expressed as $A^{4,2}_{\alpha\beta} = (p_\alpha p_\beta - \frac{1}{4} g_{\alpha\beta} p^2)\tilde{A}^{4,2}_2 = (p_\alpha p_\beta - \frac{1}{4} g_{\alpha\beta} p^2)\frac{\rho}{2m} A^{4,2}_2$ as showen in Eq. (F.2).

[#2] The expression of Eq. (F.4) is obtained from Eqs. (11) and (14) in Ref. [76], where we neglect the $\mathcal{O}(\alpha_s)$ terms in $A^{4,2}_{\alpha\beta}$ and $A^{6,2}_{\alpha\beta\lambda\sigma}$.

$$+\frac{2\rho m}{\Lambda^4}A_2^{\mathrm{u+d}}-\frac{5\rho m^3}{\Lambda^6}A_4^{\mathrm{u+d}}. \tag{F.6}$$

In the above analysis, we consider the OPE in dense matter. The quantity in hot matter corresponding to ρm^3 in Eq. (F.5) is determined as follows: From Eq. (F.1), the term of $(\tau,s)=(2,4)$ is expressed as [76]

$$\begin{aligned}\frac{1}{q^2}G_A^{(1)}{}_\mu^{\ \mu}|_{\tau=2,s=4} &= -G_A^{L(1)}|_{\tau=2,s=4}-2G_A^{T(1)}|_{\tau=2,s=4}\\ &\simeq -\frac{20\rho m^3}{(-q^2)^4}A_4^{\mathrm{u+d}}.\end{aligned} \tag{F.7}$$

On the other hand, the same matrix element in hot matter is expressed as [75]

$$\begin{aligned}\frac{1}{q^2}G_{A_\mu}{}^\mu|_{\tau=2,s=4} &= -8i\frac{q^\mu q^\nu q^\lambda q^\sigma}{Q^{10}}\Big\langle\Big(\bar u\gamma_\mu D_\nu D_\lambda D_\sigma u+\bar d\gamma_\mu D_\nu D_\lambda D_\sigma d\Big)\Big\rangle_T\\ &= \frac{16\cdot 3}{5}\left[\frac{16\pi^4T^6}{63}B_3\Big(\frac{m_\pi}{T}\Big)-\frac{\pi^2m_\pi^2T^4}{10}B_2\Big(\frac{m_\pi}{T}\Big)+\frac{m_\pi^4T^2}{48}B_1\Big(\frac{m_\pi}{T}\Big)\right]\\ &\quad\times\frac{q^\mu q^\nu q^\lambda q^\sigma}{Q^{10}}\Big(u_\mu u_\nu u_\lambda u_\sigma-\text{traces}\Big)A_4^{\mathrm{u+d}},\end{aligned} \tag{F.8}$$

where the functions B_1, B_2 and B_3 are defined by

$$\begin{aligned}B_1(z)&=\frac{6}{\pi^2}\int_z^\infty dy\,\sqrt{y^2-z^2}\frac{1}{e^y-1},\\ B_2(z)&=\frac{15}{\pi^4}\int_z^\infty dy\,y^2\sqrt{y^2-z^2}\frac{1}{e^y-1},\\ B_3(z)&=\frac{63}{8\pi^6}\int_z^\infty dy\,y^4\sqrt{y^2-z^2}\frac{1}{e^y-1},\\ A_4^{\mathrm{u+d}}(\mu^2=1\,\mathrm{GeV}^2)&=0.255\,.\end{aligned} \tag{F.9}$$

The momentum dependent part of Eq. (F.8) is expanded around $\bar q=0$ as

$$\frac{q^\mu q^\nu q^\lambda q^\sigma}{Q^{10}}\Big(u_\mu u_\nu u_\lambda u_\sigma-\text{traces}\Big)=\frac{5}{16}\frac{1}{(-q^2)^3}-\frac{5}{4}\frac{1}{(-q^2)^4}\bar q^2+\cdots. \tag{F.10}$$

From Eqs. (F.8) and (F.10), $G_A^{(1)}{}_\mu^{\ \mu}$ with $(\tau,s)=(2,4)$ takes the form

$$\begin{aligned}&\frac{1}{q^2}G_A^{(1)}{}_\mu^{\ \mu}|_{\tau=2,s=4}\\ &=-\frac{12}{(-q^2)^4}\left[\frac{16\pi^4T^6}{63}B_3\Big(\frac{m_\pi}{T}\Big)-\frac{\pi^2m_\pi^2T^4}{10}B_2\Big(\frac{m_\pi}{T}\Big)+\frac{m_\pi^4T^2}{48}B_1\Big(\frac{m_\pi}{T}\Big)\right]A_4^{\mathrm{u+d}}.\end{aligned} \tag{F.11}$$

Comparing this expression with Eq. (F.7), we find the following correspondence:

$$\rho m^3 \quad\Leftrightarrow\quad \frac{3}{5}\left[\frac{16\pi^4T^6}{63}B_3\Big(\frac{m_\pi}{T}\Big)-\frac{\pi^2m_\pi^2T^4}{10}B_2\Big(\frac{m_\pi}{T}\Big)+\frac{m_\pi^4T^2}{48}B_1\Big(\frac{m_\pi}{T}\Big)\right]. \tag{F.12}$$

Thus the expression in hot matter corresponding to Eq. (F.5) is obtained as

$$1 - V_{\pi,\mathrm{bare}}^2 = \frac{1}{G_0}\frac{6}{5}\left[\frac{16\pi^4 T^6}{63}B_3\Big(\frac{m_\pi}{T}\Big) - \frac{\pi^2 m_\pi^2 T^4}{10}B_2\Big(\frac{m_\pi}{T}\Big) + \frac{m_\pi^4 T^2}{48}B_1\Big(\frac{m_\pi}{T}\Big)\right]\frac{1}{\Lambda^6}A_4^{\mathrm{u+d}}. \quad \text{(F.13)}$$

Taking $m_\pi = 0$, Eq. (F.13) is rewritten into the same form as Eq. (4.31).

Appendix G

Hadronic Thermal Corrections to Susceptibilities

In this appendix we summarize the hadronic thermal corrections to the two-point functions of $\overline{\mathcal{A}}_\mu$-$\overline{\mathcal{A}}_\nu$, $\overline{V}_\mu$-$\overline{V}_\nu$, $\overline{\mathcal{V}}_\mu$-$\overline{\mathcal{V}}_\nu$ and $\overline{V}_\mu$-$\overline{\mathcal{V}}_\nu$.

The four components of the hadronic thermal corrections to the two point function of $\overline{\mathcal{A}}_\mu$-$\overline{\mathcal{A}}_\nu$, $\Pi_\perp$, are expressed as

$$\begin{aligned}
\bar{\Pi}^t_\perp(p_0,\bar{p};T) &= N_f(a-1)\bar{A}_0(0,T) - N_f a M_\rho^2 \bar{B}_0(p_0,\bar{p};M_\rho,0;T) \\
&\quad + N_f\frac{a}{4}\bar{B}^t(p_0,\bar{p};M_\rho,0;T)\ , \qquad \text{(G.1)} \\
\bar{\Pi}^s_\perp(p_0,\bar{p};T) &= N_f(a-1)\bar{A}_0(0,T) - N_f a M_\rho^2 \bar{B}_0(p_0,\bar{p};M_\rho,0;T) \\
&\quad + N_f\frac{a}{4}\bar{B}^s(p_0,\bar{p};M_\rho,0;T)\ , \qquad \text{(G.2)} \\
\bar{\Pi}^L_\perp(p_0,\bar{p};T) &= N_f\frac{a}{4}\bar{B}^L(p_0,\bar{p};M_\rho,0;T)\ , \qquad \text{(G.3)} \\
\bar{\Pi}^T_\perp(p_0,\bar{p};T) &= N_f\frac{a}{4}\bar{B}^T(p_0,\bar{p};M_\rho,0;T)\ . \qquad \text{(G.4)}
\end{aligned}$$

The two components $\bar{\Pi}^t$ and $\bar{\Pi}^s$ of hadronic thermal corrections to the two-point functions of $\overline{V}_\mu$-$\overline{V}_\nu$, $\overline{\mathcal{V}}_\mu$-$\overline{\mathcal{V}}_\nu$ and $\overline{V}_\mu$-$\overline{\mathcal{V}}_\nu$ are written as

$$\begin{aligned}
&\bar{\Pi}^t_V(p_0,\bar{p};T) = \bar{\Pi}^s_V(p_0,\bar{p};T) \\
&= \bar{\Pi}^t_\parallel(p_0,\bar{p};T) = \bar{\Pi}^s_\parallel(p_0,\bar{p};T) \\
&= -\bar{\Pi}^t_{V\parallel}(p_0,\bar{p};T) = -\bar{\Pi}^s_{V\parallel}(p_0,\bar{p};T) \\
&\quad = -N_f\frac{1}{4}\left[\bar{A}_0(M_\rho;T) + a^2\bar{A}_0(0;T)\right] - N_f M_\rho^2 \bar{B}_0(p_0,\bar{p};M_\rho,M_\rho;T)\ . \qquad \text{(G.5)}
\end{aligned}$$

Among the remaining components only $\bar{\Pi}^L_\parallel$ is relevant to the present analysis. This is given

by

$$\bar{\Pi}^L_{\parallel}(p_0,\bar{p};T) \;=\; N_f\frac{1}{8}\bar{B}^L(p_0,\bar{p};M_\rho,M_\rho;T)+N_f\frac{(2-a)^2}{8}\bar{B}^L(p_0,\bar{p};0,0;T)\;. \tag{G.6}$$

For obtaining the pion decay constants and velocity in subection 3.4.2 we need the limit of $p_0=\bar{p}$ of $\bar{\Pi}^t_\perp$ and $\bar{\Pi}^s_\perp$ in Eqs. (G.1) and (G.2). With Eq. (G.16), $\bar{\Pi}^t_\perp$ and $\bar{\Pi}^s_\perp$ reduce to the following forms in the limit $M_\rho\to 0$ and $a\to 1$:

$$\begin{aligned}\bar{\Pi}^t_\perp(p_0=\bar{p}+i\epsilon,\bar{p};T) &\underset{M_\rho\to 0,\,a\to 1}{\longrightarrow} -\frac{N_f}{2}\widetilde{J}^2_1(0;T)=-\frac{N_f}{24}T^2\;,\\ \bar{\Pi}^s_\perp(p_0=\bar{p}+i\epsilon,\bar{p};T) &\underset{M_\rho\to 0,\,a\to 1}{\longrightarrow} -\frac{N_f}{2}\widetilde{J}^2_1(0;T)=-\frac{N_f}{24}T^2\;.\end{aligned} \tag{G.7}$$

In the static–low-momentum limits of the functions listed in Eq. (G.17), the $(\bar{\Pi}^t_\perp-\bar{\Pi}^L_\perp)$ appearing in the axial-vector susceptibility becomes

$$\begin{aligned}&\lim_{\bar{p}\to 0}\lim_{p_0\to 0}\left[\bar{\Pi}^t_\perp(p_0,\bar{p};T)-\bar{\Pi}^L_\perp(p_0,\bar{p};T)\right]\\ &\quad=-N_f\widetilde{J}^2_1(0;T)+N_f a\,\widetilde{J}^2_1(M_\rho;T)-N_f\frac{a}{M_\rho^2}\left[\widetilde{J}^2_{-1}(M_\rho;T)-\widetilde{J}^2_{-1}(0;T)\right]\;.\end{aligned} \tag{G.8}$$

For the functions appearing in the vector susceptibility relevant to the present analysis we have

$$\lim_{\bar{p}\to 0}\lim_{p_0\to 0}\left[\bar{\Pi}^t_V(p_0,\bar{p};T)\right] \;=\; -\frac{N_f}{4}\left[2\widetilde{J}^0_{-1}(M_\rho;T)-\widetilde{J}^2_1(M_\rho;T)+a^2\,\widetilde{J}^2_1(0;T)\right]\;, \tag{G.9}$$

$$\begin{aligned}\lim_{\bar{p}\to 0}\lim_{p_0\to 0}\left[\bar{\Pi}^L_{\parallel}(p_0,\bar{p};T)\right] \;&=\; -N_f\frac{1}{4}\left[M_\rho^2\widetilde{J}^0_1(M_\rho;T)+2\widetilde{J}^2_1(M_\rho;T)\right]\\ &\quad -N_f\frac{(2-a)^2}{2}\widetilde{J}^2_1(0;T)\;.\end{aligned} \tag{G.10}$$

In the following, we list the explicit forms of the functions that figure in the hadronic thermal corrections, $\bar{A}_0$, $\bar{B}_0$ and $\bar{B}^{\mu\nu}$ in various limits relevant to the present analysis.

The function $\bar{A}_0(M;T)$ is expressed as

$$\bar{A}_0(M;T)=\widetilde{J}^2_1(M;T)\;, \tag{G.11}$$

where $\tilde{J}^2_1(M;T)$ is defined by

$$\widetilde{J}^n_l(M;T)=\int\frac{d^3\vec{k}}{(2\pi)^3}\frac{1}{e^{\omega(\vec{k};M)/T}-1}\frac{|\vec{k}|^{n-2}}{[\omega(\vec{k};M)]^l}\;, \tag{G.12}$$

with l and n being integers and $\omega(\vec{k};M)\equiv\sqrt{M^2+|\vec{k}|^2}$. In the massless limit $M=0$, the above integration can be performed analytically. Here we list the result relevant to the present analysis:

$$\widetilde{J}^2_1(0;T)=\widetilde{J}^0_{-1}(0;T)=\frac{1}{12}T^2\;. \tag{G.13}$$

It is convenient to decompose $\bar{B}^{\mu\nu}$ into four components as done for $\Pi_\perp^{\mu\nu}$ in Eq. (5.17):

$$\bar{B}^{\mu\nu} = u^\mu u^\nu \bar{B}^t + (g^{\mu\nu} - u^\mu u^\nu)\bar{B}^s + P_L^{\mu\nu}\bar{B}^L + P_T^{\mu\nu}\bar{B}^T \ . \tag{G.14}$$

We note here that, by explicit computations, the following relations are satisfied:

$$\bar{B}^t(p_0,\bar{p};M,M;T) = \bar{B}^s(p_0,\bar{p};M,M;T) = -2\bar{A}_0(M;T) = -2\widetilde{J}_1^2(M;T) \ . \tag{G.15}$$

To obtain the pion decay constants and velocity in Section 3.4.2 we need the limit of $p_0 = \bar{p}$ of the functions in Eqs. (G.1) and (G.2). As for the functions $M_\rho^2\bar{B}_0$, $\bar{B}^t$ and $\bar{B}^s$ appearing in Eqs. (G.1) and (G.2), we find that, in the limit of M_ρ going to zero, they reduce to

$$\begin{aligned}
&M_\rho^2\bar{B}_0(p_0 = \bar{p} + i\epsilon, \bar{p}; M_\rho, 0; T) \underset{M_\rho\to 0}{\longrightarrow} 0 \ , \\
&\bar{B}^t(p_0 = \bar{p} + i\epsilon, \bar{p}; M_\rho, 0; T) \underset{M_\rho\to 0}{\longrightarrow} -2\widetilde{J}_1^2(0;T) = -\frac{1}{6}T^2 \ , \\
&\bar{B}^s(p_0 = \bar{p} + i\epsilon, \bar{p}; M_\rho, 0; T) \underset{M_\rho\to 0}{\longrightarrow} -2\widetilde{J}_1^2(0;T) = -\frac{1}{6}T^2 \ .
\end{aligned} \tag{G.16}$$

The static–low-momentum limits of the functions appearing in the corrections to the axial-vector and vector susceptibility are summarized as

$$\begin{aligned}
&\lim_{\bar{p}\to 0}\lim_{p_0\to 0}\left[M_\rho^2\bar{B}_0(p_0,\bar{p};M_\rho,0;T)\right] = -\widetilde{J}_1^2(M_\rho;T) + \widetilde{J}_1^2(0;T) \ , \\
&\lim_{\bar{p}\to 0}\lim_{p_0\to 0}\left[\bar{B}^t(p_0,\bar{p};M_\rho,0;T) - \bar{B}^L(p_0,\bar{p};M_\rho,0;T)\right] \\
&\qquad = \frac{-4}{M_\rho^2}\left[-\widetilde{J}_{-1}^2(M_\rho;T) + \widetilde{J}_{-1}^2(0;T)\right] \ , \\
&\lim_{\bar{p}\to 0}\lim_{p_0\to 0}\left[M_\rho^2\bar{B}_0(p_0,\bar{p};M_\rho,M_\rho;T)\right] = \frac{1}{2}\left[\widetilde{J}_{-1}^0(M_\rho;T) - \widetilde{J}_1^2(M_\rho;T)\right] \ , \\
&\lim_{\bar{p}\to 0}\lim_{p_0\to 0}\left[\bar{B}^L(p_0,\bar{p};M_\rho,M_\rho;T)\right] = -2M_\rho^2\widetilde{J}_1^0(M_\rho;T) - 4\widetilde{J}_1^2(M_\rho;T) \ , \\
&\lim_{\bar{p}\to 0}\lim_{p_0\to 0}\left[\bar{B}^L(p_0,\bar{p};0,0;T)\right] = -4\widetilde{J}_1^2(0;T) \ .
\end{aligned} \tag{G.17}$$

Appendix H

Explicit Calculation of Quantum Correction to ΔM

In this appendix, we compute the quantum effects on the masses of 0^- (P) and 0^+ (Q^*) heavy-light $\mathcal{M}$-mesons by calculating the one-loop corrections to the two-point functions of P and Q^* denoted by Π_{PP} and $\Pi_{Q^*Q^*}$. Here we adopt the following regularization method to identify the power divergences: We first perform the integration over the temporal component of the integration momentum, and then in the remaining integration over three-momentum we make the replacements given by

$$\int^{\Lambda} \frac{d^3\vec{k}}{(2\pi)^3}\frac{1}{\bar{k}^2} \to \frac{\Lambda}{2\sqrt{2}\pi^2}\ , \quad \int^{\Lambda} \frac{d^3\vec{k}}{(2\pi)^3}\frac{1}{\bar{k}} \to \frac{\Lambda^2}{8\pi^2}\ , \quad \int^{\Lambda} \frac{d^3\vec{k}}{(2\pi)^3} \to \frac{\Lambda^3}{12\sqrt{2}\pi^2}\ . \tag{H.1}$$

Here we use the t'Hooft-Feynman gauge for fixing the gauge of the HLS.

The diagrams contributing to Π_{PP} are shown in Fig. H.1. In the limit of zero external

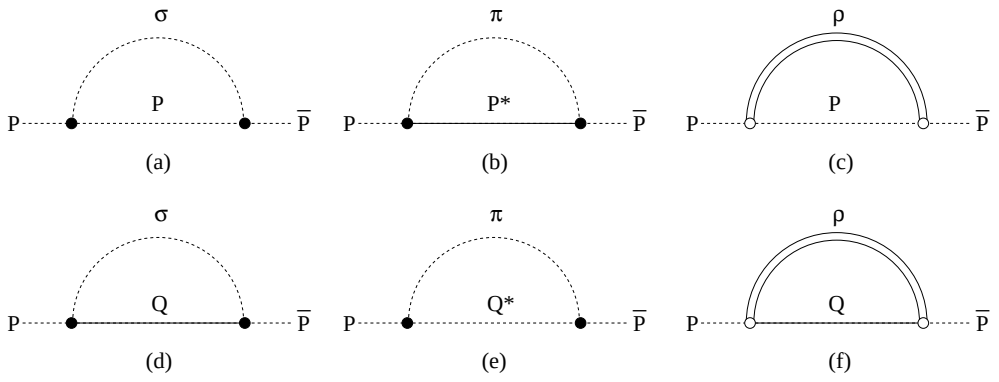

Figure H.1: Diagrams contributing to P-P two point function.

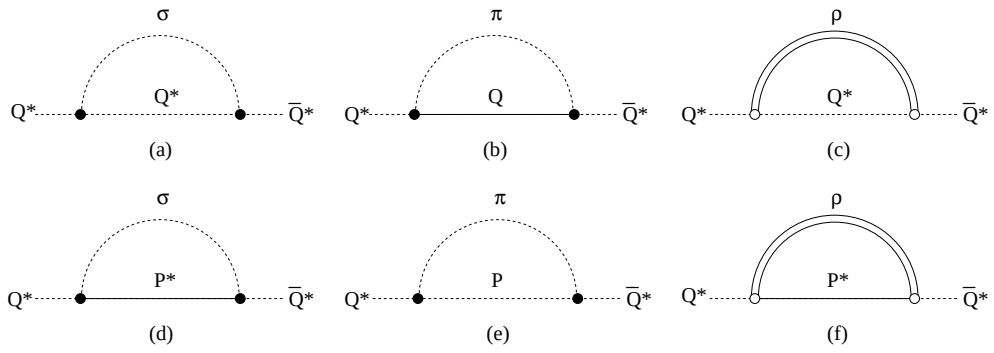

Figure H.2: Diagrams contributing to Q^*-Q^* two point function.

momentum, the divergent parts of these contributions are given by

$$\begin{aligned}
\Pi_{PP}^{(a)[\sigma P]}\Big|_{\rm div} &= \frac{2k^2}{F_\sigma^2}\left[-\frac{M_H}{(4\pi)^2}\left(\Lambda^2 - 2M_\rho \ln\Lambda\right) + \frac{M_H^2}{4\pi^2}\left(\frac{\Lambda}{\sqrt{2}} - M_H\ln\Lambda\right)\right] \ , \\
\Pi_{PP}^{(b)[\pi P^*]}\Big|_{\rm div} &= \frac{2k^2}{F_\pi^2}\left[\frac{\Lambda^3}{24\sqrt{2}\pi^2} - \frac{M_H}{(4\pi)^2}\Lambda^2 + \frac{M_H^2}{4\pi^2}\left(\frac{\Lambda}{\sqrt{2}} - M_H\ln\Lambda\right)\right] \ , \\
\Pi_{PP}^{(c)[\rho P]}\Big|_{\rm div} &= \frac{g^2}{2\pi^2}(1-k)^2\left(\frac{\Lambda}{\sqrt{2}} - M_H\ln\Lambda\right) \ , \\
\Pi_{PP}^{(d)[\sigma Q]}\Big|_{\rm div} &= \frac{2k^2}{F_\sigma^2}\left[\frac{\Lambda^3}{24\sqrt{2}\pi^2} - \frac{M_G}{(4\pi)^2}\left(\Lambda^2 - 2M_\rho^2\ln\Lambda\right) + \frac{M_G^2 - M_\rho^2}{4\pi^2}\left(\frac{\Lambda}{\sqrt{2}} - M_G\ln\Lambda\right)\right] \ , \\
\Pi_{PP}^{(e)[\pi Q^*]}\Big|_{\rm div} &= \frac{2k^2}{F_\pi^2}\left[-\frac{M_G}{(4\pi)^2}\Lambda^2 + \frac{M_G^2}{4\pi^2}\left(\frac{\Lambda}{\sqrt{2}} - M_G\ln\Lambda\right)\right] \ , \\
\Pi_{PP}^{(f)[\rho Q]}\Big|_{\rm div} &= \frac{3g^2}{2\pi^2}k^2\left(\frac{\Lambda}{\sqrt{2}} - M_G\ln\Lambda\right) \ . \qquad \text{(H.2)}
\end{aligned}$$

The particles that figure in the loop are indicated by the suffix in square bracket; e.g., $[\pi P^*]$ indicates that π and P^* enter in the internal lines. Here and henceforth, we suppress, for notational simplification, the group factor $\mathcal{C}_2(N_f)$ defined as $(T_a)_{ij}(T_a)_{jl} = \mathcal{C}_2(N_f)\delta_{il}$.

The relevant diagrams contributing to $\Pi_{Q^*Q^*}$ are shown in Fig. H.2. The divergent parts of these contributions in the low-energy limit are expressed as

$$\begin{aligned}
\Pi_{Q^*Q^*}^{(a)[\sigma Q^*]}\Big|_{\rm div} &= \frac{2k^2}{F_\sigma^2}\left[-\frac{M_G}{(4\pi)^2}\left(\Lambda^2 - 2M_\rho^2 \ln\Lambda\right) + \frac{M_G^2}{4\pi^2}\left(\frac{\Lambda}{\sqrt{2}} - M_G\ln\Lambda\right)\right] \ , \\
\Pi_{Q^*Q^*}^{(b)[\pi Q]}\Big|_{\rm div} &= \frac{2k^2}{F_\pi^2}\left[\frac{\Lambda^3}{24\sqrt{2}\pi^2} - \frac{M_G}{(4\pi)^2}\Lambda^2 + \frac{M_G^2}{4\pi^2}\left(\frac{\Lambda}{\sqrt{2}} - M_G\ln\Lambda\right)\right] \ , \\
\Pi_{Q^*Q^*}^{(c)[\rho Q^*]}\Big|_{\rm div} &= \frac{g^2}{2\pi^2}(1-k)^2\left(\frac{\Lambda}{\sqrt{2}} - M_G\ln\Lambda\right) \ , \\
\Pi_{Q^*Q^*}^{(d)[\sigma P^*]}\Big|_{\rm div} &= \frac{2k^2}{F_\sigma^2}\left[\frac{\Lambda^3}{24\sqrt{2}\pi^2} - \frac{M_H}{(4\pi)^2}\left(\Lambda^2 - 2M_\rho^2\ln\Lambda\right) + \frac{M_H^2 - M_\rho^2}{4\pi^2}\left(\frac{\Lambda}{\sqrt{2}} - M_H\ln\Lambda\right)\right] \ ,
\end{aligned}$$

$$\Pi^{(e)[\pi P]}_{Q^*Q^*}\Big|_{\rm div} = \frac{2k^2}{F_\pi^2}\left[-\frac{M_H}{(4\pi)^2}\Lambda^2 + \frac{M_H^2}{4\pi^2}\left(\frac{\Lambda}{\sqrt{2}} - M_H \ln\Lambda\right)\right] ,$$
$$\Pi^{(f)[\rho P^*]}_{Q^*Q^*}\Big|_{\rm div} = \frac{3g^2}{2\pi^2}k^2\left(\frac{\Lambda}{\sqrt{2}} - M_H \ln\Lambda\right) . \tag{H.3}$$

Now, let us compute the difference of $\Pi_{Q^*Q^*} - \Pi_{PP}$.

It is easy to show that $\Pi^{(b+e)}_{PP}\Big|_{\rm div}$ exactly cancels with $\Pi^{(b+e)}_{Q^*Q^*}\Big|_{\rm div}$. From the explicit forms given in Eqs. (H.2) and (H.3), we have

$$\Pi^{(b)[\pi Q]}_{Q^*Q^*} - \Pi^{(e)[\pi Q^*]}_{PP}\Big|_{\rm div} = \frac{2k^2}{F_\pi^2}\frac{\Lambda^3}{24\sqrt{2}\pi^2} ,$$
$$\Pi^{(e)[\pi P]}_{Q^*Q^*} - \Pi^{(b)[\pi P^*]}_{PP}\Big|_{\rm div} = -\frac{2k^2}{F_\pi^2}\frac{\Lambda^3}{24\sqrt{2}\pi^2} . \tag{H.4}$$

Note that the logarithmic, linear and quadratic divergences in $\Pi_{Q^*Q^*}$ are exactly canceled by those in Π_{PP}. This cancellation simply reflects that the external particles are chiral partners. This immediately leads to

$$\Pi^{(b+e)}_{Q^*Q^*} - \Pi^{(b+e)}_{PP}\Big|_{\rm div} = 0 . \tag{H.5}$$

The cubic divergence in $\Pi_{Q^*Q^*}$ is exactly canceled by that in Π_{PP}, reflecting that the internal particles are chiral partners to each other.

In a similar way, a partial cancellation takes place between $\Pi^{(a)}_{Q^*Q^*}$ and $\Pi^{(d)}_{PP}$ as well as between $\Pi^{(d)}_{Q^*Q^*}$ and $\Pi^{(a)}_{PP}$:

$$\Pi^{(a)[\sigma Q^*]}_{Q^*Q^*} - \Pi^{(d)[\sigma Q]}_{PP}\Big|_{\rm div} = \frac{2k^2}{F_\sigma^2}\left[-\frac{\Lambda^3}{24\sqrt{2}\pi^2} + \frac{M_\rho^2}{4\pi^2}\left(\frac{\Lambda}{\sqrt{2}} - M_G \ln\Lambda\right)\right] ,$$
$$\Pi^{(d)[\sigma P^*]}_{Q^*Q^*} - \Pi^{(a)[\sigma P]}_{PP}\Big|_{\rm div} = \frac{2k^2}{F_\sigma^2}\left[\frac{\Lambda^3}{24\sqrt{2}\pi^2} - \frac{M_\rho^2}{4\pi^2}\left(\frac{\Lambda}{\sqrt{2}} - M_H \ln\Lambda\right)\right] . \tag{H.6}$$

These lead to

$$\Pi^{(a+d)}_{Q^*Q^*} - \Pi^{(a+d)}_{PP}\Big|_{\rm div} = -g^2\frac{k^2}{2\pi^2}(M_G - M_H)\ln\Lambda , \tag{H.7}$$

where we used $M_\rho^2 = g^2F_\sigma^2$. The remaining contributions sum to

$$\Pi^{(c+f)}_{Q^*Q^*} - \Pi^{(c+f)}_{PP}\Big|_{\rm div} = -g^2\frac{1-2k-2k^2}{2\pi^2}(M_G - M_H)\ln\Lambda . \tag{H.8}$$

By summing up the contributions in Eqs. (H.5), (H.7) and (H.8), we obtain the divergent part of the correction to the mass difference:

$$\Pi_{Q^*Q^*} - \Pi_{PP}\Big|_{\rm div} = -\mathcal{C}_2(N_f)\,\frac{g^2}{2\pi^2}\Big(1-2k-k^2\Big)(M_G - M_H)\ln\Lambda , \tag{H.9}$$

where we reinstated the group factor $\mathcal{C}_2(N_f)$. The logarithmic divergence in the above expression is renormalized by the bare contribution given by

$$\Pi_{Q^*Q^*} - \Pi_{PP}\Big|_{\rm bare} = \Delta M_{\rm bare} . \tag{H.10}$$

Thus the RGE for the mass difference $\Delta M = M_G - M_H$ has the following form:

$$\mu \frac{d\,\Delta M}{d\mu} = \mathcal{C}_2(N_f)\,\frac{g^2}{2\pi^2}\Big(1 - 2k - k^2\Big)\Delta M. \tag{H.11}$$

We should stress that this RGE is exactly the same as the one in Eq. (6.32) obtained by setting $a = 1$, i.e., $F_\sigma = F_\pi$.

Note that the complete cancellation of π- and σ-loop contributions occurs even when we take into account finite renormalization effects.

References

[1] T. Hatsuda and T. Kunihiro, Phys. Rept. **247**, 221 (1994) [hep-ph/9401310].

[2] R. D. Pisarski, hep-ph/9503330.

[3] G. E. Brown and M. Rho, Phys. Rept. **269**, 333 (1996) [arXiv:hep-ph/9504250].

[4] G. E. Brown and M. Rho, Phys. Rept. **363**, 85 (2002) [arXiv:hep-ph/0103102].

[5] T. Hatsuda, H. Shiomi and H. Kuwabara, Prog. Theor. Phys. **95**, 1009 (1996) [nucl-th/9603043].

[6] R. Rapp and J. Wambach, Adv. Nucl. Phys. **25**, 1 (2000) [hep-ph/9909229].

[7] F. Wilczek, hep-ph/0003183.

[8] G. Agakishiev *et al.* [CERES Collaboration], Phys. Rev. Lett. **75**, 1272 (1995).

[9] G. Q. Li, C. M. Ko and G. E. Brown, Phys. Rev. Lett. **75**, 4007 (1995) [arXiv:nucl-th/9504025].

[10] G. E. Brown and M. Rho, Phys. Rev. Lett. **66**, 2720 (1991).

[11] M. Bando, T. Kugo, S. Uehara, K. Yamawaki and T. Yanagida, Phys. Rev. Lett. **54**, 1215 (1985).

[12] M. Bando, T. Kugo and K. Yamawaki, Phys. Rept. **164**, 217 (1988).

[13] M. Harada and K. Yamawaki, Phys. Rept. **381**, 1 (2003) [arXiv:hep-ph/0302103].

[14] M. Harada and C. Sasaki, Phys. Lett. B **537**, 280 (2002) [arXiv:hep-ph/0109034].

[15] M. Harada, Y. Kim, M. Rho and C. Sasaki, Nucl. Phys. A **727**, 437 (2003) [arXiv:hep-ph/0207012].

[16] M. Harada and C. Sasaki, Nucl. Phys. A **736**, 300 (2004) [arXiv:hep-ph/0304282].

[17] C. Sasaki, "Non-renormalization theorem originating in a new fixed point of the vector manifestation," Nucl. Phys. A **739** 151 (2004) [arXiv:hep-ph/0306005].

[18] M. Harada, Y. Kim, M. Rho and C. Sasaki, Nucl. Phys. A. **730**, 379 (2004) [arXiv:hep-ph/0308237].

[19] A. Bochkarev and J. Kapusta, Phys. Rev. D **54**, 4066 (1996) [arXiv:hep-ph/9602405].

[20] R. D. Pisarski and M. Tytgat, Phys. Rev. D **54**, R2989 (1996) [arXiv:hep-ph/9604404].

[21] M. Harada and K. Yamawaki, Phys. Rev. Lett. **86**, 757 (2001) [arXiv:hep-ph/0010207].

[22] M. Harada, Y. Kim and M. Rho, Phys. Rev. D **66**, 016003 (2002) [arXiv:hep-ph/0111120].

[23] R. L. Jaffe, Phys. Rev. D **15**, 267 (1977); Phys. Rev. D **15**, 281 (1977).

[24] N. A. Tornqvist, Z. Phys. C **68**, 647 (1995) [arXiv:hep-ph/9504372].

[25] D. Black, A. H. Fariborz, F. Sannino and J. Schechter, Phys. Rev. D **59**, 074026 (1999) [arXiv:hep-ph/9808415].

[26] K. Hagiwara *et al.* [Particle Data Group Collaboration], Phys. Rev. D **66**, 010001 (2002), and references cited therein.

[27] T. Kunihiro, S. Muroya, A. Nakamura, C. Nonaka, M. Sekiguchi and H. Wada [SCALAR Collaboration], Phys. Rev. D **70**, 034504 (2004) [arXiv:hep-ph/0310312].

[28] T. Hatsuda and T. Kunihiro, Phys. Rev. Lett. **55**, 158 (1985).

[29] P. de Forcrand *et al.* [QCD-TARO Collaboration], Phys. Rev. D **63**, 054501 (2001) [arXiv:hep-lat/0008005].

[30] E. V. Shuryak and I. Zahed, Phys. Rev. C **70**, 021901 (2004) [arXiv:hep-ph/0307267].

[31] G. E. Brown, C. H. Lee, M. Rho and E. Shuryak, Nucl. Phys. A **740**, 171 (2004) [arXiv:hep-ph/0312175].

[32] See, e.g., talk given by T. Kunihiro and Y. Nemoto at "2004 International Workshop on Dynamical Symmetry Breaking" (http://www.eken.phys.nagoya-u.ac.jp/dsb04/)

[33] M. Harada, M. Rho and C. Sasaki, Phys. Rev. D **70**, 074002 (2004) [arXiv:hep-ph/0312182].

[34] B. Aubert *et al.* [BABAR Collaboration], Phys. Rev. Lett. **90**, 242001 (2003) [arXiv:hep-ex/0304021].

[35] D. Besson *et al.* [CLEO Collaboration], Phys. Rev. D **68**, 032002 (2003) [arXiv:hep-ex/0305100].

[36] P. Krokovny *et al.* [Belle Collaboration], Phys. Rev. Lett. **91**, 262002 (2003) [arXiv:hep-ex/0308019].

[37] S. Weinberg, PhysicaA **96**, 327 (1979).

[38] J. Gasser and H. Leutwyler, Annals Phys. **158**, 142 (1984).

[39] J. Gasser and H. Leutwyler, Nucl. Phys. B **250**, 517 (1985).

[40] J. Gasser and H. Leutwyler, Nucl. Phys. B **250**, 465 (1985).

[41] G. Ecker, J. Gasser, H. Leutwyler, A. Pich and E. de Rafael, Phys. Lett. B **223**, 425 (1989).

[42] J. S. Schwinger, Phys. Lett. B **24**, 473 (1967).

[43] J. Wess and B. Zumino, Phys. Rev. **163**, 1727 (1967).

[44] S. Gasiorowicz and D. A. Geffen, Rev. Mod. Phys. **41**, 531 (1969).

[45] O. Kaymakcalan, S. Rajeev and J. Schechter, Phys. Rev. D **30**, 594 (1984).

[46] U. G. Meissner, Phys. Rept. **161**, 213 (1988).

[47] G. Ecker, J. Gasser, A. Pich and E. de Rafael, Nucl. Phys. B **321**, 311 (1989).

[48] M. C. Birse, Z. Phys. A **355**, 231 (1996) [arXiv:hep-ph/9603251].

[49] J. Schechter, Phys. Rev. D **34**, 868 (1986).

[50] K. Yamawaki, Phys. Rev. D **35**, 412 (1987).

[51] M. F. L. Golterman and N. D. Hari Dass, Nucl. Phys. B **277**, 739 (1986).

[52] U. G. Meissner and I. Zahed, Z. Phys. A **327**, 5 (1987).

[53] M. Tanabashi, Phys. Lett. B **384**, 218 (1996) [arXiv:hep-ph/9511367].

[54] See, e.g., N. Arkani-Hamed, H. Georgi and M.D. Schwartz, Ann. Phys. **305**, 96 (2003) [arXiv:hep-th/0210184].

[55] S. Weinberg, Phys. Rev. **166**, 1568 (1968).

[56] J. J. Sakurai, *Currents and Mesons*, University of Chicago Press, Chicago (1969).

[57] K. Kawarabayashi and M. Suzuki, Phys. Rev. Lett. **16**, 255 (1966); Riazuddin and Fayyazuddin, Phys. Rev. **147**, 1071 (1966).

[58] M. Bando, T. Kugo and K. Yamawaki, Nucl. Phys. B **259**, 493 (1985).

[59] M. Bando, T. Kugo and K. Yamawaki, Prog. Theor. Phys. **73**, 1541 (1985).

[60] M. Harada and K. Yamawaki, Phys. Lett. B **297**, 151 (1992) [arXiv:hep-ph/9210208].

[61] M. Harada, T. Kugo and K. Yamawaki, Phys. Rev. Lett. **71**, 1299 (1993) [arXiv:hep-ph/9303257]; Prog. Theor. Phys. **91**, 801 (1994) [arXiv:hep-ph/9303258].

[62] H. Georgi, Phys. Rev. Lett. **63** (1989) 1917; Nucl. Phys. B **331**, 311 (1990).

[63] M. Tanabashi, Phys. Lett. B **316**, 534 (1993)

[64] M. Harada and K. Yamawaki, Phys. Rev. D **64** 014023 (2001) [arXiv:hep-ph/0009163].

[65] M. Harada and K. Yamawaki, Phys. Rev. Lett. **83**, 3374 (1999) [arXiv:hep-ph/9906445].

[66] M. Veltman, Acta Phys. Polon. B **12**, 437 (1981).

[67] J. I. Kapusta, *Finite Temperature Field Theory*, Cambridge University Press (1989).

[68] M. Harada and A. Shibata, Phys. Rev. D **55**, 6716 (1997) [arXiv:hep-ph/9612358].

[69] M. Dey, V. L. Eletsky and B. L. Ioffe, Phys. Lett. B **252**, 620 (1990).

[70] U. G. Meissner, J. A. Oller and A. Wirzba, Annals Phys. **297**, 27 (2002) [arXiv:nucl-th/0109026].

[71] J. Gasser and H. Leutwyler, Phys. Lett. B **184**, 83 (1987).

[72] M. Harada and K. Yamawaki, Phys. Rev. Lett. **87**, 152001 (2001) [arXiv:hep-ph/0105335].

[73] M. A. Shifman, A. I. Vainshtein and V. I. Zakharov, Nucl. Phys. B **147** (1979) 385; Nucl. Phys. B **147** (1979) 448.

[74] W. A. Bardeen and V. I. Zakharov, Phys. Lett. B **91** (1980) 111.

[75] T. Hatsuda, Y. Koike and S. H. Lee, Nucl. Phys. B **394**, 221 (1993).

[76] B. Friman, S. H. Lee and H. C. Kim, Nucl. Phys. A **653**, 91 (1999) [arXiv:nucl-th/9903067].

[77] S. Leupold and U. Mosel, Phys. Rev. C **58**, 2939 (1998) [arXiv:nucl-th/9805024].

[78] P. Hoodbhoy, R. L. Jaffe and A. Manohar, Nucl. Phys. B **312**, 571 (1989).

[79] S. Mallik and K. Mukherjee, Phys. Rev. D **58**, 096011 (1998) [arXiv:hep-ph/9711297].

[80] F. J. Gilman and H. Harari, Phys. Rev. **165**, 1803 (1968).

[81] S. Weinberg, Phys. Rev. **177**, 2604 (1969).

[82] G. E. Brown and M. Rho, talk given at INPC2001, Berkeley, California, 2001, nucl-th/0101015.

[83] D. E. Miller, arXiv:hep-ph/0008031.

[84] For the lattice QCD calculation of quark and gluon condensates, see e.g., Refs. [115, 116, 114, 117, 83].

[85] H. J. Lee, B. Y. Park, M. Rho and V. Vento, Nucl. Phys. A **726**, 69 (2003) [arXiv:hep-ph/0304066].

[86] P. Chakraborty, M. G. Mustafa and M. H. Thoma, Eur. Phys. J. C **23** (2002) 591 [arXiv:hep-ph/0111022].

[87] T. Kunihiro, Phys. Lett. B **271** (1991) 395.

[88] J. P. Blaizot, E. Iancu and A. Rebhan, Eur. Phys. J. C **27**, 433 (2003) [arXiv:hep-ph/0206280].

[89] A. Gomez Nicola, F. J. Llanes-Estrada and J. R. Pelaez, Phys. Lett. B **550**, 55 (2002) [arXiv:hep-ph/0203134].

[90] A. Dobado, A. Gomez Nicola, F. J. Llanes-Estrada and J. R. Pelaez, Phys. Rev. C **66**, 055201 (2002) [arXiv:hep-ph/0206238].

[91] R. D. Pisarski, Phys. Rev. D **52**, 3773 (1995) [arXiv:hep-ph/9503328].

[92] C. Best *et al.*, Phys. Rev. D **56**, 2743 (1997) [arXiv:hep-lat/9703014].

[93] P. J. Sutton, A. D. Martin, R. G. Roberts and W. J. Stirling, Phys. Rev. D **45**, 2349 (1992).

[94] M. Gluck, E. Reya and A. Vogt, Z. Phys. C **48**, 471 (1990); Z. Phys. C **53**, 651 (1992).

[95] M. Gluck, E. Reya and I. Schienbein, Eur. Phys. J. C **10**, 313 (1999) [arXiv:hep-ph/9903288].

[96] D. T. Son and M. A. Stephanov, Phys. Rev. Lett. **88** (2002) 202302 [arXiv:hep-ph/0111100]; Phys. Rev. D **66** (2202) 076011 [arXiv:hep-ph/0204226].

[97] M. A. Nowak, M. Rho and I. Zahed, Phys. Rev. D **48**, 4370 (1993) [arXiv:hep-ph/9209272].

[98] W. A. Bardeen and C. T. Hill, Phys. Rev. D **49**, 409 (1994) [arXiv:hep-ph/9304265].

[99] M. A. Nowak, M. Rho and I. Zahed, Acta Phys. Polon. B **35**, 2377 (2004) [arXiv:hep-ph/0307102].

[100] N. Isgur and M. B. Wise, Phys. Lett. B **232**, 113 (1989).

[101] S. Narison, arXiv:hep-ph/0307248.

[102] S. Narison, Phys. Lett. B **210**, 238 (1988).

[103] J. Gasser and H. Leutwyler, Phys. Rept. **87**, 77 (1982).

[104] See, for a recent analysis, e.g., D. Becirevic and V. Lubicz, Phys. Lett. B **600**, 83 (2004) [arXiv:hep-ph/0403044].

[105] B. Moussallam, Eur. Phys. J. C **14**, 111 (2000) [arXiv:hep-ph/9909292].

[106] J. Schechter, A. Subbaraman and H. Weigel, Phys. Rev. D **48**, 339 (1993) [arXiv:hep-ph/9211239].

[107] M. Harada and J. Schechter, Phys. Rev. D **54**, 3394 (1996) [arXiv:hep-ph/9506473].

[108] W. A. Bardeen, E. J. Eichten and C. T. Hill, Phys. Rev. D **68**, 054024 (2003) [arXiv:hep-ph/0305049].

[109] K. Abe *et al.* [Belle Collaboration], Phys. Rev. D **69**, 112002 (2004) [arXiv:hep-ex/0307021].

[110] P. Krokovny, AIP Conf. Proc. **717**, 475 (2004) [arXiv:hep-ex/0310053].

[111] See, e.g., talk given by Y. J. Kwon [Belle Collaboration] at "2004 International Workshop on Hadron Physics: Pentaquark, Heavy-Light Hadrons and Hot/Dense Matter." (http://phya.yonsei.ac.kr∼pentaquark04/)

[112] See, e.g., M. Asakawa, T. Hatsuda and Y. Nakahara, Prog. Part. Nucl. Phys. **46**, 459 (2001) [arXiv:hep-lat/0011040], F. Karsch, Nucl. Phys. A **698**, 199 (2002) [arXiv:hep-ph/0103314], and references cited therein.

[113] K. Yamawaki, In the proceedings of 14th Symposium on Theoretical Physics: Dynamical Symmetry Breaking and Effective Field Theory, Cheju, Korea, 21-26 Jul 1995 [arXiv:hep-ph/9603293].

[114] S. Gottlieb, W. Liu, D. Toussaint, R. L. Renken and R. L. Sugar, Phys. Rev. Lett. **59**, 2247 (1987).

[115] Z. Fodor and S. D. Katz, Phys. Lett. B **534**, 87 (2002) [arXiv:hep-lat/0104001].

[116] Z. Fodor and S. D. Katz, JHEP **0203**, 014 (2002) [arXiv:hep-lat/0106002].

[117] C. R. Allton *et al.*, Phys. Rev. D **66**, 074507 (2002) [arXiv:hep-lat/0204010].